

# Mitochondrial Dehydrogenases in *Arabidopsis thaliana*

Von der Naturwissenschaftlichen Fakultät  
der Gottfried Wilhelm Leibniz Universität Hannover  
zur Erlangung des Grades  
Doktor der Naturwissenschaften  
Dr. rer. nat.

genehmigte Dissertation  
von  
M.Sc. Peter Schertl  
geboren am 13.07.1984 in Hannover

2015

Referent: Prof. Dr. Hans-Peter Braun, Leibniz Universität Hannover  
Korreferent: Prof. Dr. Christoph Peterhänsel, Leibniz Universität Hannover  
Korreferent: Prof. Dr. Stefan Binder, Universität Ulm  
Tag der Promotion: 13.01.2015

## Abstract

The mitochondrial electron transport chain (ETC) builds up a proton gradient between the mitochondrial intermembrane space and the mitochondrial matrix which is used by the ATP-synthase complex to produce ATP from ADP and  $P_i$ . This typical eukaryotic “recycling” process of ATP is called oxidative phosphorylation (OXPHOS). NADH and  $FADH_2$  are the main electron donors for the ETC. Plants as well as other eukaryotic species possess specific electron entry and exit points for the ETC. Especially plant mitochondrial dehydrogenases can be seen as a system of electron donors to the ETC. This intricate system of electron transfer pathways in plant mitochondria is poorly understood. Particularly plant mitochondria often have to cope with drastic changes in ATP requirements because of the diurnal rhythm and the fact that chloroplast only generate ATP during the day. In addition, ATP formation has to be readjusted in order to respond to several biotic and abiotic influences.

This thesis aims to contribute to a better understanding of electron pathways in the mitochondria of plants and especially to provide insights into the role of plant mitochondrial dehydrogenases. Starting with a review on the mitochondrial dehydrogenase system in plants. However, the main focus of this thesis lies on the proline dehydrogenase (ProDH), the first enzyme of the L-proline catabolism. For ProDH from *Arabidopsis thaliana* the Michaelis-Menten constant ( $K_m$ ) was determined. The influence of proline treatment on the activity of the Arabidopsis respiratory chain complexes and on other mitochondrial dehydrogenases was investigated in detail. For the first time it is shown that lactate as well as pyruvate act as competitive inhibitors for ProDH in plants. A possible rapid regulation mechanism for ProDH by the identified competitive inhibitors is discussed. It is shown that ProDH of Arabidopsis is associated to the mitochondrial membrane. In addition, analysis of Arabidopsis knock out lines allowed showing that proline breakdown represents an important electron source for the ETC under stress-release conditions. Finally, ProDH peptides from Arabidopsis were identified by mass spectrometry for the very first time in mitochondria isolated from proline treated plant cells. The second mitochondrial dehydrogenase investigated in this thesis is L-galactono-1,4-lactone dehydrogenase (GLDH). As a plant specific subunit of complex I, GLDH is responsible for the terminal step in vitamin c (ascorbate) biosynthesis as well as for the proper assembly of complex I. Three GLDH containing assembly intermediates of complex I (420 kDa, 470kDa and 850 kDa) could be identified, adding further information on the specific role of GLDH in complex I assembly in plants. Furthermore it was successfully shown that GLDH is associated to the membrane arm of complex I assembly intermediates. Finally, native gel electrophoresis methods in combination with *in-gel* activity assays are presented, methods which were of central importance for the projects of this thesis.

Keywords: plant mitochondria, dehydrogenase, proline

## Zusammenfassung

Die pflanzliche mitochondriale Elektronentransportkette (ETC) baut einen Protonengradienten zwischen dem mitochondrialen Intermembranraum und der Matrix auf. Der gebildete Protonengradient kann von der mitochondrialen ATP-Synthase genutzt werden um ATP aus ADP und  $P_i$  zu generieren. Dieser universell bei Eukaryonten vorkommende Vorgang des ATP „recyclings“ wird oxidative Phosphorylierung (OXPHOS) genannt. Die Elektronen der ETC werden überwiegend über die Co-Faktoren NADH und  $FADH_2$  in die ETC geschleust. Dabei besitzen Pflanzen, wie auch andere Eukaryonten, sowohl spezifische Stellen für den Eintritt als auch für den Austritt von Elektronen. Vor allem mitochondriale Dehydrogenasen können als ein System von „Elektron-Quellen“ für die ETC verstanden werden. Das komplexe System dieser Elektronentransportwege ist bis heute bei weitem noch nicht vollständig verstanden. Insbesondere pflanzliche Mitochondrien müssen einem oft wechselnden ATP Bedarf gerecht werden. Dies liegt vor allem am diurnalen-Rhythmus und der Tatsache, dass Chloroplasten ausschließlich am Tag einen weiteren Ort der ATP-Synthese darstellen. Ebenfalls muss der pflanzliche Metabolismus auf viele äußere biotische als auch abiotische Faktoren reagieren können. Ziel dieser Dissertation ist es, die Elektronentransportwege hin zur ETC innerhalb pflanzlicher Mitochondrien besser zu verstehen und einzelne Enzyme (Dehydrogenasen), die einen Einfluss auf die ETC haben, zu charakterisieren. Hierbei steht das erste Enzym des Prolinkatabolismus im Mittelpunkt. Für die Prolin Dehydrogenase (ProDH) aus *Arabidopsis thaliana* wurde die Michaelis-Menten-Konstante ( $K_m$ ) als enzymatische Kenngröße bestimmt. Es konnte gezeigt werden, dass durch externes Prolin Enzyme des Prolinkatabolismus als auch andere mitochondriale Dehydrogenasen induziert werden. Die Aktivität der Atmungskettenkomplexe hingegen veränderte sich nicht signifikant. Zum ersten Mal konnte gezeigt werden, dass sowohl Laktat als auch Pyruvat kompetitive Inhibitoren für eine pflanzliche ProDH darstellen. Ein schneller Regulationsmechanismus der ProDH Aktivität bei wechselnden Stressbedingungen wird diskutiert. Des Weiteren konnte eine Membranassoziation der ProDH in *Arabidopsis* gezeigt werden. Mit Hilfe von Mutanten wurde bestätigt, dass ProDH in *Arabidopsis* vorhanden sein muss, damit Prolin als Atmungskettensubstrat genutzt werden kann. Ebenfalls konnten zum ersten Mal ProDH-Peptide massenspektrometrisch in isolierten Pflanzenmitochondrien nachgewiesen werden. Die zweite mitochondriale Dehydrogenase, die im Fokus dieser Arbeit steht, ist die L-galactono-1,4-lacton Dehydrogenase (GLDH). Als pflanzenspezifische Untereinheit von Komplex I ist GLDH sowohl für den terminalen Schritt der Vitamin C (Ascorbat) Biosynthese als auch für die Assemblierung von Komplex I verantwortlich. Innerhalb dieser Arbeit konnten drei GLDH enthaltende Komplexe (420 kDa, 470 kDa und 850 kDa), die während der Assemblierung von Komplex I entstehen, identifiziert werden. Die in dieser Arbeit oft verwendete und immanent wichtige Methode der nativen Gelelektrophorese in Kombination mit *in-gel* Aktivitätstests wird in einem weiteren Teil der Arbeit detailliert beschrieben.

Schlagworte: Pflanzenmitochondrien, Dehydrogenase, Prolin

## Contents

Abbreviations .....	1
Chapter 1 - General Introduction .....	3
1.1 The Oxidative Phosphorylation (OXPHOS) System in Plants .....	3
1.2 The Alternative Oxidase (AOX) and Type II NAD(P)H Dehydrogenases .....	5
1.3 Branched Chain Amino Acid Catabolism .....	7
1.4 Proline Catabolism.....	8
1.5 Mitochondrial Dehydrogenases of the Intermembrane Space.....	10
Chapter 2 - Manuscripts .....	14
2.1 <i>Respiratory electron transfer pathways in plant mitochondria</i> .....	14
2.2 <i>Biochemical characterization of proline dehydrogenase in Arabidopsis mitochondria</i> .....	26
2.3 <i>Molecular and functional characterization of the mitochondrial proline dehydrogenase 1 in Arabidopsis thaliana</i> .....	44
2.4 <i>L-Galactono-1,4-Lactone dehydrogenase (GLDH) Forms Part of Three Subcomplexes of Mitochondrial Complex I in Arabidopsis thaliana</i> .....	88
2.5 <i>Activity measurements of mitochondrial enzymes in native gels</i> .....	103
Chapter 3 - Supplementary Discussion .....	114
3.1 On the Role of Mitochondrial Metabolism in the Light .....	114
3.2 Regulation of Proline Dehydrogenase (ProDH) activity .....	116
3.3 L-Galactono-1,4-Lactone Dehydrogenase (GLDH) as an Assembly Factor of Complex I.....	118
3.4 Supramolecular Structure of Plant Mitochondrial Enzymes .....	120
3.5 Identification of Putative Mitochondrial Dehydrogenases .....	121
Appendix.....	123
References.....	127
Curriculum Vitae.....	134

## Abbreviations

AOX	alternative oxidase
ADP	adenosine diphosphate
APX	ascorbate peroxidase
ATP	adenosine triphosphate
BCAA	branched chain amino acids
BCKDH	branched chain $\alpha$ -keto acid dehydrogenase complex
BN	blue native
<i>c</i>	cytochrome <i>c</i>
CA2	mitochondrial carbonic anhydrase 2 in Arabidopsis (At1g47260)
Complex I	NADH dehydrogenase
Complex II	succinate dehydrogenase
Complex III	cytochrome <i>c</i> reductase
Complex IV	cytochrome <i>c</i> oxidase
Complex V	ATP-synthase
cyt. G-3PDH	cytosolic NAD <sup>+</sup> -dependent G-3-P dehydrogenase
DHAP	dihydroxyacetone phosphate
DHA	dehydroascorbate
DHAR	dehydroascorbate reductase
D2HG	D-2-hydroxyglutarate
D2HGDH	D-2-hydroxyglutarate dehydrogenase
DHODH	dihydroorotate dehydrogenase
DLDH	D-lactate dehydrogenase
<i>E. coli</i>	<i>Escherichia coli</i>
ETC	electron transport chain
ETF	electron transfer flavoprotein
ETFQOR	electron transfer flavoprotein:quinone oxidoreductase
FADH <sub>2</sub>	flavin adenine dinucleotide; reduced form
FMN	flavin mononucleotide
G3-P	glycerol-3-phosphate
G3-PDH	glycerol-3-phosphate dehydrogenase
GLDH	L-galactono-1,4-lactone dehydrogenase
GR	glutathione reductase

---

GS/GOGAT	glutamine synthetase - glutamate synthase
H <sup>+</sup>	proton
IEF	isoelectric focusing
IMM	inner mitochondrial membrane
IMS	inter membrane space
IVDH	isovaleryl-CoA dehydrogenase
kDa	kilo Dalton
LLDH	L-lactate dehydrogenase
M	matrix
MDHA	monodehydroascorbate
MDHAR	monodehydroascorbate reductase
MS	mass spectrometry
NAD(P) <sup>+</sup>	nicotinamide adenine dinucleotid (phosphate); oxidized form
NAD(P)H	nicotinamide adenine dinucleotid (phosphate); reduced form
OMM	outer mitochondrial membrane
OXPPOS	oxidative phosphorylation
PAGE	polyacrylamide gel electrophoresis
P5C	pyrroline-5-carboxylate
P5CDH	pyrroline-5-carboxylate dehydrogenase
PDC	pyruvate decarboxylase complex
PEG	polyethylene glycol
P <sub>i</sub>	inorganic phosphate
ProDH	proline dehydrogenase
ROS	reactive oxygen species
UCP	uncoupling protein
UQ	ubiquinone
UQH <sub>2</sub>	ubiquinol
VAO	vanillyl-alcohol oxidase

## Chapter 1 - General Introduction

Plants can produce ATP by photophosphorylation linked to the light reaction of photosynthesis but at the same time depend on ATP formation by the mitochondrial Oxidative Phosphorylation (OXPHOS) system. The OXPHOS system consists of the respiratory chain and the ATP-synthase complex. Electrons provided to the system derive from mitochondrial catabolism. In plants, electron entry pathways into the mitochondrial respiratory chain follow unique routes. This thesis is devoted to mitochondrial dehydrogenases which are of outstanding significance for the electron transfer system of mitochondria in plants.

### 1.1 The Oxidative Phosphorylation (OXPHOS) System in Plants

Mitochondria are of central importance for energy metabolism in eukaryotes. They are responsible for the formation of adenosine triphosphate (ATP) from adenosine diphosphate (ADP). ATP is the most prevalent energy carrier in all living cells. The cleavage of its phosphoanhydride bond releases high energy. ATP is quite unstable which is due to negative charges around its triphosphate arm. On the one hand the phosphoanhydride bond is low enough in energy to be easily broken, and on the other hand the released energy is high enough to represent a strong energy source for cellular metabolism. Mitochondrial ATP synthesis relies on mitochondrial catabolism. Different organic compounds are oxidized within mitochondria and electrons are transferred by several metabolic steps to molecular oxygen. CO<sub>2</sub> represents the final oxidation product which is released from the organelles. Glycolysis which takes place in the cytosol is the preceding metabolic pathway of the process of cellular respiration. During glycolysis one molecule of glucose is oxidized forming two molecules of pyruvate in the cytosol. The following decarboxylation of pyruvate to acetyl-CoA is carried out in the mitochondrial matrix. Afterwards acetyl-CoA is the starting point of the citric acid cycle. During decarboxylation steps within the citric acid cycle two molecules CO<sub>2</sub>, three nicotinamide adenine dinucleotide (NADH) molecules and one flavin adenine dinucleotide (FADH<sub>2</sub>) molecule are produced. Most of the reducing equivalents (NADH and FADH<sub>2</sub>) produced by the citric acid cycle transfer their electrons to the respiratory electron transport chain (ETC). ETC consists of four different protein complexes. The NADH



dehydrogenase or NADH-ubiquinone-oxidoreductase (complex I), the succinate dehydrogenase or succinate - coenzyme Q reductase (complex II), the cytochrome *c* reductase or coenzyme Q : cytochrome *c* - oxidoreductase (complex III) and the cytochrome *c* oxidase (complex IV). In addition two mobile electron transporters ubiquinone (UQ) and cytochrome *c* form part of the ETC. The electrons are transferred via the respiratory chain complexes to molecular oxygen (Figure 1). During this process a proton gradient is build up across the inner mitochondrial membrane which is used by the ATP-synthase complex to form ATP.

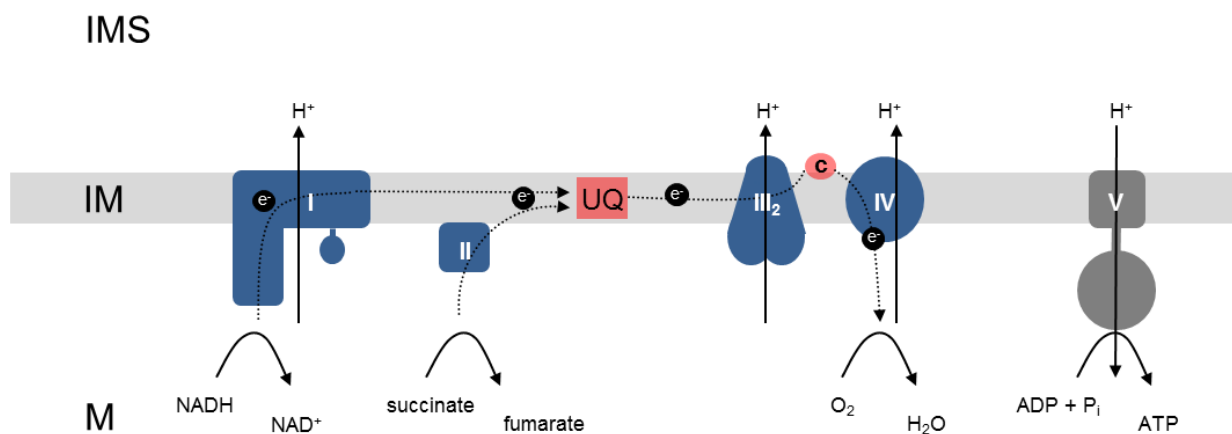


**Figure 1: The respiratory chain of the inner mitochondrial membrane, simplified.** Both, complex I and complex II transfer electrons to the mobile electron carrier ubiquinone (UQ). Subsequently, complex III transfers electrons from UQ to cytochrome *c*. The electron transfer is coupled to a proton translocation from the matrix (M) to the intermembrane space (IMS) across the inner mitochondrial membrane (IM). The emerged proton gradient is used by the ATP-synthase (complex V) to produce ATP from ADP + P<sub>i</sub>. The respiratory chain complexes I, II, III<sub>2</sub> and IV are shown in blue. ATP-synthase (complex V) is shown in grey. The two mobile electron transporters ubiquinone (UQ) and cytochrome *c* are given in red.

Complex I of the respiratory chain is the largest enzyme of the ETC. It consists of 49 subunits in plants (Klodmann *et al.* 2010). Complex I has an L-like structure with one part protruding into the mitochondrial matrix (peripheral arm) and one part embedded in the mitochondrial inner membrane (Friedrich and Böttcher 2004). Complex I oxidizes NADH using the isoalloxazine ring of flavin mononucleotide (FMN) as an electron acceptor. Subsequently, the electrons are transferred via numerous iron-sulfur clusters within complex I to ubiquinone (UQ). UQ is reduced to ubiquinol (UQH<sub>2</sub>) by the uptake of two electrons. Coupled to this process four protons are transferred from the matrix to the intermembrane space (Sazanov *et al.* 2013). UQH<sub>2</sub> can freely move within the inner mitochondrial membrane. The electrons coming from UQH<sub>2</sub> are transferred via complex III to cytochrome *c*. A Q-cycle-like

mechanism within complex III couples electron transport and proton translocation across the inner mitochondrial membrane. The electron transfer within complex III is accomplished by cytochrome b and c<sub>1</sub>, and one iron sulfur cluster (rieske centrum). For each reduced cytochrome c molecule two protons are released in the intermembrane space. Furthermore, complex II transfers electrons onto UQ, too. Within this complex the transport of electrons from succinate to UQ is accomplished by FAD and iron-sulfur clusters and fumarate is produced (Kenney 1975). At this step no proton translocation occurs. Complex II is directly involved in the citric acid cycle.

Complex IV oxidizes cytochrome c. Within complex IV, cytochrome a and a<sub>3</sub> as well as two copper ions are involved in the electron transfer. During this step further protons are transported across the inner mitochondrial membrane to the intermembrane space. Electrons are finally transferred onto molecular oxygen within complex IV (Millar et al. 2004).

The F<sub>0</sub>F<sub>1</sub>-ATP-synthase uses the proton gradient across the inner mitochondrial membrane for the synthesis of ATP from ADP and phosphate. The F<sub>1</sub>-part protrudes into the matrix. Here, ADP + P<sub>i</sub> are bound and ATP is released. The F<sub>0</sub>-part of the ATP-synthase forms a channel for the protons through the inner mitochondrial membrane (Abrahams et al. 1994). Interestingly, all protein complexes of the OXPHOS system include some extra proteins in plants. Their functional roles are only partially understood (Klodmann et al. 2010).

## **1.2 The Alternative Oxidase (AOX) and Type II NAD(P)H Dehydrogenases**

Besides the above mentioned “standard components” of the mitochondrial respiratory chain, plants have quite a number of enzymes which enable alternative electron transfer pathways. These enzymes are important to maintain the redox balance of the plant cell. The “alternative oxidase” (AOX) transfers electrons directly from UQH<sub>2</sub> to molecular oxygen (Rasmusson *et al.* 2004). In this way complex III and complex IV of the respiratory chain are bypassed and proton translocation is reduced (Figure 2). Five AOX isoforms are encoded by the *Arabidopsis thaliana* genome. The expression of the different isoforms depends on the developmental stage, cellular redox status and external factors (Wagner and Krab 1995, Van der Straeten *et al.* 1995, Millenaar and Lambers 2003, Clifton *et al.* 2006). Pyruvate especially activates AOX, probably by interaction with specific cysteine residues within AOX.

These cysteines are also involved in dimer-formation of AOX (Rhoads *et al.* 1998; Vanlerberghe *et al.* 1998). This process causes increased activity of AOX during high glycolysis. Excess of NADH can be oxidized by the action of type II NADH(P)H dehydrogenases in plants. All type II NADH(P)H dehydrogenases are attached to the inner mitochondrial membrane. In Arabidopsis the external type II NADH(P)H dehydrogenases NDB1, NDB2, NDB3 and NDB4 are facing the intermembrane space. These enzymes are able to oxidize NAD(P)H from the cytoplasm, whereas the internal type II NADH(P)H dehydrogenases NDA1, NDA2 and NDC1 are exposed to the mitochondrial matrix. These enzymes exclusively oxidize NAD(P)H which is localized in the matrix (reviewed in Rasmusson *et al.* 2008) (Figure 2). (Solely matrix localized NADH is accessible to these enzymes due to the fact that NADH cannot traverse the inner mitochondrial membrane (Tobin *et al.* 1980)). A characteristic feature of type II NAD(P)H dehydrogenases in plants is their differential dependence on  $\text{Ca}^{2+}$ . Some enzymes strictly depend on  $\text{Ca}^{2+}$ , whereas others do not. Type II NAD(P)H dehydrogenases transfer electrons onto UQ. Thus, similar to AOX, no proton translocation occurs at the inner mitochondrial membrane. AOX and type II NAD(P)H dehydrogenases are not contributing to the proton gradient which causes decreased ATP formation by the ATP-synthase complex. By this mechanism, plant cells regulate their redox balance and ATP production. Furthermore the uncoupling protein (UCP) is able to regulate energy homeostasis. Protons are channeled back from the intermembrane space to the matrix thereby releasing stored energy as heat (reviewed in Nicholls and Rial 1999).

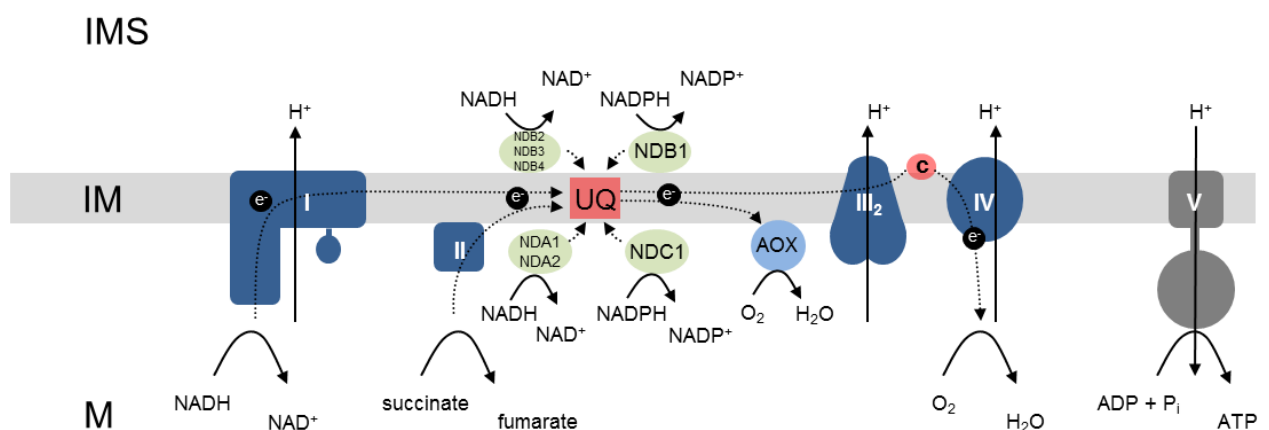


**Figure 2: Integration of alternative NAD(P)H dehydrogenases and AOX into the ETC in plants.** Type II NAD(P)H dehydrogenases (given in light green) transfer electrons to UQ. The external type II NADH(P)H dehydrogenases NDB1, NDB2, NDB3 and NDB4 are facing the intermembrane space (IMS). The internal type II NADH(P)H dehydrogenases NDA1, NDA2 and NDC1 are localized on the matrix (M) side. AOX is able to transfer electrons directly from  $\text{UQH}_2$  to molecular oxygen. (For abbreviations see Figure 1).

### 1.3 Branched Chain Amino acid Catabolism

Besides the citric acid cycle several other catabolic pathways take place in mitochondria which also contribute electrons to the respiratory chain. Especially the degradation of amino acids is of great importance. For example, electrons generated during proline, valine, leucine and isoleucine degradation can enter the ETC. The three amino acids valine, leucine and isoleucine belong to the group of branched chain amino acids (BCAA). Break down of BCAAs was found to be very important as an alternative source of electrons for plant cells under carbon starvation conditions (Ishizaki *et al.* 2005, Ishizaki *et al.* 2006, Araujo *et al.* 2010). A transamination is the starting reaction of BCAA degradation in plant mitochondria. By this reaction  $\alpha$ -keto acids are produced. Subsequently the branched chain  $\alpha$ -keto acid dehydrogenase complex (BCKDH) converts  $\alpha$ -keto acids to acyl-CoAs (reviewed in Binder 2010). In Arabidopsis the isovaleryl-CoA dehydrogenase (IVDH), which belongs to the acyl-CoA dehydrogenase family, is able to use different acyl-CoAs as substrates (coming from the different BCAAs) and produces enoyl-CoAs (Däschner *et al.* 2001). After this step the degradation of leucine proceeds via methylcrotonyl-CoA carboxylase, which forms 3-methylglutaconyl-CoA (reviewed in Binder 2010). The next step in leucine degradation is carried out by an enoyl-CoA hydratase. It is assumed that 3-methylglutaconyl-CoA (leucine breakdown) as well as the enoyl-CoAs of valine and isoleucine are putative substrates for enoyl-CoA hydratases in Arabidopsis (reviewed in Binder 2010) (Figure 3). IVDH is the link of BCAA breakdown and the respiratory chain. Via its flavo group IVDH transfers electrons to the electron transfer flavoprotein (ETF) system. In mammals ETF accepts electrons from nine different dehydrogenases involved in  $\beta$ -oxidation and amino acid degradation (reviewed in Watmough and Ferman 2010). In addition the sarcosine dehydrogenase and dimethylglycine dehydrogenase, which are involved in one-carbon metabolism in mammals, are also able to transfer electrons to ETF. In contrast to mammals, only IVDH and additionally D-2-hydroxyglutarate dehydrogenase (D2HGDH) are currently known to transfer electrons to ETF, in plants. Via the electron transfer flavoprotein : ubiquinone oxidoreductase (ETFQOR) electrons are transferred from ETF to UQ. The expression of ETFQOR is highly increased during senescence, in sucrose-starved plants and cell cultures as well as in plants grown in the presence of continuous darkness (Ishizaki *et al.* 2005 and reviewed in Binder 2010).

The matrix localized enzyme D2HGDH converts D-2-hydroxyglutarate (D2HG) to  $\alpha$ -ketoglutarate. In peroxisomes one possible source of D2HG is the condensation of propionyl-CoA and glyoxylate to D2HG. This reaction is carried out by the 2-hydroxyglutarate synthase (Engqvist *et al.* 2009). Propionyl-CoA can be produced during membrane lipid, chlorophyll and protein turnover (Engqvist *et al.* 2009). Thus it seems that D2HGDH can act as a central player of coupling these catabolic processes with the ETC.

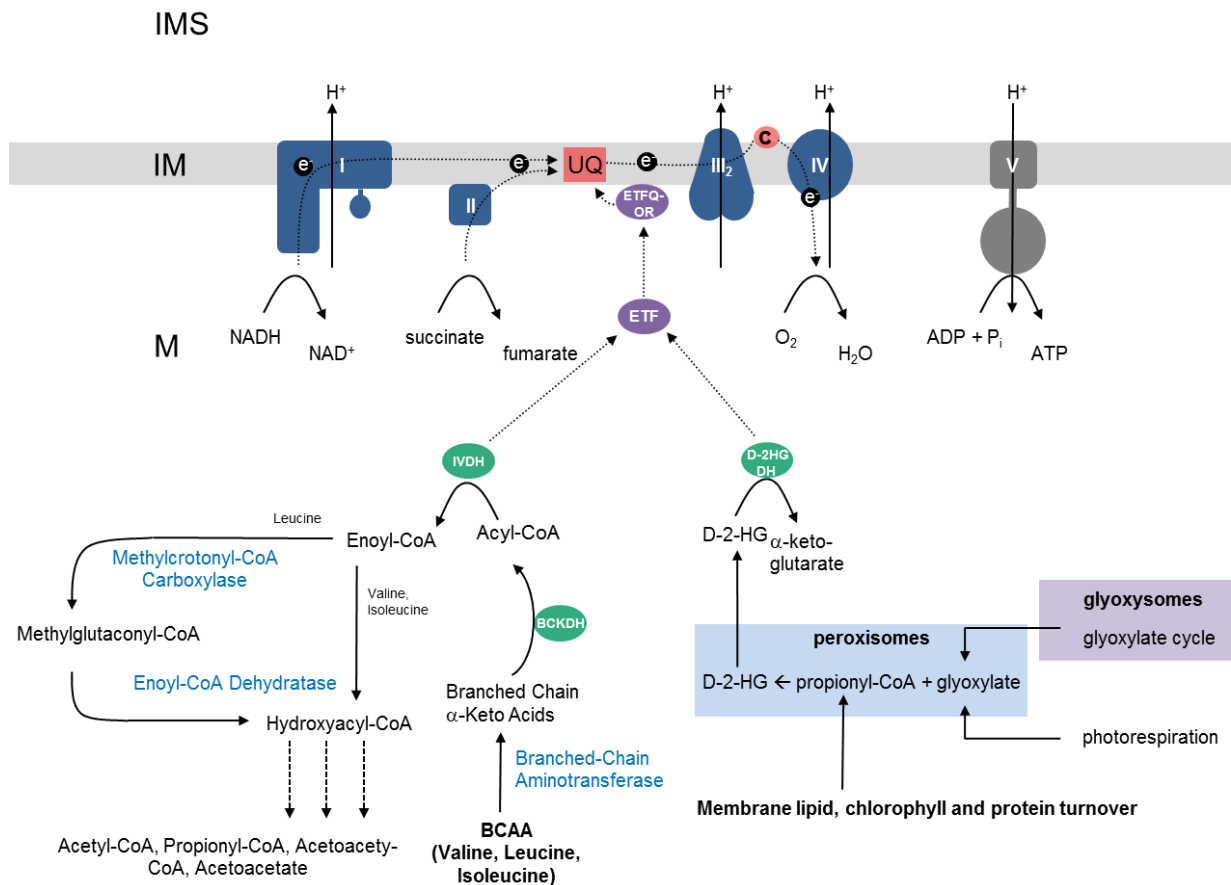


**Figure 3: The ETF – ETFQOR system in plant mitochondria.** Until today only two plant mitochondrial dehydrogenases (IVDH and D2HGDH) are known to transfer electrons from amino acid catabolism onto UQ. IVDH is involved in the catabolism of BCAAs (Binder 2010). D2HGDH receives electrons from the membrane lipids, chlorophyll and protein turnover. Mitochondrial dehydrogenases are shown in green. The names of other enzymes are given in blue. Metabolites are written in black (For abbreviations see Figure 1).

## 1.4 Proline Catabolism

The ETF system is not the only way to transfer electrons from amino acid catabolism onto UQ. For instance, proline dehydrogenase (ProDH) can directly insert electrons into the respiratory chain. ProDH converts proline to pyrroline-5-carboxylate (P5C). It is assumed that electrons from proline are directly transferred to ubiquinone. Especially under stress

conditions leading to dehydration of cells (e.g. drought and salinity stress) proline accumulates to a high level in plants (Verslues and Bray 2006). Also abiotic stress like heavy metal toxicity (Sharma and Dietz 2009) and biotic stress like pathogen infection cause induction of proline levels in plants (Fabro *et al.* 2004). In contrast, stress release conditions lead to enhanced proline degradation and subsequently to an enhanced electron flow from proline to the ETC (Figure 4).

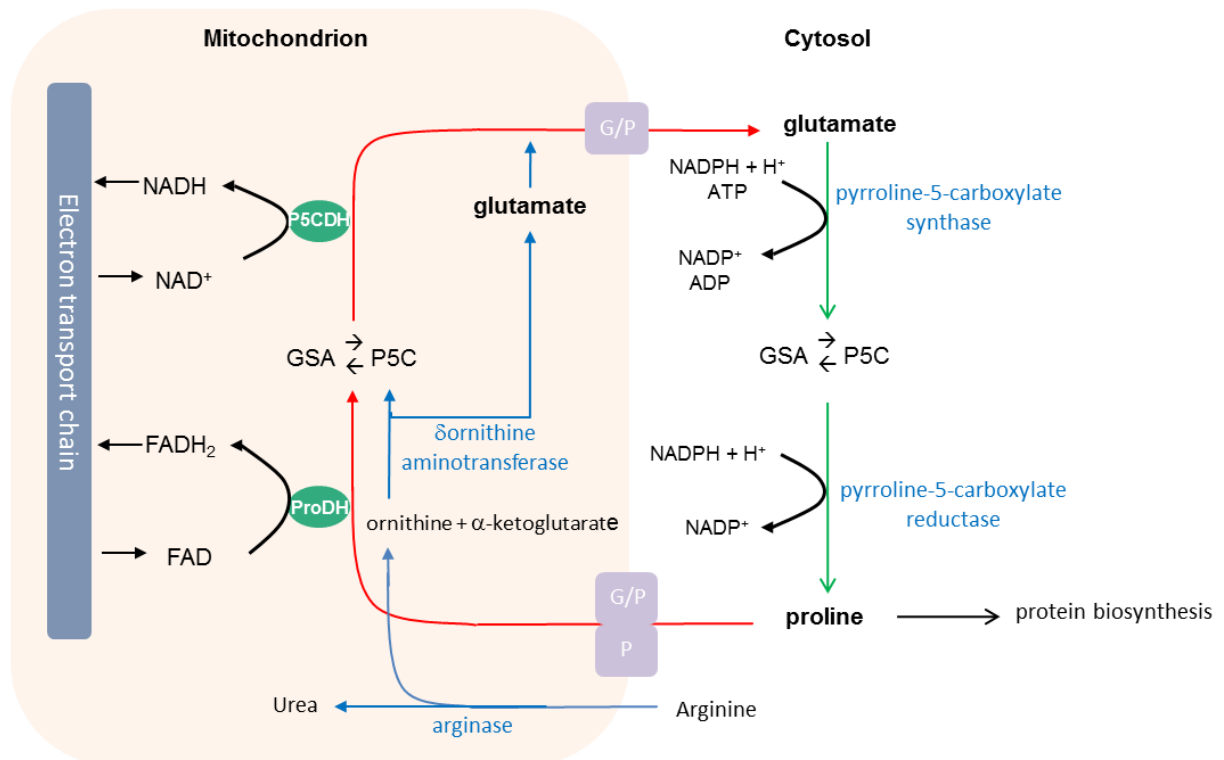


**Figure 4: Proline metabolism in higher plants (Szabadós and Savouré 2010, modified).** Biosynthesis of proline takes place in the cytosol (green lines). Starting from glutamate, proline is formed by the subsequent action of pyrroline-5-carboxylate synthase and pyrroline-5-carboxylate reductase. Proline degradation takes place in mitochondria (red lines). In mitochondria proline dehydrogenase (ProDH) and pyrroline-5-carboxylate dehydrogenase (P5CDH) oxidize proline to glutamate. The ornithine pathway uses arginine and produces pyrroline-5-carboxylate (P5C) and glutamate. (A former suggested biosynthesis pathway of proline localized in chloroplast is not shown. The existence of this pathway is not clarified yet; personal correspondence Arnould Savouré) Enzyme names are given in blue. Metabolites are indicated in black. Transporters are shown as purple boxes. Abbreviations: G/P, mitochondrial glutamate/proline antiporter; P, mitochondrial proline transporter; GSA, glutamate-semialdehyde; P5C, pyrroline-5-carboxylate.

ProDH is not the only enzyme of the proline catabolism that can transfer electrons to the ETC. The second enzyme of the proline degradation pathway, pyrroline-5-carboxylate dehydrogenase (P5CDH), uses NAD<sup>+</sup> as electron acceptor. The formed NADH subsequently

can be used by complex I and the internal type II NADH(P)H dehydrogenases to feed electrons into the ETC (Figure 4).

### 1.5 Mitochondrial Dehydrogenases of the Intermembrane Space

In the mitochondrial matrix as well as in the mitochondrial intermembrane space dehydrogenases are localized which can transfer electrons directly to ubiquinone. In animals one of these dehydrogenases is the dihydroorotate dehydrogenase (DHODH). It catalyses the fourth step of the pyrimidine biosynthesis pathway. Thereby it converts dihydroorotate to orotate. DHODH is a flavoenzyme and it is able to transfer electrons directly to ubiquinone via a flavin mononucleotide (FMN) group. DHODH from *Arabidopsis* was recombinantly expressed and characterized for substrate specificity and inhibition properties (Ullrich *et al.* 2002).

Another dehydrogenase localized in the intermembrane space is assumed to transfer electrons directly to UQ. The glycerol-3-phosphate dehydrogenase (G3-PDH) converts glycerol-3-phosphate (G3-P) to dihydroxyacetone phosphate (DHAP) (Shen *et al.* 2003). Shen *et al.* (2003, 2006) present evidence that a mitochondrial FAD-dependent G3-PDH occurs in *Arabidopsis* which is bound to the inner mitochondrial membrane and which is linked to oxygen consumption. The authors suggest a G-3-P-shuttle that links cytosolic G-3-P metabolism to carbon source utilization and energy metabolism in plants (Shen *et al.* 2003). Similar to the animal system the G-3-P-shuttle consists of a cytosolic NAD<sup>+</sup>-dependent G-3-P dehydrogenase (cyt. G3-PDH) and the mitochondrial localized G3-PDH. NADH is consumed by cyt. G3-PDH to generate G-3-P from DHAP. G-3-P can diffuse through the outer mitochondrial membrane. In the intermembrane space the mitochondrial localized G3-PDH converts G-3-P back to DHAP and donates electrons to the mitochondrial ubiquinone pool (Shen *et al.* 2006) (Figure 5). In this way reducing equivalents are shuttled from the cytosol to mitochondria without involving a metabolite transporter. This shuttle system can contribute to a fine tuning of cellular redox balance (Shen *et al.* 2006).

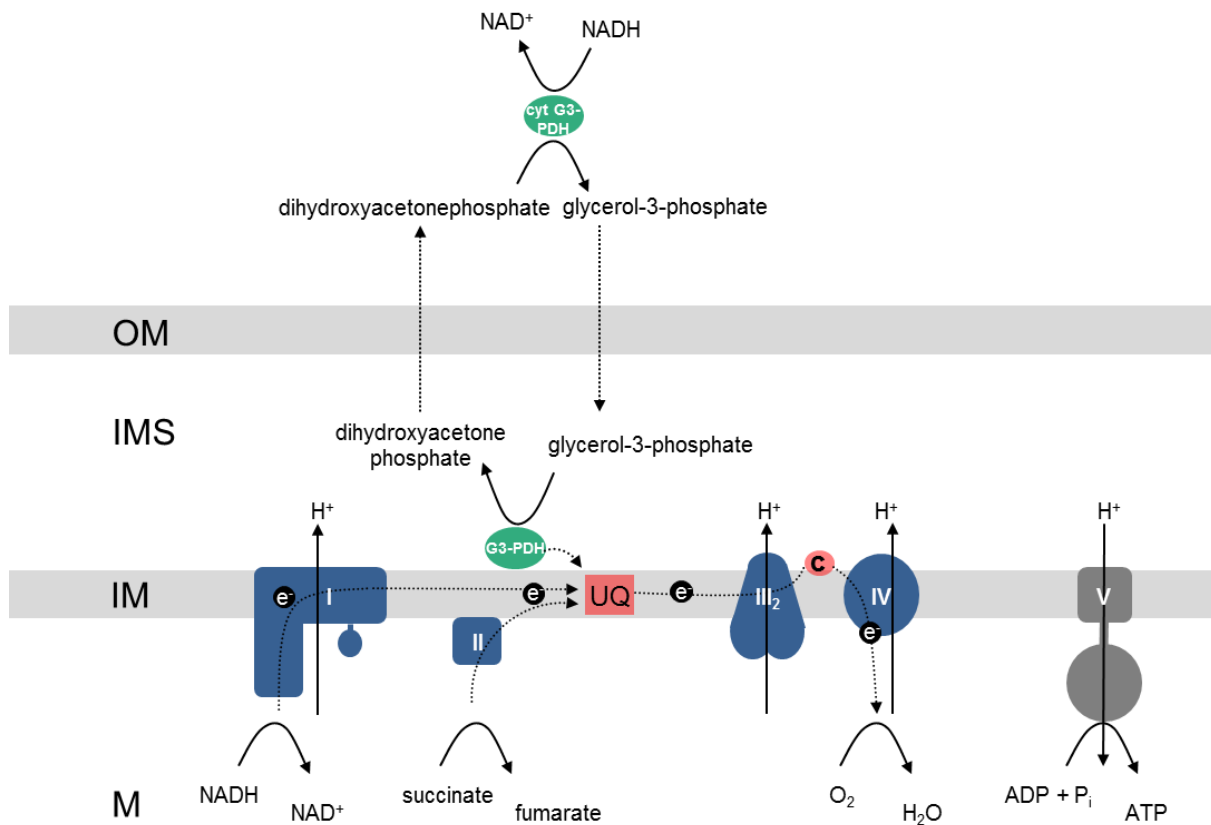


**Figure 5: Model for the involvement of the G-3-P-Shuttle in redox regulation (Shen et al. 2006, modified).** The mitochondrial G-3-P-shuttle consists of two G3-PDHs. One is located in the cytosol (cyt. G3-PDH) and another one is located in the mitochondrial intermembrane space (IMS). NADH is consumed by cyt. G3-PDH to generate G-3-P from dihydroxyacetonephosphate. G-3-P can diffuse through the outer mitochondrial membrane. In the intermembrane space the mitochondrial localized G3-PDH converts G-3-P back to dihydroxyacetonephosphate and donates electrons to the mitochondrial ubiquinone pool. (For abbreviations see Figure 1)

Two further dehydrogenases, L-galactono-1,4-lactone dehydrogenase (GLDH) and D-lactate dehydrogenase (DLDH) also seem to be localized in the intermembrane space of plant mitochondria. Both enzymes use oxidized cytochrome *c* as electron acceptor.

GLDH is a plant specific subunit of complex I (Millar *et al.* 2003). The enzyme catalyses the last step in the so called Smirnoff-Wheeler pathway of the vitamin *c* (L-ascorbate) biosynthesis pathway in plants. In the final step L-galactono-1,4-lactone is converted to L-ascorbate by the activity of GLDH. The enzyme is an aldonolactone oxidoreductase. These oxidoreductases belong to the vanillyl-alcohol oxidase (VAO) family, containing a conserved FAD-binding domain. During the conversion of L-galactono-1,4-lactone to L-ascorbate, GLDH transfers two electrons to cytochrome *c* (Bartoli *et al.* 2000). Since cytochrome *c* only accepts one electron, GLDH requires two oxidized cytochrome *c* molecules for the oxidation of one molecule L-galactono-1,4-lactone. It is known that GLDH is the sole enzyme in the



Smirnoff-Wheeler pathway that is localized in mitochondria. By the reduction of cytochrome *c* the enzyme is able to introduce electrons into the respiratory chain (Millar *et al.* 2003). In addition to its role during ascorbate formation, it has been shown that GLDH is involved in the assembly of complex I and that GLDH is obligatorily required for the accumulation of complex I (Pineau *et al.* 2008). Interestingly, the enzyme only is part of a smaller version of complex I (850 kDa) but absent in the mature form of complex I (1000 kDa) (Heazlewood *et al.* 2003; Millar *et al.* 2003). It currently is not known which subunits are lacking in this smaller version of complex I.

Like GLDH, also DLDH utilize oxidized cytochrome *c* as an electron acceptor. The Arabidopsis protein is a homodimer and each of the 59 kDa subunits possesses a FAD group (Engqvist *et al.* 2009). Substrate screening revealed activity of the enzyme with D- and L-lactate, D-2-hydroxybutyrate, glycerate and glycolate, with a higher activity with D-lactate than with glycolate (Engqvist *et al.* 2009). Until now it is not clarified which the preferred substrate is *in vivo*. Complementation experiments showed that *E. coli* mutants impaired in glycolate oxidation can be complemented by expression of the Arabidopsis protein (Bari *et al.* 2004). The authors suggest a role of DLDH during photorespiration. Photorespiration is initiated by the oxygenase activity of RuBisCo, leading to the production of phosphoglycolate in plastids. In higher plants oxidation of glycolate is carried out within peroxisomes. In contrast several algae oxidize glycolate in mitochondria. The authors propose that the basic photorespiratory system of algae is also conserved in higher plants (Bari *et al.* 2004). Another possibility is that DLDH is involved in the detoxification of methylglyoxal *in planta* (Engqvist *et al.* 2009). The main role of DLDH within the plant mitochondrial metabolism and its connection to the respiratory chain remains elusive.

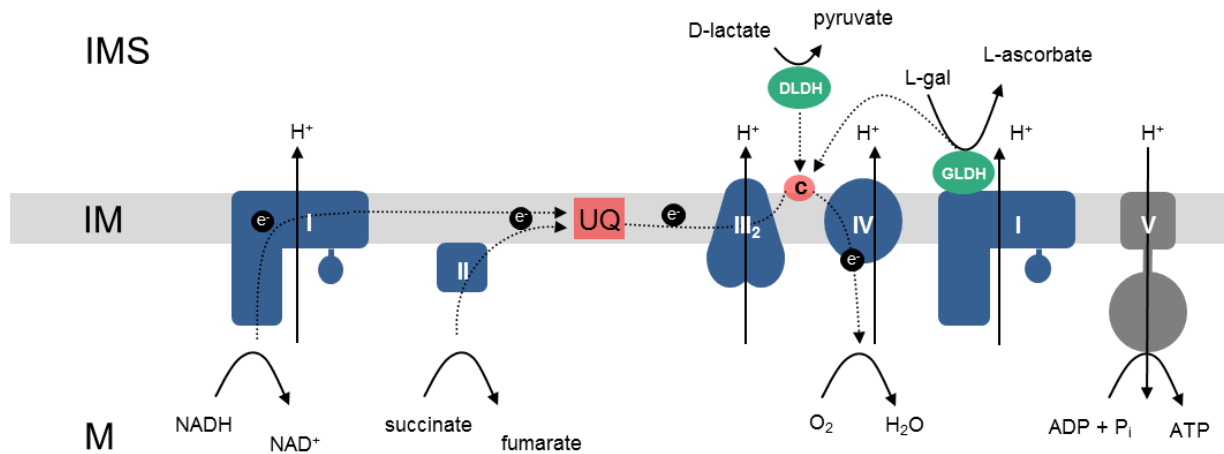


**Figure 6: Integration of L-galactono-1,4-lactone dehydrogenase (GLDH) and D-lactate dehydrogenase (DLDH) into the ETC.** GLDH and DLDH transfer electrons to cytochrome c. GLDH forms part of complex I assembly intermediates. Up to date it is not known if DLDH is a soluble or membrane bound enzyme. (For abbreviations see Figure 1).

In summary, numerous electron entry pathways into the respiratory chain exist, especially in plants. Objective of this thesis is a systematic investigation of enzymes involved in mitochondrial catabolism and supply of electrons for the plant ETC. Previous investigations point to a highly dynamic system of dehydrogenases and oxidoreductases which act in a highly regulated manner in dependence of the metabolic state of the plant cell. Manuscripts presented in the following chapter refer to investigations on selected dehydrogenases. Furthermore, a review is presented which summarizes properties of the entire electron transfer system in plants. Finally, an approach to identify so far unknown mitochondrial dehydrogenases has been carried out and is presented in the end of the supplementary discussion of this thesis (Chapter 3).

## Chapter 2 - Manuscripts

### Publication I

#### ***2.1 Respiratory electron transfer pathways in plant mitochondria***

Peter Schertl and Hans-Peter Braun

Institut für Pflanzengenetik, Abteilung Pflanzenproteomik, Leibniz Universität Hannover,  
Herrenhäuser Str. 2, 30419 Hannover, Germany

Type of authorship:	first author
Type of article:	review article
Share of the work:	50 %
Contribution to the publication:	drawing of all figures with captions, preparation of the complete table and references
Journal:	Frontiers in Plant Science
Impact Factor:	3,637
Date of publication:	published in April 2014
Number of citations (9 <sup>th</sup> of October 2014)	2
DOI:	10.3389/fpls.2014.00163
PubMed-ID:	24808901



# Respiratory electron transfer pathways in plant mitochondria

Peter Schertl and Hans-Peter Braun \*

Abteilung Pflanzenproteomik, Institut für Pflanzengenetik, Leibniz Universität Hannover, Hannover, Germany

## Edited by:

Daniel H. Gonzalez, *Universidad Nacional del Litoral, Argentina*

## Reviewed by:

Joshua L. Heazlewood, *Lawrence Berkeley National Laboratory, USA*  
Nicolas L. Taylor, *The University of Western Australia, Australia*

## \*Correspondence:

Hans-Peter Braun, *Institut für Pflanzengenetik, Abteilung Pflanzenproteomik, Leibniz Universität Hannover, Herrenhäuser Str. 2, 30419 Hannover, Germany*  
e-mail: braun@genetik.uni-hannover.de

The respiratory electron transport chain (ETC) couples electron transfer from organic substrates onto molecular oxygen with proton translocation across the inner mitochondrial membrane. The resulting proton gradient is used by the ATP synthase complex for ATP formation. In plants, the ETC is especially intricate. Besides the “classical” oxidoreductase complexes (complex I–IV) and the mobile electron transporters cytochrome c and ubiquinone, it comprises numerous “alternative oxidoreductases.” Furthermore, several dehydrogenases localized in the mitochondrial matrix and the mitochondrial intermembrane space directly or indirectly provide electrons for the ETC. Entry of electrons into the system occurs via numerous pathways which are dynamically regulated in response to the metabolic state of a plant cell as well as environmental factors. This mini review aims to summarize recent findings on respiratory electron transfer pathways in plants and on the involved components and supramolecular assemblies.

**Keywords:** plant mitochondria, electron transport chain, dehydrogenase, alternative oxidase, respiratory supercomplex

## INTRODUCTION

During cellular respiration, organic compounds are oxidized to generate usable chemical energy in the form of ATP. The respiratory electron transport chain (ETC) of mitochondria is at the center of this process. Its core consists of four oxidoreductase complexes, the NADH dehydrogenase (complex I), the succinate dehydrogenase (complex II), the cytochrome c reductase (complex III) and the cytochrome c oxidase (complex IV), as well as of two mobile electron transporters, cytochrome c, and the lipid ubiquinone. Overall, electrons are transferred from the coenzymes NADH or FADH<sub>2</sub> onto molecular oxygen which is reduced to water. Three of the four oxidoreductase complexes (complexes I, III and IV) couple their electron transfer reactions with proton translocation across the inner mitochondrial membrane. As a result, a proton gradient is formed which can be used by the ATP synthase complex (complex V) for the phosphorylation of ADP. In its classically described form, cellular respiration is based on a linear ETC (from NADH via complexes I, III, and IV to molecular oxygen). However, electrons can enter and leave the ETC at several alternative points. This is especially true for the plant ETC system, which is highly branched. In this review we aim to integrate current knowledge on the ETC system in plants with respect to its components, electron transport pathways and supramolecular structure.

## COMPONENTS OF THE PLANT ETC SYSTEM

The “classical” oxidoreductase complexes of the respiratory chain (given in dark blue in **Figure 1**) resemble their homologues in animal mitochondria but at the same time have some clear distinctive features (reviewed in Millar et al., 2008, 2011; Rasmusson and Moller, 2011; van Dongen et al., 2011; Jacoby et al., 2012). *Complex I* is especially large in plant mitochondria and includes

nearly 50 different subunits (Braun et al., 2014). Compared to its homologs from bacteria and other eukaryotic lineages it has an extra domain which includes carbonic anhydrase-like proteins. The function of this additional domain is currently unclear but it has been suggested to be important in the context of an intercellular CO<sub>2</sub> transfer mechanism to provide mitochondrial CO<sub>2</sub> for carbon fixation in chloroplasts (Braun and Zabaleta, 2007; Zabaleta et al., 2012). *Complex II* is composed of four subunits in bacteria and mitochondria of animals and fungi. In plants complex II includes homologs of these subunits but additionally four extra proteins of unknown function (Millar et al., 2004; Huang and Millar, 2013). In contrast, the subunit composition of *complex III* from plants is highly similar to the ones in yeast and bovine mitochondria (Braun and Schmitz, 1995a). The two largest subunits of this protein complex, termed “core proteins” in animals and fungi, are homologous to the two subunits of the mitochondrial processing peptidase (MPP) which removes pre-sequences of nuclear-encoded mitochondrial proteins after their import into mitochondria. In animal mitochondria, the core proteins are proteolytically inactive. Instead, an active MPP is present within the mitochondrial matrix. In contrast, the core subunits of complex III from plants have intact active sites (Braun et al., 1992; Glaser et al., 1994). Indeed, complex III isolated from plant mitochondria efficiently removes pre-sequences of mitochondrial pre-proteins. The differing functional states of complex III in diverse eukaryotic lineages might reflect different evolutionary stages of this protein complex (Braun and Schmitz, 1995b). Also *complex IV* has some extra subunits in mitochondria of plants (Millar et al., 2004). Eight subunits are homologous to complex IV subunits from other groups of eukaryotes and another six putative subunits represent proteins of unknown functions.

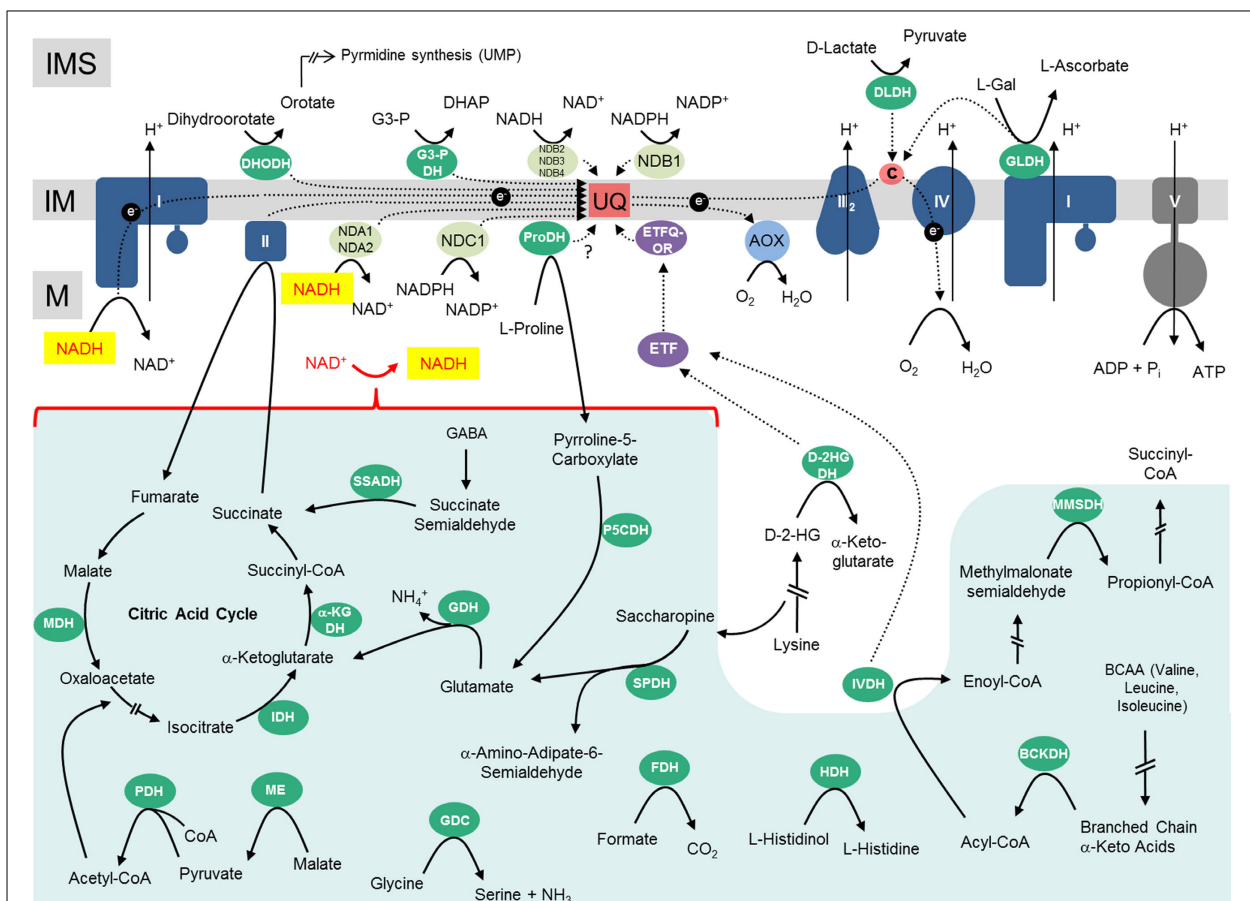


**FIGURE 1 | Mitochondrial dehydrogenases and the respiratory chain.**

Within the mitochondrial matrix (M) numerous dehydrogenases generate NADH by oxidizing various carbon compounds. NADH subsequently is re-oxidized at the inner mitochondrial membrane (IM) by the respiratory electron transfer chain (ETC). The electrons of NADH can enter the ETC through complex I or at the ubiquinone level via alternative NAD(P)H-dehydrogenases. Besides, some dehydrogenases of the mitochondrial matrix transfer electrons to ubiquinone via the ETF/ETFQOR system. Proline dehydrogenase possibly directly transfers electrons onto ubiquinone. In the intermembrane space (IMS), electrons from NAD(P)H generated in the cytoplasm can be inserted into the ETC via alternative NAD(P)H dehydrogenases. Furthermore, some dehydrogenases of the IMS can directly transfer electrons onto ubiquinone or cytochrome c. Color code—dark blue, protein complexes of the ETC; blue, AOX; purple, ETF/ETFQOR system; light green, alternative NAD(P)H dehydrogenases of the ETC; green, dehydrogenases; red, ubiquinone and cytochrome c; yellow, NADH produced by dehydrogenases of the mitochondrial matrix/NADH re-oxidized by complex I or internal alternative NADH dehydrogenases; dark gray, ATP synthase complex; light green background, NADH producing

dehydrogenases of the mitochondrial matrix. Abbreviations—*alphabetically ordered*. I, complex I; II, complex II; III, complex III; IV, complex IV; V, complex V;  $\alpha$ -KGDH,  $\alpha$ -ketoglutarate dehydrogenase complex; c, cytochrome c; D-2HGDH, D-2-hydroxyglutarate dehydrogenase; DHODH, dihydroorotate dehydrogenase; DLDH, D-lactate dehydrogenase; ETF, electron transfer flavoprotein; ETFQOR, electron transfer flavoprotein ubiquinone oxidoreductase; FDH, formate dehydrogenase; GDC, glycine dehydrogenase; GDH, glutamate dehydrogenase; GLDH, L-galactono-1,4-lactone dehydrogenase; G3-PDH, glyceraldehyde 3-phosphate dehydrogenase; HDH, histidinol dehydrogenase; IDH, isocitrate dehydrogenase; IVDH, isovaleryl-coenzyme A dehydrogenase; MDH, malate dehydrogenase; ME, malic enzyme; MMSDH, methylmalonate-semialdehyde dehydrogenase; NDA1/2, NDB2/3/4, alternative NADH dehydrogenase; NDC1, NDB1, alternative NADPH dehydrogenase; P5CDH, pyrroline-5-carboxylate dehydrogenase; PDH, pyruvate dehydrogenase; ProDH, proline dehydrogenase; SPDH, saccharopine dehydrogenase; SSADH, succinic semialdehyde dehydrogenase; UQ, ubiquinone. For further information of the enzymes see **Table 1**.

The ETC of plant mitochondria additionally includes several so-called “alternative oxidoreductases”: the alternative oxidase (AOX; light blue in **Figure 1**) and several functionally distinguishable alternative NAD(P)H dehydrogenases (alternative NDs, light green in **Figure 1**). Findings on their functional roles have been reviewed recently (Rasmusson et al., 2008; Rasmusson and Moller, 2011; Moore et al., 2013). AOX directly transfers

electrons from ubiquinol to molecular oxygen and therefore constitutes an alternative electron exit point of the ETC. As a result, complexes III and IV are excluded from respiratory electron transport. The alternative NAD(P)H dehydrogenases serve as alternative electron entry points of the plant ETC and may substitute complex I. They differ with respect to co-factor requirement and localization at the outer or inner surface of

**Table 1 | Mitochondrial dehydrogenases in *Arabidopsis thaliana*<sup>a</sup>.**

Enzyme	Accession no. <sup>b</sup> subunits isoforms etc.	Catalysed reaction	Oligomeric state Native mass/monomer mass according to GelMap <sup>c</sup> (according to other data in the literature)	Publication <sup>d</sup> for <i>Arabidopsis</i> (for other plants)
Malate dehydrogenase	At1g53240 At3g15020	Malate + NAD <sup>+</sup> ⇌ Oxaloacetate + NADH	At1g53240: 89 kDa/42 kDa At3g47520: 157 kDa/38 kDa	Journet et al., 1981 Gietl, 1992 Krömer, 1995 Nunes-Nesi et al., 2005 Lee et al., 2008 Tomaz et al., 2010
Isocitrate dehydrogenase	At4g35260 At5g14590 At4g35650 At3g09810 At5g03290 At2g17130	Isocitrate + NAD <sup>+</sup> ⇌ α-Ketoglutarate + CO <sub>2</sub> + NADH	At4g35260: 89 kDa/42 kDa At5g14590: 140 kDa/53 kDa At3g09810: 138 kDa/40 kDa At5g03290: 138 kDa/40 kDa	Behal and Oliver, 1998 Lancien et al., 1998 Lin et al., 2004 Lemaitre and Hodges, 2006 Lemaitre et al., 2007
α-Ketoglutarate dehydrogenase complex	At3g55410 (E1) At5g65750 (E1) At4g26910 (E2) At5g55070 (E2) At3g17240 (E3) At1g48030 (E3) At3g13930 (E3)	α-Ketoglutarate + coenzyme A + NAD <sup>+</sup> ⇌ succinyl-CoA + CO <sub>2</sub> + NADH	At5g65750: 207 kDa/91 kDa At3g55410: 207 kDa/91 kDa (1.7 MDa complex)	Poulsen and Wedding, 1970 Wedding and Black, 1971a,b Dry and Wiskich, 1987 Millar et al., 1999 Araújo et al., 2008 Araújo et al., 2013
Glutamate dehydrogenase	At5g18170 At5g07440 At3g03910	Glutamate + H <sub>2</sub> O + NAD <sup>+</sup> ⇌ α-Ketoglutarate + NH <sub>4</sub> <sup>+</sup> + NADH	At5g18170: 209 kDa/48 kDa At5g07440: 209 kDa/48 kDa At3g03910: 209 kDa/48 kDa	Yamaya et al., 1984 Turano et al., 1997 Aubert et al., 2001 Miyashita and Good, 2008a,b Fontaine et al., 2012 Tarasenko et al., 2013 Fontaine et al., 2012
Malic enzyme	At2g13560 At4g00570 At1g79750	Malate + NAD <sup>+</sup> ⇌ Pyruvate + NADH + CO <sub>2</sub>	At2g13560: 370 kDa/63 kDa At4g00570: 370 kDa/63 kDa	Jenner et al., 2001 Tronconi et al., 2008 Tronconi et al., 2010 Tronconi et al., 2012
Pyruvate dehydrogenase complex	At1g59900 (E1) At1g24180 (E1) At5g50850 (E1) At3g52200 (E2) At1g54220 (E2) At3g13930 (E3) At3g17240 (E3) At1g48030 (E3)	Pyruvate + coenzyme A + NAD <sup>+</sup> ⇌ Acetyl-CoA + CO <sub>2</sub> + NADH	At3g13930: 1500 kDa/54 kDa At1g24180: 470 kDa/41 kDa At5g50850: 150 kDa/39 kDa At1g59900: 138 kDa/44 kDa (9.5 MDa complex)	Luethy et al., 1994 Grof et al., 1995 Zou et al., 1999 Tovar-Méndez et al., 2003 Szurmak et al., 2003 Yu et al., 2012
Glycine dehydrogenase complex	At4g33010 (P) At2g26080 (P) At1g32470 (H) At2g35120 (H) At2g35370 (H) At1g11860 (T) At4g12130 (T) At3g17240 (L) At1g48030 (L)	Glycine + H <sub>4</sub> folate + NAD <sup>+</sup> ⇌ methylene-H <sub>4</sub> folate + CO <sub>2</sub> + NH <sub>3</sub> + NADH	At4g33010: 144 kDa/91 kDa At2g26080: 209 kDa/91 kDa At1g11860: 148 kDa/46 kDa (1.3 MDa complex)	Somerville and Ogren, 1982 Oliver et al., 1990 Oliver, 1994 Srinivasan and Oliver, 1995 Douce et al., 2001

(Continued)

Table 1 | Continued

Enzyme	Accession no. <sup>b</sup> subunits isoforms etc.	Catalysed reaction	Oligomeric state Native mass/monomer mass according to GelMap <sup>c</sup> (according to other data in the literature)	Publication <sup>d</sup> for Arabidopsis (for other plants)
Branched-chain alpha keto acid dehydrogenase complex	At5g09300 (E1) At1g21400 (E1) At1g55510 (E1) At3g13450 (E1) At3g06850 (E2) At3g13930 (E3) At3g17240 (E3) At1g48030 (E3)	Branched chain alpha keto-acids + CoA + NAD <sup>+</sup> ⇌ Acyl-CoA + NADH	At1g55510: 150 kDa/39 kDa  (0.95 MDa complex)	Fujiki et al., 2000 Mooney et al., 2000 Fujiki et al., 2001 Fujiki et al., 2002 Taylor et al., 2004 Binder, 2010
Formate dehydrogenase	At5g14780	Formate + NAD <sup>+</sup> ⇌ CO <sub>2</sub> + NADH	(200 kDa complex)	Halliwell, 1974 Colas des Francs-Small et al., 1993 Hourton-Cabassa et al., 1998 Jänsch et al., 1996 Bykova et al., 2003 Baack et al., 2003 Olson et al., 2000 Alekseeva et al., 2011
Methylmalonate semialdehyde dehydrogenase	At2g14170	(S)-methylmalonate- semialdehyde + coenzyme A + NAD <sup>+</sup> + H <sub>2</sub> O ⇌ propanoyl-CoA + bicarbonate + NADH	At2g14170: 200 kDa/59 kDa	Oguchi et al., 2004 Tanaka et al., 2005 Kirch et al., 2004
Isovaleryl-CoA dehydrogenase	At3g45300	Isovaleryl-CoA + acceptor (ETF) ⇌ 3-methylbut-2-enoyl-CoA + reduced acceptor (ETF) (also considerable activity with other acyl-CoAs)	At3g45300: 132 kDa/46 kDa  (homodimeric complex)	Däschner et al., 1999 Reinard et al., 2000 Faire-Nitschke et al., 2001 Däschner et al., 2001 Goetzman et al., 2005 Araújo et al., 2010
D-2-Hydroxyglutarate dehydrogenase	At4g36400	D-2-hydroxyglutarate + acceptor (ETF) ⇌ 2-oxoglutarate + reduced acceptor (ETF)	(homodimeric complex)	Engqvist et al., 2009 Araújo et al., 2010 Engqvist et al., 2011
Saccharopine dehydrogenase	At5g39410	Saccharopine + NAD <sup>+</sup> + H <sub>2</sub> O ⇌ Glutamate + -Amino adipate semialdehyde + NADH	not known	Zhu et al., 2000 Heazlewood et al., 2003
Pyrraline-5- carboxylate dehydrogenase	At5g62530	Pyrraline-5-carboxylate + NAD <sup>+</sup> ⇌ Glutamate (Glutamate-5- semialdehyde) + NADH	At5g62530: 158 kDa/59 kDa	Forlani et al., 1997 Deuschle et al., 2001 Deuschle et al., 2004 Miller et al., 2009
Proline dehydrogenase	At3g30775 At5g38710	L-Proline ⇌ Pyrraline-5-Carboxylate	not known	Elthon and Stewart, 1981 Verbruggen et al., 1996 Kiyosue et al., 1996 Mani et al., 2002 Szabados and Saviouré, 2010 Funck et al., 2010 Sharma and Verslues, 2010 Schertl et al., in press

(Continued)

Table 1 | Continued

Enzyme	Accession no. <sup>b</sup> subunits isoforms etc.	Catalysed reaction	Oligomeric state Native mass/monomer mass according to GelMap <sup>c</sup> (according to other data in the literature)	Publication <sup>d</sup> for Arabidopsis (for other plants)
L-Galactono-1,4-lactone dehydrogenase	At3g47930	L-Galactono-1,4-Lactone $\leftrightarrow$ L-Ascorbate	(420 kDa, 470 kDa, 850 kDa complexes)	Mapson and Breslow, 1958 Siendones et al., 1999 Leferink et al., 2008 Pineau et al., 2008 Leferink et al., 2009 Schertl et al., 2012
D-Lactate dehydrogenase	At5g06580	D-Lactate $\leftrightarrow$ Pyruvate	(homodimeric complex)	Bari et al., 2004 Atlante et al., 2005 Engqvist et al., 2009 Wienstroer et al., 2012
Glycerol-3-phosphate dehydrogenase	At3g10370	Glycerol 3-phosphate $\leftrightarrow$ Dihydroxyacetonephosphate	At3g10370: 160 kDa/65 kDa	Shen et al., 2003 Shen et al., 2006
Dihydroorotate dehydrogenase	At5g23300	Dihydroorotate $\leftrightarrow$ Orotate	At5g23300: 156 kDa/49 kDa	Ullrich et al., 2002 Doremus and Jagendorf, 1985 Miersch et al., 1987
Succinic semialdehyde dehydrogenase	At1g79440	Succinic semialdehyde $\leftrightarrow$ Succinate	At1g79440: 163 kDa/55 kDa	Busch and Fromm, 1999 Bouché et al., 2003 Kirch et al., 2004 Toyokura et al., 2011
Histidinol dehydrogenase	At5g63890	L-histidinol + NAD <sup>+</sup> $\leftrightarrow$ L-histidine + NADH	At5g63890: 115 kDa/51 kDa	Nagai and Scheidegger, 1991 Ingle, 2011
Alternative NAD(P)H dehydrogenases (NDA1, NDB4, NDA2, NDB2, NDB3, NDB1, NDC1)	At1g07180 At2g20800 At2g29990 At4g05020 At4g21490 At4g28220 At5g08740	NAD(P)H + UQ $\leftrightarrow$ NAD(P) <sup>+</sup> + UQH <sub>2</sub>	At2g20800: 160 kDa/65 kDa At2g29990: 163 kDa/55 kDa At4g05020: 160 kDa/65 kDa	Escobar et al., 2004 Rasmusson et al., 2004 Rasmusson et al., 2008 Wulff et al., 2009 Wallström et al., 2014a,b

<sup>a</sup>Mitochondrial dehydrogenases without complex I (NADH dehydrogenase) and complex II (succinate dehydrogenase) of the respiratory chain. This list corresponds to the dehydrogenases shown in **Figure 1**.

<sup>b</sup>Accession numbers in accordance with The Arabidopsis Information Resource (TAIR).

<sup>c</sup>Oligomeric state: native mass and monomer mass according to GelMap (<https://gelmap.de/231>).

<sup>d</sup>Key publications for Arabidopsis (other plants).

the inner mitochondrial membrane (external alternative NDs, internal alternative NDs). Some of the genes encoding alternative NDs are activated by light (Rasmusson et al., 2008; Rasmusson and Moller, 2011). The latter enzymes are considered to be important during photorespiration and all alternative enzymes during various stress conditions. Since none of the alternative oxidoreductases couple electron transfer with proton translocation across the inner mitochondrial membrane, their enzymatic function is believed to be important in the context of an overflow protection mechanism for the ETC which is especially relevant during high-light conditions.

Finally, dehydrogenases (dark green in **Figure 1**; **Table 1**) can directly or indirectly insert electrons into the respiratory chain (Rasmusson et al., 2008; Rasmusson and Moller, 2011). Numerous dehydrogenases of the mitochondrial matrix

generate NADH which is re-oxidized by complex I and the internal alternative NDs. However, some dehydrogenases directly transfer electrons onto ubiquinone [dihydroorotate dehydrogenase (DHODH), glyceraldehyde 3-phosphate dehydrogenase (G3-PDH) and possibly proline dehydrogenase (ProDH)] or onto cytochrome c [L-galactone-1,4-lactone dehydrogenase (GLDH) and D-lactate dehydrogenase (DLDH)]. Furthermore, at least two dehydrogenases [isovaleryl-coenzyme A dehydrogenase (IVDH) and D-2-hydroxyglutarate dehydrogenase (D-2HGDH)] transfer electrons onto ubiquinone via a short electron transfer chain composed of the “electron transfer flavoprotein” and the “electron transfer flavoprotein-ubiquinone oxidoreductase” (ETF and ETFQ-OR, purple in **Figure 1**) (Ishizaki et al., 2005, 2006; Araújo et al., 2010). IVDH is involved in the branched chain amino acid catabolism and D-2HGDH in the catabolism of lysine. In



plants, degradation of amino acids for respiration was shown to be especially important during carbon starvation conditions, e.g., extended darkness (Araújo et al., 2011). In contrast to animal mitochondria, fatty acid oxidation does not take place in plant mitochondria and the involved dehydrogenases consequently are absent. Instead, additional metabolic pathways occur in plants, e.g., the final step of an ascorbic acid biosynthesis pathway, which is catalyzed by GLDH. Electrons of L-galactono-1,4-lactone (GL) oxidation are inserted into the ETC via cytochrome c (Bartoli et al., 2000). Proline, besides being a building block for protein biosynthesis, is used as an osmolyte in plant cells. Proline is catabolized in mitochondria by a two-step process involving pyrroline-5-carboxylate dehydrogenase (P5CDH) and ProDH (Szabados and Savouré, 2010). P5CDH produces NADH, whereas ProDH represents a flavoenzyme which is assumed to transfer electrons directly or indirectly onto ubiquinone. Some additional dehydrogenases occur in plant mitochondria in the mitochondrial matrix and the intermembrane space

which also contribute electrons to the ETC (Figure 1, Table 1). However, in some cases their mitochondrial localization is not entirely certain and should be further investigated by future research.

### ELECTRON ENTRY PATHWAYS INTO THE ETC

All electrons enter the ETC via NAD(P)H (generated by a variety of dehydrogenases in the mitochondrial matrix or the intermembrane space/the cytoplasm) or via flavine nucleotides (FADH<sub>2</sub>, FMNH<sub>2</sub>), which generally are bound to proteins termed flavoproteins. Consequently, the following electron entry pathways into the ETC can be defined: (i) the Matrix NAD(P)H pathway, (ii) the Matrix-FADH<sub>2</sub> pathway, (iii) the Intermembrane-space-NAD(P)H pathway, and (iv) the Intermembrane-space-FADH<sub>2</sub>/FMDH<sub>2</sub> pathway (Figure 2).

Different metabolic processes, which vary depending on the physiological state of the plant cell, contribute to the four electron entry pathways. During stable carbohydrate conditions, electrons

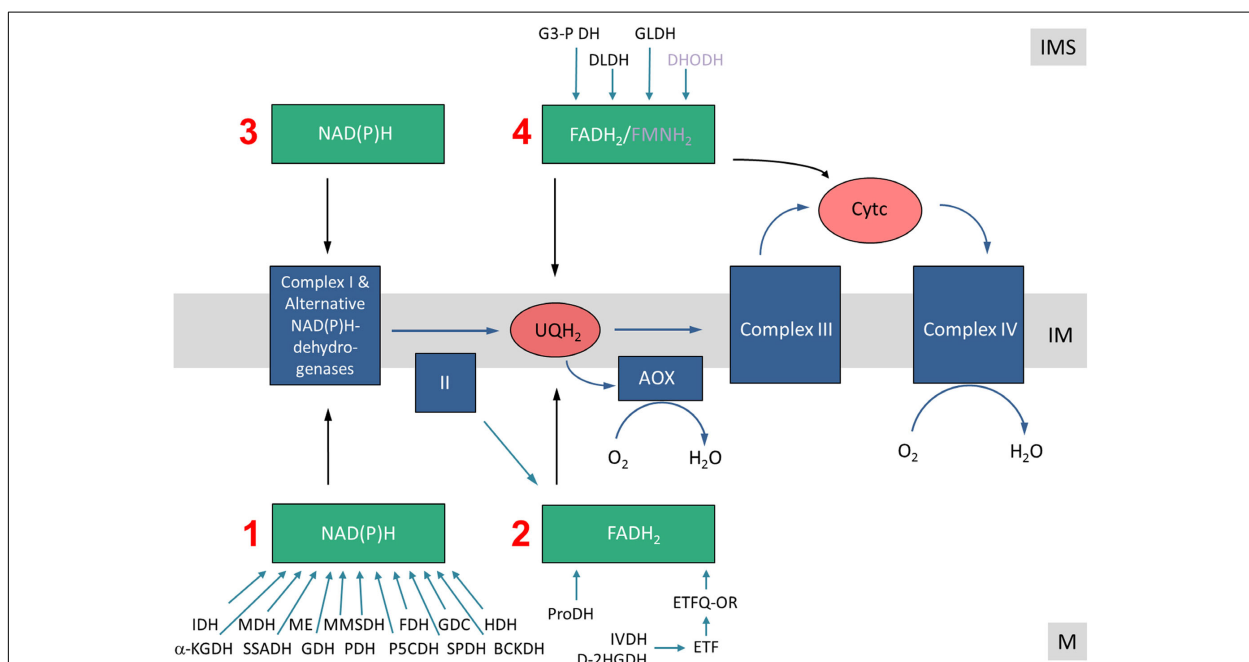


**FIGURE 2 | Electron entry pathways into the mitochondrial electron transport chain in plants.** Electrons enter the respiratory chain via four different pathways. (1) The Matrix-NAD(P)H pathway. Various dehydrogenases oxidize carbon compounds in the mitochondrial matrix. Electrons are transferred in the form of NADH to the ETC. NADH is re-oxidized by complex I or the internal alternative NAD(P)H dehydrogenases. (2) The Matrix-FADH<sub>2</sub> pathway. FAD-containing enzymes oxidize carbon compounds in the mitochondrial matrix and directly (ProDH?) or indirectly (via the ETF/ETFQ system) transfer electrons to the ubiquinone pool. (3) The IMS-NAD(P)H pathway. Cytoplasmically formed NAD(P)H is re-oxidized via external alternative dehydrogenases. (4) The IMS-FADH<sub>2</sub> pathway. FAD/FMN-containing enzymes oxidize carbon compounds in the mitochondrial intermembrane space. Electrons are transferred either to the ubiquinone or the cytochrome c. M, matrix; IM, inner membrane; IMS, intermembrane space. Abbreviations—*alphabetically ordered*. I,

complex I; II, complex II; III, complex III; IV, complex IV;  $\alpha$ -KGDH,  $\alpha$ -ketoglutarate dehydrogenase; AOX, alternative oxidase; BCKDH, branched-chain  $\alpha$ -ketoacid dehydrogenase complex; Cyt c, cytochrome c; D-2HGDH, D-2-hydroxyglutarate dehydrogenase; DHODH, dihydroorotate dehydrogenase; DLDH, D-lactate dehydrogenase; ETF, electron transfer flavoprotein; ETFQOR, electron transfer flavoprotein ubiquinone oxidoreductase; FDH, formate dehydrogenase; GDC, glycine dehydrogenase; GDH, glutamate dehydrogenase; GLDH, L-galactono-1,4-lactone dehydrogenase; G3-PDH, glyceraldehyde 3-phosphate dehydrogenase; HDH, histidinol dehydrogenase; IDH, isocitrate dehydrogenase; IVDH, isovaleryl-coenzyme A dehydrogenase; MDH, malate dehydrogenase; ME, malic enzyme; MMSDH, methylmalonate-semialdehyde dehydrogenase; P5CDH, pyrroline-5-carboxylate dehydrogenase; PDH, pyruvate dehydrogenase; ProDH, proline dehydrogenase; SPDH, saccharopine dehydrogenase; SSADH, succinic semialdehyde dehydrogenase; UQH<sub>2</sub>, ubiquinol.

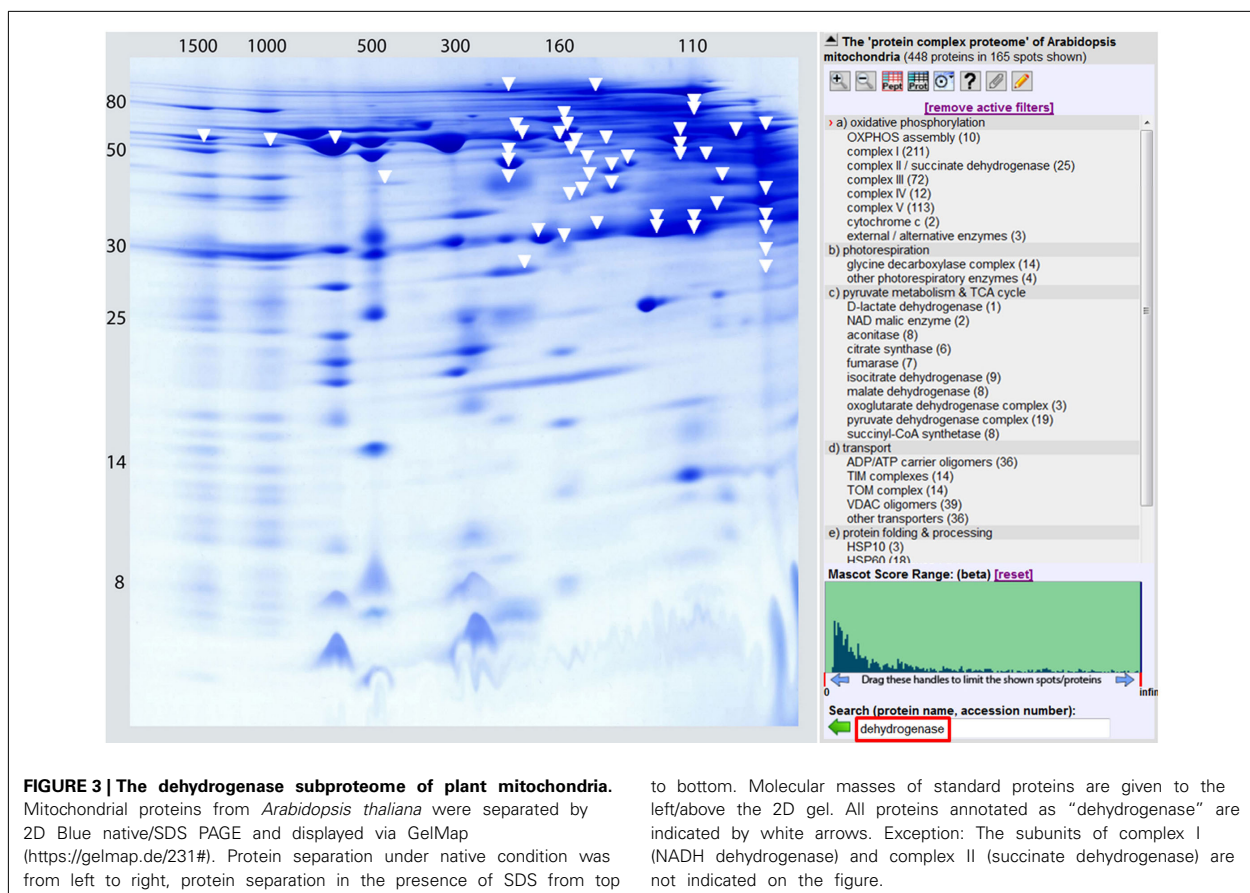
for the respiratory chain can be supplied by NADH and FADH<sub>2</sub> provided by the tricarboxylic acid (TCA) cycle. This is believed to be the standard mode of cellular respiration in non-green plant tissues or green tissues at night and resembles the basic situation in animal cells. However, during photosynthesis, NADH generation of the TCA cycle is reduced because some of its intermediates are used for anabolic reactions (reviewed in Sweetlove et al., 2010). Furthermore, the pyruvate dehydrogenase (PDH) complex is deactivated in plant mitochondria in the light by phosphorylation (Budde and Randall, 1990). At the same time photorespiration leads to an increase in NADH formation in the mitochondrial matrix by the activity of the glycine dehydrogenase complex (GDC). Indeed, at high-light conditions, NADH formed by GDC is believed to be the main substrate of the ETC, and not the NADH formed by the enzymes of the TCA cycle. At the same time, plant cells might become over-reduced in the presence of high-light. In this situation alternative oxidoreductases can insert excess electrons into the respiratory chain without contributing to the proton gradient. Upon carbon starvation conditions (e.g., extended darkness) electrons from the breakdown of amino acids are provided to the ETC (Araújo et al., 2011). Especially after release of salt stress the amino acid proline is used as an electron source (Szabados and Savouré, 2010). In summary, electron entry into the ETC is a highly flexible process in plants

which much depends on light, the metabolic state of the cell as well as environmental stress factors.

### SUPRAMOLECULAR STRUCTURE OF THE ETC SYSTEM

The ETC is based on defined protein-protein interactions. Most stable interactions occur within the four “classical” oxidoreductase complexes of the respiratory chain. Indeed, complexes I to IV can be isolated in intact form by various biochemical and electrophoretic procedures. Furthermore, several lines of evidence indicate that complexes I, III and IV interact within the inner mitochondrial membrane forming respiratory supercomplexes (reviewed in Dudkina et al., 2008). Complex I as well as complex IV associate with dimeric complex III (I + III<sub>2</sub> and IV<sub>2</sub> + III<sub>2</sub> supercomplexes). An even larger supercomplex includes complexes I, III<sub>2</sub>, and IV and was proposed to be called “respirasome” because it can autonomously catalyzes the overall ETC reaction in the presence of ubiquinone and cytochrome c. The alternative oxidoreductases of the plant ETC seem not to be part of the respiratory supercomplexes. However, alternative NDs were found to be part of other protein complexes of about 160 kDa (Klodmann et al., 2011) or 150–700 kDa (Rasmusson and Agius, 2001).

Experimental data also indicate that several of the mitochondrial dehydrogenases form protein complexes. TCA cycle



enzymes can assemble forming multienzyme clusters (Barnes and Weitzman, 1986). In addition, some of the mitochondrial dehydrogenases interact with ETC complexes, e.g., malate dehydrogenase has been reported to interact with complex I in animal mitochondria (Fukushima et al., 1989; see Braun et al., 2014 for review). Information on the native state of mitochondrial dehydrogenases furthermore comes from the GelMap project (Klodmann et al., 2011). Using 2D Blue native/SDS PAGE and systematic protein identifications, various dehydrogenases were described (Figure 3, Table 1). Native molecular mass of the dehydrogenases in many cases much exceeds the molecular mass of the monomeric proteins (Table 1, column 3). This indicates that probably most mitochondrial dehydrogenases form part of defined higher order structures.

## CONCLUSION AND OUTLOOK

Cellular respiration in plants is an especially dynamic system. The classical protein complexes of the ETC have extra functions and several alternative oxidoreductases occur. A network of mitochondrial dehydrogenases directly or indirectly supplies electrons for the respiratory chain. Insertion of electrons via various pathways is highly dependent on the metabolic state of the plant cell. The regulation of electron entry pathways into the respiratory chain is only partially understood and might, besides others, depend on the formation of supramolecular structures. Non-invasive experimental procedures will be necessary to physiologically investigate the function of these structures by future research.

## ACKNOWLEDGMENTS

We thank Tatjana Hildebrandt and Holger Eubel, Leibniz University Hannover, for critically reading the manuscript. This research project was supported by the Deutsche Forschungsgemeinschaft (DFG), grant Br 1829/10-2. Furthermore we acknowledge support by the Open Access Publishing Fund of Leibniz Universität Hannover, which is funded by the DFG.

## REFERENCES

- Alekseeva, A. A., Savin, S. S., and Tishkov, V. I. (2011). NAD (+) -dependent formate dehydrogenase from plants. *Acta Nat.* 3, 38–54.
- Araújo, W. L., Ishizaki, K., Nunes-Nesi, A., Larson, T. R., Tohge, T., Krahnert, I., et al. (2010). Identification of the 2-hydroxyglutarate and isovaleryl-CoA dehydrogenases as alternative electron donors linking lysine catabolism to the electron transport chain of Arabidopsis mitochondria. *Plant Cell* 22, 1549–1563. doi: 10.1105/tpc.110.075630
- Araújo, W. L., Nunes-Nesi, A., Trenkamp, S., Bunik, V. I., and Fernie, A. R. (2008). Inhibition of 2-oxoglutarate dehydrogenase in potato tuber suggests the enzyme is limiting for respiration and confirms its importance in nitrogen assimilation. *Plant Physiol.* 148, 1782–1796. doi: 10.1104/pp.108.126219
- Araújo, W. L., Tohge, T., Ishizaki, K., Leaver, C. J., and Fernie, A. R. (2011). Protein degradation - an alternative respiratory substrate for stressed plants. *Trends Plant Sci.* 16, 489–498. doi: 10.1016/j.tplants.2011.05.008
- Araújo, W. L., Trofimova, L., Mkrtchyan, G., Steinhauser, D., Krall, L., Graf, A., et al. (2013). On the role of the mitochondrial 2-oxoglutarate dehydrogenase complex in amino acid metabolism. *Amino Acids* 44, 683–700. doi: 10.1007/s00726-012-1392-x
- Atlante, A., de Bari, L., Valenti, D., Pizzuto, R., Paventi, G., and Passarella, S. (2005). Transport and metabolism of D-lactate in Jerusalem artichoke mitochondria. *Biochim. Biophys. Acta* 1708, 13–22. doi: 10.1016/j.bbabi.2005.03.003
- Aubert, S., Bligny, R., Douce, R., Gout, E., Ratcliffe, R. G., and Roberts, J. K. (2001). Contribution of glutamate dehydrogenase to mitochondrial glutamate metabolism studied by (13)C and (31)P nuclear magnetic resonance. *J. Exp. Bot.* 52, 37–45. doi: 10.1093/jxb/52.354.37
- Baack, R. D., Markwell, J., Herman, P. L., and Osterman, J. C. (2003). Kinetic behavior of the *Arabidopsis thaliana* leaf formate dehydrogenase is thermally sensitive. *J. Plant Physiol.* 160, 445–450. doi: 10.1078/0176-1617-00995
- Bari, R., Kebeish, R., Kalamajka, R., Rademacher, T., and Peterhänsel, C. (2004). A glycolate dehydrogenase in the mitochondria of *Arabidopsis thaliana*. *J. Exp. Bot.* 55, 623–630. doi: 10.1093/jxb/erh079
- Barnes, S. J., and Weitzman, P. D. (1986). Organization of citric acid cycle enzymes into a multienzyme cluster. *FEBS Lett.* 201, 267–270. doi: 10.1016/0014-5793(86)80621-4
- Bartoli, C. G., Pastori, G. M., and Foyer, C. H. (2000). Ascorbate biosynthesis in mitochondria is linked to the electron transport chain between complexes III and IV. *Plant Physiol.* 123, 335–344. doi: 10.1104/pp.123.1.335
- Behal, R. H., and Oliver, D. J. (1998). NAD(+)-dependent isocitrate dehydrogenase from *Arabidopsis thaliana*. Characterization of two closely related subunits. *Plant Mol. Biol.* 36, 691–698. doi: 10.1023/A:1005923410940
- Binder, S. (2010). Branched-chain amino acid metabolism in *Arabidopsis thaliana*. *Arabidopsis Book* 8, e0137. doi: 10.1199/tab.0137
- Bouché, N., Fait, A., Bouchez, D., Møller, S. G., and Fromm, H. (2003). Mitochondrial succinic-semialdehyde dehydrogenase of the gamma-aminobutyrate shunt is required to restrict levels of reactive oxygen intermediates in plants. *Proc. Natl. Acad. Sci. U.S.A.* 100, 6843–6848. doi: 10.1073/pnas.1037532100
- Braun, H. P., Binder, S., Brennicke, A., Eubel, H., Fernie, A. R., Finkemeier, I., et al. (2014). The life of plant mitochondrial complex I. *Mitochondrion*. doi: 10.1016/j.mito.2014.02.006. [Epub ahead of print].
- Braun, H. P., Emmermann, M., Kruft, V., and Schmitz, U. K. (1992). The general mitochondrial processing peptidase from potato is an integral part of cytochrome c reductase of the respiratory chain. *EMBO J.* 11, 3219–3227.
- Braun, H. P., and Schmitz, U. K. (1995a). The bifunctional cytochrome c reductase/processing peptidase complex from plant mitochondria. *J. Bioenerg. Biomembr.* 27, 423–436. doi: 10.1007/BF02110005
- Braun, H. P., and Schmitz, U. K. (1995b). Are the “core” proteins of the mitochondrial bc1 complex evolutionary relics of a processing peptidase? *Trends Biochem. Sci.* 20, 171–175. doi: 10.1016/S0968-0004(00)88999-9
- Braun, H. P., and Zabaleta, E. (2007). Carbonic anhydrase subunits of the mitochondrial NADH dehydrogenase complex (complex I) in plants. *Physiologia Plantarum* 129, 114–122. doi: 10.1111/j.1399-3054.2006.00773.x
- Budde, R. J., and Randall, D. D. (1990). Pea leaf mitochondrial pyruvate dehydrogenase complex is inactivated *in vivo* in a light-dependent manner. *Proc. Natl. Acad. Sci. U.S.A.* 87, 673–676. doi: 10.1073/pnas.87.2.673
- Busch, K. B., and Fromm, H. (1999). Plant succinic semialdehyde dehydrogenase. Cloning, purification, localization in mitochondria, and regulation by adenine nucleotides. *Plant Physiol.* 121, 589–597. doi: 10.1104/pp.121.2.589
- Bykova, N. V., Stensballe, A., Egsgaard, H., Jensen, O. N., and Møller, I. M. (2003). Phosphorylation of formate dehydrogenase in potato tuber mitochondria. *J. Biol. Chem.* 278, 26021–26030. doi: 10.1074/jbc.M300245200
- Colas des Francs-Small, C., Ambard-Bretteville, F., Small, I. D., and Rémy, R. (1993). Identification of a major soluble protein in mitochondria from nonphotosynthetic tissues as NAD-dependent formate dehydrogenase. *Plant Physiol.* 102, 1171–1177. doi: 10.1104/pp.102.4.1171
- Däschner, K., Couée, I., and Binder, S. (2001). The mitochondrial isovaleryl-coenzyme a dehydrogenase of Arabidopsis oxidizes intermediates of leucine and valine catabolism. *Plant Physiol.* 126, 601–612. doi: 10.1104/pp.126.2.601
- Däschner, K., Thalheim, C., Guha, C., Brennicke, A., and Binder, S. (1999). In plants a putative isovaleryl-CoA-dehydrogenase is located in mitochondria. *Plant Mol. Biol.* 39, 1275–1282.
- Deuschle, K., Funck, D., Forlani, G., Stransky, H., Biehl, A., Leister, D., et al. (2004). The role of [Delta]1-pyrroline-5-carboxylate dehydrogenase in proline degradation. *Plant Cell* 16, 3413–3425. doi: 10.1105/tpc.104.023622
- Deuschle, K., Funck, D., Hellmann, H., Däschner, K., Binder, S., and Frommer, W. B. (2001). A nuclear gene encoding mitochondrial Delta-pyrroline-5-carboxylate dehydrogenase and its potential role in protection from proline toxicity. *Plant J.* 27, 345–356. doi: 10.1046/j.1365-313X.2001.01101.x

- Doremus, H. D., and Jagendorf, A. T. (1985). Subcellular localization of the pathway of de novo pyrimidine nucleotide biosynthesis in pea leaves. *Plant Physiol.* 79, 856–861. doi: 10.1104/pp.79.3.856
- Douce, R., Bourguignon, J., Neuburger, M., and Rébeillé, F. (2001). The glycine decarboxylase system: a fascinating complex. *Trends Plant Sci.* 6, 167–176. doi: 10.1016/S1360-1385(01)01892-1
- Dry, I. B., and Wiskich, J. T. (1987). 2-Oxoglutarate dehydrogenase and pyruvate dehydrogenase activities in plant mitochondria: interaction via a common coenzyme a pool. *Arch. Biochem. Biophys.* 257, 92–99. doi: 10.1016/0003-9861(87)90546-7
- Dudkina, N. V., Sunderhaus, S., Boekema, E. J., and Braun, H.-P. (2008). The higher level of organization of the oxidative phosphorylation system: mitochondrial supercomplexes. *J. Bioenerg. Biomembr.* 40, 419–424. doi: 10.1007/s10863-008-9167-5
- Elthon, T. E., and Stewart, C. R. (1981). Submitochondrial location and electron transport characteristics of enzymes involved in proline oxidation. *Plant Physiol.* 67, 780–784. doi: 10.1104/pp.67.4.780
- Engqvist, M., Drincovich, M. F., Flügge, U.-I., and Maurino, V. G. (2009). Two D-2-hydroxy-acid dehydrogenases in *Arabidopsis thaliana* with catalytic capacities to participate in the last reactions of the methylglyoxal and beta-oxidation pathways. *J. Biol. Chem.* 284, 25026–25037. doi: 10.1074/jbc.M109.021253
- Engqvist, M. K. M., Kuhn, A., Wienstroer, J., Weber, K., Jansen, E. E. W., Jakobs, C., et al. (2011). Plant D-2-hydroxyglutarate dehydrogenase participates in the catabolism of lysine especially during senescence. *J. Biol. Chem.* 286, 11382–11390. doi: 10.1074/jbc.M110.194175
- Escobar, M. A., Franklin, K. A., Svensson, A. S., Salter, M. G., Whitlam, G. C., and Rasmuson, A. G. (2004). Light regulation of the Arabidopsis respiratory chain. Multiple discrete photoreceptor responses contribute to induction of type II NAD(P)H dehydrogenase genes. *Plant Physiol.* 136, 2710–2721. doi: 10.1104/pp.104.046698
- Faivre-Nitschke, S. E., Couée, I., Vermel, M., Grienberger, J. M., and Gualberto, J. M. (2001). Purification, characterization and cloning of isovaleryl-CoA dehydrogenase from higher plant mitochondria. *Eur. J. Biochem.* 268, 1332–1339. doi: 10.1046/j.1432-1327.2001.01999.x
- Fontaine, J.-X., Tercé-Laforgue, T., Armengaud, P., Clément, G., Renou, J.-P., Pelletier, S., et al. (2012). Characterization of a NADH-dependent glutamate dehydrogenase mutant of Arabidopsis demonstrates the key role of this enzyme in root carbon and nitrogen metabolism. *Plant Cell* 24, 4044–4065. doi: 10.1105/tpc.112.103689
- Fontaine, J.-X., Tercé-Laforgue, T., Bouton, S., Pageau, K., Lea, P. J., Dubois, F., et al. (2013). Further insights into the isoenzyme composition and activity of glutamate dehydrogenase in *Arabidopsis thaliana*. *Plant Signal. Behav.* 8, e23329. doi: 10.4161/psb.23329
- Forlani, G., Scainelli, D., and Nielsen, E. (1997). [ $\delta$ ]1-pyrroline-5-carboxylate dehydrogenase from cultured cells of potato (purification and properties). *Plant Physiol.* 113, 1413–1418.
- Fujiki, Y., Ito, M., Itoh, T., Nishida, I., and Watanabe, A. (2002). Activation of the promoters of Arabidopsis genes for the branched-chain alpha-keto acid dehydrogenase complex in transgenic tobacco BY-2 cells under sugar starvation. *Plant Cell Physiol.* 43, 275–280. doi: 10.1093/pcp/pcf032
- Fujiki, Y., Ito, M., Nishida, I., and Watanabe, A. (2001). Leucine and its keto acid enhance the coordinated expression of genes for branched-chain amino acid catabolism in Arabidopsis under sugar starvation. *FEBS Lett.* 499, 161–165. doi: 10.1016/S0014-5793(01)02536-4
- Fujiki, Y., Sato, T., Ito, M., and Watanabe, A. (2000). Isolation and characterization of cDNA clones for the  $\epsilon$ 1beta and  $\epsilon$ 2 subunits of the branched-chain alpha-ketoacid dehydrogenase complex in Arabidopsis. *J. Biol. Chem.* 275, 6007–6013. doi: 10.1074/jbc.275.8.6007
- Fukushima, T., Decker, R. V., Anderson, W. M., and Spivey, H. O. (1989). Substrate channeling of NADH in mitochondrial redox processes. *J. Biol. Chem.* 264, 16483–16488.
- Funck, D., Eckard, S., and Müller, G. (2010). Non-redundant functions of two proline dehydrogenase isoforms in Arabidopsis. *BMC Plant Biol.* 10:70. doi: 10.1186/1471-2229-10-70
- Gietl, C. (1992). Malate dehydrogenase isoenzymes: cellular locations and role in the flow of metabolites between the cytoplasm and cell organelles. *Biochim. Biophys. Acta* 1100, 217–234. doi: 10.1016/0167-4838(92)90476-T
- Glaser, E., Eriksson, A., and Sjöling, S. (1994). Bifunctional role of the bc1 complex in plants. Mitochondrial bc1 complex catalyses both electron transport and protein processing. *FEBS Lett.* 346, 83–87. doi: 10.1016/0014-5793(94)00312-2
- Goetzman, E. S., Mohsen, A.-W. A., Prasad, K., and Vockley, J. (2005). Convergent evolution of a 2-methylbutyryl-CoA dehydrogenase from isovaleryl-CoA dehydrogenase in *Solanum tuberosum*. *J. Biol. Chem.* 280, 4873–4879. doi: 10.1074/jbc.M412640200
- Grof, C. P., Winning, B. M., Scaysbrook, T. P., Hill, S. A., and Leaver, C. J. (1995). Mitochondrial pyruvate dehydrogenase. Molecular cloning of the E1 alpha subunit and expression analysis. *Plant Physiol.* 108, 1623–1629. doi: 10.1104/pp.108.4.1623
- Halliwel, B. (1974). Oxidation of formate by peroxisomes and mitochondria from spinach leaves. *Biochem. J.* 138, 77–85.
- Heazlewood, J. L., Howell, K. A., Whelan, J., and Millar, A. H. (2003). Towards an analysis of the rice mitochondrial proteome. *Plant Physiol.* 132, 230–242. doi: 10.1104/pp.102.018986
- Hourton-Cabassa, C., Ambard-Bretteville, F., Moreau, F., and Davy de Virville, J., Rémy, R., and Francs-Small, C. C. (1998). Stress induction of mitochondrial formate dehydrogenase in potato leaves. *Plant Physiol.* 116, 627–635. doi: 10.1104/pp.116.2.627
- Huang, S., and Millar, A. H. (2013). Succinate dehydrogenase: the complex roles of a simple enzyme. *Curr. Opin. Plant Biol.* 16, 344–349. doi: 10.1016/j.pbi.2013.02.007
- Ingle, R. A. (2011). Histidine biosynthesis. *Arabidopsis Book* 9, e0141. doi: 10.1199/tab.0141
- Ishizaki, K., Larson, T. R., Schauer, N., Fernie, A. R., Graham, I. A., and Leaver, C. J. (2005). The critical role of Arabidopsis electron-transfer flavoprotein:ubiquinone oxidoreductase during dark-induced starvation. *Plant Cell* 17, 2587–2600. doi: 10.1105/tpc.105.035162
- Ishizaki, K., Schauer, N., Larson, T. R., Graham, I. A., Fernie, A. R., and Leaver, C. J. (2006). The mitochondrial electron transfer flavoprotein complex is essential for survival of Arabidopsis in extended darkness. *Plant J.* 47, 751–760. doi: 10.1111/j.1365-313X.2006.02826.x
- Jacoby, R. P., Li, L., Huang, S., Pong Lee, C., Millar, A. H., and Taylor, N. L. (2012). Mitochondrial composition, function and stress response in plants. *J. Integr. Plant Biol.* 54, 887–906. doi: 10.1111/j.1744-7909.2012.01177.x
- Jansch, L., Kruft, V., Schmitz, U. K., and Braun, H. P. (1996). New insights into the composition, molecular mass and stoichiometry of the protein complexes of plant mitochondria. *Plant J.* 9, 357–368. doi: 10.1046/j.1365-313X.1996.09030357.x
- Jenner, H. L., Winning, B. M., Millar, A. H., Tomlinson, K. L., Leaver, C. J., and Hill, S. A. (2001). NAD malic enzyme and the control of carbohydrate metabolism in potato tubers. *Plant Physiol.* 126, 1139–1149. doi: 10.1104/pp.126.3.1139
- Journet, E. P., Neuburger, M., and Douce, R. (1981). Role of glutamate-oxaloacetate transaminase and malate dehydrogenase in the regeneration of NAD for glycine oxidation by spinach leaf mitochondria. *Plant Physiol.* 67, 467–469. doi: 10.1104/pp.67.3.467
- Kirch, H.-H., Bartels, D., Wei, Y., Schnable, P. S., and Wood, A. J. (2004). The ALDH gene superfamily of Arabidopsis. *Trends Plant Sci.* 9, 371–377. doi: 10.1016/j.tplants.2004.06.004
- Kiyosue, T., Yoshida, Y., Yamaguchi-Shinozaki, K., and Shinozaki, K. (1996). A nuclear gene encoding mitochondrial proline dehydrogenase, an enzyme involved in proline metabolism, is upregulated by proline but downregulated by dehydration in Arabidopsis. *Plant Cell* 8, 1323–1335.
- Klodmann, J., Senkler, M., Rode, C., and Braun, H.-P. (2011). Defining the protein complex proteome of plant mitochondria. *Plant Physiol.* 157, 587–598. doi: 10.1104/pp.111.182352
- Krömer, S. (1995) Respiration during photosynthesis. *Annu. Rev. Plant Physiol. Plant Mol. Biol.* 46, 47–70. doi: 10.1146/annurev.pp.46.060195.000401
- Lancien, M., Gadal, P., and Hodges, M. (1998). Molecular characterization of higher plant NAD-dependent isocitrate dehydrogenase: evidence for a heteromeric structure by the complementation of yeast mutants. *Plant J.* 16, 325–333. doi: 10.1046/j.1365-313x.1998.00305.x
- Lee, C. P., Eubel, H., O'Toole, N., and Millar, A. H. (2008). Heterogeneity of the mitochondrial proteome for photosynthetic and non-photosynthetic Arabidopsis metabolism. *Mol. Cell Proteomics* 7, 1297–1316. doi: 10.1074/mcp.M700535-MCP200
- Lefterink, N. G. H., van den Berg, W. A. M., and van Berkel, W. J. H. (2008). L-Galactono-gamma-lactone dehydrogenase from *Arabidopsis thaliana*,

- a flavoprotein involved in vitamin C biosynthesis. *FEBS J.* 275, 713–726. doi: 10.1111/j.1742-4658.2007.06233.x
- Leferink, N. G. H., van Duijn, E., Barendregt, A., Heck, A. J. R., and van Berkel, W. J. H. (2009). Galactonolactone dehydrogenase requires a redox-sensitive thiol for optimal production of vitamin C. *Plant Physiol.* 150, 596–605. doi: 10.1104/pp.109.136929
- Lemaitre, T., and Hodges, M. (2006). Expression analysis of *Arabidopsis thaliana* NAD-dependent isocitrate dehydrogenase genes shows the presence of a functional subunit that is mainly expressed in the pollen and absent from vegetative organs. *Plant Cell Physiol.* 47, 634–643. doi: 10.1093/pcp/pcj030
- Lemaitre, T., Urbanczyk-Wochniak, E., Flesch, V., Bismuth, E., Fernie, A. R., and Hodges, M. (2007). NAD-dependent isocitrate dehydrogenase mutants of *Arabidopsis* suggest the enzyme is not limiting for nitrogen assimilation. *Plant Physiol.* 144, 1546–1558. doi: 10.1104/pp.107.100677
- Lin, M., Behal, R. H., and Oliver, D. J. (2004). Characterization of a mutation in the IDH-II subunit of the NAD<sup>+</sup>-dependent isocitrate dehydrogenase from *Arabidopsis thaliana*. *Plant Sci.* 166, 983–988. doi: 10.1016/j.plantsci.2003.12.012
- Luethy, M. H., Miernyk, J. A., and Randall, D. D. (1994). The nucleotide and deduced amino acid sequences of a cDNA encoding the E1 beta-subunit of the *Arabidopsis thaliana* mitochondrial pyruvate dehydrogenase complex. *Biochim. Biophys. Acta* 1187, 95–98. doi: 10.1016/0005-2728(94)90171-6
- Mani, S., van de Cotte, B., van Montagu, M., and Verbruggen, N. (2002). Altered levels of proline dehydrogenase cause hypersensitivity to proline and its analogs in *Arabidopsis*. *Plant Physiol.* 128, 73–83. doi: 10.1104/pp.010572
- Mapson, L. W., and Breslow, E. (1958). Biological synthesis of ascorbic acid: L-galactono-gamma-lactone dehydrogenase. *Biochem. J.* 68, 395–406.
- Miersch, J., Grancharov, K., Krauss, G. J., Spassovska, N., Karamanov, G., Maneva, L., et al. (1987). Biological activity and mode of action of some dihydroorotic and dihydroazaorotic acid derivatives. *Biomed. Biochim. Acta* 46, 307–315.
- Millar, A. H., Eubel, H., Jansch, L., Kruft, V., Heazlewood, J. L., and Braun, H.-P. (2004). Mitochondrial cytochrome c oxidase and succinate dehydrogenase complexes contain plant specific subunits. *Plant Mol. Biol.* 56, 77–90. doi: 10.1007/s11103-004-2316-2
- Millar, A. H., Hill, S. A., and Leaver, C. J. (1999). Plant mitochondrial 2-oxoglutarate dehydrogenase complex: purification and characterization in potato. *Biochem. J.* 343(Pt 2), 327–334. doi: 10.1042/0264-6021:3430327
- Millar, A. H., Small, I. D., Day, D. A., and Whelan, J. (2008). Mitochondrial biogenesis and function in *Arabidopsis*. *Arabidopsis Book* 6, e0111. doi: 10.1199/tab.0111
- Millar, A. H., Whelan, J., Soole, K. L., and Day, D. A. (2011). Organization and regulation of 1822 mitochondrial respiration in plants. *Annu. Rev. Plant Biol.* 62, 79–104. doi: 10.1146/annurev-arplant-042110-103857
- Miller, G., Honig, A., Stein, H., Suzuki, N., Mittler, R., and Zilberstein, A. (2009). Unraveling delta<sup>1</sup>-pyrroline-5-carboxylate-proline cycle in plants by uncoupled expression of proline oxidation enzymes. *J. Biol. Chem.* 284, 26482–26492. doi: 10.1074/jbc.M109.009340
- Miyashita, Y., and Good, A. G. (2008a). Glutamate deamination by glutamate dehydrogenase plays a central role in amino acid catabolism in plants. *Plant Signal. Behav.* 3, 842–843. doi: 10.4161/psb.3.10.5936
- Miyashita, Y., and Good, A. G. (2008b). NAD(H)-dependent glutamate dehydrogenase is essential for the survival of *Arabidopsis thaliana* during dark-induced carbon starvation. *J. Exp. Bot.* 59, 667–680. doi: 10.1093/jxb/erm340
- Mooney, B. P., Henzl, M. T., Miernyk, J. A., and Randall, D. D. (2000). The dihydrolipoyl acyltransferase (BCE2) subunit of the plant branched-chain alpha-ketoacid dehydrogenase complex forms a 24-mer core with octagonal symmetry. *Protein Sci.* 9, 1334–1339. doi: 10.1110/ps.9.7.1334
- Moore, A. L., Shiba, T., Young, L., Harada, S., Kita, K., and Ito, K. (2013). Unraveling the heater: new insights into the structure of the alternative oxidase. *Annu. Rev. Plant Biol.* 64, 637–663. doi: 10.1146/annurev-arplant-042811-105432
- Nagai, A., and Scheidegger, A. (1991). Purification and characterization of histidinol dehydrogenase from cabbage. *Arch. Biochem. Biophys.* 284, 127–132. doi: 10.1016/0003-9861(91)90274-M
- Nunes-Nesi, A., Carrari, F., Lytovchenko, A., Smith, A. M. O., Loureiro, M. E., Ratcliffe, R. G., et al. (2005). Enhanced photosynthetic performance and growth as a consequence of decreasing mitochondrial malate dehydrogenase activity in transgenic tomato plants. *Plant Physiol.* 137, 611–622. doi: 10.1104/pp.104.055566
- Oguchi, K., Tanaka, N., Komatsu, S., and Akao, S. (2004). Methylmalonate-semialdehyde dehydrogenase is induced in auxin-stimulated and zinc-stimulated root formation in rice. *Plant Cell Rep.* 22, 848–858. doi: 10.1007/s00299-004-0778-y
- Oliver, D. J. (1994). The glycine decarboxylase complex from plant mitochondria. *Annu. Rev. Plant Physiol. Plant Mol. Biol.* 45, 323–338. doi: 10.1146/annurev.pp.45.060194.001543
- Oliver, D. J., Neuburger, M., Bourguignon, J., and Douce, R. (1990). Interaction between the component enzymes of the glycine decarboxylase multienzyme complex. *Plant Physiol.* 94, 833–839. doi: 10.1104/pp.94.2.833
- Olson, B. J., Skavdahl, M., Ramberg, H., Osterman, J. C., and Markwell, J. (2000). Formate dehydrogenase in *Arabidopsis thaliana*: characterization and possible targeting to the chloroplast. *Plant Sci.* 159, 205–212. doi: 10.1016/S0168-9452(00)00337-X
- Pineau, B., Layoune, O., Danon, A., and Paepe, R., de (2008). L-galactono-1,4-lactone dehydrogenase is required for the accumulation of plant respiratory complex I. *J. Biol. Chem.* 283, 32500–32505. doi: 10.1074/jbc.M805320200
- Poulsen, L. L., and Wedding, R. T. (1970). Purification and properties of the alpha-ketoglutarate dehydrogenase complex of cauliflower mitochondria. *J. Biol. Chem.* 245, 5709–5717.
- Rasmusson, A. G., and Agius, S. C. (2001). Rotenone-insensitive NAD(P)H dehydrogenases in plants: immunodetection and distribution of native proteins in mitochondria. *Plant Physiol. Biochem.* 39, 1057–1066. doi: 10.1016/S0981-9428(01)01334-1
- Rasmusson, A. G., Geisler, D. A., and Møller, I. M. (2008). The multiplicity of dehydrogenases in the electron transport chain of plant mitochondria. *Mitochondrion* 8, 47–60. doi: 10.1016/j.mito.2007.10.004
- Rasmusson, A. G., and Møller, I. M. (2011). “Mitochondrial electron transport and plant stress,” in *Plant Mitochondria*, ed F. Kempken (New York, NY: Springer), 357–381.
- Rasmusson, A. G., Soole, K. L., and Elthon, T. E. (2004). Alternative NAD(P)H dehydrogenases of plant mitochondria. *Annu. Rev. Plant Biol.* 55, 23–39. doi: 10.1146/annurev.arplant.55.031903.141720
- Reinard, T., Janke, V., Willard, J., Buck, F., Jacobsen, H. J., and Vockley, J. (2000). Cloning of a gene for an acyl-CoA dehydrogenase from *Pisum sativum* L. and purification and characterization of its product as an isovaleryl-CoA dehydrogenase. *J. Biol. Chem.* 275, 33738–33743. doi: 10.1074/jbc.M004178200
- Schertl, P., Cabassa, C., Saadallah, K., Bordenave, M., Savouré, A., and Braun, H.P. (in press). Biochemical characterization of ProDH activity in *Arabidopsis* mitochondria. *FEBS J.* doi: 10.1111/febs.12821
- Schertl, P., Sunderhaus, S., Klodmann, J., Grozoff, G. E. G., Bartoli, C. G., and Braun, H.-P. (2012). L-galactono-1,4-lactone dehydrogenase (GLDH) forms part of three subcomplexes of mitochondrial complex I in *Arabidopsis thaliana*. *J. Biol. Chem.* 287, 14412–14419. doi: 10.1074/jbc.M111.305144
- Sharma, S., and Verslues, P. E. (2010). Mechanisms independent of abscisic acid (ABA) or proline feedback have a predominant role in transcriptional regulation of proline metabolism during low water potential and stress recovery. *Plant Cell Environ.* 33, 1838–1851. doi: 10.1111/j.1365-3040.2010.02188.x
- Shen, W., Wei, Y., Dauk, M., Tan, Y., Taylor, D. C., Selvaraj, G., et al. (2006). Involvement of a glycerol-3-phosphate dehydrogenase in modulating the NADH/NAD<sup>+</sup> ratio provides evidence of a mitochondrial glycerol-3-phosphate shuttle in *Arabidopsis*. *Plant Cell* 18, 422–441. doi: 10.1105/tpc.105.039750
- Shen, W., Wei, Y., Dauk, M., Zheng, Z., and Zou, J. (2003). Identification of a mitochondrial glycerol-3-phosphate dehydrogenase from *Arabidopsis thaliana*: evidence for a mitochondrial glycerol-3-phosphate shuttle in plants. *FEBS Lett.* 536, 92–96. doi: 10.1016/S0014-5793(03)00033-4
- Siendones, E., Gonzalez-Reyes, J. A., Santos-Ocana, C., Navas, P., and C rdoba, F. (1999). Biosynthesis of ascorbic acid in kidney bean. L-galactono-gamma-lactone dehydrogenase is an intrinsic protein located at the mitochondrial inner membrane. *Plant Physiol.* 120, 907–912. doi: 10.1104/pp.120.3.907
- Somerville, C. R., and Ogren, W. L. (1982). Mutants of the cruciferous plant *Arabidopsis thaliana* lacking glycine decarboxylase activity. *Biochem. J.* 202, 373–380.
- Srinivasan, R., and Oliver, D. J. (1995). Light-dependent and tissue-specific expression of the H-protein of the glycine decarboxylase complex. *Plant Physiol.* 109, 161–168. doi: 10.1104/pp.109.1.161
- Sweetlove, L. J., Beard, K. F. M., Nunes-Nesi, A., Fernie, A. R., and Ratcliffe, R. G. (2010). Not just a circle: flux modes in the plant TCA cycle. *Trends Plant Sci.* 15, 462–470. doi: 10.1016/j.tplants.2010.05.006

- Szabados, L., and Savouré, A. (2010). Proline: a multifunctional amino acid. *Trends Plant Sci.* 15, 89–97. doi: 10.1016/j.tplants.2009.11.009
- Szurmak, B., Strokovskaya, L., Mooney, B. P., Randall, D. D., and Miernyk, J. A. (2003). Expression and assembly of *Arabidopsis thaliana* pyruvate dehydrogenase in insect cell cytoplasm. *Protein Expr. Purif.* 28, 357–361. doi: 10.1016/S1046-5928(02)00712-X
- Tanaka, N., Takahashi, H., Kitano, H., Matsuoka, M., Akao, S., Uchimiya, H., et al. (2005). Proteome approach to characterize the methylmalonate-semialdehyde dehydrogenase that is regulated by gibberellin. *J. Proteome Res.* 4, 1575–1582. doi: 10.1021/pr050114f
- Tarasenko, V. I., Garnik, E. Y., and Konstantinov, Y. M. (2013). Rate of alternative electron transport in *Arabidopsis* mitochondria affects the expression of the glutamate dehydrogenase gene *gdh2*. *Dokl. Biochem. Biophys.* 452, 234–236. doi: 10.1134/S1607672913050037
- Taylor, N. L., Heazlewood, J. L., Day, D. A., and Millar, A. H. (2004). Lipoic acid-dependent oxidative catabolism of alpha-keto acids in mitochondria provides evidence for branched-chain amino acid catabolism in *Arabidopsis*. *Plant Physiol.* 134, 838–848. doi: 10.1104/pp.103.035675
- Tomaz, T., Bagard, M., Pracharoenwattana, I., Lindén, P., Lee, C. P., Carroll, A. J., et al. (2010). Mitochondrial malate dehydrogenase lowers leaf respiration and alters photorespiration and plant growth in *Arabidopsis*. *Plant Physiol.* 154, 1143–1157. doi: 10.1104/pp.110.161612
- Tovar-Méndez, A., Miernyk, J. A., and Randal, D. D. (2003) Regulation of pyruvate dehydrogenase complex activity in plant cells. *Eur. J. Biochem.* 270, 1043–1049. doi: 10.1046/j.1432-1033.2003.03469.x
- Toyokura, K., Watanabe, K., Oiwaka, A., Kusano, M., Tameshige, T., Tatematsu, K., et al. (2011). Succinic semialdehyde dehydrogenase is involved in the robust patterning of *Arabidopsis* leaves along the adaxial-abaxial axis. *Plant Cell Physiol.* 52, 1340–1353. doi: 10.1093/pcp/pcr079
- Tronconi, M. A., Fahnenstich, H., Gerrard Weehler, M. C., Andreo, C. S., Flügge, U.-I., Drincovich, M. F., et al. (2008). *Arabidopsis* NAD-malic enzyme functions as a homodimer and heterodimer and has a major impact on nocturnal metabolism. *Plant Physiol.* 146, 1540–1552. doi: 10.1104/pp.107.114975
- Tronconi, M. A., Gerrard Wheeler, M. C., Drincovich, M. F., and Andreo, C. S. (2012). Differential fumarate binding to *Arabidopsis* NAD<sup>+</sup>-malic enzymes 1 and -2 produces an opposite activity modulation. *Biochimie* 94, 1421–1430. doi: 10.1016/j.biochi.2012.03.017
- Tronconi, M. A., Maurino, V. G., Andreo, C. S., and Drincovich, M. F. (2010). Three different and tissue-specific NAD-malic enzymes generated by alternative subunit association in *Arabidopsis thaliana*. *J. Biol. Chem.* 285, 11870–11879. doi: 10.1074/jbc.M109.097477
- Turano, F. J., Thakkar, S. S., Fang, T., and Weisemann, J. M. (1997). Characterization and expression of NAD(H)-dependent glutamate dehydrogenase genes in *Arabidopsis*. *Plant Physiol.* 113, 1329–1341. doi: 10.1104/pp.113.4.1329
- Ullrich, A., Knecht, W., Piskur, J., and Löffler, M. (2002). Plant dihydroorotate dehydrogenase differs significantly in substrate specificity and inhibition from the animal enzymes. *FEBS Lett.* 529, 346–350. doi: 10.1016/S0014-5793(02)03425-7
- van Dongen, J. T., Gupta, K. J., Ramirez-Aguilar, S. J., Araújo, W. L., Nunes-Nesi, A., and Fernie, A. R. (2011). Regulation of respiration in plants: a role for alternative metabolic pathways. *J. Plant Physiol.* 168, 1434–1443. doi: 10.1016/j.jplph.2010.11.004
- Verbruggen, N., Hua, X. J., May, M., and van Montagu, M. (1996). Environmental and developmental signals modulate proline homeostasis: evidence for a negative transcriptional regulator. *Proc. Natl. Acad. Sci. U.S.A.* 93, 8787–8791. doi: 10.1073/pnas.93.16.8787
- Wallström, S. V., Florez-Sarasa, I., Araújo, W. L., Aidemark, M., Fernández-Fernández, M., Fernie, A. R., et al. (2014a). Suppression of the external mitochondrial NADPH dehydrogenase, NDB1, in *Arabidopsis thaliana* affects central metabolism and vegetative growth. *Mol. Plant* 7, 356–368. doi: 10.1093/mp/ss115
- Wallström, S. V., Florez-Sarasa, I., Araújo, W. L., Escobar, M. A., Geisler, D. A., Aidemark, M., et al. (2014b). Suppression of NDA-type alternative mitochondrial NAD(P)H dehydrogenases in *Arabidopsis thaliana* modifies growth and metabolism, but not high light stimulation of mitochondrial electron transport. *Plant Cell Physiol.* doi: 10.1093/pcp/pcu021. [Epub ahead of print].
- Wedding, R. T., and Black, M. K. (1971a). Evidence for tighter binding of magnesium-thiamine pyrophosphate to -ketoglutarate dehydrogenase when activated by adenosine monophosphate. *J. Biol. Chem.* 246, 4097–4099.
- Wedding, R. T., and Black, M. K. (1971b). Nucleotide activation of cauliflower alpha-ketoglutarate dehydrogenase. *J. Biol. Chem.* 246, 1638–1643.
- Wienstroer, J., Engqvist, M. K. M., Kunz, H.-H., Flügge, U.-I., and Maurino, V. G. (2012). D-Lactate dehydrogenase as a marker gene allows positive selection of transgenic plants. *FEBS Lett.* 586, 36–40. doi: 10.1016/j.febslet.2011.11.020
- Wulff, A., Oliveira, H. C., Saviani, E. E., and Salgado, I. (2009) Nitrite reduction and superoxide-dependent nitric oxide degradation by *Arabidopsis* mitochondria: influence of external NAD(P)H dehydrogenases and alternative oxidase in the control of nitric oxide levels. *Nitric Oxide* 21, 132–139. doi: 10.1016/j.niox.2009.06.003
- Yamaya, T., Oaks, A., and Matsumoto, H. (1984). Characteristics of glutamate dehydrogenase in mitochondria prepared from corn shoots. *Plant Physiol.* 76, 1009–1013. doi: 10.1104/pp.76.4.1009
- Yu, H., Du, X., Zhang, F., Zhang, F., Hu, Y., Liu, S., et al. (2012). A mutation in the E2 subunit of the mitochondrial pyruvate dehydrogenase complex in *Arabidopsis* reduces plant organ size and enhances the accumulation of amino acids and intermediate products of the TCA cycle. *Planta* 236, 387–399. doi: 10.1007/s00425-012-1620-3
- Zabaleta, E., Martin, M. V., and Braun, H.-P. (2012). A basal carbon concentrating mechanism in plants? *Plant Sci.* 187, 97–104. doi: 10.1016/j.plantsci.2012.02.001
- Zhu, X., Tang, G., and Galili, G. (2000) Characterization of the two saccharopine dehydrogenase isozymes of lysine catabolism encoded by the single composite AtLKR=SDH locus of *Arabidopsis*. *Plant Physiol.* 124, 1363–1372. doi: 10.1104/pp.124.3.1363
- Zou, J., Qi, Q., Katavic, V., Marillia, E. F., and Taylor, D. C. (1999). Effects of antisense repression of an *Arabidopsis thaliana* pyruvate dehydrogenase kinase cDNA on plant development. *Plant Mol. Biol.* 41, 837–849. doi: 10.1023/A:1006393726018

**Conflict of Interest Statement:** The authors declare that the research was conducted in the absence of any commercial or financial relationships that could be construed as a potential conflict of interest.

Received: 28 February 2014; accepted: 07 April 2014; published online: 29 April 2014.  
Citation: Schertl P and Braun H-P (2014) Respiratory electron transfer pathways in plant mitochondria. *Front. Plant Sci.* 5:163. doi: 10.3389/fpls.2014.00163

This article was submitted to *Plant Physiology*, a section of the journal *Frontiers in Plant Science*.

Copyright © 2014 Schertl and Braun. This is an open-access article distributed under the terms of the Creative Commons Attribution License (CC BY). The use, distribution or reproduction in other forums is permitted, provided the original author(s) or licensor are credited and that the original publication in this journal is cited, in accordance with accepted academic practice. No use, distribution or reproduction is permitted which does not comply with these terms.

## Publication II

### ***2.2 Biochemical characterization of proline dehydrogenase in Arabidopsis mitochondria***

Peter Schertl<sup>1</sup>, Cécile Cabassa<sup>2</sup>, Kaouthar Saadallah<sup>2</sup>, Marianne Bordenave<sup>2</sup>, Arnould Savouré<sup>2</sup> and Hans-Peter Braun<sup>1</sup>

<sup>1</sup> Institute of Plant Genetics, Plant Proteomics, Leibniz University Hannover, Germany

<sup>2</sup> Université Pierre & Marie Curie (UPMC), Université Paris 6, France

Type of authorship:	first author
Type of article:	research article
Share of the work:	85 %
Contribution to the publication:	planned and performed all experiments, analyzed data, prepared all figures and wrote the paper
Journal:	FEBS Journal
Impact Factor:	3,986
Date of publication:	published in April 2014
Number of citations (9 <sup>th</sup> of October 2014)	1
DOI:	10.1111/febs.12821
PubMed-ID:	24751239

## Biochemical characterization of proline dehydrogenase in *Arabidopsis* mitochondria

Peter Schertl<sup>1</sup>, Cécile Cabassa<sup>2</sup>, Kaouthar Saadallah<sup>2</sup>, Marianne Bordenave<sup>2</sup>, Arnould Savouré<sup>2</sup> and Hans-Peter Braun<sup>1</sup>

<sup>1</sup> Institute of Plant Genetics, Plant Proteomics, Leibniz University Hannover, Germany

<sup>2</sup> Université Pierre & Marie Curie (UPMC), Université Paris 6, France

### Keywords

At3g30775; dehydrogenase; enzyme inhibitor; mitochondria; plant; proline; proline dehydrogenase (ProDH); stress response

### Correspondence

H.-P. Braun, Institute of Plant Genetics, Plant Proteomics, Leibniz University Hannover, Herrenhäuser Str. 2, 30419 Hannover, Germany  
 Fax: +49 511 7623608  
 Tel: +49 511 7622674  
 E-mail: braun@genetik.uni-hannover.de  
 A. Savouré, Université Pierre & Marie Curie (UPMC), Université Paris 6, URF5 APCE, Case 156, 4 place Jussieu, 75252 Paris cedex 05, France  
 Fax: +33 (0)144 276151  
 Tel: +33 (0)144 272672  
 E-mail: arnould.savoure@upmc.fr

(Received 21 January 2014, revised 14 March 2014, accepted 11 April 2014)

doi:10.1111/febs.12821

Proline has multiple functions in plants. Besides being a building block for protein biosynthesis proline plays a central role in the plant stress response and in further cellular processes. Here, we report an analysis on the integration of proline dehydrogenase (ProDH) into mitochondrial metabolism in *Arabidopsis thaliana*. An experimental system to induce ProDH activity was established using cell cultures. Induction of ProDH was measured by novel photometric activity assays and by a ProDH *in gel* activity assay. Effects of increased ProDH activity on other mitochondrial enzymes were systematically investigated. Activities of the protein complexes of the respiratory chain were not significantly altered. In contrast, some mitochondrial dehydrogenases had markedly changed activities. Activity of glutamate dehydrogenase substantially increased, indicating upregulation of the entire proline catabolic pathway, which was confirmed by co-expression analyses of the corresponding genes. Furthermore, activity of D-lactate dehydrogenase was increased. D-lactate was identified to be a competitive inhibitor of ProDH in plants. We suggest that induction of D-lactate dehydrogenase activity allows rapid upregulation of ProDH activity during the short-term stress response in plants.

## Introduction

In plants the amino acid proline is not only used to build up proteins. Rather, it is involved in several additional cellular processes. It is well known that plants accumulate proline under different environmental stress conditions [1–4]. These stress conditions can be both biotic and abiotic. For example, biosynthesis of proline is highly upregulated during drought stress and high salt [5–7]. Increased proline concentration

was also observed in response to heavy metals [8] and plant pathogens [9]. Under these conditions, proline does not only act as an osmolyte adjusting the osmolality of a cell. Besides, it can directly act as a chaperone enhancing protein stability and integrity [10]. Proline can also buffer the cytosolic pH and influence the cell redox status [11]. Furthermore, it has been suggested that proline metabolism acts as an electron

### Abbreviations

CN PAGE, clear native PAGE; DCIP, 2,6-dichloroindophenol; DLDH, D-lactate dehydrogenase; GluDH, glutamate dehydrogenase; MG, methylglyoxal; OXPHOS, oxidative phosphorylation; P5C, pyrroline-5-carboxylate; P5CDH, P5C dehydrogenase; ProDH, proline dehydrogenase.



shuttle between chloroplasts and mitochondria, thereby influencing the redox state of these organelles [12].

The biosynthesis of proline takes place in the cytosol and most probably also in chloroplasts [3]. In plants, the starting compound of proline biosynthesis is glutamate. In contrast to its biosynthesis, proline breakdown takes place in mitochondria [13]. Proline dehydrogenase (ProDH), a mitochondrial flavoenzyme, is especially induced upon stress release conditions [13]. ProDH converts proline to pyrroline-5-carboxylate (P5C). Electrons from proline are transferred directly or indirectly to ubiquinone. As a next step, P5C dehydrogenase (P5CDH) catalyzes the oxidation of P5C to glutamate, which involves formation of glutamic semialdehyde as a reaction intermediate. P5CDH uses either  $\text{NAD}^+$  or  $\text{NADP}^+$  as an electron acceptor [14]. Glutamate can be exported from mitochondria or converted within mitochondria to  $\alpha$ -ketoglutarate catalyzed by glutamate dehydrogenase (GluDH). Finally,  $\alpha$ -ketoglutarate can be introduced into the citric acid cycle.

Mitochondrial localization of ProDH has been revealed by several investigations. Boggess and Koeppe [15] demonstrated that isolated mitochondria from different plant species efficiently oxidize proline. In a later study, Elthon and Stewart [16] showed that proline oxidation is catalyzed by an enzyme associated with the inner mitochondrial membrane in *Zea mays*. Furthermore, mitochondrial localization of ProDH from *Arabidopsis* was proved by immunoblotting [17,18]. In *Arabidopsis*, ProDH occurs in two closely related isoforms termed ProDH1 (At3g30775) and ProDH2 (At3g38710). ProDH1 was reported to be the predominantly expressed isoform under most conditions and in most tissues [19].

The regulation of proline metabolism in plants is not fully understood. Accumulation of proline is believed to depend on simultaneous increase in proline biosynthesis and decrease in proline degradation. Dehydration, low water potential and salinity downregulate the genes encoding ProDH [11,17,19–21]. In contrast, stress release conditions induce expression of ProDH [11,20,22–24]. Additionally it has been shown that exogenously added proline induces ProDH expression [17,20].

Here we report an investigation on the integration of ProDH into mitochondrial metabolism in plants. An experimental system to substantially induce ProDH was established by external addition of proline to an *Arabidopsis thaliana* cell culture. Increase of enzyme activity in mitochondrial fractions was monitored by newly developed photometric ProDH activity assays

and by a ProDH *in gel* activity assay. Next, effects of increased proline catabolism on other mitochondrial enzymes were systematically characterized. Activities of the protein complexes of the respiratory chain were largely unchanged. In contrast, some mitochondrial dehydrogenases had markedly changed activities. Increase of GluDH indicates upregulation of the entire proline catabolic pathway. Also D-lactate dehydrogenase activity was upregulated in proline-treated cells. D-lactate was identified to represent a competitive inhibitor of ProDH which is assumed to play an important role during the rapid stress response of plants.

## Results

### Induction of ProDH

Plant mitochondria have been extensively characterized by proteome analyses (reviewed in [25]). Based on these investigations, more than 800 distinct proteins could be assigned to this subcellular compartment in *Arabidopsis* (for detailed information see the subcellular localization database for *Arabidopsis* proteins, SUBA (<http://suba.plantenergy.uwa.edu.au/>) [26]). However, in none of these studies was ProDH identified. We conclude that ProDH is of very low abundance if plants are cultivated under standard conditions. It has been shown previously that ProDH activity is much induced during stress release conditions or direct proline treatment [17]. We decided to establish a cell culture based system to investigate ProDH in *Arabidopsis* under defined conditions. *Arabidopsis* cell cultures were shown to be an ideal starting material for mitochondrial preparations [27]. For ProDH induction, the cell culture was treated with 50 mM L-proline for 21 h. Mitochondria were isolated in parallel from treated and non-treated cells (Fig. S1).

### Measurement of ProDH activity in mitochondrial fractions

ProDH activity of mitochondrial fractions was measured using an established assay which is based on the proline-dependent reduction of the artificial electron acceptor 2,6-dichloroindophenol (DCIP) at 600 nm [28]. Induction of ProDH activity was 6-fold in proline-treated versus non-treated *Arabidopsis* cells (Fig. 1A). To confirm these results, two novel photometric ProDH assays were established that use cytochrome *c* or decylubiquinone as electron acceptors. Both methods revealed 4- to 5-fold induction of ProDH in proline-treated versus non-treated

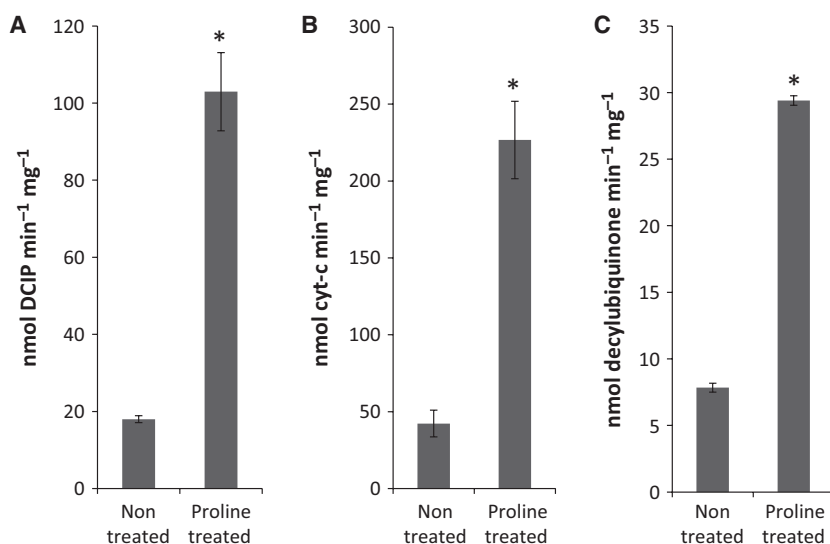


**Fig. 1.** Activity of ProDH as determined by three different photometrical methods. The activity of mitochondrial ProDH was measured in mitochondria isolated from cells which were treated with 50 mM L-proline for 21 h (proline treated) or from non-treated cells. Methods of determining the ProDH activity are based on different electron acceptors: (A) DCIP; (B) cytochrome c; (C) decylubiquinone. Standard errors are based on three biological replicates. \*Significantly different ( $P < 0.05$ ) between proline-treated and non-treated fractions.

Arabidopsis cells (Fig. 1B,C). Finally, a DCIP-based *in gel* assay was developed to monitor ProDH activity. For this approach, proteins of mitochondrial fractions from proline-treated and non-treated cells were separated by clear native (CN) PAGE. Upon *in gel* ProDH activity staining a white diffuse band becomes visible in the proline-treated but not in the control fraction (Fig. 2). DCIP is blue in the oxidized state but becomes colorless upon reduction. The position of the band nicely corresponds to a ProDH signal on a parallel immunoblot which was developed using an antibody directed against Arabidopsis ProDH1 [5]. Subsequent Coomassie staining of the activity-stained gels did not reveal any visible differences between the proline-treated and non-treated fractions with respect to protein complexes.

#### Immunological identification of ProDH in mitochondrial fractions

Increase in ProDH activity could be caused by enzyme activation and/or *de novo* synthesis of ProDH. An immunoblotting experiment was carried out to investigate this issue. Mitochondrial fractions from proline-treated and non-treated cells were separated by SDS/PAGE, blotted onto nitrocellulose and probed using the antibody directed against Arabidopsis ProDH (Fig. 3). Immunopositive bands at about 55 and 57 kDa become visible in the proline-treated fraction. Only after much longer exposure times were these bands also detectable in the control fraction (Fig. S2). This result is in accordance with the native immunoblot shown in Fig. 2B. Furthermore, proline treatment also induces ProDH *in planta* (Fig. S2).

#### Activities of the respiratory chain complexes in proline-treated Arabidopsis cells

Like several other amino acids, proline represents a substrate for the respiratory chain [15]. In consequence, cultivation of Arabidopsis in the presence of proline could cause a decrease or increase in one or the other activity of complex I–IV of the respiratory chain. This hypothesis was tested for mitochondrial fractions of proline-treated and non-treated cells. Activities of all four complexes did not differ significantly (Fig. 4). At the same time, occurrence of the mitochondrial protein complexes was unchanged in proline-treated and non-treated cells as revealed by CN PAGE (Fig. 2). We conclude that the oxidative phosphorylation (OXPHOS) system does not adapt structurally or physiologically in response to proline treatment. This is in line with previous findings that the OXPHOS system of plant mitochondria is expressed constitutively rather than dynamically adapted in response to changing external factors [29].

#### Activities of other dehydrogenases in proline-treated Arabidopsis cells

Mitochondria include numerous other dehydrogenases which are involved in the citric acid cycle, amino acid catabolism and other processes. Some dehydrogenases are highly induced upon stress [30]. We tested the activities of various dehydrogenases in mitochondrial fractions of proline-treated and non-treated cells. Most dehydrogenases displayed unchanged activities. However, two dehydrogenases clearly had increased activities in proline-treated Arabidopsis cells: GluDH and

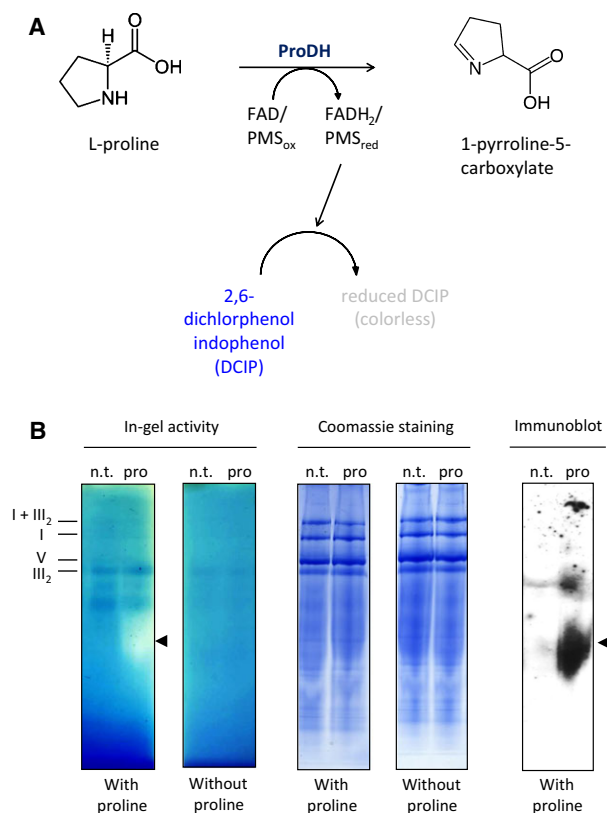


**Fig. 2.** ProDH *in gel* activity assay. (A) Reaction scheme (PMS, phenazinemetosulfate). (B) *In gel* assay. Mitochondria were solubilized by 2.5% digitonin and subsequently separated by one-dimensional CN PAGE. *In gel* ProDH activity was measured directly after completion of the electrophoretic run (left). The identical gel was Coomassie stained afterwards (right). pro, mitochondrial protein from cells which were treated with 50 mM proline for 21 h; n.t., mitochondrial protein from non-treated cells. Identities of protein complexes of the respiratory chain are given on the left. The immunoblot (right) was developed with polyclonal IgG directed against *Arabidopsis* ProDH1.

D-lactate dehydrogenase (DLDH). GluDH activity was increased by 30%, while DLDH activity even went up by 40% (Fig. 5). Since glutamate is generated by the proline degradation pathway in mitochondria, increase in GluDH activity was expected. However, it was not clear why DLDH activity is increased in proline-treated cells.

### L- and D-lactate are competitive inhibitors of ProDH in plants

A review of the literature on ProDH revealed a study reporting that lactate was identified as an inhibitor of ProDH in mammalian mitochondria [31]. Similar results were found in bacteria [32]. We therefore

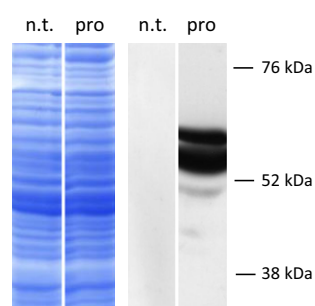


**Fig. 3.** Identification of ProDH by immunoblotting. Mitochondrial protein isolated from non-treated (n.t.) and proline-treated (pro) *Arabidopsis* cells was separated by SDS/PAGE and either Coomassie stained (left) or blotted onto nitrocellulose membranes (right). The blots were developed using polyclonal IgG directed against *Arabidopsis* ProDH1. Masses of standard proteins are given to the right of the blots.

directly tested the effect of D-lactate on ProDH activity in proline-treated *Arabidopsis* cells (Fig. 6B). In the absence of D-lactate, the  $K_m$  value of ProDH was 31 mM and  $V_{max}$  was approximately 120 nmol DCIP  $\text{min}^{-1} \cdot \text{mg}^{-1}$  (measured at pH 7.5). The comparatively high  $K_m$  value indicates that ProDH is active when proline concentrations are high. In the presence of 1 mM D-lactate,  $V_{max}$  is not altered but  $K_m$  is increased to 95 mM. Hence, D-lactate represents a competitive inhibitor of ProDH in plants. The inhibitory effect of D-lactate depends on its concentration. Besides D-lactate, also L-lactate inhibits *A. thaliana* ProDH (data not shown).

### Discussion and conclusions

In plants, proline is a multifunctional amino acid which, besides its role for protein biosynthesis, plays a central role in the plant stress response. Nevertheless, proline catabolism, which takes place in mitochondria, is not quite understood. An experimental system was established for *A. thaliana* to investigate ProDH, the first enzyme of the proline degradation pathway. Three different photometric assays clearly revealed strong induction of ProDH activity upon treatment of *Arabidopsis* cells by 50 mM proline for 21 h (Fig. 1). Two of these assays are newly developed and either use cytochrome *c* or decylubiquinone as electron acceptors. In comparison to the DCIP assay [28], absolute ProDH activities obtained by the cytochrome *c* based assay were twice as high (227 versus 103 nmol reduced electron acceptor per minute and milligram protein in mitochondrial fractions of proline-treated cells, and 42 versus 18 nmol reduced electron acceptor per minute and milligram protein in mitochondrial fractions of

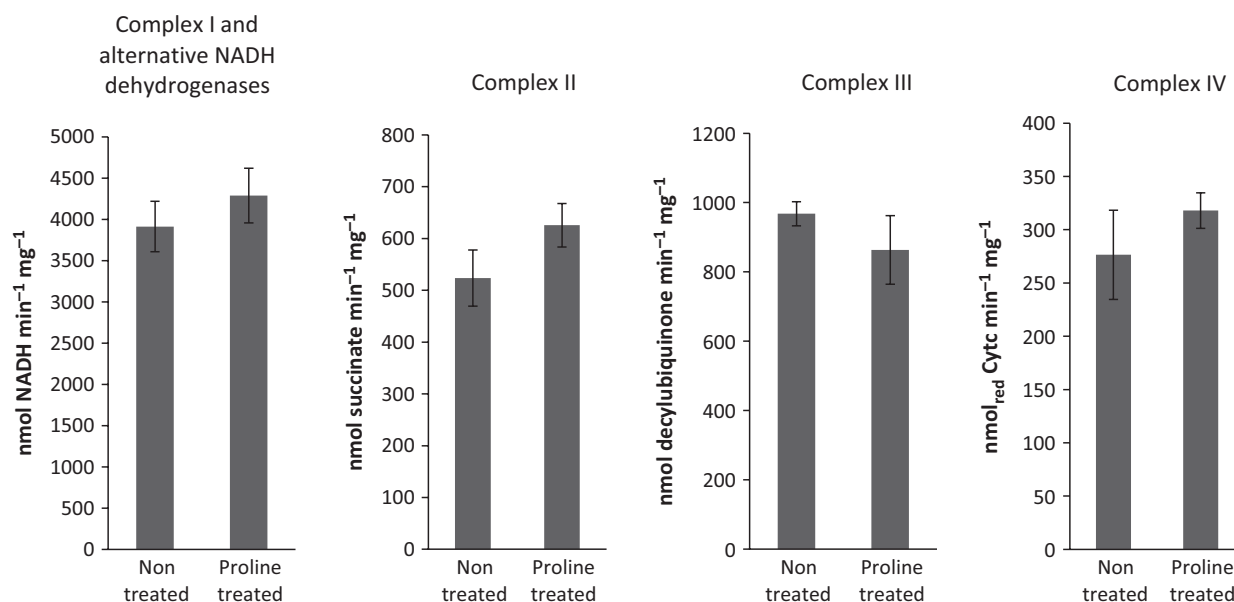


**Fig. 4.** Activity of the oxidoreductase complexes of the respiratory chain in proline-treated and non-treated cells. Assays were carried out as described in Materials and methods using mitochondrial fractions. Standard errors are based on three biological replicates.

non-treated cells). This result reflects that DCIP can accept two electrons while cytochrome *c* only accepts one electron. The cytochrome *c* based ProDH activity assay should be useful for future ProDH research but is only applicable in mitochondrial fractions because

cytochrome *c* does not represent a direct electron acceptor of ProDH (reduction of cytochrome *c* depends on the presence of additional components, e.g. complex III). In contrast, the novel decylubiquinone based activity assay should also work with purified recombinant ProDH. However, absolute ProDH activity is lower compared with the other two photometric assays, which most probably reflects that decylubiquinone is a ubiquinone analog and not the naturally occurring ProDH electron acceptor.

Furthermore, a DCIP-based *in gel* ProDH activity assay was developed (Fig. 2). DCIP reduction causes a shift in color from blue to colorless. Therefore, ProDH separated in a native gel becomes visible by whitish bands on a blue background in the presence of proline. A good separation of mitochondrial proteins under native conditions is achievable by blue native (BN) PAGE [33]. However, the blue background of this PAGE system interferes with the DCIP-based *in gel* assay. We therefore used CN PAGE [34] for the ProDH assay. The ProDH band is somehow diffuse which has been reported before for other membrane proteins separated by CN PAGE [35]. Unfortunately, CN PAGE does not allow determination of native molecular mass information because migration of proteins in the gel partly depends on intrinsic charges. The novel ProDH *in gel* assay confirms a strong induction of ProDH in mitochondria isolated from proline-treated *Arabidopsis* cells. The *in gel* assay

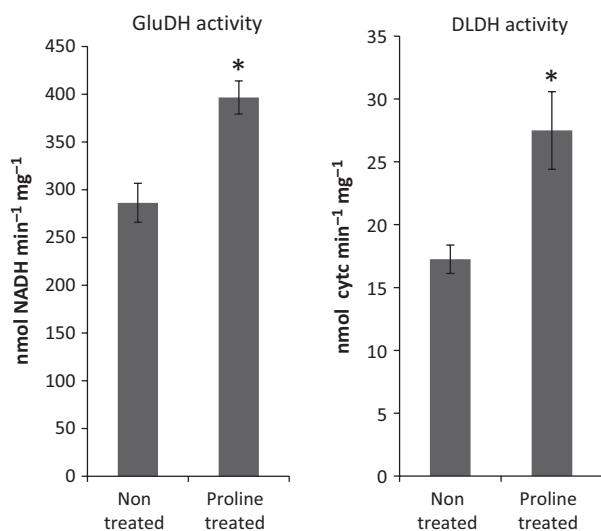


**Fig. 5.** Activity of glutamate dehydrogenase (GluDH) and D-lactate dehydrogenase (DLDH) in mitochondrial fractions isolated from non-treated and L-proline-treated cells. Standard errors are based on three biological replicates. \*Significantly different ( $P < 0.05$ ) between proline-treated and non-treated fractions.

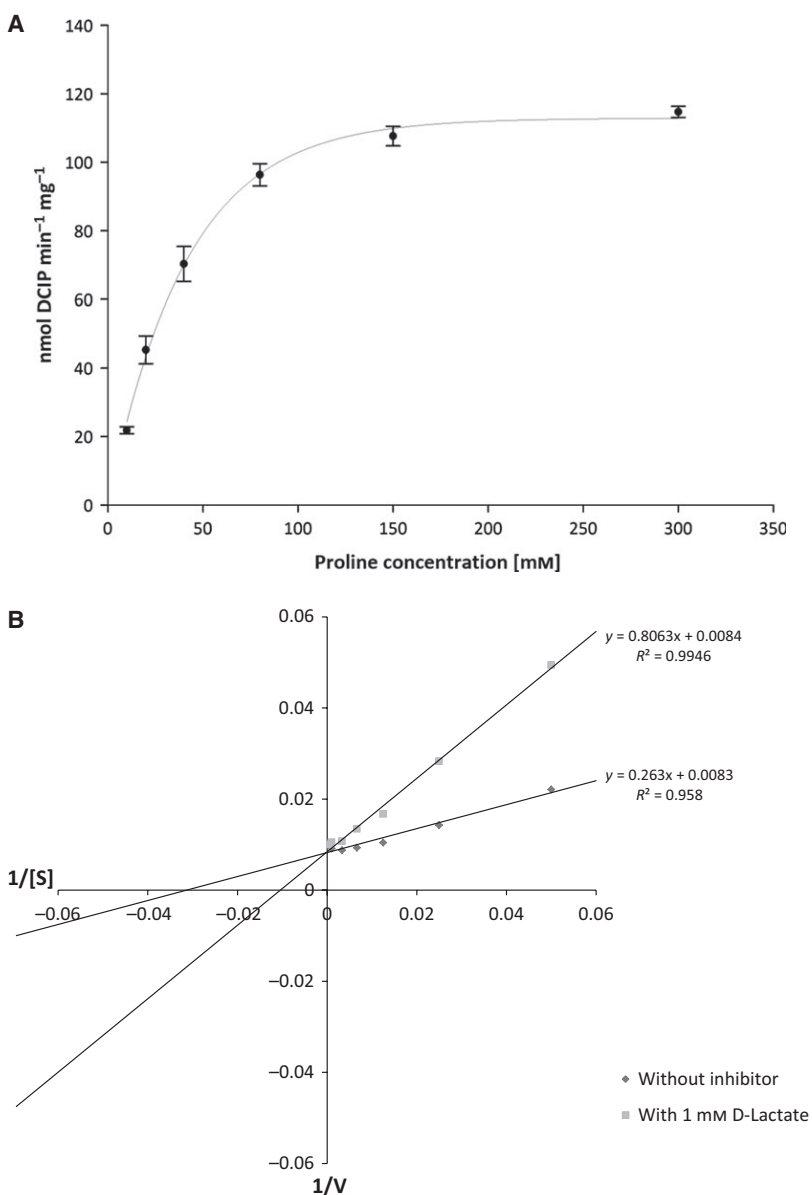


**Fig. 6.** Kinetic properties of ProDH from *Arabidopsis*. (A) ProDH activity in the presence of varying substrate concentrations in mitochondrial fractions of L-proline-treated *Arabidopsis* cells. Standard errors are based on three technical replicates. (B) Lineweaver–Burke double reciprocal plot of ProDH activity measured in the presence/absence of 1 mM D-lactate.

$V_{\max}$  and  $K_m$  values for ProDH without inhibitor and in the presence of 1 mM D-lactate:

$V_{\max}$ (without inhibitor)	$V_{\max}$ (in the presence of 1 mM D-lactate)	$K_m$ (without inhibitor)	$K_m$ (in the presence of 1 mM D-lactate)
120.48 nmol DCIP min <sup>-1</sup> mg <sup>-1</sup>	119.04 nmol DCIP min <sup>-1</sup> mg <sup>-1</sup>	31.69 mM	95.69 mM

should be useful to monitor ProDH activity in total protein fractions from plants cultivated under various stress conditions.

Increase of ProDH activity in mitochondria of proline-treated *Arabidopsis* cells is well correlated to induction of ProDH synthesis in *Arabidopsis* as shown by immunoblotting (Figs 2 and 3). Upon separation by SDS/PAGE, ProDH bands are visible at 55 kDa

and 57 kDa, which closely correspond to the calculated molecular mass of ProDH1 and ProDH2 (55 and 53 kDa). Gene expression data indicated that *ProDH1* is much more expressed in *Arabidopsis* than *ProDH2*, especially in response to exogenously applied proline [19]. We speculate that the main band on our immunoblot (55 kDa) represents ProDH1. The 57 kDa band might represent a post-translationally modified version

of ProDH1 or ProDH2. The molecular biology of ProDH1 and ProDH2 of *Arabidopsis* should be further investigated.

*Arabidopsis* cells containing strongly induced ProDH levels were next used to investigate the integration of ProDH into mitochondrial metabolism in plants. Proline catabolism is linked to the generation of reducing equivalents at two points. First, ProDH, via its flavin group, can probably directly transfer electrons on ubiquinone. Second, conversion of P5C into glutamate by P5CDH is linked to reduction of NAD<sup>+</sup> or NADP<sup>+</sup>. As a consequence, cultivation of plants in the presence of excess proline could cause changes with respect to the activities of the oxidoreductases of the respiratory chain. However, photometric activity assays for complexes I–IV did not reveal any differences between proline-treated and non-treated cells (Fig. 4). We conclude that the OXPHOS complexes are not individually regulated in response to high proline concentrations under the conditions tested.

In contrast, the activities of two mitochondrial dehydrogenases are clearly enhanced if cells are cultivated in the presence of proline: GluDH and DLDH (Fig. 5). GluDH is part of the proline catabolic pathway because glutamate is generated from P5C, the product formed by ProDH. Induction of GluDH by cultivation of cells at high proline concentration indicates that the entire catabolic pathway is upregulated. Induction of GluDH activity by proline furthermore indicates that glutamate formed from proline degradation is at least partially converted into  $\alpha$ -ketoglutarate

within mitochondria and most likely further oxidized by reactions of the citric acid cycle. At the same time part of the glutamate and/or  $\alpha$ -ketoglutarate might be exported from the mitochondria into the cytoplasm to become part of other metabolic pathways, e.g. nitrogen fixation. Co-expression analyses indeed confirm that regulation of ProDH and GluDH synthesis are closely connected (Figs S3 and S4; Tables S1 and S2). Figure 7 summarizes the current knowledge on the integration of ProDH into mitochondrial metabolism in plants.

Interestingly, DLDH activity is induced in proline-treated *Arabidopsis* cells. D-lactate is mainly formed from methylglyoxal (MG), which is a non-enzymatic by-product of glycolysis. Conversion of MG into D-lactate is carried out by the glyoxylase system [36]. D-lactate can be transported into mitochondria by a D-lactate/H<sup>+</sup> symporter or a D-lactate/malate antiporter [36,37]. Alternatively, upstream intermediates of the MG side-way of glycolysis are transported into mitochondria and D-lactate is produced in the matrix. In *Arabidopsis*, D-lactate is a competitive inhibitor of ProDH (Fig. 6).

It has been previously reported that D-lactate represents an inhibitor of ProDH in mammalian mitochondria [31]. The D-lactate concentration reflects the metabolic flux through glycolysis and might function as a signal. In addition, experimental evidence points to an upregulation of the MG-initiated side branch of glycolysis during stress [38]. Within mitochondria, D-lactate mediated inactivation of ProDH could prevent

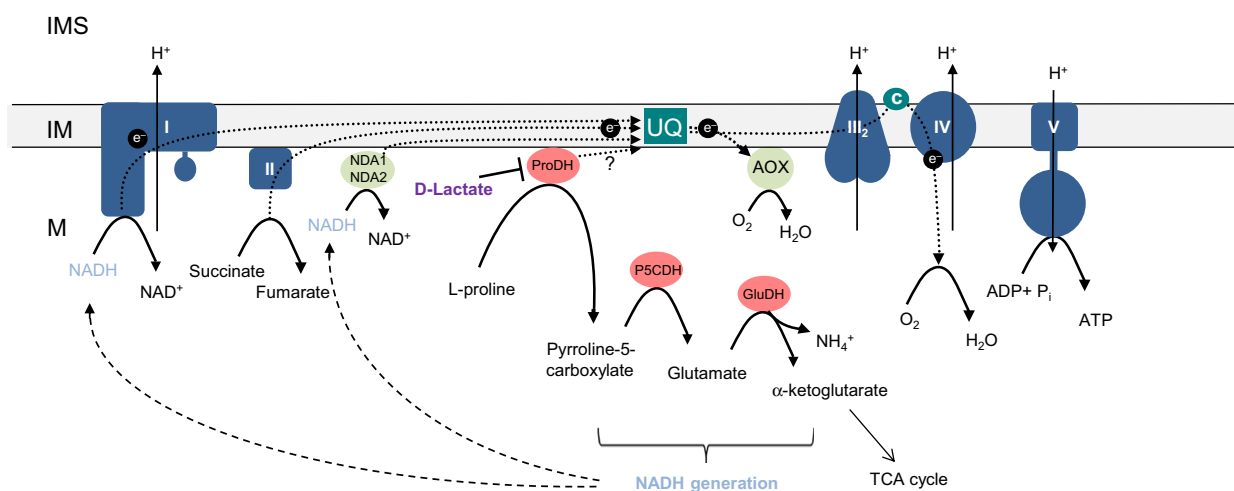


**Fig. 7.** Integration of proline dehydrogenase into mitochondrial metabolism in plants: blue, enzymes of the respiratory chain are indicated with numbers; red, enzymes involved in proline catabolism (ProDH, proline dehydrogenase; P5CDH, pyrroline-5-carboxylate dehydrogenase; GluDH, glutamate dehydrogenase); green, electron carriers (UQ, ubiquinone/ubiquinol; c, cytochrome c); light green, alternative respiratory enzymes (NDA1 and NDA2, alternative NADH dehydrogenases; AOX, alternative oxidase).

usage of this amino acid as a substrate for OXPHOS under high carbohydrate conditions. In plants, D-lactate might additionally have a role for regulating proline metabolism during the stress response. We speculate that D-lactate is involved in a rapid mechanism for regulating ProDH activity during changing salt stress. Upon release of salt stress, ProDH becomes induced for increase of proline breakdown. If salt stress increases again, ProDH activity should become inhibited for proline re-increase. Increase of DLDH activity in proline-treated *Arabidopsis* cells may contribute to rapidly reduce inactivation of ProDH in plants. Most intriguingly, proline was reported to stabilize the structural integrity of a rabbit muscle M4 lactate dehydrogenase, thereby protecting its activity [39]. In summary, observations made in different experimental systems indicate that lactate and proline are embedded into reciprocal regulatory mechanisms which might be of special importance during the plant stress response.

## Materials and methods

### Cultivation of *A. thaliana* suspension culture cells

All experiments were carried out using a suspension cell culture of *A. thaliana* (var. Columbia-0). Conditions for establishing and maintaining the cell culture were taken from [40]. In short, cells were cultivated at 24–26 °C under continuous shaking at 90 rpm. The medium was changed once a week and contained the following ingredients: 3% (w/v) sucrose, 0.0001% (w/v) 2,4-dichlorophenoxyacetic acid, 0.00001% (w/v) kinetin, 0.316% (w/v) B5 medium, pH 5.7 adjusted with KOH. In order to induce ProDH, cells were treated with 50 mM L-proline. The time of L-proline treatment was set at 21 h in accordance with the literature (proline-induced expression of the ProDH gene has been reported to reach a maximum between 10 and 24 h [17]).

### Isolation of mitochondria

Isolation of mitochondria was carried out according to [41]. Organelles were extracted using a buffer containing 450 mM sucrose, 15 mM 3-(*N*-morpholino) propanesulfonic acid (MOPS), 1.5 mM EGTA, 0.6% (w/v) polyvinylpyrrolidone (PVP40), 0.2% bovine serum albumin, 0.2 mM phenylmethylsulfonyl fluoride (PMSF), pH 7.4 (KOH). After cell disruption in a Waring blender 14.3 mM  $\beta$ -mercaptoethanol was added. To remove cell debris the suspension was centrifuged twice for 5 min at 2700 g and once for 10 min at 8300 g. Afterwards mitochondria were sedimented at 17 000 g for 10 min. The mitochondria pellet was

resuspended in 3–5 mL washing buffer containing 300 mM sucrose, 10 mM MOPS, 1 mM EGTA and 0.2 mM PMSF.

The pH was adjusted with KOH to 7.2. Subsequently the suspension was homogenized using a potter (two strokes). Next, the mitochondria suspension was transferred on Percoll gradients and centrifuged for 45 min at 70 000 g using an ultracentrifuge. The Percoll gradients consisted of 40%, 23% and 18% Percoll in 0.3 M sucrose and 10 mM MOPS, pH 7.2 (KOH). After centrifugation mitochondria are localized at the 23%/40% interphase. Collected mitochondria were washed two to three times with resuspension buffer (400 mM mannitol, 10 mM Tricine, 1 mM EGTA and 0.2 mM PMSF, pH 7.2 with KOH) at 14 300 g for 10 min.

### SDS and CN PAGE

One-dimensional SDS/PAGE was carried out according to [42]. One-dimensional CN PAGE was carried out using pre-cast 4–16% Bis-Tris Native Gels (Life Technologies GmbH, Darmstadt, Germany). Before gel loading, mitochondria were solubilized with 2.5% digitonin in 50 mM Tris/HCl pH 7.2. After incubation for 10 min insoluble material was sedimented at 21 700 g for another 10 min. Samples were mixed with native loading buffer (62.5 mM Tris/HCl pH 6.8, 10% (w/v) glycerol, 0.00125 (w/v) bromophenol blue). Running conditions for CN gels were 3.5 h at 375 V and 4 °C using an XCell SureLock Mini-Electrophoresis System (Life Technologies GmbH). The running buffer contained 25 mM Tris and 19.2 mM glycine.

### In gel ProDH activity assay

After completion of the electrophoresis run, the gel was incubated for 10 min with 1.2 mM DCIP in 50 mM Tris/HCl pH 7.2 while gently shaking. After this incubation step the DCIP solution was discarded and the gel was incubated with ProDH activity staining solution (50 mM Tris/HCl pH 7.15, 5 mM MgCl<sub>2</sub>, 0.25 mM flavin adenine dinucleotide, 0.5 mM phenazinemethosulfate, 100 mM L-proline) without shaking for 1.5 h in the dark.

### Immunoblotting

Proteins separated in polyacrylamide gels were blotted on nitrocellulose membranes using the Trans-Blot SD Semi-Dry Transfer Cell (Bio-Rad, Hercules, CA, USA). The transfer of proteins was carried out at 400 mA, maximum 23 V, for 90 min using transfer buffer (25 mM Tris, 192 mM glycine, 20% v/v methanol). Equal protein loading and integrity of protein samples were checked by Ponceau S red staining of the blot membrane. Immunostaining was carried out by incubating the nitrocellulose membrane in NaCl/Tris/Tween with 5% nonfat dry milk and 0.05% (v/

v) Tween 20 for 1 h at room temperature and then in NaCl/Tris/Tween with 1 : 1000 ProDH antibody for 2 h at room temperature. The antibody raised against ProDH was obtained by rabbit immunization with AtProDH1 (amino acids 1–522) as described earlier [5]. Subsequently the membrane was incubated for 1 h with a 1 : 5000 diluted secondary antibody directly coupled to the horseradish peroxidase. ProDH was detected using the ECL prime chemiluminescence detection kit from GE Healthcare (Munich, Germany).

### Enzyme activity measurements

Enzyme assays were carried out at 25 °C using an Epoch Microplate Spectrophotometer (Biotek, Winooski, VT, USA). All activity assays were carried out in a total volume of 300 µL. Kinetic values were corrected by values obtained in parallel control experiments (assays without substrate or added protein). Protein quantification was carried out using Pierce™ Coomassie (Bradford) Protein Assay (Thermo Scientific, Bonn, Germany). All measurements were carried out with mitochondria which were frozen before (membranes are permeable). ProDH was measured using three different photometric methods. In method A, the DCIP method [28], ProDH was measured in a reaction mixture containing 250 mM Tris/HCl, pH 7.5, 5 mM MgCl<sub>2</sub>, 1 mM KCN, 0.06 mM DCIP, 0.25 mM flavin adenine dinucleotide, 0.5 mM phenazinmethosulfate, 2 µg of whole mitochondrial protein. The reaction was initiated with 100 mM L-proline. The reduction of DCIP was monitored at 600 nm ( $E = 19.1 \text{ mm}^{-1}\cdot\text{cm}^{-1}$ ). Method B, the Cyt-C method, used 250 mM Tris/HCl, pH 8.4, 60 µM cytochrome *c*, 1 mM KCN and 2 µg of whole mitochondrial protein. The reaction was initiated with 100 mM L-proline. The reduction of cytochrome *c* was monitored at 550 nm ( $E = 19 \text{ mm}^{-1}\cdot\text{cm}^{-1}$ ). Method C, the decylubiquinone method, used 250 mM Tris/HCl, pH 8.4, 1 mM KCN, 100 µM decylubiquinone and 25 µg of whole mitochondrial protein. The reaction was initiated with 100 mM L-proline. Reduction of decylubiquinone was monitored at 275 nm ( $E = 15 \text{ mm}^{-1}\cdot\text{cm}^{-1}$ ).

GluDH activity was determined following the reduction of NAD<sup>+</sup> at 340 nm. The reaction mixture contained 50 mM Tris/HCl, pH 8.4, 2 mM NAD<sup>+</sup> and 2.5 µg of soluble mitochondrial proteins. To separate most of the membrane bound proteins from soluble proteins mitochondria underwent a thaw–freeze cycle twice. Afterwards, membrane bound proteins were sedimented at 25 000 *g*. The reaction was started with the addition of 30 mM glutamate.

D-lactate dehydrogenase activity was determined by monitoring the increase in absorbance at 550 nm. The assay mixture contained 50 mM Tris/HCl, pH 8.4, 60 µM cytochrome *c*, 1 mM KCN and 2.5 µg of soluble mitochondrial proteins. To separate most of the membrane bound proteins from soluble proteins mitochondria underwent a

thaw–freeze cycle twice before the membrane bound proteins were sedimented at 25 000 *g*. The reaction was started by adding 100 mM D-lactate.

Complex I activity was measured according to [43] and [44]. The assay mixture contained 0.5 mM K<sub>3</sub>Fe(CN)<sub>6</sub>, 0.2 mM NADH, 50 mM Tris/HCl pH 7.4 and 2 µg mitochondrial protein. Reduction of K<sub>3</sub>Fe(CN)<sub>6</sub> was monitored at 420 nm ( $E = 1 \text{ mm}^{-1}\cdot\text{cm}^{-1}$ ).

Complex II was measured according to [45]: 5 mM MgCl<sub>2</sub>, 20 mM succinate, 0.3 mM ATP, 50 mM Tris/HCl pH 7.4 and 15 µg mitochondrial protein were mixed and incubated for 5 min to repeal inhibition through oxaloacetate. Afterwards 0.5 mM SHAM, 100 µM decylubiquinone (oxidized) and 2 mM KCN were added to the solution. The reaction was started with 50 µM DCIP and the reduction of DCIP was measured at 600 nm ( $E = 19.1 \text{ mm}^{-1}\cdot\text{cm}^{-1}$ ).

Complex III was measured according to [45]. The assay mixture contained 5 mM MgCl<sub>2</sub>, 2 mM KCN, 30 µM cytochrome *c* (oxidized), 100 µM decylubiquinone (reduced with sodium borohydrate), 50 mM Tris/HCl pH 7.4 and 2 µg mitochondrial protein. Reduction of cytochrome *c* was monitored at 550 nm ( $E = 19 \text{ mm}^{-1}\cdot\text{cm}^{-1}$ ).

Complex IV was measured according to [45]. The assay mixture contained 15 µM cytochrome *c* (reduced with sodium dithionite), 0.3 mM dodecylmaltoside, 50 mM Tris/HCl pH 7.4 and 1 µg mitochondrial protein. Oxidation of cytochrome *c* was followed at 550 nm ( $E = 19 \text{ mm}^{-1}\cdot\text{cm}^{-1}$ ).

### Statistical analyses

A minimum of three biological replicates were measured for each experiment. Significant differences between means were evaluated. The extinction of each enzyme was calculated using a linear mixed model [46] of the form  $y_{ijk} = \beta_j + \delta_j x_{ijk} + b_i + \varepsilon_{ijk}$  with  $i = 1, 2, j = 1, 2, 3, k = 1, \dots, nij$  where  $\beta_j$  denotes the treatment-specific intercept,  $\delta_j$  the treatment-specific slope at time  $x_{ijk}$  and  $b_i$  the block effect representing the different biological replicates. To compare the enzyme activity between the two treatment groups the treatment-specific regression slopes were compared using the *t* test statistic. Because multiple null hypotheses were tested simultaneously the Bonferroni–Holm procedure [47] was applied to control the pre-specified overall type I error rate  $\alpha = 0.05$ . For the statistical analysis the open source statistic software R (<http://www.r-project.org/>) was used.

### Acknowledgements

We thank Marianne Langer, Christa Ruppelt and Dagmar Lewejohann for expert technical assistance. Furthermore, we thank Andreas Kitsche for advice with respect to statistical analyses. This research project is supported by the PROCOPE program of the Deutsche Akademische Austauschdienst (DAAD)



funded by the Bundesministerium für Bildung und Forschung (BMBF), Project ID 55903318.

## Author contributions

PS: planned and performed experiments, analyzed data, wrote the paper. CC: performed experiments. KS: performed experiments. MB: performed experiments. AS: initiated project, planned and coordinated experiments. HPB: planned and coordinated experiments, wrote the paper.

## References

- Hare PD & Cress WA (1997) Metabolic implications of stress-induced proline accumulation in plants. *Plant Growth Regul* **21**, 79–102.
- Verbruggen N & Hermans C (2008) Proline accumulation in plants: a review. *Amino Acids* **35**, 753–759.
- Szabados L & Savouré A (2010) Proline: a multifunctional amino acid. *Trends Plant Sci* **15**, 89–97.
- Verslues PE & Sharma S (2010) Proline metabolism and its implications for plant–environment interaction. *Arabidopsis Book* **8**, e0140.
- Thiery L, Leprince AS, Lefebvre D, Ghars MA, Debarbieux E & Savouré A (2004) Phospholipase D is a negative regulator of proline biosynthesis in *Arabidopsis thaliana*. *J Biol Chem* **279**, 14812–14818.
- Parre E, Ghars MA, Leprince AS, Thiery L, Lefebvre D & Bordenave M (2007) Calcium signaling via phospholipase C is essential for proline accumulation upon ionic but not nonionic hyperosmotic stresses in *Arabidopsis*. *Plant Physiol* **144**, 503–512.
- Ghars MA, Richard L, Lefebvre-De Vos D, Leprince AS, Parre E, Bordenave M, Abdely A & Savouré A (2012) Phospholipases C and D modulate proline accumulation in *Thellungiella halophila/salsuginea* differently according to the severity of salt or hyperosmotic stress. *Plant Cell Physiol* **53**, 183–192.
- Sharma S & Dietz KJ (2009) The relationship between metal toxicity and cellular redox imbalance. *Trends Plant Sci* **14**, 43–50.
- Fabro G, Kovács I, Pavet V, Szabados L & Alvarez ME (2004) Proline accumulation and AtP5CS2 gene activation are induced by plant–pathogen incompatible interactions in *Arabidopsis*. *Mol Plant Microbe Interact* **17**, 343–350.
- Arakawa T & Timasheff SN (1985) The stabilization of proteins by osmolytes. *Biophys J* **47**, 411–414.
- Sharma S & Verslues PE (2010) Mechanisms independent of abscisic acid (ABA) or proline feedback have a predominant role in transcriptional regulation of proline metabolism during low water potential and stress recovery. *Plant, Cell Environ* **33**, 1838–1851.
- Jacoby RP, Taylor NL & Millar AH (2011) The role of mitochondrial respiration in salinity tolerance. *Trends Plant Sci* **16**, 614–623.
- Servet C, Ghelis T, Richard L, Zilberstein A & Savouré A (2012) Proline dehydrogenase: a key enzyme in controlling cellular homeostasis. *Front Biosci (Landmark Ed)* **17**, 607–620.
- Forlani G, Scainelli D & Nielsen E (1997) [ $\delta$ ]-Pyrroline-5-carboxylate dehydrogenase from cultured cells of potato (purification and properties). *Plant Physiol* **113**, 1413–1418.
- Bogges SF & Koeppe DE (1978) Oxidation of proline by plant mitochondria. *Plant Physiol* **62**, 22–25.
- Elthon TE & Stewart CR (1981) Submitochondrial location and electron transport characteristics of enzymes involved in proline oxidation. *Plant Physiol* **67**, 780–784.
- Kiyosue T, Yoshida Y, Yamaguchi-Shinozaki K & Shinozaki K (1996) A nuclear gene encoding mitochondrial proline dehydrogenase, an enzyme involved in proline metabolism, is upregulated by proline but downregulated by dehydration in *Arabidopsis*. *Plant Cell* **8**, 1323–1335.
- Mani S, van de Cotte B, van Montagu M & Verbruggen N (2002) Altered levels of proline dehydrogenase cause hypersensitivity to proline and its analogs in *Arabidopsis*. *Plant Physiol* **128**, 73–83.
- Funck D, Eckard S & Müller G (2010) Non-redundant functions of two proline dehydrogenase isoforms in *Arabidopsis*. *BMC Plant Biol* **10**, 70.
- Verbruggen N, Hua XJ, May M & van Montagu M (1996) Environmental and developmental signals modulate proline homeostasis: evidence for a negative transcriptional regulator. *Proc Natl Acad Sci USA* **93**, 8787–8791.
- Verslues PE, Kim YS & Zhu JK (2007) Altered ABA, proline and hydrogen peroxide in an *Arabidopsis* glutamate: glyoxylate aminotransferase mutant. *Plant Mol Biol* **64**, 205–217.
- Peng Z, Lu Q & Verma DP (1996) Reciprocal regulation of  $\delta$  1-pyrroline-5-carboxylate synthetase and proline dehydrogenase genes controls proline levels during and after osmotic stress in plants. *Mol Genet* **253**, 334–341.
- Yoshida Y, Kiyosue T, Nakashima K, Yamaguchi-Shinozaki K & Shinozaki K (1997) Regulation of levels of proline as an osmolyte in plants under water stress. *Plant Cell Physiol* **38**, 1095–1102.
- Satoh R, Nakashima K, Seki M, Shinozaki K & Yamaguchi-Shinozaki K (2002) ACTCAT, a novel *cis*-acting element for proline- and hypoosmolarity-responsive expression of the ProDH gene encoding proline dehydrogenase in *Arabidopsis*. *Plant Physiol* **130**, 709–719.

- 25 Lee CP, Taylor NL & Millar AH (2013) Recent advances in the composition and heterogeneity of the Arabidopsis mitochondrial proteome. *Front Plant Sci* **4**, 4.
- 26 Tanz SK, Castleden I, Hooper CM, Vacher M, Small I & Millar HA (2013) SUBA3: a database for integrating experimentation and prediction to define the SUBcellular location of proteins in Arabidopsis. *Nucleic Acids Res*, **41** (Database issue), D1185–D1191.
- 27 Davy de Virville J, Aaron Y, Alin MF & Moreau F (1994) Isolation and properties of mitochondria from *Arabidopsis thaliana* cell suspension culture. *Plant Physiol Biochem* **32**, 159–166.
- 28 Huang AH & Cavalieri AJ (1979) Proline oxidase and water stress-induced proline accumulation in spinach leaves. *Plant Physiol* **63**, 531–535.
- 29 Atkin OK & Macherel D (2009) The crucial role of plant mitochondria in orchestrating drought tolerance. *Ann Bot* **103**, 581–597.
- 30 Araújo WL, Tohge T, Ishizaki K, Leaver CJ & Fernie AR (2011) Protein degradation – an alternative respiratory substrate for stressed plants. *Trends Plant Sci* **16**, 489–498.
- 31 Kowaloff EM, Phang JM, Granger AS & Downing SJ (1977) Regulation of proline oxidase activity by lactate. *Proc Natl Acad Sci USA* **74**, 5368–5371.
- 32 Zhang M, White TA, Schuermann JP, Baban BA, Becker DF & Tanner JJ (2004) Structures of the *Escherichia coli* PutA proline dehydrogenase domain in complex with competitive inhibitors. *Biochemistry* **43**, 12539–12548.
- 33 Wittig I & Schägger H (2007) Electrophoretic methods to isolate protein complexes from mitochondria. *Methods Cell Biol* **80**, 723–741.
- 34 Wittig I & Schägger H (2005) Advantages and limitations of clear-native PAGE. *Proteomics* **5**, 4338–4346.
- 35 Wittig I & Schägger H (2009) Native electrophoretic techniques to identify protein–protein interactions. *Proteomics* **9**, 5214–5223.
- 36 Atlante A, de Bari L, Valenti D, Pizzuto R, Paventi G & Passarella S (2005) Transport and metabolism of D-lactate in Jerusalem artichoke mitochondria. *Biochim Biophys Acta* **1708**, 13–22.
- 37 de Bari L, Valenti D, Pizzuto R, Paventi G, Atlante A & Passarella S (2005) Jerusalem artichoke mitochondria can export reducing equivalents in the form of malate as a result of D-lactate uptake and metabolism. *Biochem Biophys Res Commun* **335**, 1224–1230.
- 38 Yadav SK, Singla-Pareek SL, Ray M, Reddy MK & Sopory SK (2005) Methylglyoxal levels in plants under salinity stress are dependent on glyoxalase I and glutathione. *Biochem Biophys Res Commun* **337**, 61–67.
- 39 Rajendrakumar CS, Reddy BV & Reddy AR (1994) Proline–protein interactions: protection of structural and functional integrity of M4 lactate dehydrogenase. *Biochem Biophys Res Commun* **201**, 957–963.
- 40 Sunderhaus S, Dudkina N, Jänsch L, Klodmann J, Heinemeyer J, Perales M, Zabaleta E, Boekema E & Braun HP (2006) Carbonic anhydrase subunits form a matrix-exposed domain attached to the membrane arm of mitochondrial complex I in plants. *J Biol Chem* **281**, 6482–6488.
- 41 Klein M, Binder S & Brennicke A (1998) Purification of mitochondria from Arabidopsis. *Methods Mol Biol* **82**, 49–53.
- 42 Laemmli UK (1970) Cleavage of structural proteins during the assembly of the head of bacteriophage T4. *Nature* **227**, 680–685.
- 43 Singer TP (1974) Determination of the activity of succinate, NADH, choline, and alpha-glycerophosphate dehydrogenases. *Methods Biochem Anal* **22**, 123–175.
- 44 Zhou G, Jiang W, Zhao Y, Ma G, Xin W, Yin J & Zhao B (2003) Sodium tanshinone IIA sulfonate mediates electron transfer reaction in rat heart mitochondria. *Biochem Pharmacol* **65**, 51–57.
- 45 Birch-Machin MA, Briggs HL, Saborido AA, Bindoff LA & Turnbull DM (1994) An evaluation of the measurement of the activities of complexes I–IV in the respiratory chain of human skeletal muscle mitochondria. *Biochem Med Metab Biol* **51**, 35–42.
- 46 Pinheiro JC & Bates DM (2000) Mixed-Effects Models in S and S-PLUS. Springer, New York.
- 47 Holm S (1979) A simple sequentially rejective multiple test procedure. *Scand J Stat* **6**, 6570.

## Supporting information

Additional supporting information may be found in the online version of this article at the publisher's web site:

**Fig. S1.** Experimental strategy.

**Fig. S2.** Identification of ProDH in mitochondrial fractions from Arabidopsis non-green cell cultures and green seedlings.

**Fig. S3.** Co-expression analysis of ProDH (At3 g30775) using the Atted-II database (<http://atted.jp/>).

**Fig. S4.** Co-expression analysis of ProDH (At3 g30775) using Genevestigator ([www.genevestigator.com](http://www.genevestigator.com)).

**Table S1.** Atted-II co-expression analysis results.

**Table S2.** Genevestigator co-expression analysis results.



WILEY  
Blackwell

the **FEBS**  
Journal

[www.febsjournal.org](http://www.febsjournal.org)

## **Biochemical characterization of proline dehydrogenase in Arabidopsis mitochondria**

Peter Schertl, Cécile Cabassa, Kaouthar Saadallah, Marianne Bordenave, Arnould Savouré and Hans-Peter Braun

DOI: 10.1111/febs.12821

**Supplementary Material**

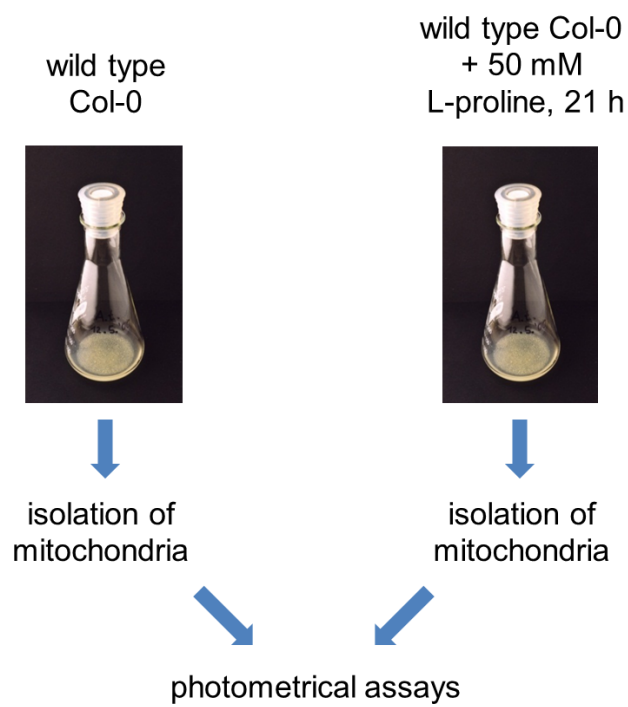
**Biochemical characterization of proline dehydrogenase in Arabidopsis mitochondria**

**Peter Schertl<sup>1</sup>, Cécile Cabassa<sup>2</sup>, Kaouthar Saadallah<sup>2</sup>, Marianne Bordenave<sup>2</sup>,  
Arnould Savouré<sup>2</sup>, and Hans-Peter Braun<sup>1</sup>**

<sup>1</sup>From the Institute of Plant Genetics, Plant Proteomics, Leibniz University Hannover,  
Herrenhäuser Str. 2, 30419 Hannover, Germany

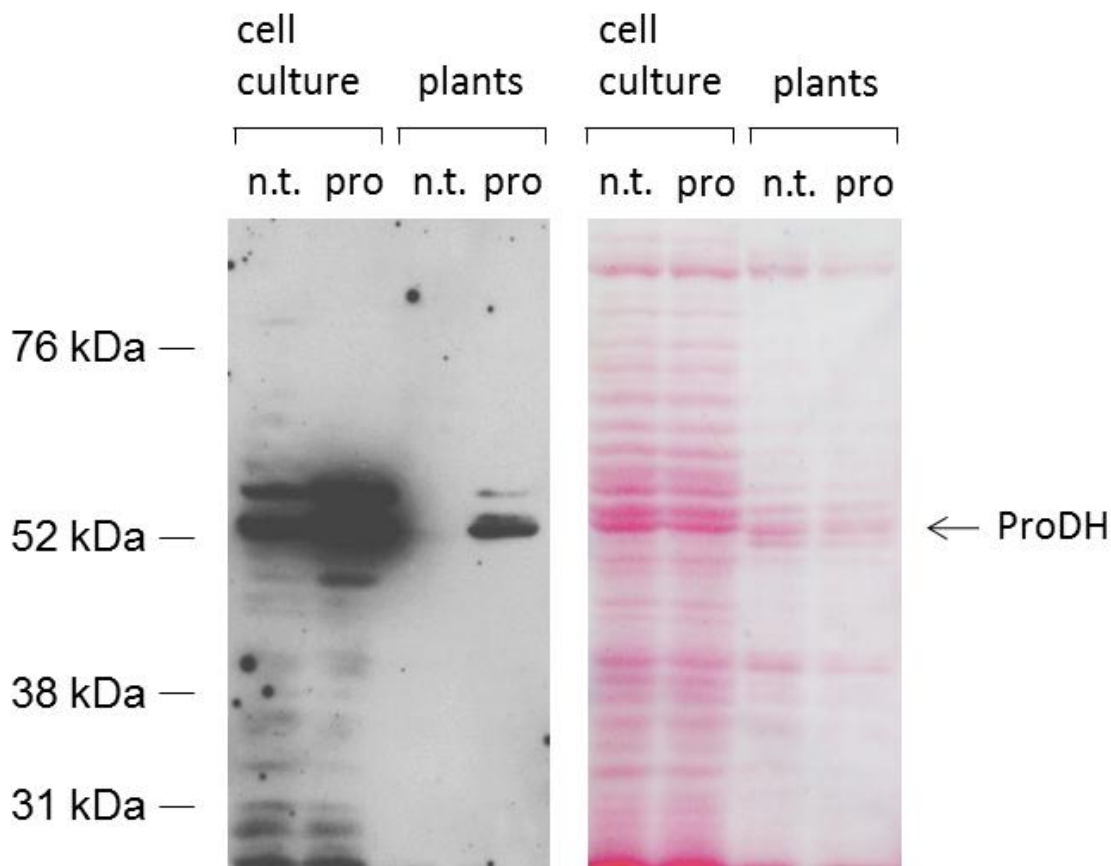
<sup>2</sup>Physiologie Moléculaire et Cellulaire des Plantes, Université Pierre et Marie Curie Paris 6, UR5  
EAC7180 CNRS, 4 Place Jussieu, 75005 Paris, France

Supp. Figure 1:



Supp. Figure 1: Experimental strategy. *Arabidopsis thaliana* Columbia suspension culture cells were treated with 50 mM L-proline. After incubation of 21 h mitochondria were isolated from treated and non-treated cells.

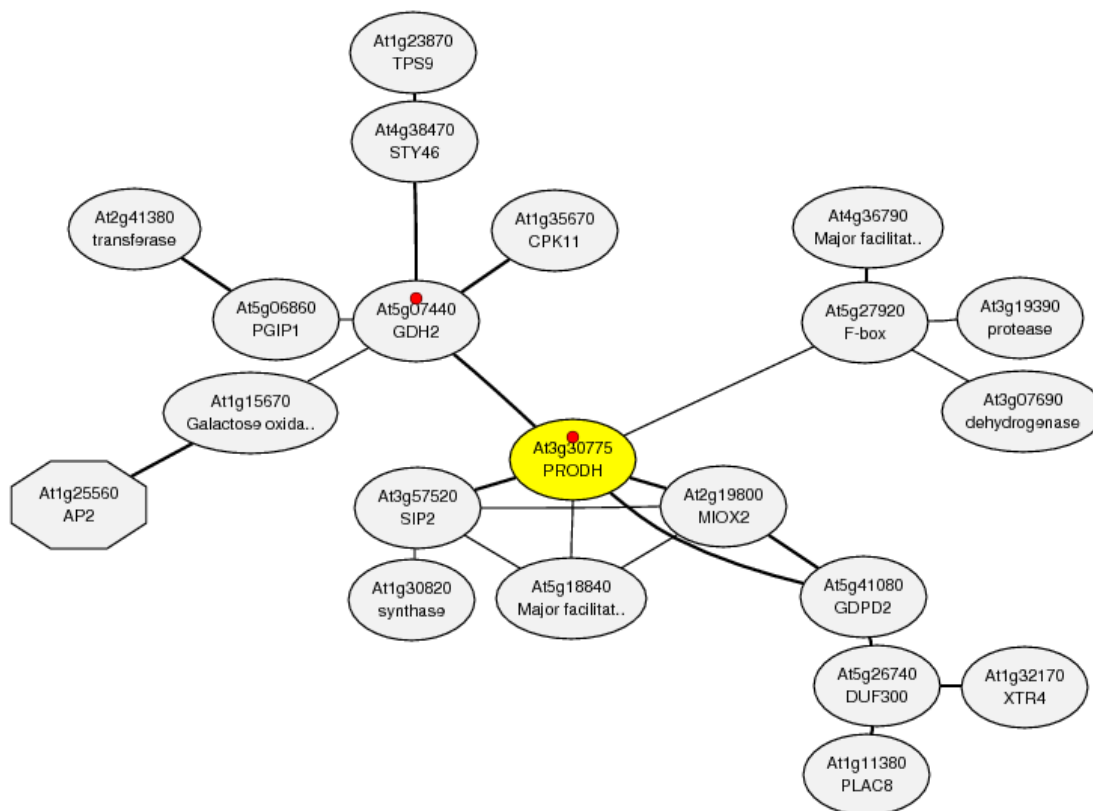
Supp. Figure 2:



Supp. Figure 2: Identification of ProDH in mitochondrial fractions from Arabidopsis non-green cell cultures and green seedlings. Cells and seedlings were either proline treated (pro) or not treated by proline (n.t.). Proline treatment of the cell cultures was carried out as specified in the Material and Methods section. For proline treatment of plants, seedlings were cultivated on  $\frac{1}{2}$  Murashige & Skoog medium (0.8 % agar). After 12 days, seedlings were transferred onto 50 mM proline containing  $\frac{1}{2}$  Murashige & Skoog medium for additional 24 h. Mitochondrial fractions were separated by SDS PAGE and blotted onto nitrocellulose. First, total protein of the blot was visualized by Ponceau staining (right part of the figure). Afterwards, ProDH was identified by immunostaining (left part of the figure). Masses of standard proteins are given to the left of the blots.

Note: protein load is identical between the mitochondrial fractions of pro-treated and non-treated cells on one hand and between those isolated from pro-treated and non-treated seedlings on the other. However, protein load between cells and seedlings differed by ca. factor 4. In mitochondrial fractions isolated from both sources (cells and seedlings), proline treatment clearly induces ProDH.

Supp. Figure 3:



Supp. Figure 3: Co-expression analysis of ProDH (At3g30775) using the Atted-II data base (<http://atted.jp/>). ProDH1 (At3g30775) and GluDH2 (At5g97440) are indicated by red dots.

To define co-expressed genes, gene expression profiles were compared. The profiles were constructed from Gene- Chip data downloaded from TAIR. To quantify the similarity of the gene expression profiles, pairwise Pearson's correlation coefficients were used (Obayashi et al 2007).

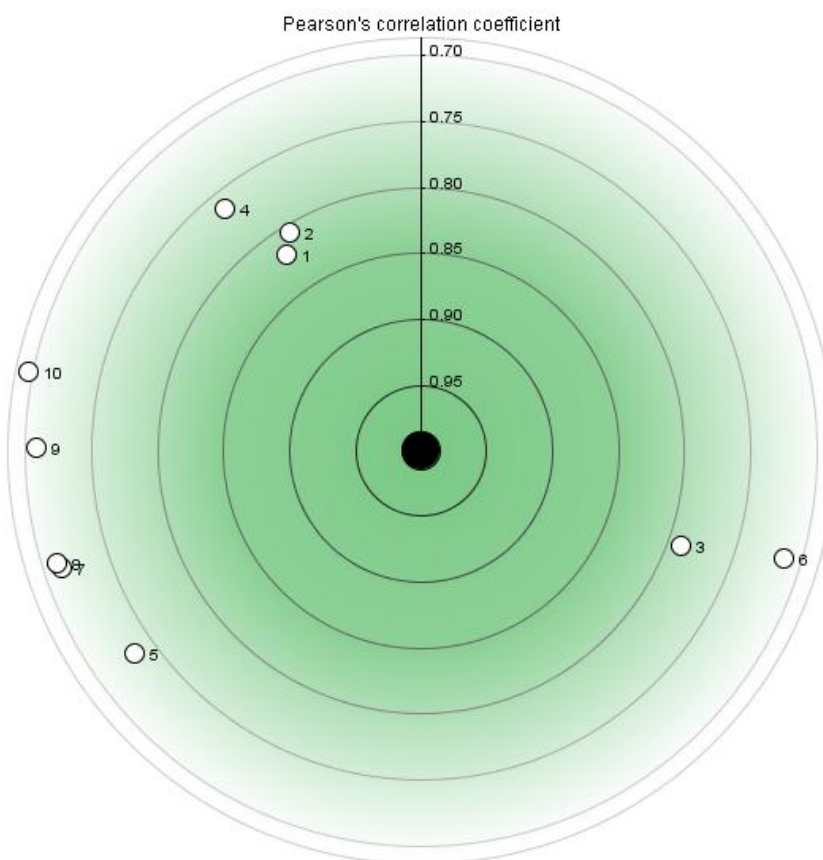
Table S1: Atted-II Co-expression analysis results.

MR <sup>a</sup>	Gene <sup>b</sup>	Description <sup>c</sup>
	At3g30775	proline dehydrogenase
1.0	At2g19800	myo-inositol oxygenase 2
1.4	At5g41080	PLC-like phosphodiesterases superfamily protein
2.0	At3g57520	seed imbibition 2
3.5	At5g07440	glutamate dehydrogenase 2
6.7	At5g27920	F-box family protein
27.2	At5g18840	Major facilitator superfamily protein

<sup>a</sup> Mutual Rank is a geometrically averaged correlation rank, which is based on weighted Pearson correlation coefficients, <sup>b</sup> gene accession number, <sup>c</sup> description of protein function

*Reference:* Obayashi T, Kinoshita K, Nakai K, Shibaoka M, Hayashi S, Saeki M, Shibata D, Saito K, Ohta H. (2007) ATTED-II: a database of co-expressed genes and cis elements for identifying co-regulated gene groups in Arabidopsis. *Nucleic Acids Res.*, 35, D863-D869.

Supp. Figure 4:



Supp. Figure 4: Co-expression analysis of ProDH (At3g30775) using Genevestigator ([www.genevestigator.com](http://www.genevestigator.com); Nebion, Hruz et al., 2008). A two-step workflow has been applied: First, microarray experiments with a significant change ( $p < 0.05$ ) of at least 1.5-fold in ProDH expression were selected using the perturbations tool. Genes with most similar expression patterns in these experiments were then identified with the co-expression tool using the Pearson correlation coefficient as a measure of similarity.

Table S2: Genevestigator Co-expression analysis results.

No <sup>a</sup>	Score <sup>b</sup>	Gene <sup>c</sup>	Description <sup>d</sup>
1	0.82	At2g19800	myo-inositol oxygenase 2
2	0.81	At5g41080	PLC-like phosphodiesterase superfamily protein
3	0.79	At1g32460	unknown protein
4	0.76	At3g57520	seed imbibition 2
5	0.73	At1g03090	methylcrotonyl-CoA carboxylase alpha chain
6	0.71	At5g07440	glutamate dehydrogenase 2
7	0.71	At2g30600	BTB/POZ domain-containing protein
8	0.71	At2g39570	ACT domain-containing protein
9	0.71	At5g21170	5'-AMP-activated family protein
10	0.70	At5g20250	glutamin-dependent asparagine synthase

<sup>a</sup> Protein number given in the figure, <sup>b</sup> Pearson's correlation coefficient, <sup>c</sup> gene accession number  
<sup>d</sup> description of protein function

Reference: Hruz T, Laule O, Szabo G, Wessendorp F, Bleuler S, Oertle L, Widmayer P, Gruissem W, and Zimmermann P. (2008). Genevestigator v3: A reference expression database for the meta-analysis of transcriptomes. *Adv. Bioinforma.* 2008: 420747.



## Publication III

### ***2.3 Molecular and functional characterization of the mitochondrial proline dehydrogenase 1 in Arabidopsis thaliana***

Cécile Cabassa-Hourton<sup>1</sup>, Peter Schertl<sup>2</sup>, Marianne Bordenave-Jacquemin<sup>1</sup>, Kaouthar Saadallah<sup>1,3</sup>, Anne Guivarc'h<sup>1</sup>, Séverine Planchais<sup>1</sup>, Jennifer Klodmann<sup>2</sup>, Holger Eubel<sup>2</sup>, Delphine Lefebvre-De Vos<sup>1</sup>, Thanos Ghelis<sup>1</sup>, Luc Richard<sup>1</sup>, Sandine Lebreton<sup>1</sup>, Chedly Abdelly<sup>3</sup>, Pierre Carol<sup>1</sup>, Hans-Peter Braun<sup>2</sup>, Arnould Savouré<sup>1</sup>

<sup>1</sup> Sorbonne Universités, UPMC Univ Paris 06, Adaptation de Plantes aux Contraintes Environnementales, URF5, Case 156, 4 place Jussieu, F-75252 Paris cedex 05, France

<sup>2</sup> Institute of Plant Genetics, Plant Proteomics, Leibniz University Hannover, Herrenhäuser Str. 2, 30419 Hannover, Germany

<sup>3</sup> Laboratoire des Plantes Extrêmophiles, Centre de Biotechnologie de Borj-Cedria (CBBC), BP 901, Hammam-Lif 2050, Tunisia

Type of authorship:	Co-author
Type of article:	research article
Share of the work:	25 %
Contribution to the publication:	isolation of mitochondria from suspension cell cultures, analyses of mitochondrial fractions by 2D BN/SDS PAGE, western blotting, analysis of MS-data, support in establishing ProDH activity assays in Paris
Journal:	Plant Physiology
Impact Factor:	7.908
Date of publication:	in revision

Running head: Proline dehydrogenase 1 in Arabidopsis mitochondria

Corresponding authors:

A. Savouré, Université Pierre & Marie Curie (UPMC), Université Paris 6, URF5 APCE, Case 156, 4 place Jussieu, 75252 Paris cedex 05, France

Fax: +33 (0)144 276151

Tel: +33 (0)144 272672

E-mail: [arnould.savoure@upmc.fr](mailto:arnould.savoure@upmc.fr)

H.-P. Braun, Institute of Plant Genetics, Plant Proteomics, Leibniz University Hannover, Herrenhäuser Str. 2, 30419 Hannover, Germany

Fax: +49 511 7623608

Tel: +49 511 7622674

E-mail: [braun@genetik.uni-hannover.de](mailto:braun@genetik.uni-hannover.de)

Research Area : Biochemistry and Metabolism

Key-words:

Arabidopsis, Electron transfer chain, Mitochondria, Proline dehydrogenase, Proline

---

# Molecular and functional characterization of the mitochondrial proline dehydrogenase 1 in *Arabidopsis thaliana*

Cécile Cabassa-Hourton<sup>1</sup>, Peter Schertl<sup>2</sup>, Marianne Bordenave-Jacquemin<sup>1</sup>, Kaouthar Saadallah<sup>1,3</sup>, Anne Guivarc'h<sup>1</sup>, Séverine Planchais<sup>1</sup>, Jennifer Klodmann<sup>2</sup>, Holger Eubel<sup>2</sup>, Delphine Lefebvre-De Vos<sup>1</sup>, Thanos Ghelis<sup>1</sup>, Luc Richard<sup>1</sup>, Sandine Lebreton<sup>1</sup>, Chedly Abdelly<sup>3</sup>, Pierre Carol<sup>1</sup>, Hans-Peter Braun<sup>2</sup>, Arnould Savouré<sup>1</sup>

<sup>1</sup> Sorbonne Universités, UPMC Univ Paris 06, Adaptation de Plantes aux Contraintes Environnementales, URF5, Case 156, 4 place Jussieu, F-75252 Paris cedex 05, France

<sup>2</sup> Institute of Plant Genetics, Plant Proteomics, Leibniz University Hannover, Herrenhäuser Str. 2, 30419 Hannover, Germany

<sup>3</sup> Laboratoire des Plantes Extrêmophiles, Centre de Biotechnologie de Borj-Cedria (CBBC), BP 901, Hammam-Lif 2050, Tunisia

## Summary

PRODH1 is a key enzyme in mitochondrial proline oxidation in *Arabidopsis*

## Footnotes

## Financial source

We thank the UMPC (Paris) and the Leibniz University Hannover for financial support. This research project was also supported by the PROCOPE program between Germany (Project 55903318 of the Deutsche Akademische Austauschdienst [DAAD] funded by the Bundesministerium für Bildung und Forschung [BMBF]) and France (Project n°28404PH funded by the Ministry of Foreign Affairs). Part of this work was supported by the Tunisian-French UTIQUE network (n°13G0929).

Present address(es) of authors if different from heading;

Delphine Lefebvre-De Vos

Institut Jean-Pierre Bourgin, UMR 1318 INRA-AgroParisTech, Centre INRA Versailles,  
78026 Versailles Cedex, France.

Corresponding authors:

A. Savouré

E-mail: [arnould.savoure@upmc.fr](mailto:arnould.savoure@upmc.fr)

H.-P. Braun

E-mail: [braun@genetik.uni-hannover.de](mailto:braun@genetik.uni-hannover.de)

**Abstract**

Proline is accumulated in many plant species in response to environmental stresses. Upon relief from stress, proline is rapidly oxidized in mitochondria by two enzymes, proline dehydrogenase (ProDH) and pyrroline-5-carboxylate dehydrogenase (P5CDH), the former being the limiting step in proline catabolism. Although two ProDH isoforms have been identified in the Arabidopsis genome, little is known about the function of these isoforms. A viable double *prodh1prodh2* mutant was generated. We show that root growth as well as root density are differentially affected in *prodh1*, *prodh2* and double *prodh1prodh2* mutants in response to proline. We also demonstrate that ProDH activity is tightly correlated to ProDH protein content under our experimental conditions. To evaluate the contribution of each isoform to proline oxidation, oxygen consumption using proline as substrate was measured in mitochondria isolated from wild-type, *prodh1*, *prodh2*, *prodh1prodh2* and *p5cdh* mutants. Results indicate a key role of ProDH1 in proline oxidation, ProDH2 not being able to compensate the lack of ProDH1 isoform. In addition we show that ProDH1 is linked to the mitochondrial membrane and forms part of a low molecular weight complex. Finally, protein separation by 2D Blue native / SDS PAGE in combination with immunoblotting and protein analysis by mass spectrometry allowed the identification of ProDH1 peptides in mitochondria. These observations have many implications for further investigating the role of this mitochondrial ProDH complex in relation to organelle functions.

## Introduction

Proline is a proteinogenic secondary amino acid known to play an essential role in primary metabolism, redox homeostasis, osmotic adjustment, protection against stress and signalling in many organisms, such as prokaryotes, yeasts, mammals and plants (for review, see Szabados and Saviouré, 2010). Today, the proline biosynthetic pathway is well documented but less is known about its catabolism, which contributes to generate important molecules such as ATP, reactive oxygen species (ROS) or reducing power (Servet et al., 2012). In response to water stress, plants usually accumulate proline. Proline biosynthesis occurs both in the cytosol and chloroplasts (Szekely et al., 2008). Upon recovery from stress, the accumulated proline is oxidized in mitochondria by two distinct enzymes: proline dehydrogenase (ProDH) (Kiyosue et al., 1996; Peng et al., 1996; Verbruggen et al., 1996) and delta-1-pyrroline-5-carboxylate dehydrogenase (P5CDH) (Deuschle et al., 2001). The first and limiting step of proline oxidation is under the control of ProDH, the flavin-dependent oxidation of proline to delta-1-pyrroline-5-carboxylate (P5C). P5C is then non-enzymatically converted into glutamate semialdehyde (GSA), which is then oxidised to glutamate by P5CDH. In most bacteria, a single bifunctional enzyme known as Proline utilization A (PutA) is a membrane-associated dehydrogenase with combined ProDH and P5CDH activities while in all eukaryote cells, ProDH and P5CDH are monofunctional enzymes (Servet et al., 2012). In prokaryotes and yeasts, ProDH has been shown to be a flavoenzyme transferring electrons to the respiratory chain via ProDH-FAD complexes while P5CDH reduces  $\text{NAD}^+$  (Tanner 2008; Wanduragala et al., 2010). In plants, it can be hypothesised that the first ProDH-catalysed step of proline oxidation also produces  $\text{FADH}_2$  and the second P5CDH-catalysed step generates NADH. Both reducing equivalents finally provide electrons to the mitochondrial electron transfer chain (ETC) (Schertl and Braun, 2014).

Proline oxidation activity has been reported for maize, wheat, barley, soybean and mung bean (Boggess et al., 1978; Elthon and Stewart, 1981) by L-proline dependent  $\text{O}_2$  consumption measurements of isolated mitochondria. Other abundant mitochondrial amino acids like glutamate and glycine can also be used as respiratory substrates by Arabidopsis mitochondria (Keech et al., 2005) while wheat mitochondria cannot support  $\text{O}_2$  consumption from glycine, arginine, serine and alanine (Boggess et al., 1978). This indicates substrate and plant specificities in providing the mitochondrial respiratory chain. P5C, product of proline oxidation, was found to be used as a respiratory substrate in maize mitochondria (Elthon and Stewart, 1981) thus demonstrating the existence of a direct electron transfer pathway from

P5CDH to the respiratory chain. In contrast, the ability of ProDH to directly transfer electrons to the mitochondrial respiratory chain remains to be demonstrated in plants.

In Arabidopsis, there are two closely related ProDH isoforms (75% amino acid sequence identity), ProDH1 and ProDH2. Analysis of the *ProDH1* promoter has led to the identification of a PRE (Proline or hypoosmolarity-Responsive Element) motif that is involved in the regulation of its expression (Nakashima et al., 1998; Servet et al., 2012). *ProDH1* expression has been found to be repressed by dehydration when proline accumulates but increased after recovery after water stress, exogenous proline addition and hypoosmolarity (Kiyosue et al., 1996; Verbruggen et al., 1996; Nakashima et al., 1998). *ProDH1* and *ProDH2* are both scarcely expressed in vegetative organs when Arabidopsis seedlings are cultivated in standard conditions and differentially regulated by various bZIP transcription factors (Weltmeier et al., 2006; Hanson et al., 2008). Specific expression patterns were nevertheless found using promoter-GUS fusion studies as the *ProDH1* promoter directs high expression in floral organs such as pollen and stigma while *ProDH2* expression is preferentially localized to vascular tissues and abscission zones (Funck et al., 2010). *ProDH2* transcript accumulation might also be induced by pathogen attack or UV stress (Arabidopsis eFP Browser: <http://bar.utoronto.ca/efp/cgi-bin/efpWeb.cgi>) and in the presence of 20 mM proline or 200 mM NaCl (Funck et al., 2010).

The first step of proline catabolism is thus a highly regulated process, an essential feature regarding its possible impact on cell ROS and energy production or in maintaining the redox balance (Cecchini et al., 2011; Ben Rejeb et al., 2014). The subcellular location of proline catabolism enzymes is of crucial importance to ensure its role for providing electrons to the respiratory chain. ProDH1 has been clearly demonstrated to be mitochondrial (Kiyosue et al., 1996; Mani et al., 2002) but due to contradictory ProDH-GFP fusion analyses, subcellular location of ProDH2 is still under debate (Funck et al., 2010; Van Aken et al., 2009). P5CDH has been identified in mitochondrial proteome analyses (Kruft et al. 2001; Millar et al. 2001; Heazlewood et al. 2004). It possibly represents a dual-targeted protein because it also was identified in the course of proteome analyses of chloroplasts (Kleffmann et al., 2004). So far, ProDH1 and ProDH2 could not be identified by any organelle-based proteome project in plants.

Although proline metabolism has been extensively investigated, the biochemical characterization of ProDH remains elusive. Therefore and to further characterize how ProDH participates in resuming growth after stress, we first developed an experimental system to induce ProDH accumulation leading to high ProDH activity in Arabidopsis seedlings. ProDH

accumulation and activity were localized in the mitochondrial membrane fraction. L-proline dependent O<sub>2</sub> consumption analyses were performed on isolated mitochondria from wild-type and various Arabidopsis proline catabolism knockout mutants to precisely define the proteins involved in the electron transfer from L-proline to the respiratory chain in Arabidopsis. Analyses using a *p5cdh* knockout mutant demonstrated for the first time a direct electron transfer pathway from L-proline to the respiratory chain *via* the first step of proline catabolism. Investigations using *prodh1* and *prodh2* mutants provided evidences that ProDH1 is the only isoform involved in transferring electrons to the Arabidopsis respiratory chain when plants are treated with external proline. This result was confirmed by the identification of ProDH1 peptides in Arabidopsis mitochondria of L-proline-treated plants using 2D Blue-native (BN) / SDS PAGE and western blot analyses in combination with mass spectrometry.



## Results

### Molecular characterization of *prodh* mutants

In order to assess the functions of ProDH1, we genetically characterized allelic T-DNA insertion mutants of *ProDH1* (*prodh1-3* and *prodh1-4*) and *ProDH2* (*prodh2-2* and *prodh2-3*) (Fig. 1). Insertions in *prodh1-3*, *prodh1-4* and *prodh2-2* are located in an intron as previously described by Funck and co-workers (Funck et al., 2010), while *prodh2-3* mutant has a T-DNA insertion in the promoter (Fig. 1A). The homozygous lines were confirmed by PCR genotyping experiments (Fig. 1B). Next, the impact of *prodh* mutations were investigated on ProDH protein content. Arabidopsis seedlings of wild-type as well as *prodh1-4*, *prodh2-2* and the double *prodh1-4prodh2-2* lines were subjected to L-proline treatment for 24 h to trigger ProDH accumulation. Western blot analysis using an antibody directed against ProDH revealed a very utqpi immunoreactive signal (around 54 kDa) in response to exogenous L-proline, which became much fainter with mitochondrial extracts from non-treated seedlings (Fig. 1C). This signal was absent in the *prodh1-4* mutant as well as in the double *prodh1prodh2* mutant. This suggests that the signal can be attributed to ProDH1 isoform and that *prodh1-4* is a complete loss-of-function allele. The absence of any band in both *prodh1* and in the double mutant as well as the fact that it is much more intense in response to proline clearly confirms that the 54 kDa band corresponds to ProDH1 isoform.

As a control, we also performed western blots with an excess of recombinant ProDH1, which can bind the ProDH antibody before its binding to the blotted proteins. As expected, the ProDH signal was not visible anymore in both proline-treated and not-treated seedlings extracts (supplemental Figure 1).

### ProDH1 is required for root development on high proline concentration but not ProDH2

To get deeper insights into the physiological role of ProDH, *prodh* mutants were grown *in vitro* in order to test their root development in presence of exogenous proline (Fig. 2). In absence of proline, single *prodh1-4* mutant and *prodh1prodh2* double mutant showed a root growth identical to wild-type, but *prodh2-2* mutant had a slightly increased primary root growth after eight days of culture (Fig. 2). To better quantify the responses of *prodh* mutants to exogenous proline on root system development, the length of the primary root was analysed during plant growth in presence of proline (Fig. 2A and B). First, presence of proline did not affect wild-type plants. However, in presence of proline, primary root growth of the *prodh2-2* mutant was slightly delayed at 4 days but later became identical to wild-type. *prodh1-4* mutant and *prodh1prodh2* double mutant had more striking phenotypes: primary

root growth of these mutants was clearly inhibited during development in presence of proline, 46% delay for *prodh1* and 43% for *prodh1prodh2* after 12 days of 10 mM proline treatment; this growth inhibition was more severe with 10 mM proline as early as four days after germination (Fig. 2B). Thus absence of ProDH1 causes an inhibition of the root growth in presence of exogenous proline, while the absence of ProDH2 did not.

The number of secondary roots was also investigated. In general, proline exposure had a slight negative effect on the number of secondary roots, which was more severe in the *prodh* mutants than in wild-type plants (Supplementary Fig. 2). However, compared to changes in primary root growth, changes were less substantial and at the borderline of significance. Finally, the development of the aerial parts was not affected by proline. Wild-type and mutants had the same number of leaves that displayed the same size and morphology (data not shown).

### **L-proline treatment triggers ProDH1 protein content and activity**

ProDH1 is induced in seedlings in response to externally added proline (Fig. 1). ProDH activity was monitored in mitochondria isolated from wild-type and mutant plant lines exposed to proline using a modified version of the 2,6-dichloroindophenol- (DCIP) based assay (Schertl et al., 2014) previously established by Huang and Cavalieri (1979). In presence of proline, 32.1 nmol reduced DCIP  $\text{min}^{-1} \text{mg protein}^{-1}$  ProDH activity was measured in wild-type (Fig. 3). This ProDH activity was slightly higher in the *prodh2* mutant than wild-type. In contrast, ProDH activity was decreased by 80% in *prodh1*. In *prodh1prodh2* double mutant, ProDH activity was close to background level. Thus ProDH activities tightly correlate with ProDH protein contents, with a high ProDH activity dependent on the presence of the proline-induced ProDH1.

### **Proline-treated seedlings displayed a higher mitochondrial respiration**

First we measured and compared standard respiration parameters in mitochondria from proline-treated and non-treated seedlings. Mitochondrial respiratory parameters were recorded using isolated mitochondria and various respiratory substrates (Supplemental Fig. 3). NADH and succinate respiratory substrates were used in order to define the intrinsic parameters of the various mitochondria tested. As presented in Table I, in control conditions (NT), wild-type mitochondria displayed a state 3  $\text{O}_2$  consumption rate around 144  $\text{nmol O}_2 \text{min}^{-1} \text{mg protein}^{-1}$  and a state 4 rate around 72  $\text{nmol O}_2 \text{min}^{-1} \text{mg protein}^{-1}$ . The respiratory coupling rate (RCR) of 2.0 indicates a rather good capability to readjust electron flow. These mitochondria were

also normally coupled with a phosphorylating yield of 1.4 using NADH and succinate as substrates. More generally, they displayed a high CytC pathway (96% of total electron flow) and a weak alternative oxidase (AOX) capacity ( $13.3 \text{ nmol O}_2 \text{ min}^{-1} \text{ mg protein}^{-1}$ ). Proline-treated plants displayed higher respiratory rates in both phosphorylating state (around  $168 \text{ nmol O}_2 \text{ min}^{-1} \text{ mg protein}^{-1}$  in state 3 and 84 in state 4) than non-treated plants. The RCR parameter was again around 2.0, similar to what was previously observed in proline-non-treated mitochondria. By contrast, the ADP/O ratio was dramatically lower (1.0 versus 1.4), indicating that more electrons had to be transferred to oxygen to produce the same ATP content. This feature could explain the higher respiratory rates observed in these mitochondria. As proline catabolism is known to induce ROS production (Miller et al., 2009; Cecchini et al., 2011; Ben Rejeb et al., 2014), we also measured AOX capacity. A 40% higher AOX capacity in proline-treated seedlings could be measured ( $19 \text{ nmol O}_2 \text{ min}^{-1} \text{ mg protein}^{-1}$ ), leading to smaller participation of the CytC pathway (85% of total electron flow). This result indicates an oxidative stress response of the proline-treated plants. As AOX is one of the uncoupling plant mitochondria systems, the high AOX capacity measured when plants are exogenously supplied with L-proline could partially explain the low phosphorylating yield observed in these mitochondria.

### **L-proline provides electrons to the respiratory chain**

L-proline oxidation in mitochondria isolated from Arabidopsis leaves was tested and compared with standard respiration measurements. As shown in Table I, specific L-Proline dependent respiration could be measured in mitochondria from wild-type proline-treated plants ( $29 \text{ nmol O}_2 \text{ min}^{-1} \text{ mg protein}^{-1}$  for the CytC pathway and up to  $36.4 \text{ nmol O}_2 \text{ min}^{-1} \text{ mg protein}^{-1}$  for the AOX pathway). No L-proline dependent electron flow could be measured in non-proline-treated plants. Interestingly proline-related substrates like D-proline or L-hydroxyproline could not lead to any respiratory chain-dependent  $\text{O}_2$  consumption even in mitochondria isolated from L-proline-treated plants (supplementary figure 3 C). Thus, only mitochondria containing high ProDH level displayed L-proline dependent oxygen consumption, indicating that a ProDH content or activity threshold should be reached to allow measurable L-proline respiration in isolated mitochondria.

P5C, the product of ProDH catabolism, was shown to function as a respiratory substrate in maize mitochondria (Elthon and Stewart, 1981) thus demonstrating the existence of a direct electron transfer to the respiratory chain involving P5CDH. However, the ability of ProDH to directly provide electrons to the mitochondrial respiratory chain remained elusive. To address

this question, proline-dependent mitochondrial respiration was investigated using a *p5cdh* knockout mutant. *p5cdh* had a slightly higher mitochondrial ProDH content in response to proline treatment than wild-type (supplemental Fig. 4). Respiratory rates of *prodh* and *p5cdh* mutants were investigated using different respiratory substrates as well as proline (Table I). Mitochondria were isolated from wild-type and mutants that were treated with or without proline. State 3 rates were similar in wild-type and *p5cdh* mitochondria from non-treated plants while RCR was significantly lower in *p5cdh* mutants (1.8 versus 2.0) because of higher state 4 rates (around 78 versus 72 nmol O<sub>2</sub> min<sup>-1</sup> mg protein<sup>-1</sup>). ADP/O ratio was also reduced in non-treated *p5cdh* mutant line (1.23 versus 1.4), which indicates poorly coupled mitochondria in control conditions. Interestingly upon proline treatment, *p5cdh* uncoupling did not change and wild-type mitochondria became even more uncoupled than the mutant ones (ADP/O decreasing up to 1.0). AOX capacity was also slightly higher in the NT *p5cdh* mutant but at an intermediate rate between NT and proline treated wild-type plants. In contrast, proline treatment induced an increase of the AOX capacity in the *p5cdh* mutant (36.6 nmol O<sub>2</sub> min<sup>-1</sup> mg protein<sup>-1</sup>). The reduced phosphorylating yield and enhanced AOX capacity observed in this mutant under control conditions indicate that these plants behaved as stressed plants. The contradictory response to proline treatment in the mutant line (high increase of AOX capacity but no change in phosphorylating yield) may indicate a modification in mitochondrial membrane properties upon proline treatment that decreases proton leakage, which compensate the uncoupling increased by the AOX pathway in these mitochondria. L-proline dependent O<sub>2</sub> uptake could be observed in *p5cdh* mitochondria when isolated from proline-treated plants but with reduced rates when compared to wild-type plants (about 17.9 versus 29 nmol O<sub>2</sub> min<sup>-1</sup> mg protein<sup>-1</sup> in wild-type for the cytochrome pathway and 19 versus 36.4 nmol O<sub>2</sub> min<sup>-1</sup> mg protein<sup>-1</sup> in wild-type for the AOX pathway). The reduced L-proline dependent oxidation rates measured in the *p5cdh* mutant compared to wild-type could be explained by the lack of electron transfer from P5CDH in the ETC. Thus the ability of this mutant lacking the second step of L-proline oxidation to use L-proline as sole respiratory substrate indicates that ProDH can directly deliver electrons to the respiratory chain.

### **ProDH is associated with mitochondrial membrane fraction in Arabidopsis**

Elthon and Stewart (1981) showed that a proline oxidation activity was associated with the inner mitochondrial membrane in *Zea mays*. In order to test this protein localization in Arabidopsis, mitochondria were purified using Percoll density gradient ultra centrifugation from 15 days-old wild-type seedlings treated for 24 h by 50 mM L-proline. Mitochondrial

membrane (MB) and soluble fractions (S) were then separated and tested for the presence of ProDH by western blot analysis. The purity of the two fractions was assessed using antibodies against the membrane integrated adenylate translocator (ANT) and the matrix-localized isocitrate dehydrogenase (ICDH). Figure 4A shows a specific ProDH signal in the membrane fraction, confirmed by the fraction purity controls in B and C. These results demonstrate a physical association between ProDH and the mitochondrial membranes in Arabidopsis.

### **ProDH1 is essential for L-proline dependent respiration**

We wanted to know which ProDH isoform is the main provider of electrons to the mitochondrial respiratory chain. We therefore performed respiratory measurements with mitochondria isolated from *prodh* mutants either treated or not treated by exogenous L-proline. As presented in Table I, when tested with NADH and succinate as respiratory substrates, all mutant lines behaved like wild-type regarding the increases in the respiratory parameters upon proline treatment. When plants were treated with proline, AOX capacity was only slightly increased in the *prodh1* mutant and even decreased in *prodh2* lines. But this AOX value is already very high in all mutant lines (between 29 to 45.6 nmol O<sub>2</sub> min<sup>-1</sup> mg protein<sup>-1</sup>) under proline-treated and non-treated conditions. ADP/O ratios were also similar between wild-type and *prodh2* while *prodh1* displayed very low phosphorylating yields (1.18 in NT plants and 0.85 in proline-treated ones), which is in accordance with their specifically high AOX capacity (up to 44 nmol O<sub>2</sub> min<sup>-1</sup> mg protein<sup>-1</sup>).

The *prodh1* mutant mitochondria could not support any L-proline dependent respiration independently of the treatments. On the contrary *prodh2*, mitochondria isolated from proline-treated plants displayed L-proline dependent respiration (up to 23.3 nmol O<sub>2</sub> min<sup>-1</sup> mg protein<sup>-1</sup> for the CytC pathway and 18.3 nmol O<sub>2</sub> min<sup>-1</sup> mg protein<sup>-1</sup> for the AOX pathway). Thus, L-proline dependent respiration could only be observed in mitochondria from wild-type and *prodh2* mutant lines treated with proline, when ProDH1 was present at high level. These experiments demonstrate that ProDH1 is the only isoform located in mitochondria under the tested conditions and that this enzyme is able to transfer electrons from L-proline to the ETC.

### **ProDH1 is associated with low molecular weight complexes in Arabidopsis mitochondria**

In plants, ProDH is scarcely abundant even after relief from stress. Only few ProDH peptides have been reported today in the frame of global Arabidopsis shot gun proteome analyses (Baerenfaller et al. 2008). No ProDH peptides have been identified until now in any plant using organelle-based proteome analysis. In order to identify ProDH in mitochondria, we used

a cell suspension culture recently developed by Schertl et al. (2014) that allows a massive ProDH induction suitable for biochemical characterization of this enzyme. Proteins from mitochondria purified on Percoll density gradients were separated by 2D Blue native (BN) / SDS PAGE. As shown by the immune-blotting experiment in Fig. 5, spots were revealed using ProDH antibody in proline-treated cells. No signal was detectable on the corresponding 2D gel of proline non-treated cells using identical film exposure time. Immuno-positive proteins of purified mitochondria from proline-treated cells had an apparent molecular mass of ~54-55 kDa on the second gel dimension. The oligomeric state of ProDH is not quite clear so far because the immune-positive proteins migrate in the range of 70 to 140 kDa on the first blue native gel dimension. Several film exposure times were used out in order to compare the signals between BN / SDS PAGE gels from non-treated and proline-treated mitochondrion samples (Fig. 6). Similar signals were observed in a 150-fold difference in exposure time (2 seconds in mitochondria of proline-treated cells versus 300 seconds in non-treated cells), indicating an estimated 150-fold difference in ProDH content between the two samples. Additional experiments were also carried out using mitochondria isolated from non-treated and proline-treated *Arabidopsis* seedlings. Interestingly, very similar spot patterns were observed in 2D BN / SDS PAGE, but of very much lower intensity (supplemental Fig. 5). To obtain similar ProDH signals, much longer exposure times, minutes in comparison to seconds, were needed, indicating again that ProDH is of much higher concentrations in cell cultures than in seedlings.

Spots recognized by the ProDH antibody and differentially expressed between NT and proline-treated material were further analysed by mass spectrometry (MS). Only ProDH1 peptides were detected in four spots of mitochondria from proline-treated cell suspension (Fig. 7), indicating that the ProDH2 isoform is not present or not at a sufficient level in these mitochondria. The peptides are well distributed along the ProDH1 protein (Fig. 8). In mitochondria isolated from seedlings, only ProDH1 peptides were also detected in the corresponding spots (data not shown). These results support our respiratory data demonstrating that ProDH1 is the only active isoform located in mitochondria of proline-treated plants that provides electrons to the ETC when L-proline is used as a substrate.

## Discussion

Proline is accumulated in response to various environmental stresses in many plant species. When stress is relieved, proline is rapidly degraded in mitochondria through the sequential action of two enzymes, ProDH and P5CDH. The limiting step of proline degradation is

controlled by ProDH (for review, see Servet et al., 2012). Although proline biosynthesis is well characterized at molecular and biochemical levels, only few information is available on the role and function of ProDH in proline degradation. Physiological, biochemical and proteomic analysis have been carried out to get better insight into the physiological role of this key enzyme. The use of a specific ProDH antibody allowed, for the first time, to investigate ProDH content in different mutants. One important step in ProDH characterization was the generation of a viable double *prodh1prodh2* mutant. Using a root growth assay, we could demonstrate that proline hypersensitivity was due to the lack of *prodh1* and not *prodh2*, a phenotype which is conserved in the double *prodh1prodh2* mutant. Also proline-dependent respiration was investigated in mitochondria isolated from these different genotypes. Results again indicate a key role of ProDH1 in proline oxidation. A good correlation was observed between ProDH activity and its protein content. We therefore pursued to investigate some biochemical properties of ProDH. We could demonstrate that ProDH is linked to mitochondrial membrane and is part of a low molecular weight complex. Finally, protein separation by 2D Blue native / SDS PAGE in combination with immunoblotting and protein analysis by mass spectrometry allowed for the first time the identification of ProDH1 peptides in a mitochondrial fraction. These observations have many implications for further investigating how ProDH1 interacts with the inner mitochondrial membrane and for better understanding the respective roles of the two ProDH isoforms.

### **ProDH1 and ProDH2 have distinct roles in proline hypersensitivity**

In order to characterize the role of ProDH, a double mutant *prodh1prodh2* was generated. ProDH accumulation was totally impaired in this mutant in response to proline. To our surprise, this double mutant did not show any obvious developmental phenotype. It notably has growth as wild-type and can produce viable seeds, suggesting that proline degradation is not essential for vegetative and reproductive plant growth. The use of double mutant in the investigation of proline hypersensitivity demonstrated the key role of ProDH1 in primary root length growth, which is in accordance to previous published work (Mani et al. 2002, Nanjo et al., 2003). However the root density was affected in *prodh2*. All these data indicate different adaptation of the root system to the presence of exogenous proline which further indicates that the two ProDH isoforms have distinct roles, at least in plant development (Funck et al., 2010) with an essential role of ProDH1 in proline oxidation.

### **Proline is a respiratory substrate for ProDH1 but not for ProDH2**

The use of *prodh* mutants allowed investigating the role of each ProDH isoform in mitochondrial respiration. ProDH1 plays an essential role in L-proline dependent respiration in mitochondria. Recently it was shown by Funck et al. (2010) that *ProDH2* is induced by proline but repressed by sucrose at least at the transcript level. This was not observed in our study at the mitochondrial protein level because ProDH2 isoform was not detectable in the *prodh1* mutant background in response to proline. However, it cannot be excluded that the amount of ProDH2 is too low to be detected on western blots. Furthermore *prodh1* did not show any measurable proline dependent respiration in isolated mitochondria although this mutant had been previously treated by proline. These findings suggest that ProDH2 is not accumulated in mitochondria in response to proline and more importantly ProDH2 cannot compensate the lack of ProDH1. Deuschle et al. (2004) reported that the *p5cdh* mutant, which is a single copy gene in Arabidopsis, was unable to completely degrade exogenously applied <sup>14</sup>C-labeled proline into glutamine or glutamate but could accumulate P5C. This is in accordance with our results where mitochondria isolated from *p5cdh* mutant displayed slightly higher ProDH1 content and a L-dependent proline respiration, although at a lower extent than in wild-type seedlings. This indicates that ProDH1 is able to oxidize proline even when P5CDH is lacking thus providing electrons to the ETC. This reduced *p5cdh* respiration could be explained by the lack of electron transfer from P5CDH to the ETC. The finding that ProDH and P5CDH can function independently is surprising because the analysis of structural data of the bifunctional ProDH and P5CDH enzyme PutA revealed a dynamic tunnel system that allows a substrate-channelling path between the two active sites (Singh et al., 2014). A detailed characterization of the interaction between ProDH and P5CDH in plants will help to answer this question.

Hydroxyproline, a proline derivative containing a hydroxyl group attached to the gamma carbon atom, is known to represent a substrate for the vertebrate ProDH (Ostrander et al., 2009). As shown by oxygen consumption measurements, hydroxyproline could not be used as a respiratory substrate for any mitochondria isolated from either wild-type or *prodh* mutants. A tyrosine 540 residue was found to be an important determinant for preventing hydroxyproline to bind to the substrate-binding site (Ostrander et al., 2009). Both Arabidopsis ProDH protein sequences show high sequence similarity and possess, as vertebrate ProDH1, a tyrosine residue in analogous position (Servet et al., 2012). Also in this respect the ProDH isoforms of plants should be further investigated.



It is well known that proline is an essential energy substrate for insect flights (Auerswald et al., 1998; Sacaraffia and Wells, 2003). However plant L-proline dependent respiration was always weak compared to canonical substrates like NADH or succinate and highly dependent on the uncoupling AOX activity. It is thus unlikely that L-proline oxidation could be used as the sole energy substrate for resuming growth after stress in plants. Proline oxidation might rather help in increasing respiratory rates and regulating redox balance and ROS generation.

### **ProDH forms part of low molecular weight complex in mitochondria**

Availability of specific ProDH antibody allowed us for the first time to identify ProDH peptides in a plant mitochondrial fraction. Using external proline treatment, ProDH first was substantially induced (Schertl et al., 2014). Next, proteins were separated by 2D BN / SDS PAGE and ProDH was visualized by immunoblotting. The ProDH signal runs at about 70 to 140 kDa on the native gel dimension, indicating that ProDH might represent a dimer or that it binds to another so far unknown protein. This issue has to be further investigated. The fact that ProDH somehow “smears” on the first BN gel dimension between 70 and 140 kDa is a commonly observed phenomenon on blue native gels, because protein separation takes place under very mild conditions. This may cause lipids or detergent molecules to stick to proteins. On the second gel dimension, the ProDH signal runs at 54 kDa, as expected. The corresponding gel region was cut out and analysed by mass spectrometry. Overall, seven unique ProDH peptides were identified, which cover different regions of the protein from the N- to its C-terminus. All peptides exactly match the predicted amino acid sequence of ProDH1. In accordance with our other data, ProDH2 peptides could not be identified. We conclude that ProDH1 is the far more prominent ProDH isoform in mitochondria under the conditions tested. ProDH1 associates to the mitochondrial membrane and forms part of a low molecular weight complex.

Dehydrogenases are of key importance for mitochondrial catabolism. Besides pyruvate dehydrogenase and dehydrogenases of the citric acid cycle, several further dehydrogenases occur, some of which are specific for plant mitochondria (Schertl and Braun 2014). Dehydrogenases transfer electrons either onto  $\text{NAD}^+$  or FAD, forming NADH and  $\text{FADH}_2$ , respectively. NADH-producing enzymes are often localized in the mitochondrial matrix or attached to the inner mitochondrial membrane. The NADH is re-oxidized by complex I of the respiratory chain or alternative NADH dehydrogenases, which are especially prominent in plant mitochondria. In contrast,  $\text{FAD}^+/\text{FADH}_2$  normally is tightly bound to dehydrogenases. Based on current knowledge, electrons of  $\text{FADH}_2$  are always directly transferred onto

ubiquinone, which requires tight linkage of the corresponding enzymes to the inner mitochondrial membrane. The proline catabolic pathway includes two dehydrogenases, ProDH and P5CDH, the former transferring electrons onto FAD and the latter onto NAD<sup>+</sup>. In accordance to other FAD-containing mitochondrial dehydrogenases, ProDH is tightly linked to the mitochondrial membrane and most likely transfers electrons directly onto ubiquinone. It is known that electron entry pathways into the respiratory chain of plant mitochondria can much vary depending on the biochemical state of a plant cell (Schertl and Braun 2014). Electron entry via proline certainly is of great importance during stress release conditions. The precise mode of action of the 70-140 kDa ProDH complex during electron transfer from proline to the ETC should be addressed by future research.

## Materials and Methods

### *Plant material and growth conditions*

*Arabidopsis* (*Arabidopsis thaliana* (L.) Heynh. ecotype Col0 and *prodh1-3* (GABI\_308F08), *prodh1-4* (SALK\_119334), *prodh2-2* (GABI\_328G05), and *prodh2-3* (SALK\_918D08) T-DNA insertion lines were obtained from the Salk Institute, La Jolla, USA (Alonso et al., 2003) and the Center for Biotechnology, Universitat Bielefeld, Germany (Kleinboelting et al., 2012). Presence of the T-DNA and allelic status were verified by PCR and sequencing of the T-DNA flanking sequences. In the crosses between *prodh1-4* and *prodh2-2*, double *prodh1-4prodh2-2* F<sub>2</sub> seedlings were selected by PCR. Gene and T-DNA-specific primers are listed in supplemental Table I. The mutant *p5cdh* T-DNA line (Salk\_018453) has been previously described (Deuschle et al. 2004).

Surface-sterilized seeds of *Arabidopsis* wild-type (Col0) and mutant lines were sown onto grids placed on half-strength agar-solidified Murashige and Skoog (MS) medium in square Petri dishes according to Thiery et al. (2004). After 24 h at 4°C to break dormancy, seedlings were allowed to grow at 22°C under continuous light (90 μmol photons m<sup>-2</sup> s<sup>-1</sup>). Fifteen-day-old *Arabidopsis* seedlings were exposed to proline or to water as control for 24 h.

For root growth assays, 24 h old-seedlings were transferred onto agar-solidified MS/2 medium supplied or not with proline and then were cultivated in growth chamber under a 16 h light (90 μmol m<sup>-2</sup> s<sup>-1</sup>)/ 8 h dark cycle at 22°C. Treatments with up to 10 mM proline were used for root growth assays and 50 mM proline for biochemical and proteomic analysis.

*Mitochondria isolation and subfractionation*

Mitochondria were isolated at 4°C from leaves of 15 day-old Arabidopsis plantlets. 50 g of fresh leaves were used for purification to undergo respiratory measurements and 130 g for purification on Percoll gradients to undergo subcellular ProDH localization. Leaves were ground in a blender with three volumes of grinding buffer (sucrose 0.3 M, KH<sub>2</sub>PO<sub>4</sub> 10 mM, Na<sub>4</sub>-pyrophosphate 25 mM, Na-ascorbate 20 mM, EDTA 2 mM, PVP 40 1%, PMF 0.2 mM and BSA 1% ; pH 7.5), filtered onto miracloth and blutex filters, then a cycle of two steps differential centrifugations were performed as follows: contaminants were pelleted with a 2,500xg centrifugation for 5 min and mitochondria contained in the supernatant were sedimented by a 15 000xg centrifugation for 20 minutes. Pellets of crude mitochondria were resuspended in washing buffer (sucrose 0.3 M, TES buffer 10 mM, BSA FFA 0.1%, pH 7.5), aggregates were destroyed using a Potter homogenizer. Crude mitochondria were washed using one more cycle as describe above.

For respiratory measurements, mitochondria were washed again with another cycle of two steps differential centrifugations process and BSA removed by several high-speed sedimentation steps (15,000xg) in washing buffer without BSA.

For protein subcellular localization, mitochondria were purified on a 5 steps Percoll gradient (80%, 40%, 30%, 20% and 15% in washing buffer without BSA) by ultra-centrifugation at 15,000xg for at least 45 minutes. Highly purified mitochondria were found at the 40%/30% interphase, carefully removed and diluted up to 100 time. Percoll was eliminated by several centrifugations at 15,000xg during 15 min until getting well aggregate pellets. BSA was then removed by additional 15,000xg sedimentation steps in washing buffer depleted in BSA. Whatever the purification level, mitochondrial protein concentration was determined according to Lowry et al. (1951) using bovine serum albumin (BSA) as a standard.

Matrix and membrane fractions of Percoll gradient-purified mitochondria were separated as previously described in Sunderhaus et al. (2006) with some modifications. Mitochondria were resuspended in a sonication buffer (10mM TES, 1 mM EDTA, 1 mM EGTA and 0.2 mM PMSF, pH 7.2) at 1 mg/mL protein concentration. 1.5 mL of mitochondria was broken by three freeze-thaw cycles and 4 sonication steps during 16 seconds using a Branson Sonifier 250. Unbroken mitochondria were sedimented by 7 min centrifugation at 5,000xg and discarded. The supernatant was then centrifuged 100 min at 140,000xg in a 70 Ti rotor. The resulting pellet containing mitochondrial membranes was resuspended in sonication buffer. The soluble fraction corresponding to matrix and inter-membrane space compartments was precipitated using pure acetone. Proteins were then centrifuged for 1 h at maximum speed in a

bench centrifuge. Pellets were resuspended in sonication buffer. Proteins were further analysed by western blots.

### *Respiratory measurements*

Oxygen consumption were performed on isolated mitochondria using a Clark-type O<sub>2</sub> electrode system (Hansatech, Norfolk, United Kingdom) in a stirred temperature-controlled (25°C) 1 ml reaction buffer (sucrose 0.3 M ; KH<sub>2</sub>PO<sub>4</sub> 5 mM ; TES buffer 10 mM pH 7.2; KCL 10 mM ; MgSO<sub>4</sub> 2 mM, BSA FFA 0.1 %). Each assay contained 300 µg mitochondrial proteins. Respiratory substrates were used at final concentrations as follows: 1 mM NADH, 10 mM succinate, 6 mM L-(D- or hydroxy-) proline. Alternative oxidase capacity was obtained in the presence of 1 mM KCN and by adding 1 mM DTT and 5 mM pyruvate. CytC dependent O<sub>2</sub> uptake was specifically inhibited by 1 mM cyanid while AOX pathway was inhibited by 0.5 mM n-propyl gallate. RCR and ADP/O ratios were measured as previously described in Hourton-Cabassa *et al.* (2009). State 3 rates are oxidation rates under phosphorylating conditions (in the presence of ADP), state 4 rates are oxidation rates under non phosphorylating conditions (lack of ADP), RCR is the respiratory control rate (state 3 rate /state 4 rate) which provides indications about the ability of the respiratory chain to readjust its electron flow with the ADP content and ADP/O ratio which represents the phosphorylating yield of the chain by measuring the quantity of molecular oxygen necessary to consume all the ADP added. The CytC rate represents the quantity of electron flow directed to the Cytochrome pathway by calculating the state 4 rate minus the remaining oxidation rate measured in the presence of cyanide, a CytC oxidase specific inhibitor. AOX capacity was also checked in the presence of cyanide, pyruvate and DTT to fully reduce and activate AOX enzymes.

### *ProDH immunodetection*

Mitochondria were resuspended in Laemmli buffer containing freshly added β-mercaptoethanol. Proteins were separated by SDS-PAGE in 11 % (v/v) polyacrylamide gels and transferred to nitrocellulose membranes (Bio-Rad) in a Trans-Blot Semi-Dry Electrophoretic Transfer Cell (Bio-Rad) for 30 min at 135 mA using transfer buffer (25 mM Tris, 192 mM glycine, 20 % v/v methanol, pH 8.3). Equal protein loading and integrity of protein samples were checked by Ponceau S red staining of the blot membrane. For immunodetection, the nitrocellulose filter was incubated in TBS (TBS-T) with 5% non-fat dry milk and 0.05% (v/v) Tween 20 for 30 minutes at room temperature and then in TBS-T with

1:1000 ProDH antibody overnight at 4°C. Antibodies raised against ProDH were obtained by rabbits immunization with AtProDH1 (amino acids 1–522) as described in Thiery et al. (2004). The secondary antibody, an anti-rabbit horseradish peroxidase conjugate was diluted at 1:4000. ProDH was detected with a chemiluminescence detection kit ECL prime from GE Healthcare (France).

*Blue native / SDS PAGE and molecular identification of ProDH1*

Molecular identification of ProDH of Arabidopsis was carried out using mitochondria isolated from either Arabidopsis seedlings (growth conditions see above) or from Arabidopsis cell cultures (for details see Schertl et al. (2014)). Mitochondrial proteins were separated by BN / SDS PAGE (according to Wittig et al. (2006); experimental parameters as given in Klodmann et al. (2011)). The 2D gels were either Coomassie-stained (Neuhoff et al., 1988), or used for Western Blotting and immunodetection experiments (as described above). Tryptic digestion of the selected proteins was carried out as highlighted in Klodmann et al. (2010). Analyses of the extracted peptides were carried out by tandem mass spectrometry using a micrOTOF Q-II mass spectrometer (Bruker, Bremen, Germany) as described previously (Klodmann et al. 2011).

**LITERATURE CITED**

- Alonso JM, Stepanova AN, Leisse TJ, Kim CJ, Chen H, Shinn P, Stevenson DK, Zimmerman J, Barajas P, Cheuk R, Gadrinab C, Heller C, Jeske A, Koesema E, Meyers CC, Parker H, Prednis L, Ansari Y, Choy N, Deen H, Geralt M, Hazari N, Hom E, Karnes M, Mulholland C, Ndubaku R, Schmidt I, Guzman P, Aguilar-Henonin L, Schmid M, Weigel D, Carter DE, Marchand T, Risseuw E, Brogden D, Zeko A, Crosby WL, Berry CC, Ecker JR (2003) Genome-wide insertional mutagenesis of *Arabidopsis thaliana*. *Science* 301: 653-657
- Auerswald L, Schneider P, Gäde G (1998) Proline powers pre-flight warm-up in the African fruit beetle *Pachnoda sinuata* (Cetoniinae). *JEB* 201: 1651-1657
- Baerenfaller K, Grossmann J, Grobei MA, Hull R, Hirsch-Hoffmann M, Yalovsky S, Zimmermann P, Grossniklaus U, Gruissem W, Baginsky S (2008) Genome-scale proteomics reveals *Arabidopsis thaliana* gene models and proteome dynamics. *Science* 320: 938-941
- Ben Rejeb K, Abdelly C, Sauré A. (2014) How reactive oxygen species and proline face stress together. *PPB* 80: 278-84
- Cecchini NM, Monteoliva MI, Alvarez ME. (2011) Proline dehydrogenase contributes to pathogen defense in *Arabidopsis*. *Plant Physiol* 155:1947-59
- Cecchini NM, Monteoliva MI, Alvarez ME. (2011) Proline dehydrogenase is a positive regulator of cell death in different kingdoms. *Plant Signal Behav* 6:1195-7
- Boggess SF, Koeppe DE, Stewart CR (1978) Oxidation of proline by plant mitochondria. *Plant Physiol* 62: 22-25
- Deuschle K, Funck D, Hellmann H, Däschner K, Binder S, Frommer WB (2001) A nuclear gene encoding mitochondrial Delta-pyrroline-5-carboxylate dehydrogenase and its potential role in protection from proline toxicity. *Plant J* 27: 345-56
- Deuschle K, Funck D, Forlani G, Stransky H, Biehl A, Leister D, van der Graaff E, Kunze R, Frommer WB (2004) The role of delta-1-pyrroline-5-carboxylate dehydrogenase in proline degradation. *Plant Cell* 16: 3413-3425
- Elthon TE, Stewart CR (1981) Submitochondrial location and electron transport characteristics of enzymes involved in proline oxidation. *Plant Physiol* 67: 780-784
- Foreman J, Demidchik V, Bothwell JH, Mylona P, Miedema H, Torres MA, Linstead P, Costa S, Brownlee C, Jones JD, et al (2003) Reactive oxygen species produced by NADPH oxidase regulate plant cell growth. *Nature* 422: 442-446
- Funck D, Eckard S, Muller G (2010) Non-redundant functions of two proline dehydrogenase isoforms in *Arabidopsis*. *BMC Plant Biol* 10: 70
- Hanson J, Hanssen M, Wiese A, Hendriks MM and Smeekens S (2008) The sucrose regulated transcription factor bZIP11 affects amino acid metabolism by regulating the expression of *ASPARAGINE SYNTHETASE1* and *PROLINE DEHYDROGENASE2*. *Plant J* 53: 935-949

- Heazlewood JL, Tonti-Filippini JS, Gout AM, Day DA, Whelan J, Millar AH (2004) Experimental analysis of the *Arabidopsis* mitochondrial proteome highlights signaling and regulatory components, provides assessment of targeting prediction programs, and indicates plant-specific mitochondrial proteins. *Plant Cell* 16: 241-256
- Hourton-Cabassa C, Matos AR, Arrabaça J, Demandre C, Zachowski A, Moreau F (2009) Genetically modified *Arabidopsis thaliana* cells reveal the involvement of mitochondrial fatty acid composition in membrane basal and uncoupling protein mediated proton leaks. *Plant Cell Physiol* 50: 2084-2091
- Huang AH, Cavalieri AJ (1979) Proline oxidase and water stress-induced proline accumulation in spinach leaves. *Plant Physiol* 63: 531-535
- Keech O, Dizengremel P, Gardeström P (2005) Preparation of leaf mitochondria from *Arabidopsis thaliana*. *Physiologia Plantarum* 124: 403-409
- Kiyosue T, Yoshida Y, Yamaguchi-Shinozaki K, Shinozaki K (1996) A nuclear gene encoding mitochondrial proline dehydrogenase, an enzyme involved in proline metabolism, is upregulated by proline but downregulated by dehydration in *Arabidopsis*. *Plant Cell* 8: 1323-1335
- Kleffmann T, Russenberger D, von Zychlinski A, Christopher W, Sjölander K, Grissem W, Baginsky S (2004) The *Arabidopsis thaliana* chloroplast proteome reveals pathway abundance and novel protein functions. *Current Biology* 14: 354-362
- Kleinboelting N, Huet G, Kloetgen A, Viehovec P, Weisshaar B (2012) GABI-Kat SimpleSearch: new features of the *Arabidopsis thaliana* T-DNA mutant database. *Nucleic Acids Res* 40 (Database issue): D1211-1215
- Klodmann J, Sunderhaus S, Nimtz M, Jansch L, Braun HP (2010) Internal architecture of mitochondrial complex I from *Arabidopsis thaliana*. *Plant Cell* 22: 797-810
- Klodmann J, Senkler M, Rode C, Braun HP (2011) Defining the protein complex proteome of plant mitochondria. *Plant Physiol* 157: 587-598
- Kruft V, Eubel H, Jansch L, Werhahn W, Braun HP (2001) Proteomic approach to identify novel mitochondrial proteins in *Arabidopsis*. *Plant Physiol* 127: 1694-1710
- Kwak JM, Mori IC, Pei ZM, Leonhardt N, Torres MA, Dangl JL, Bloom RE, Bodde S, Jones JD, Schroeder JI (2003) NADPH oxidase *AtrbohD* and *AtrbohF* genes function in ROS-dependent ABA signaling in *Arabidopsis*. *EMBO J* 22: 2623-2633
- Lowry OH, Rosenbrough HJ, Farr AL, Randall RJ (1951) Protein measurements with the Folin phenol reagent. *J Biol Chem* 193: 265-275
- Mani S, Van De Cotte B, Van Montagu M, Verbruggen N (2002) Altered levels of proline dehydrogenase cause hypersensitivity to proline and its analogs in *Arabidopsis*. *Plant Physiol* 128: 73-83
- Millar AH, Sweetlove LJ, Giegé P, Leaver CJ (2001) Analysis of the *Arabidopsis* mitochondrial proteome. *Plant Physiol* 127: 1711-1727
- Miller G, Honig A, Stein H, Suzuki N, Mittler R, Zilberstein A (2009) Unraveling delta1-

---

pyrroline-5-carboxylate-proline cycle in plants by uncoupled expression of proline oxidation enzymes. *J Biol Chem* 284: 26482-26492

Monteoliva MI, Rizzi YS, Cecchini NM, Hajirezaei MR, Alvarez ME (2014) Context of action of proline dehydrogenase (ProDH) in the Hypersensitive Response of Arabidopsis. *BMC Plant Biol* 13: 14:21

Nakashima K, Satoh R, Kiyosue T, Yamaguchi-Shinozaki K, Shinozaki K (1998) A gene encoding proline dehydrogenase is not only induced by proline and hypoosmolarity, but is also developmentally regulated in the reproductive organs of Arabidopsis. *Plant Physiol* 118: 1233-1241

Nanjo T, Fujita M, Seki M, Kato T, Tabata S, Shinozaki K (2003) Toxicity of free proline revealed in an Arabidopsis T-DNA-tagged mutant deficient in proline dehydrogenase. *Plant Cell Physiol* 44: 541-548

Neuhoff V, Arold N, Taube D, Ehrhardt W (1988) Improved staining of proteins in polyacrylamide gels including isoelectric focusing gels with clear background at nanogram sensitivity using Coomassie Brilliant Blue G-250 and R-250. *Electrophoresis* 9: 255-262

Ostrander EL, Larson JD, Schuermann JP, Tanner JJ (2009) A conserved active site tyrosine residue of proline dehydrogenase helps enforce the preference for proline over hydroxyproline as the substrate. *Biochemistry* 48: 951-959

Peng Z, Lu Q, Verma DP (1996) Reciprocal regulation of delta 1-pyrroline-5-carboxylate synthetase and proline dehydrogenase genes controls proline levels during and after osmotic stress in plants. *Mol Gen Genet* 253: 334-341

Scaraffia PY, Wells MA (2003) Proline can be utilized as an energy substrate during flight of *Aedes aegypti* females. *Journal of Insect Physiology* 49: 591-601

Schertl P, Braun HP (2014) Respiratory electron transfer pathways in plant mitochondria. *Front Plant Sci* 5: 163

Schertl P, Cabassa C, Saadallah K, Bordenave M, Savouré A, Braun HP (2014) Biochemical characterization of proline dehydrogenase in Arabidopsis mitochondria. *FEBS J* 281: 2794-2804

Servet C, Ghelis T, Richard L, Zilberstein A, Savouré A (2012). Proline dehydrogenase: a key enzyme in controlling cellular homeostasis. *Font Biosci* 17: 607-620

Singh H, Arentson BW, Becker DF, Tanner JJ (2014) Structures of the PutA peripheral membrane flavoenzyme reveal a dynamic substrate-channeling tunnel and the quinone-binding site. *Proc Natl Acad Sci U S A* 111: 3389-3394

Sunderhaus S, Dudkina NV, Jansch L, Klodmann J, Heinemeyer J, Perales M, Zabaleta E, Boekema EJ, Braun HP (2006) Carbonic anhydrase subunits form a matrix-exposed domain attached to the membrane arm of mitochondrial complex I in plants. *J Biol Chem* 281: 6482-6488



- Szabados L, Savouré A (2010) Proline: a multifunctional amino acid. *Trends Plant Sci* 15: 89-97
- Szekely G, Abraham E, Cseplo A, Rigo G, Zsigmond L, Csiszar J, Ayaydin F, Strizhov N, Jasik J, Schmelzer E, Koncz C, Szabados L (2008) Duplicated *P5CS* genes of *Arabidopsis* play distinct roles in stress regulation and developmental control of proline biosynthesis. *Plant J* 53: 11-28
- Tanner JJ (2008) Structural biology of proline catabolism. *Amino Acids* 35: 719-30
- Thiery L, Leprince AS, Lefebvre D, Ghars MA, Debarbieux E, Savouré A (2004) Phospholipase D is a negative regulator of proline biosynthesis in *Arabidopsis thaliana*. *J Biol Chem* 279: 14812–14818
- Van Aken O, Zhang B, Carrie C, Uggalla V, Paynter E, Giraud E, Whelan J (2009) Defining the Mitochondrial Stress Response in *Arabidopsis thaliana*. *Mol Plant* 2: 1310- 24
- Verbruggen N, Hua XJ, May M, Van Montagu M (1996) Environmental and developmental signals modulate proline homeostasis: evidence for a negative transcriptional regulator. *Proc Natl Acad Sci USA* 93: 8787-91
- Wanduragala S, Sanyal N, Liang X, Becker DF (2010) Purification and characterization of Put1p from *Saccharomyces cerevisiae*. *Arch Biochem Biophys* 498: 136-142
- Weltmeier F, Ehlert A, Mayer CS, Dietrich K, Wang X, Schutze K, Alonso R, Harter K, Vicente-Carbajosa J, Droge-Laser W (2006) Combinatorial control of *Arabidopsis* proline dehydrogenase transcription by specific heterodimerisation of bZIP transcription factors. *EMBO J* 25: 3133-3143
- Wittig I, Braun HP, Schägger H (2006) Blue native PAGE. *Nat Protoc* 1: 418-428

### Figure legends

Figure 1: Molecular characterization of the *Arabidopsis prodh* mutants. A. Map of T-DNA insertion loci in four mutant lines with the primer references used for genotyping. Primers are listed in supplemental table I. Gray box indicates the promoter region, white and black boxes represent the 5' and 3' untranslated regions and coding exons respectively, dash lines show intron regions. *prodh1-3* and *prodh1-4* carried inverted T-DNA tandem repeats. B. Genomic DNAs were extracted from either wild-type Col0 (wt), *prodh1-3*, *prodh1-4*, *prodh2-2* or *prodh2-3* seedlings and PCR products were separated in a 0.8 % agarose gel. C. Western blot analysis of ProDH content was performed on mitochondria isolated from 15 day-old wild-type, *prodh1-3*, *prodh1-4*, *prodh2-2* or the double mutant *prodh1-4prodh2-2* (*p1xp2*) seedlings non-treated or treated with 50 mM L-proline for 24 h.

Figure 2: Growth response of wild-type (WT), *prodh1-4*, *prodh2-2* and *prodh1-4/prodh2-2* seedlings to proline. A. Photographs of 12 days-old wild-type Col0 (WT), *prodh1-4*, *prodh2-2* and *prodh1-4/prodh2-2* seedlings grown on medium without or with 10 mM proline (P). B. Primary root elongation of WT, *prodh1-4*, *prodh2-2* and *prodh1-4/prodh2-2* seedlings grown on medium without (0 mM) or with 1 mM, 5 mM or 10 mM proline for 4, 8 and 12 days. For B, data shown are means of four to five independent experiments including each 12 plants. Small letters represent significant differences compared to the WT as indicated by an unpaired *t* test (a :  $P < 0,05$ ; b :  $P < 0,01$ ).

Figure 3: ProDH activity in wild-type and in *prodh1-4*, *prodh2-2* and *prodh1-4prodh2-2* (*p1xp2*) mutants treated with proline. Crude mitochondria were purified from 15 days-old plants treated with 50 mM L-proline for 24 h. ProDH activity measurements were performed using 2,6-dichlorindophenol (DCIP) as an electron acceptor. Standard errors are based on at least three biological replicates.

Figure 4: ProDH is associated with mitochondrial membranes. Mitochondria were purified from 15 days-old seedlings treated for 24 h with 0.1M L-proline using a Percoll density gradient ultra centrifugation. Mitochondrial membrane (MB) and soluble (S) fractions were then separated by SDS PAGE (10  $\mu$ g of each fraction per lane). Western Blots shown in A, B and C were probed with IgGs directed against ProDH, the adenine nucleotide translocase (ANT) or the isocitrate dehydrogenase (ICDH) as indicated.

Figure 5: Immunological identification of ProDH1 in mitochondrial fractions of proline-treated *Arabidopsis* cells. Total mitochondrial proteins of proline treated / untreated cells were separated by 2D blue native / SDS PAGE. Proteins were either Coomassie stained (top) or blotted onto nitrocellulose (bottom). Blots were developed using an antibody directed against ProDH from *Arabidopsis*. Molecular masses of standard proteins are given to the left (in kDa), identities of the OXPHOS complexes are indicated above the gels. I+III<sub>2</sub>: supercomplex formed of complexes I and dimeric complex III; I: complex I; V: complex V; III<sub>2</sub>: dimeric complex III; F<sub>1</sub>: F<sub>1</sub> part of complex V; IV: complex IV; II: complex II. The lipamide dehydrogenase (L protein of the glycine dehydrogenase complex; mtLPD) is indicated on the gels.

Figure 6. ProDH1 is strongly induced upon proline treatment in *Arabidopsis*. Total mitochondrial protein of proline treated / untreated cells was separated by 2D blue native / SDS PAGE and blotted onto nitrocellulose. The blot was incubated with antibodies directed against *Arabidopsis* ProDH. Immune signals were visualized after 2, 5, 120 and 300 seconds.

Figure 7: Identification of ProDH1 by mass spectrometry. Total mitochondrial protein of proline-treated *Arabidopsis* cells was separated by 2D Blue native / SDS PAGE and Coomassie-stained (A). Four gel spots were cut out from the gel at positions corresponding to ProDH signals obtained on a parallel immunoblot (B) and analysed by mass spectrometry (C).

Figure 8: Peptides of ProDH1 identified by mass spectrometry. Top: amino acid sequence of ProDH1 with the location of the corresponding peptides. Bottom: Peptides identified within spots 1-4 (as indicated on Figure 7).

Table I: Respiratory parameters of L-proline-treated wild-type and *p5cdh* and *prodh* mutant seedlings measured using isolated mitochondria. Crude mitochondria were obtained from 15 days-old seedlings of either wild-type, *p5cdh*, *prodh1-3*, *prodh1-4*, *prodh2-2* or *prodh2-3* genotypes treated without (NT) or with 50 mM L-proline (Pro) for 24 h. Respiratory rates are expressed in nmol O<sub>2</sub> min<sup>-1</sup> mg protein<sup>-1</sup> and are the mean of at least three biological replicates for wild-type and *p5cdh* genotypes for each condition. For *prodh1* and *prodh2*, results correspond to a mean of three independent experiments for each *prodh1-4* and *prodh1-3* mutants and for each *prodh2-2* and *prodh2-3* mutants, respectively. “State 3” and “state 4” respiration represent phosphorylation and non-phosphorylation modes of the respiratory chain

(ADP sufficiently present *versus* not present), respectively. CytC rate and AOX capacity were determined in the presence of KCN and SHAM, which block one or the other respiratory electron transfer pathway. RCR is the respiratory coupling rate (state3/state4 rate) and ADP/O is the phosphorylation yield.

Supplemental Figure 1. Proline treatment increases ProDH content in seedlings. Mitochondria were purified from 15 day-old Col0 seedlings non treated (1) or treated with 50 mM L-proline (2) for 24 h. A and B, Western blot analysis of ProDH content using 40 µg of mitochondrial proteins. B, ProDH antibody were used in competition with a purified ProDH1 recombinant protein. Ponceau stainings of the corresponding blots are presented on the right. The masses of standard proteins are given in kDa.

Supplemental Figure 2. Root architecture analysis in wild-type and *prodh* mutants in response to exogenously applied proline. A. Mean number of secondary roots of WT, *prodh1-4*, *prodh2-2* and *prodh1-4/prodh2-2* seedlings after 12 days of growth on medium without or with 1mM, 5 mM or 10 mM proline. B. Root density of WT, *prodh1-4*, *prodh2-2* and *prodh1-4/prodh2-2* seedlings after 12 days of growth on medium without (0 mM) or with 1mM, 5 mM or 10 mM proline. Root density was calculated for each plant as the ratio of the number of secondary root /length of the primary root. For A and B, data shown are means of four to five independent experiments including each 12 plants. Small letters represent significant differences compared to the WT as indicated by an unpaired *t* test (a :  $P < 0,05$ ; b :  $P < 0,01$ ).

Supplemental Figure 3. Respiratory measurement of isolated mitochondria from Arabidopsis. Primary experimental results using either a combination of NADH and succinate (A: NADH + Succ) or L-proline (B) or D-proline (C) as respiratory substrates. ADP, adenosine diphosphate; DTT, dithiothreitol; KCN, potassium cyanide; MP, purified mitochondria; PG, propyl gallate.

Supplemental Figure 4. Molecular characterization of *p5cdh* mutant. A. Map of the T-DNA insertion in the *p5cdh* mutant. Representation of the gene is the same as in figure 1. B. PCR genotyping of *p5cdh* using genomic DNA isolated from either wild-type or *p5cdh* seedlings. PCR products were separated on a 0.8 % agarose gel. C. Western blot using mitochondria isolated from *p5cdh* and wild-type seedlings treated with 50 mM proline for 24 h.

Supplemental Figure 5. Immunological identification of ProDH1 in mitochondrial fractions isolated from 15-days old Arabidopsis seedlings either treated or not treated with 50 mM proline for 24 h. Total mitochondrial proteins were separated by 2D Blue native / SDS PAGE. Proteins were either Coomassie stained (top) or blotted onto nitrocellulose (bottom). Blots were developed using an antibody directed against ProDH from Arabidopsis and immune signals were visualized after 2, 30 and 60 minutes.

Supplemental Table I. List of the primers used for genotyping the different *prodh* and *p5cdh* mutants.

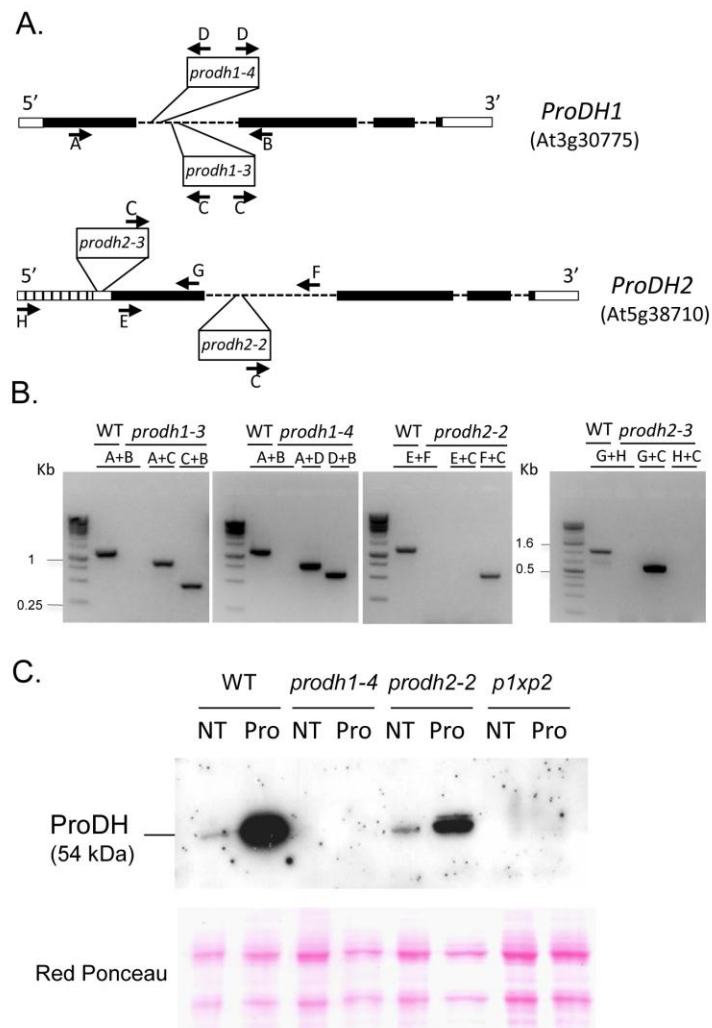


Figure 1: Molecular characterization of the *Arabidopsis prodh* mutants. A. Map of T-DNA insertion loci in four mutant lines with the primer references used for genotyping. Primers are listed in supplemental table I. Dash boxes indicate the promoter regions, dash lines show intron regions, boxes represent the 5' and 3' untranslated regions (white) and coding exons (black). *prodh1-3* and *prodh1-4* carried inverted T-DNA tandem repeats. B. Genomic DNAs were extracted from either wild-type Col0 (wt), *prodh1-3*, *prodh1-4*, *prodh2-2* or *prodh2-3* seedlings and PCR products were separated in a 0.8 % agarose gel. C. Western blot analysis of ProDH content was performed on mitochondria isolated from 15 day-old wild-type, *prodh1-3*, *prodh1-4*, *prodh2-2* or the double mutant *prodh1-4prodh2-2* (*p1xp2*) seedlings non-treated or treated with 50 mM L-proline for 24 h.

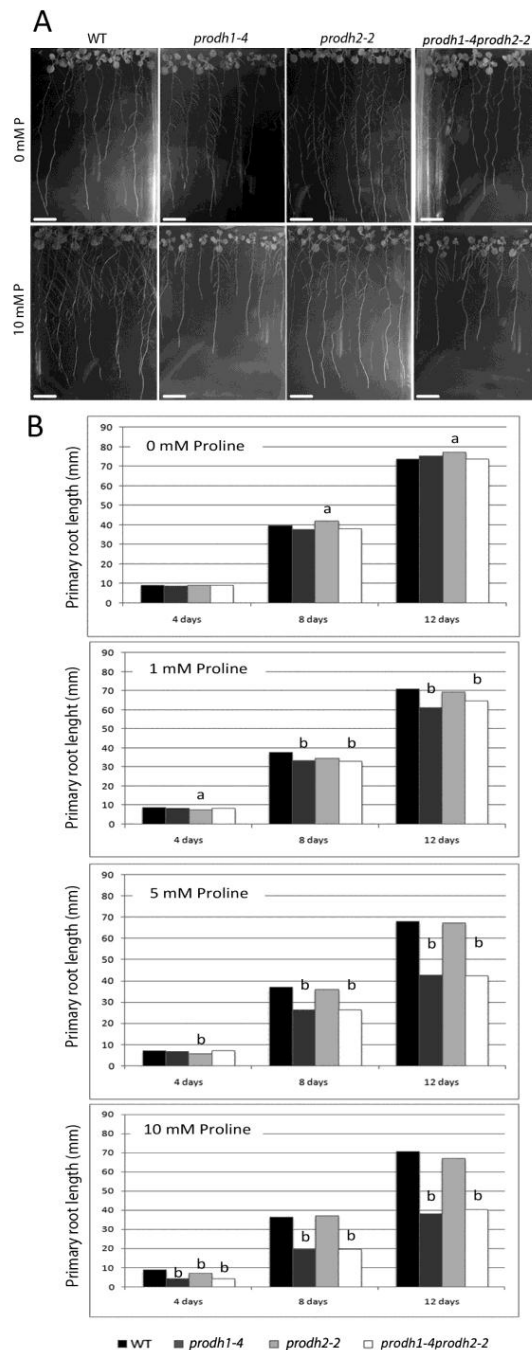


Figure 2: Growth response of wild-type (WT), *prodh1-4*, *prodh2-2* and *prodh1-4/prodh2-2* seedlings to proline. A. Photographs of 12 days-old wild-type Col0 (WT), *prodh1-4*, *prodh2-2* and *prodh1-4/prodh2-2* seedlings grown on medium without or with 10 mM proline (P). B. Primary root elongation of WT, *prodh1-4*, *prodh2-2* and *prodh1-4/prodh2-2* seedlings grown on medium without (0 mM) or with 1 mM, 5 mM or 10 mM proline for 4, 8 and 12 days. For B, data shown are means of four to five independent experiments including each 12 plants. Small letters represent significant differences compared to the WT as indicated by an unpaired *t* test (a :  $P < 0,05$ ; b :  $P < 0,01$ ).

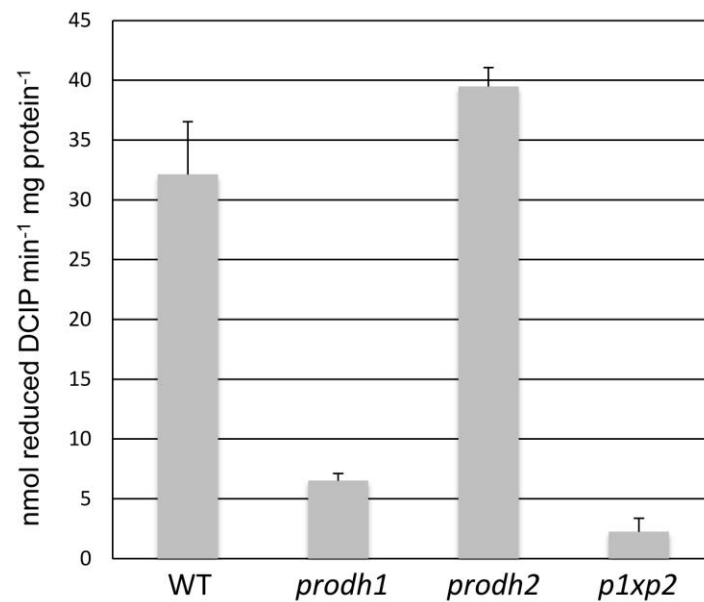


Figure 3: ProDH activity in wild-type and in *prodh1-4*, *prodh2-2* and *prodh1-4prodh2-2* (*p1xp2*) mutants treated with proline. Crude mitochondria were purified from 15 days-old plants treated with 50 mM L-proline for 24 h. ProDH activity measurements were performed using 2,6-dichlorindophenol (DCIP) as an electron acceptor. Standard errors are based on at least three biological replicates.



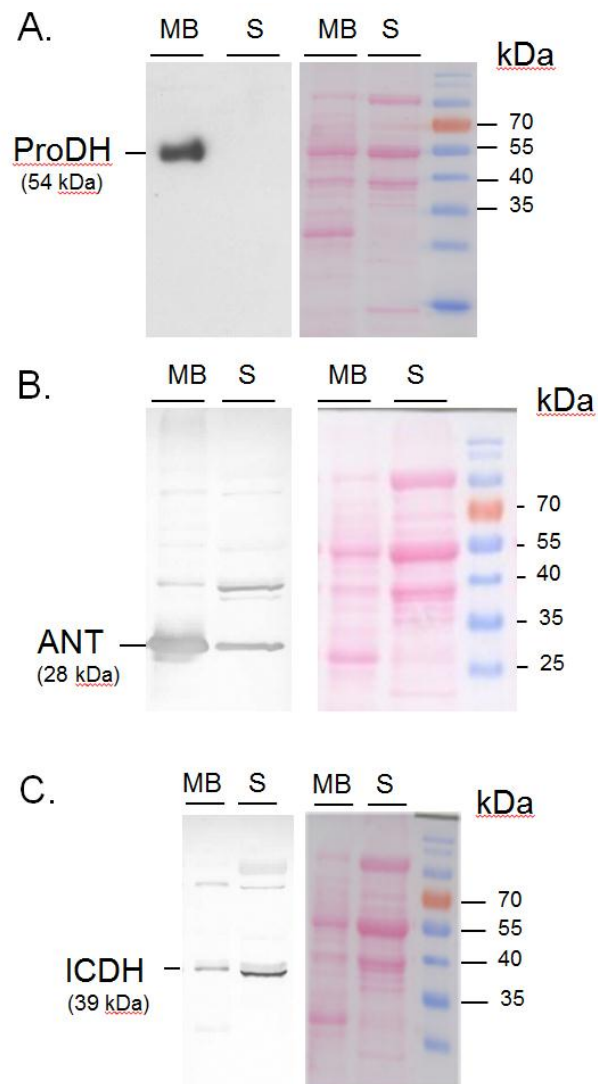


Figure 4: ProDH is associated with mitochondrial membranes. Mitochondria were purified from 15 days-old seedlings treated for 24 h with 0.1M L-proline using a Percoll density gradient ultra centrifugation. Mitochondrial membrane (MB) and soluble (S) fractions were then separated by SDS PAGE (10  $\mu$ g of each fraction per lane). Western Blots shown in A, B and C were probed with IgGs directed against ProDH, the adenine nucleotide translocase (ANT) or the isocitrate dehydrogenase (ICDH) as indicated.

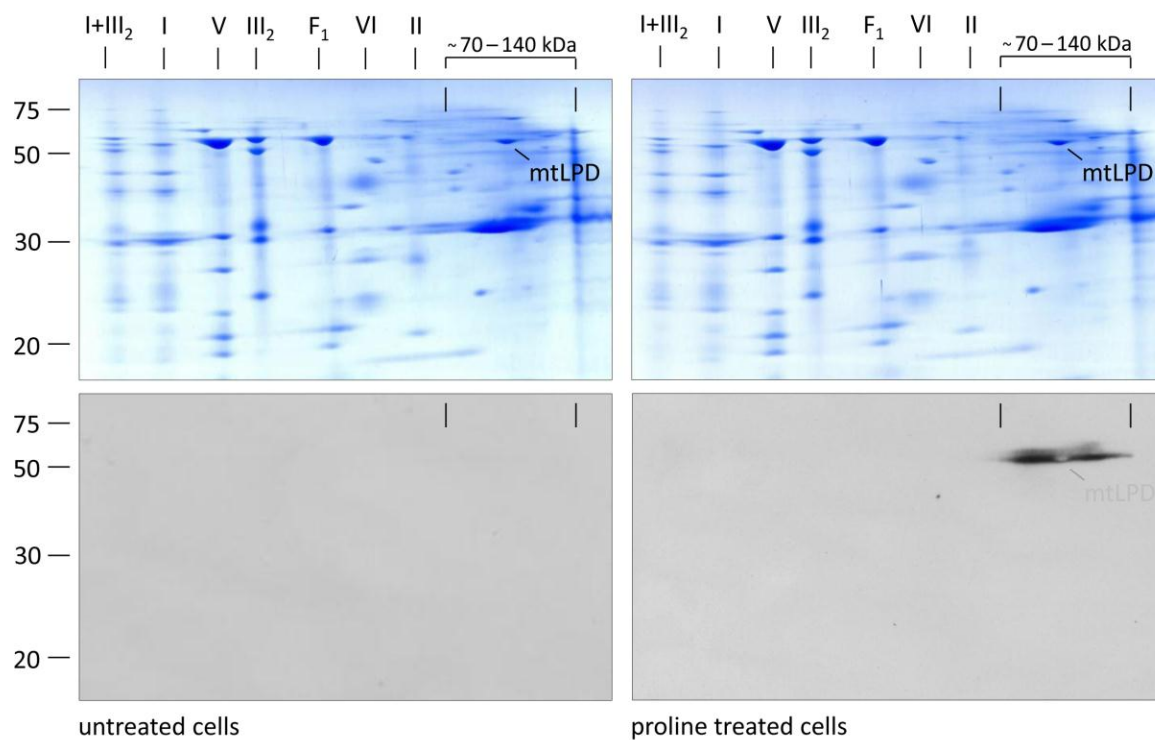


Figure 5: Immunological identification of ProDH1 in mitochondrial fractions of proline-treated Arabidopsis cells. Total mitochondrial proteins of proline treated / untreated cells were separated by 2D blue native / SDS PAGE. Proteins were either Coomassie stained (top) or blotted onto nitrocellulose (bottom). Blots were developed using an antibody directed against ProDH from Arabidopsis. Molecular masses of standard proteins are given to the left (in kDa), identities of the OXPHOS complexes are indicated above the gels. I+III<sub>2</sub>: supercomplex formed of complexes I and dimeric complex III; I: complex I; V: complex V; III<sub>2</sub>: dimeric complex III; F<sub>1</sub>: F<sub>1</sub> part of complex V; IV: complex IV; II: complex II. The lipoamide dehydrogenase (L protein of the glycine dehydrogenase complex; mtLPD) is indicated on the gels.

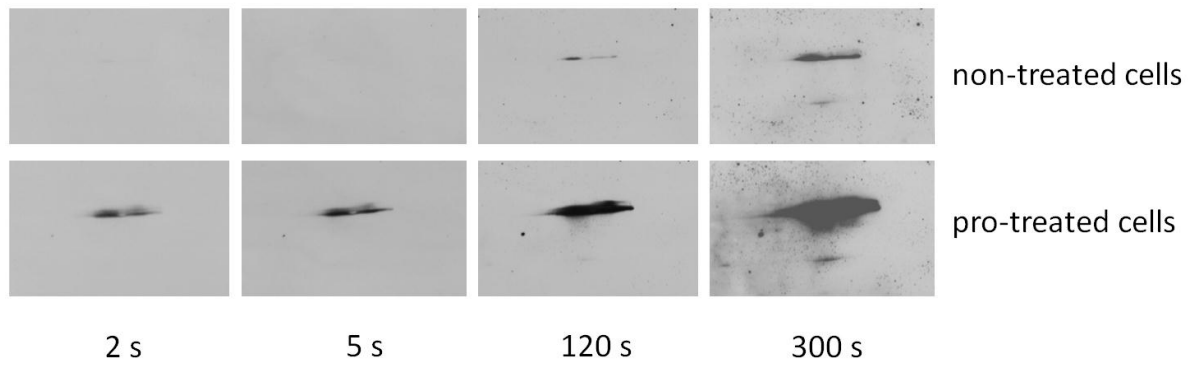


Figure 6. ProDH1 is strongly induced upon proline treatment in Arabidopsis. Total mitochondrial protein of proline treated / untreated cells was separated by 2D blue native / SDS PAGE and blotted onto nitrocellulose. The blot was incubated with antibodies directed against Arabidopsis ProDH. Immune signals were visualized after 2, 5, 120 and 300 seconds.

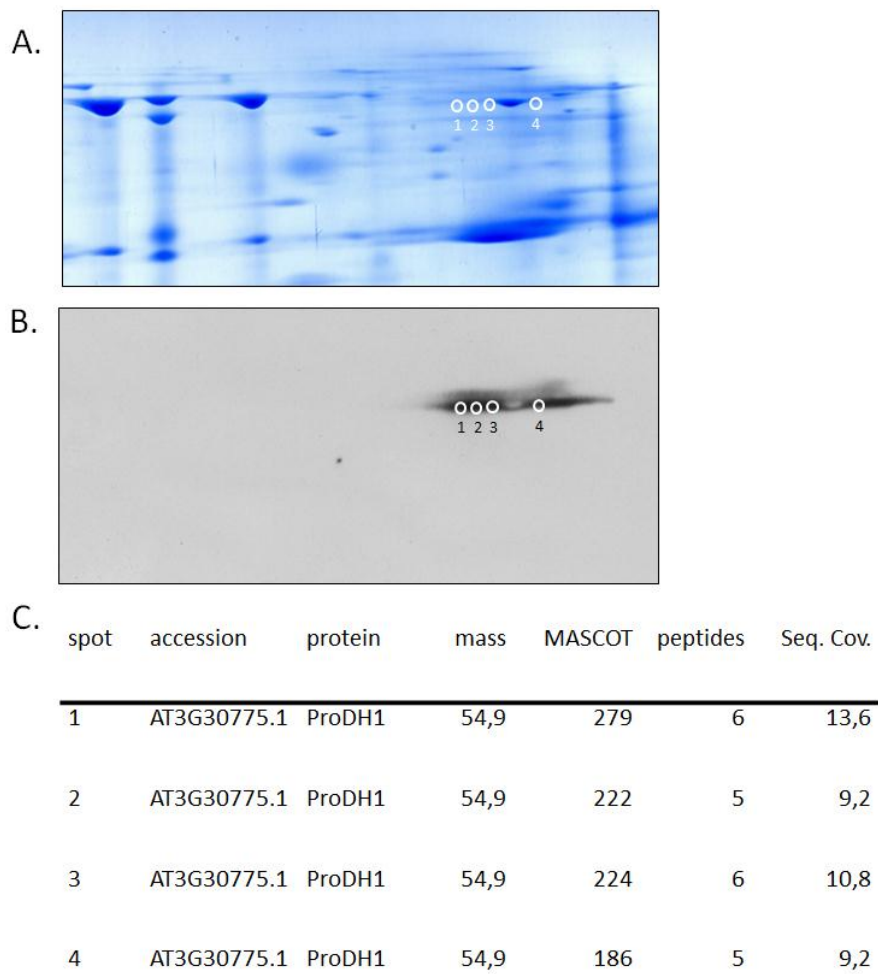


Figure 7: Identification of ProDH1 by mass spectrometry. Total mitochondrial protein of proline-treated *Arabidopsis* cells was separated by 2D Blue native / SDS PAGE and Coomassie-stained (A). Four gel spots were cut out from the gel at positions corresponding to ProDH signals obtained on a parallel immunoblot (B) and analysed by mass spectrometry (C).

MATRLLRRTNF	IRRSYRLPAF	SPVGPPTVTA	STAVVPEILS	FGQQAPEPPL
HHPKPTEQSH	DGLDLSQAR	LFSS IPTSDL	LRSTAVLHAA	AIGPMVDLGT
WVMSSK LMDA	SVTRGMVLGL	VKSTFYDHFC	AGEDADAAAE	RVRSVYEATG
LKGM LVYGVE	HADDAVSCDD	NMQQFIRTIE	AAKSLPTSHF	SSVVVKITAI
CPISLLKRVS	DLLRWEYKSP	NFKLSWKLKS	FPVFSESSPL	YHTNSEPEPL
TAEERELEA	AHGRIQEICR	KCQESNVPLL	IDAEDTILQP	AIDYMAYSSA
IMFNADKDRP	IVYNTIQAYL	RDAGERLHLA	VQNAEKENVP	MGFKLV RGAY
MSSEASLADS	LGCKSPVHDT	IQDTHSCYND	CMTFLMEKAS	NGSGFGV VLA
THNADSGRLA	SRKASDLGID	KQNGKIEFAQ	LYGMSDALS F	GLKRAGFNVS
KYMPFGPVAT	AIPYLLRRAY	ENRGM MATGA	HDRQLMRMEL	KRRLIAGIA

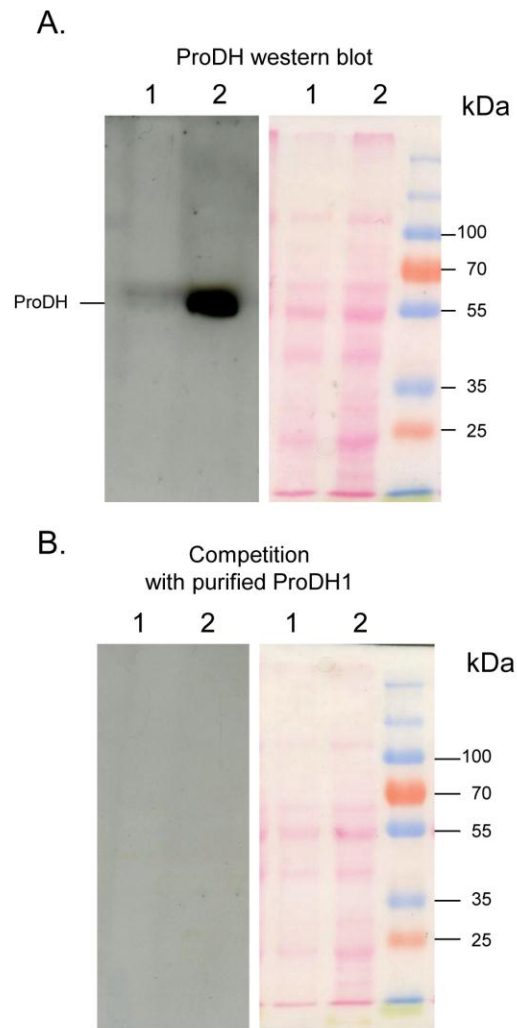
  

spot 1	spot 3
R. GMVLGLVK. S	R. GMVLGLVK. S
K. LMDASVTR. G	K. LMDASVTR. G
K. ITAICPISLLK. R	R. IQEICR. K
R. SVYEATGLK. G	K. ITAICPISLLK. R
R. LFSS IPTSDLLR. S	R. SVYEATGLK. G
K. ASNGSGFGV VLA THNADSGR. L	R. LFSS IPTSDLLR. S
spot 2	spot 4
K. LMDASVTR. G	K. LMDASVTR. G
R. IQEICR. K	R. IQEICR. K
K. ITAICPISLLK. R	K. ITAICPISLLK. R
R. SVYEATGLK. G	R. SVYEATGLK. G
R. LFSS IPTSDLLR. S	R. LFSS IPTSDLLR. S

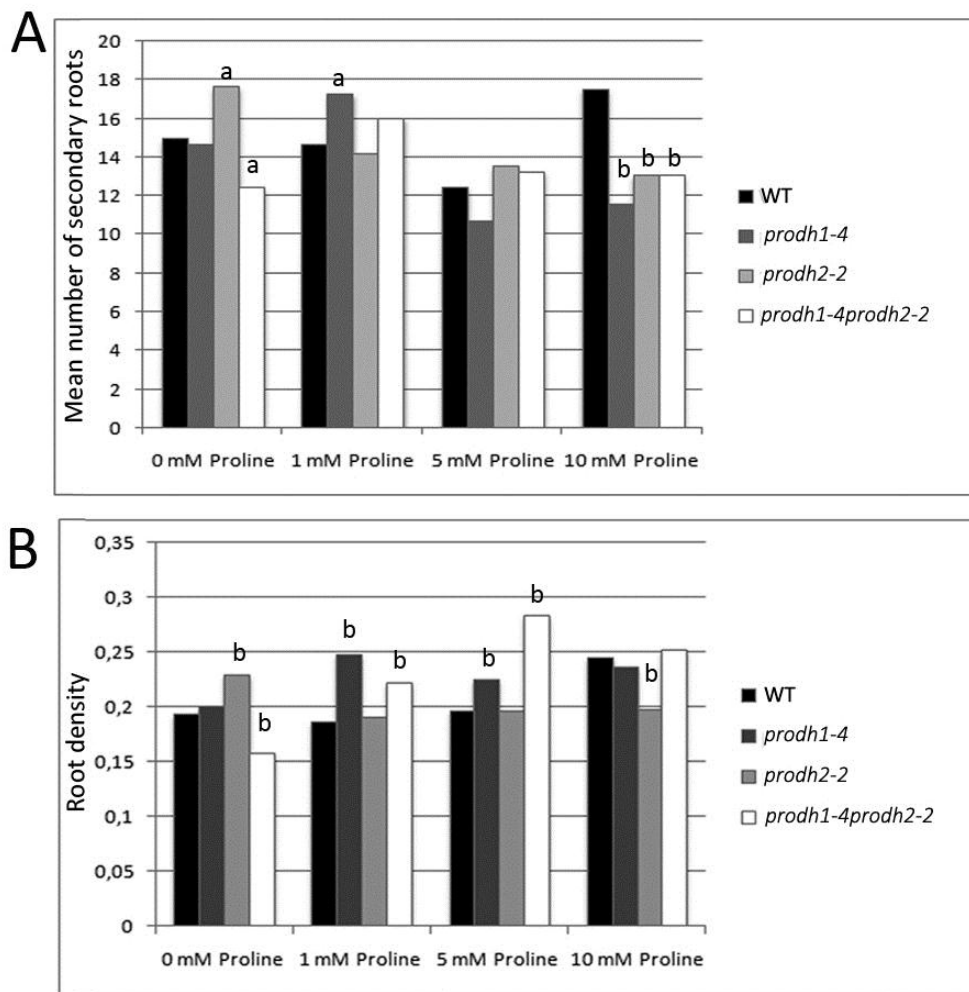
Figure 8: Peptides of ProDH1 identified by mass spectrometry. Top: amino acid sequence of ProDH1 with the location of the corresponding peptides. Bottom: Peptides identified within spots 1-4 (as indicated on Figure 7).

Genotype and treatment	Respiratory substrate = NADH + succinate						Respiratory substrate L-proline	
	State 3 rate	State 4 rate	CytC rate	AOX capacity	RCR	ADP/O	L-proline cytC	L-proline AOX
Wt NT	144.5 ± 0.5	72.29 ± 1.5	69.39 ± 1.6	13.30 ± 1.3	2.00 ± 0.05	1.40 ± 0.00	0 ± 0.0	0 ± 0.0
Wt +Pro	166.7 ± 5.2	83.42 ± 3.6	71.60 ± 3.5	18.80 ± 3.0	2.00 ± 0.04	1.00 ± 0.22	29.1 ± 2.8	36.4 ± 4.07
<i>p5cdh</i> NT	145 ± 0.7	78.6 ± 0.4	70.74 ± 0.6	15.72 ± 2.5	1.84 ± 0.02	1.23 ± 0.01	0 ± 0.0	0 ± 0.0
<i>p5cdh</i> +Pro	142.2 ± 8.6	102.0 ± 6.8	88.07 ± 8.8	36.64 ± 4.3	1.50 ± 0.01	1.25 ± 0.09	17.9 ± 4.7	19 ± 2.6
<i>prodh1</i> NT	132.5 ± 2.5	77.59 ± 3.7	58.82 ± 2.2	43.10 ± 4.1	1.71 ± 0.05	1.18 ± 0.10	0 ± 0.0	0 ± 0.0
<i>prodh1</i> +Pro	137.4 ± 8.8	84.38 ± 3.2	60.11 ± 2.1	45.60 ± 6.7	1.63 ± 0.05	0.85 ± 0.16	0 ± 0.0	0 ± 0.0
<i>prodh2</i> NT	142.4 ± 2.4	75.16 ± 0.7	60.46 ± 2.2	32.75 ± 0.2	1.90 ± 0.02	1.45 ± 0.08	0 ± 0.0	0 ± 0.0
<i>prodh2</i> +Pro	156 ± 2.0	82.1 ± 0.2	69.50 ± 0.4	29.00 ± 2.5	1.90 ± 0.02	1.15 ± 0.01	23.3 ± 3	18.3 ± 1.8

Table I: Respiratory parameters of L-proline-treated wild-type and *p5cdh* and *prodh* mutant seedlings measured using isolated mitochondria. Crude mitochondria were obtained from 15 days-old seedlings of either wild-type, *p5cdh*, *prodh1-3*, *prodh1-4*, *prodh2-2* or *prodh2-3* genotypes treated without (NT) or with 50 mM L-proline (Pro) for 24 h. Respiratory rates are expressed in  $\text{nmol O}_2 \text{ min}^{-1} \text{ mg protein}^{-1}$  and are the mean of at least three biological replicates for wild-type and *p5cdh* genotypes for each condition. For *prodh1* and *prodh2*, results correspond to a mean of three independent experiments for each *prodh1-4* and *prodh1-3* mutants and for each *prodh2-2* and *prodh2-3* mutants, respectively. “State 3” and “state 4” respiration represent phosphorylation and non-phosphorylation modes of the respiratory chain (ADP sufficiently present *versus* not present), respectively. CytC rate and AOX capacity were determined in the presence of KCN and SHAM, which block one or the other respiratory electron transfer pathway. RCR is the respiratory coupling rate (state3/state4 rate) and ADP/O is the phosphorylation yield.

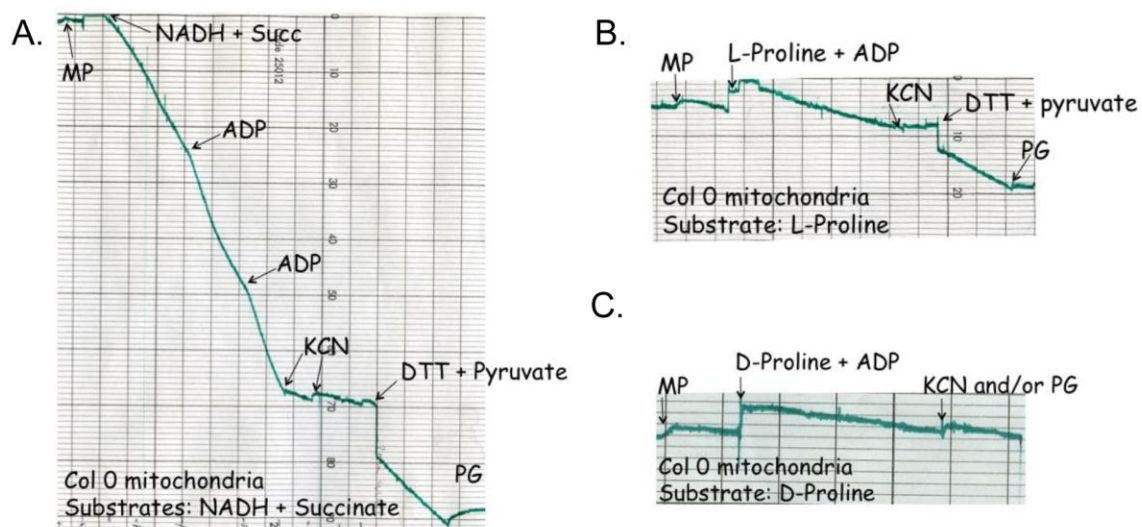


Supplemental Figure 1. Proline treatment increases ProDH content in seedlings. Mitochondria were purified from 15 day-old Col0 seedlings treated with 50 mM L-proline (1) or not treated (2) for 24 h. A and B, Western blot analysis of ProDH content using 40  $\mu$ g of mitochondrial proteins. B, ProDH antibody were used in competition with a purified ProDH1 recombinant protein. Ponceau stainings of the corresponding blots are presented on the right. The masses of standard proteins are given in kDa.

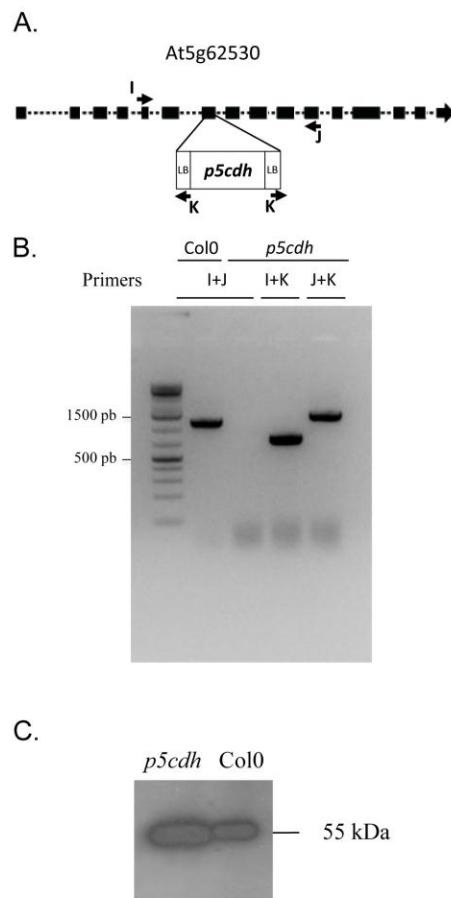


Supplemental Figure 2. Root architecture analysis in wild-type and *prodh* mutants in response to exogenously applied proline. A. Mean number of secondary roots of WT, *prodh1-4*, *prodh2-2* and *prodh1-4/prodh2-2* seedlings after 12 days of growth on medium without or with 1mM, 5 mM or 10 mM proline. B. Root density of WT, *prodh1-4*, *prodh2-2* and *prodh1-4/prodh2-2* seedlings after 12 days of growth on medium without (0 mM) or with 1mM, 5 mM or 10 mM proline. Root density was calculated for each plant as the ratio of the number of secondary root /length of the primary root. For A and B, data shown are means of four to five independent experiments including each 12 plants. Small letters represent significant differences compared to the WT as indicated by an unpaired *t* test (a :  $P < 0,05$ ; b :  $P < 0,01$ ).

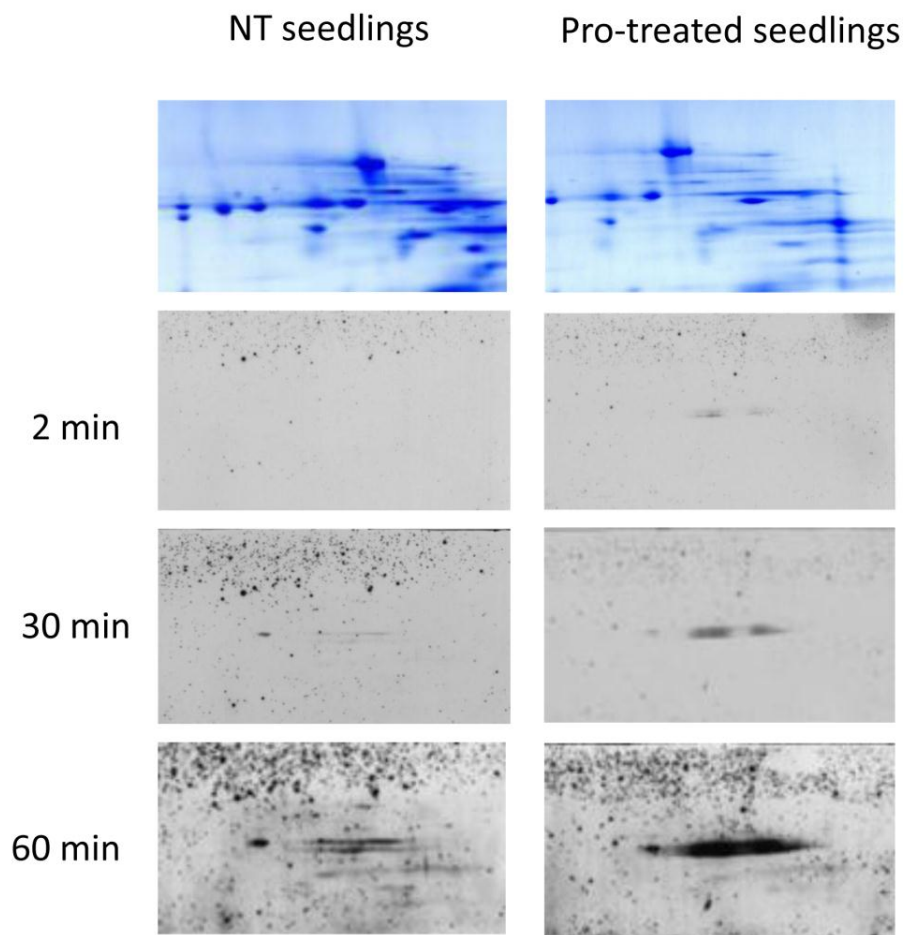




Supplemental Figure 3. Respiratory measurement of isolated mitochondria from Arabidopsis. Primary experimental results using either a combination of NADH and succinate (A: NADH + Succ) or L-proline (B) or D-proline (C) as respiratory substrates. ADP, adenosine diphosphate; DTT, dithiothreitol; KCN, potassium cyanide; MP, purified mitochondria; PG, propyl gallate.



Supplemental Figure 4. Molecular characterization of *p5cdh* mutant. A. Map of the T-DNA insertion in the *p5cdh* mutant. Representation of the gene is the same as in figure 1. B. PCR genotyping of *p5cdh* using genomic DNA isolated from either wild-type or *p5cdh* seedlings. PCR products were separated on a 0.8 % agarose gel. C. Western blot using mitochondria isolated from *p5cdh* and wild-type seedlings treated with 50 mM proline for 24 h.



Supplemental Figure 5. Immunological identification of ProDH1 in mitochondrial fractions isolated from 15-days old *Arabidopsis* seedlings either treated or not treated with 50 mM proline for 24 h. Total mitochondrial proteins were separated by 2D Blue native / SDS PAGE. Proteins were either Coomassie stained (top) or blotted onto nitrocellulose (bottom). Blots were developed using an antibody directed against ProDH from *Arabidopsis* and immune signals were visualized after 2, 30 and 60 minutes.

### List of the primers used for the genotyping

A: CGTGGGTCATGAGCTCTAAAC  
B: TAAACGATTGGTCGGTCTTTG  
C: ATATTGACCATCATACTCATTGC  
D: GCGTGGACCGCTTGCTGCAACT  
E: AAACCTCATCCACCGTTTCTC  
F: CGACGTGACTTTGATTGTTATTTT  
G: GGTAGGGTTTTAGCAGCTTCG  
H: AATACTTTCAGTAACTTTGATCAAACAC  
I: CAGCTCATATGCTCGCCTTAC  
J: CATCTTGATCACATTGCCATG  
K: TGGTTCACGTAGTGGGCCTCG

Supplemental Table I. List of the primers used for genotyping the different *prodh* and *p5cdh* mutants.

## Publication IV

### ***2.4 L-Galactono-1,4-Lactone dehydrogenase (GLDH) Forms Part of Three Subcomplexes of Mitochondrial Complex I in Arabidopsis thaliana***

Peter Schertl<sup>‡</sup>, Stephanie Sunderhaus<sup>‡</sup>, Jennifer Klodmann<sup>‡</sup>, Gustavo E. Gergoff Grozeff<sup>§</sup>, Carlos G. Bartoli<sup>§</sup>, and Hans-Peter Braun<sup>‡1</sup>

From the <sup>‡</sup>Institut für Pflanzengenetik, Abteilung Pflanzenproteomik, Universität Hannover, Herrenhäuser Str. 2, 30419 Hannover, Germany and the <sup>§</sup>Instituto de Fisiología Vegetal, Facultad de Ciencias Agrarias y Forestales, Universidad Nacional de La Plata CCT CONICET La Plata, CC 327 (1900) La Plata, Buenos Aires, Argentina

Approximately 80 % of this publication was obtained during my M.Sc. thesis.

Type of authorship:	first author
Type of article:	research article
Share of the work:	75 %
Contribution to the publication:	planned and performed experiments, analyzed data, prepared all figures and wrote the paper
Journal:	Journal of Biological Chemistry
Impact Factor:	4,6
Date of publication:	published in February 2012
Number of citations (9 <sup>th</sup> of October 2014)	18
DOI:	10.1074/jbc.M111.305144
PubMed-ID:	22378782

Supplemental Material can be found at:  
<http://www.jbc.org/content/suppl/2012/02/29/M111.305144.DC1.html>

THE JOURNAL OF BIOLOGICAL CHEMISTRY VOL. 287, NO. 18, PP. 14412–14419, APRIL 27, 2012  
 © 2012 BY THE AMERICAN SOCIETY FOR BIOCHEMISTRY AND MOLECULAR BIOLOGY, INC. PUBLISHED IN THE U.S.A.

# L-Galactono-1,4-lactone dehydrogenase (GLDH) Forms Part of Three Subcomplexes of Mitochondrial Complex I in *Arabidopsis thaliana*<sup>\*S</sup>

Received for publication, September 16, 2011, and in revised form, February 29, 2012. Published, JBC Papers in Press, February 29, 2012, DOI 10.1074/jbc.M111.305144

Peter Schertl<sup>‡</sup>, Stephanie Sunderhaus<sup>‡</sup>, Jennifer Klodmann<sup>‡</sup>, Gustavo E. Gergoff Grozeff<sup>§</sup>, Carlos G. Bartoli<sup>§</sup>, and Hans-Peter Braun<sup>‡1</sup>

From the <sup>‡</sup>Institut für Pflanzengenetik, Abteilung Pflanzenproteomik, Universität Hannover, Herrenhäuser Str. 2, 30419 Hannover, Germany and the <sup>§</sup>Instituto de Fisiología Vegetal, Facultad de Ciencias Agrarias y Forestales, Universidad Nacional de La Plata CCT CONICET La Plata, CC 327 (1900) La Plata, Buenos Aires, Argentina

**Background:** L-Galactono-1,4-lactone dehydrogenase (GLDH) catalyzes the final step of the L-ascorbate biosynthesis pathway and at the same time is essential for complex I accumulation.

**Results:** The active GLDH is localized within three different subcomplexes of complex I.

**Conclusion:** Evidence is increasing that GLDH represents a complex I assembly factor.

**Significance:** New insights into mitochondrial complex I assembly in *Arabidopsis thaliana*.

L-Galactono-1,4-lactone dehydrogenase (GLDH) catalyzes the terminal step of the Smirnov-Wheeler pathway for vitamin C (L-ascorbate) biosynthesis in plants. A GLDH *in gel* activity assay was developed to biochemically investigate GLDH localization in plant mitochondria. It previously has been shown that GLDH forms part of an 850-kDa complex that represents a minor form of the respiratory NADH dehydrogenase complex (complex I). Because accumulation of complex I is disturbed in the absence of GLDH, a role of this enzyme in complex I assembly has been proposed. Here we report that GLDH is associated with two further protein complexes. Using native gel electrophoresis procedures in combination with the *in gel* GLDH activity assay and immunoblotting, two mitochondrial complexes of 470 and 420 kDa were identified. Both complexes are of very low abundance. Protein identifications by mass spectrometry revealed that they include subunits of complex I. Finally, the 850-kDa complex was further investigated and shown to include the complete “peripheral arm” of complex I. GLDH is attached to a membrane domain, which represents a major fragment of the “membrane arm” of complex I. Taken together, our data further support a role of GLDH during complex I formation, which is based on its binding to specific assembly intermediates.

Ascorbate (vitamin C) is of central importance for several biological processes. In plants, it was shown to be essential for growth (1), programmed cell death (2), pathogen response (3), signal transduction (4), and the stress response with respect to ozone (5), UV radiation (6), high temperature (7), and high light (8). Ascorbate is the cofactor of several enzymes and one of the major components adjusting the redox state of cells. In plant tissue, it can reach millimolar concentrations and form up to

10% of the soluble carbohydrate content. Biosynthesis of ascorbate in plants mainly takes place via the “L-galactose” also known as “Smirnov-Wheeler” pathway (9). The terminal step of this pathway, the conversion of L-galactono-1,4-lactone (GL)<sup>2</sup> into ascorbate, is catalyzed by L-galactono-1,4-lactone dehydrogenase (GLDH). GLDH is localized in mitochondria. During ascorbate formation, GLDH needs oxidized cytochrome *c* as the electron acceptor (10–12). Indeed, GL represents a respiratory substrate for oxidative phosphorylation in plants (12, 13).

GLDH has been purified and characterized for several plant species (11, 14, 15). The primary GLDH translation product has a molecular mass of about 68 kDa but is processed to a mature protein of 56–58 kDa. Processing is based on removal of an N-terminal peptide of about 100 amino acids and probably takes place during transport of GLDH into mitochondria (15, 16). GLDH is most active with L-galactono-1,4-lactone but also has some low L-gulono-1,4-lactone activity (14, 16). The enzyme needs noncovalently bound FAD as a co-factor. GLDH so far has not been crystallized but amino acid positions essential for regulation and activity were identified by the investigation of recombinant forms of the enzyme (16–19).

GLDH is localized in the inner mitochondrial membrane (12, 20, 21). Because the mature protein lacks membrane spanning segments (16) it most likely is peripherally attached to the inner mitochondrial membrane. If overexpressed in *Escherichia coli*, GLDH forms part of the soluble fraction of this bacterium (16). About a decade ago, it surprisingly was discovered that GLDH is attached to the mitochondrial NADH dehydrogenase complex (complex I) of the respiratory chain (22). Complex I has a molecular mass of 1000 kDa and in plants includes at least 48 different subunits, several of which represent proteins specific for this enzyme complex in plants (23, 24). Some of these extra subunits integrate side activities into this respiratory complex, e.g. carbonic anhydrase (CA) subunits, which were proposed to

\* This work was supported by Deutsche Forschungsgemeinschaft (DFG) Grant Br 1829/10-1.

<sup>S</sup> This article contains supplemental Tables S1 and S2 and Figs. S1–S3.

<sup>1</sup> To whom correspondence should be addressed. Tel.: 49-5117622674; Fax: 49-5117623608; E-mail: braun@genetik.uni-hannover.de.

<sup>2</sup> The abbreviations used are: GL, L-galactono-1,4-lactone; GLDH, L-galactono-1,4-lactone dehydrogenase; CA, carbonic anhydrase; BN, blue native.

## GLDH Forms Part of Three Complex I Subcomplexes in Arabidopsis

support CO<sub>2</sub> transfer from mitochondria to chloroplasts in plant cells (25). However, GLDH was not found to be attached to the 1000-kDa holoenzyme, but only to a slightly smaller version of complex I, which is of comparatively low abundance (13, 22, 26). This complex has a molecular mass of about 850 kDa and obviously lacks some of the subunits present in the main form of complex I. The identity of these subunits is not known so far. GLDH activity is inhibited in the presence of rotenone, an inhibitor of electron transfer within complex I, if pyruvate and malate are used as respiratory substrates (13). It therefore was speculated that a subpopulation of complex I particles are important for GLDH regulation by monitoring the rate of NADH-driven electron flow through complex I (13).

Silencing of the gene encoding GLDH in tomato does not much affect ascorbate concentration, indicating that GLDH activity is not rate-limiting for ascorbate formation (27). However, silenced plants have a clearly retarded growth and produce smaller fruits. At the same time, the central metabolism of plant mitochondria is significantly changed. It is concluded that GLDH is important for other processes besides ascorbate formation. Recently, characterization of an *Arabidopsis* knock-out mutant lacking the gene encoding GLDH was found to have drastically reduced amounts of complex I (26). In contrast, the amounts of the other protein complexes of the respiratory chain were not changed. It therefore is speculated that GLDH, besides its role in ascorbate formation, represents an assembly factor for complex I.

Here we present a biochemical investigation on GLDH localization within plant mitochondria. Protein complexes of the inner mitochondrial membrane were carefully solubilized by the use of nonionic detergents and resolved protein complexes were separated by blue native PAGE. Using a newly developed *in gel* GLDH activity assay and immunoblotting, three distinct GLDH containing protein complexes of 850, 470, and 420 kDa were discovered. The 850-kDa complex represents the known smaller version of mitochondrial complex I. GLDH is shown to be attached to the membrane arm of the 850-kDa complex I. Subunits of the novel 470 and 420 kDa complexes were identified by mass spectrometry. Like the 850-kDa complex, they also include complex I subunits. We propose that GLDH has a more extended function in complex I assembly by specifically binding to several of its assembly intermediates.

### EXPERIMENTAL PROCEDURES

**Arabidopsis thaliana Cultivation and Isolation of Mitochondria**—*A. thaliana* cells (var. Columbia-0) were cultivated as previously described (28). Isolation of mitochondria was performed according to Werhahn *et al.* (29).

**Gel Electrophoresis Procedures and Immunoblotting**—One-dimensional BN-PAGE and two-dimensional BN/SDS-PAGE was performed as previously described (30). Two-dimensional BN/BN-PAGE was carried out as outlined in Sunderhaus *et al.* (31). For the experiments of the current investigation, first dimension BN-PAGE was carried out in the presence of digitonin, second dimension BN-PAGE in the presence of Triton X-100. Proteins were visualized by Coomassie colloidal staining (32, 33). After separation on polyacrylamide gels proteins were blotted onto a nitrocellulose membrane using the Trans Blot

Cell from Bio-Rad. The transfer of proteins was performed as described in Kruff *et al.* (34). Immunostainings were carried out using the VectaStain ABC Kit (Vector Laboratories, Burlingame, CA). The carbonic anhydrase antibody was provided by Eduardo Zabaleta (Mar del Plata University, Argentina). The GLDH antibody was purchased from Agrisera Antibodies (Vännäs, Sweden).

**In Gel Activity Stainings**—*In gel* staining for NADH-ubiquinone-oxidoreductase was carried out as previously described (35).

*In gel* activity staining of GLDH was performed as follows. After half-completion of the electrophoretic run of a BN-PAGE the Coomassie-containing cathode buffer was replaced by a cathode buffer without Coomassie for dye reduction within the gel. The gel was incubated in 100 ml of GLDH staining solution (40 mM Tris(hydroxymethyl)aminomethane, 2 mM L-galactono-1,4-lactone, 1 mg/ml of nitro blue tetrazolium chloride, 200 μM phenazine methosulfate) in the dark. The pH of the solution was adjusted to 8.8 (HCl). GLDH activity becomes visible as purple bands or spots after 15–30 min. The activity staining was stopped by rinsing the gel with water. To improve visualization and destain the background the gel was transferred into destaining solution (40% methanol and 10% acetic acid) overnight. The resulting gels were finally scanned on a transmission scanner (PowerLook III, UMAX).

**Mass Spectrometry (MS)**—Tryptic digestion of proteins and MS were performed as described previously (23). Protein identifications were based on the MASCOT search algorithm using the *A. thaliana* protein data base, release TAIR10 ([www.arabidopsis.org](http://www.arabidopsis.org)).

### RESULTS

**Identification of GLDH Containing Protein Complexes**—Immunoblotting experiments were carried out to first get information on GLDH localization in plant mitochondria. For this approach, mitochondria were isolated from a suspension cell culture of *A. thaliana*. Isolated organelles were solubilized by 5% digitonin and protein complexes were subsequently separated by two-dimensional blue native (BN)/SDS-PAGE (Fig. 1). Upon Coomassie staining, subunits of the mitochondrial protein complexes are visible as reported before (36). The main form of complex I runs at about 1000 kDa. In addition, a slightly smaller version of complex I is visible in accordance with previous investigations (13, 22, 26). On our gels, it runs at 850 kDa on the first gel dimension and is designated complex I\*. It also includes an additional 58-kDa subunit not present in the main form of complex I. This protein represents GLDH as shown by a parallel immunoblotting experiment. Furthermore, the 58-kDa immune signal is detectable at two further regions on the two-dimensional gels, which correspond to 470 and 420 kDa on the native gel dimension. Finally, the 58-kDa GLDH signal is visible in the <100 kDa region of the native gel dimension. This signal represents the monomeric form of GLDH, which was reported previously (36); see the two-dimensional BN/SDS-PAGE GelMap of Arabidopsis mitochondria ([www.gelmap.de/47](http://www.gelmap.de/47), spot 116). We conclude that GLDH not only forms part of the 850-kDa complex I\*, but additionally of two unknown protein complexes of 470 and 420 kDa.

## GLDH Forms Part of Three Complex I Subcomplexes in Arabidopsis

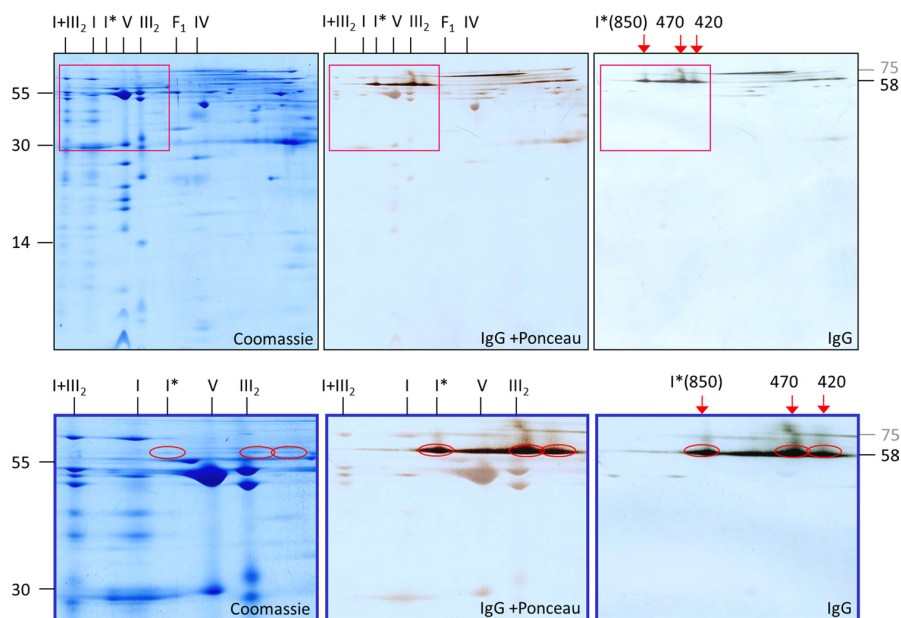


**FIGURE 1. Immunological detection of L-galactono-1,4-lactone dehydrogenase in a mitochondrial protein fraction of *A. thaliana*.** Proteins were separated by BN/SDS-PAGE and either stained by Coomassie Blue (left) or blotted onto nitrocellulose membranes for immunological GLDH detection (center and right). The blot in the center additionally was stained with Ponceau for background visualization. Enlargements of the boxed regions are given in the lower line of the figure. Red circles indicate GLDH. A molecular mass standard is given to the left. Nomenclature of protein complexes: I, complex I; I\*, 850-kDa subcomplex of complex I; V, complex V; III<sub>2</sub>, dimeric complex III; F<sub>1</sub>, F<sub>1</sub> part of complex V; IV, complex IV; I+III<sub>2</sub>, supercomplex composed of complex I + dimeric complex III; 850, 470, and 420 kDa, GLDH containing protein complexes (the 850-kDa complex corresponds to I\*). GLDH is detected on the second gel dimension at 58 kDa. The 58-kDa signal on the right side of the two-dimensional gel represents monomeric GLDH. Another signal at about 75 kDa represents a cross-reaction with an unknown protein (see supplemental Table S1 and supplemental Fig. 1).

An *in gel* activity assay was developed to investigate if the 850-, 470-, and 420-kDa complexes have GLDH activity. The assay includes 2 mM L-galactono-1,4-lactone to avoid substrate inhibition, which was reported to take place at higher concentrations (16). Oxidized cytochrome *c* was substituted by the electron acceptor phenazine methosulfate, which increases sensitivity of the assay. The pH of the assay solution was adjusted to 8.8 in accordance with the pH optimum of GLDH reported previously (16). Finally, nitro blue tetrazolium was used for GLDH activity visualization. This redox dye is yellow in its oxidized form and purple upon reduction into formazan (37). Reduction takes place in the presence of ascorbate. Additionally, reduced phenazine methosulfate can directly reduce nitro blue tetrazolium, which may enhance the ascorbate-mediated color reaction. Nitro blue tetrazolium itself cannot be reduced directly by the GLDH. Using this assay, GLDH activity becomes visible on native protein gels as purple bands or spots. The principle of the assay is summarized in Fig. 2A and the details are given under “Experimental Procedures.”

For performing the GLDH *in gel* activity assay, mitochondria were solubilized by digitonin and protein complexes were subsequently separated by one-dimensional BN PAGE (Fig. 2B). The 850-, 470-, and 420-kDa complexes exhibit strong GLDH activity. No activity is detectable in the absence of GL. The activity-stained bands exactly correspond to the signals obtained by immunoblotting (Fig. 2B). The bands at 850, 470, and 420 kDa are not visible on a parallel Coomassie-stained gel indicating that the *in gel* GLDH activity assay has very high sensitivity.

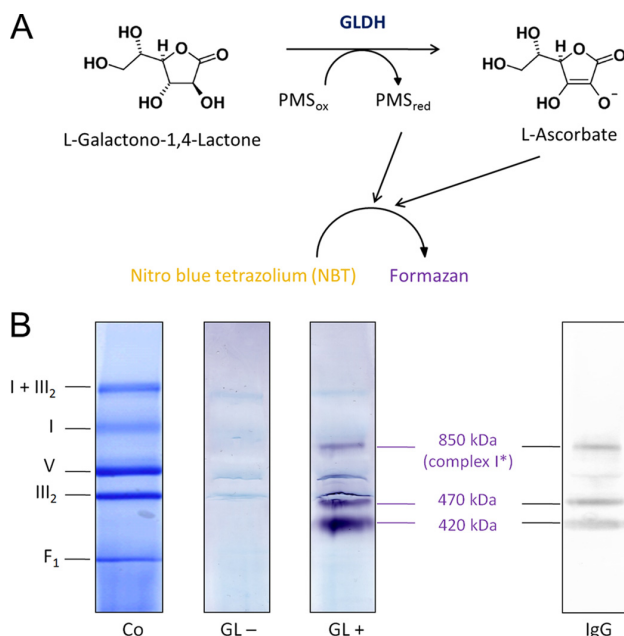


**FIGURE 2. L-Galactono-1,4-lactone dehydrogenase *in gel* activity assay.** A, reaction scheme of the *in gel* activity assay. B, *in gel* activity assay for GLDH. Mitochondrial membrane proteins were solubilized by 5% digitonin and subsequently separated by one-dimensional blue native PAGE. Co, Coomassie stain. GL<sup>-</sup>/GL<sup>+</sup>, *in gel* GLDH activity stain in the presence (GL<sup>+</sup>) or absence (GL<sup>-</sup>) of the substrate L-galactono-1,4-lactone. IgG, immunoblot for GLDH detection. The identities of protein complexes are given on the right, the GLDH-containing protein complexes are indicated in the center (for nomenclature see Fig. 1). The faint signals between the 470- and 850-kDa complexes are caused by local overloading of the gel in the regions of complexes III and V.



## GLDH Forms Part of Three Complex I Subcomplexes in Arabidopsis

For further investigation of the 470- and 420-kDa complexes, a mitochondrial protein fraction was resolved by two-dimensional BN/BN PAGE (Fig. 3). First dimension BN PAGE was carried out in the presence of digitonin, second dimension BN PAGE in the presence of Triton X-100. On the resulting two-dimensional gels, most protein complexes are positioned on a diagonal line, but resolution is increased in comparison to one-

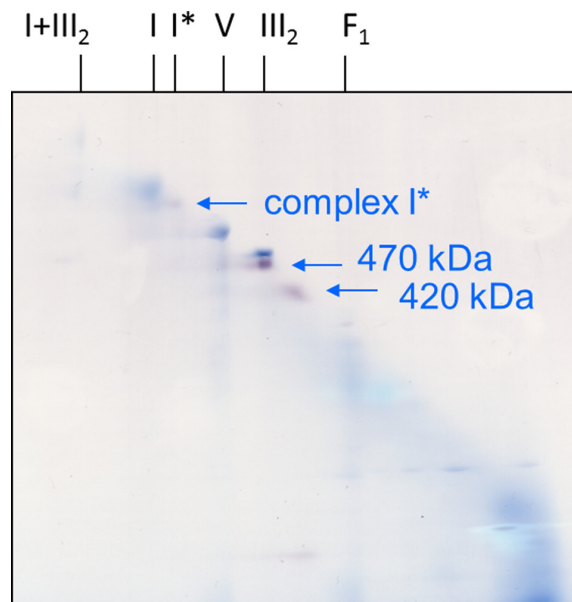


**FIGURE 3. Detection of GLDH-containing protein complexes on a two-dimensional BN/BN gel by activity staining.** Isolated mitochondria from *A. thaliana* were treated with digitonin for protein solubilization and protein complexes were subsequently separated by two-dimensional BN-digitonin/BN-Triton X-100 PAGE. The gel was stained for GLDH activity (purple spots). Background complexes are visible due to Coomassie Blue present during the electrophoresis run (the gel was not stained with Coomassie after completion of the electrophoresis run). Identities of protein complexes are given on top of the gels (for nomenclature, see Fig. 1). The arrows indicate GLDH-containing complexes identified by the *in gel* activity assay. Another GLDH signal at the lower border of the two-dimensional gel below the 420-kDa complex most likely represents GLDH, which became detached from the 420-kDa complex during the second native gel dimension. Two more extensively GLDH activity stained BN/BN gels are presented in supplemental Fig. S2. A comparison of a two-dimensional BN/BN gel before and after GLDH activity staining is presented in supplemental Fig. S3.

**TABLE 1**  
Proteins of the two-dimensional BN/BN gel (Fig. 3) identified by MS

Only complex I subunits are shown. For complete list of the identified proteins see supplemental Table S2.

Sample <sup>a</sup>	Accession No. <sup>b</sup>	Protein <sup>c</sup>	Mass <sup>d</sup>	Mascot score <sup>e</sup>	No. peptides <sup>f</sup>	S.C. <sup>g</sup>	Complex
			<i>kDa</i>			%	
470 kDa	At3g47930	GLDH	68.5	201	4	11.8	Complex I
470 kDa	At1g47260	CA2	30.0	178	4	25.5	Complex I
470 kDa	At3g48680	CAL2	27.9	154	3	17.6	Complex I
470 kDa	At1g04630	GRIM19	16.1	65	1	7.0	Complex I
420 kDa	At1g47260	CA2	30.0	204	4	24.5	Complex I
420 kDa	At3g48680	CAL2	27.9	177	3	13.7	Complex I
420 kDa	At3g47930	GLDH	68.5	170	4	8.5	Complex I
420 kDa	At5g66510	CA3	27.8	101	1	15.5	Complex I
420 kDa	AtMg00285	NAD 2A	54.8	84	2	4.2	Complex I

<sup>a</sup> Analyzed protein complex (Fig. 3).

<sup>b</sup> Accession numbers of identified proteins as given by TAIR.

<sup>c</sup> Names of identified proteins.

<sup>d</sup> Calculated molecular mass of the identified proteins as deduced from the corresponding gene.

<sup>e</sup> Probability score for the protein identifications based on MS analysis and MASCOT search.

<sup>f</sup> Number of unique peptides.

<sup>g</sup> Sequence coverage of the proteins by identified peptides.

dimensional BN PAGE due to differential effects of the two detergents on the individual protein complexes. Visualization of 850-, 470-, and 420-kDa complexes was carried out by *in gel* GLDH activity staining (Fig. 3). Both, the 470- and 420-kDa complexes again were not visible on a parallel Coomassie-stained BN/BN gel due to their low concentration (supplemental Fig. S3). The 470-kDa complex runs close to dimeric complex III (500 kDa).

Although present at extremely low concentrations, gel spots representing the 470- and 420-kDa complexes were further analyzed by mass spectrometry. As expected, both protein complexes include GLDH (Table 1). Furthermore, and as expected, MS analysis of the 470-kDa complex revealed identification of complex III subunits (supplemental Table S2). This complex is of very high abundance and migrates in very close proximity to the 470-kDa complex on the BN/BN gel. However, the GLDH activity stain clearly is not at the position of complex III (Fig. 3). Strikingly, the 470-kDa complex additionally includes the CA2, CAL2, and Grim-19 subunits, which form part of the membrane arm of complex I in plants. Similarly, MS analysis of the 420-kDa complex revealed, besides GLDH, several subunits of the membrane arm of complex I: CA2, CA3, CAL2, and NAD2 (Table 1). Further complex I subunits were not identified, probably due to the low abundance of the 470- and 420-kDa complexes and due to the fact that the membrane arm of complex I mainly includes very hydrophobic subunits, which are difficult to detect by MS. Besides, some proteins of the HSP60 and malic enzyme complexes and the F1-part of ATP synthase were identified in the spot representing the 420-kDa complex (supplemental Table S2). However, as in the case of the 470-kDa complex, identification of these subunits rather reflects spot overlappings on our BN/BN gel than physical association of these proteins with GLDH, because these complexes run in very close proximity to the 420-kDa complex and are of very high abundance.

MS analyses of the 850-kDa complex revealed, as expected, several complex I subunits, which form part of the membrane and the peripheral arm (supplemental Table S2). Also in this data set, some subunits of other protein complexes were identified, which represent components of highly abundant protein

## GLDH Forms Part of Three Complex I Subcomplexes in Arabidopsis

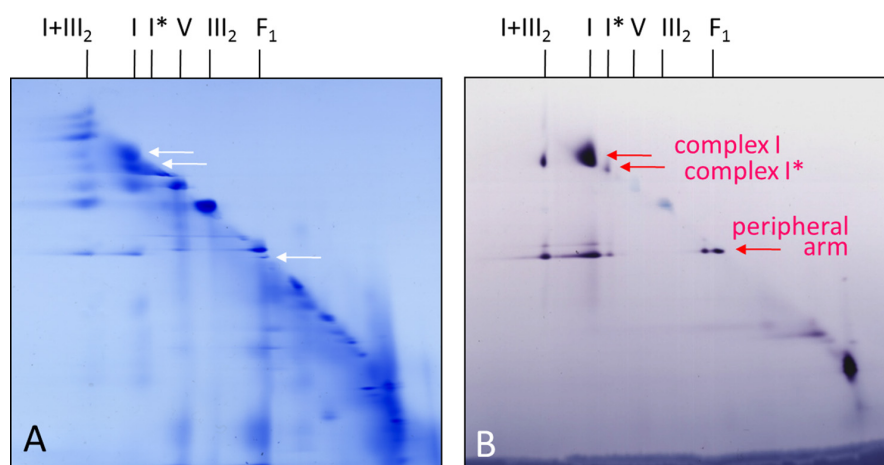


FIGURE 4. **Detection of NADH dehydrogenase complexes on a two-dimensional BN/BN gel by activity staining.** Isolated mitochondria from *A. thaliana* were treated with digitonin for protein solubilization and protein complexes were subsequently separated by two-dimensional BN-digitonin/BN-Triton X-100 PAGE. **A**, Coomassie colloidal stained gel. **B**, NADH dehydrogenase activity stained gel. Identities of protein complexes are given on top of the gels (for nomenclature see Fig. 1). The arrows indicate NADH dehydrogenase complexes identified by the *in gel* activity assay. The signals in the low molecular mass region of the two-dimensional gel (bottom, right) represent alternative NADH-dehydrogenases.

complexes running in close proximity to the 850-kDa complex on the BN/BN gel.

**Localization of GLDH within Complex I**—GLDH forms part of the 850-kDa complex I\* and possibly of further complex I subcomplexes. However, precise localization of GLDH within complex I so far is not clear. Complex I consists of two longish domains, which together form an L-like structure. One domain is embedded in the inner mitochondrial membrane (“membrane arm”), whereas the other protrudes into the mitochondrial matrix (“peripheral arm”). NADH oxidation takes place at the peripheral arm, whereas proton translocation is mediated by the membrane arm. Both processes are probably coupled through conformational changes (38–40).

At which position does GLDH bind to mitochondrial complex I in plants? To address this question, further experiments were carried out using the two-dimensional BN/BN PAGE system in combination with *in gel* activity staining and immunoblotting. First dimension BN PAGE was carried out in the presence of digitonin, second dimension BN PAGE in the presence of Triton X-100. Because Triton X-100 has a slightly reduced mildness during membrane solubilization compared with digitonin, some protein complexes partly get dissected into subcomplexes during the second gel dimension. On the resulting two-dimensional gels, these subcomplexes migrate below the diagonal line. For example, the 1500-kDa I + III<sub>2</sub> supercomplex, which is composed of complexes I and III<sub>2</sub>, is dissected into its two components on the second native gel dimension (28). Furthermore, complex I is partially dissected on the second native gel dimension into two subcomplexes representing the membrane arm (550 kDa) and the peripheral arm (370 kDa) (23, 28).

In the first experiment, a mitochondrial fraction of *Arabidopsis* was separated by two-dimensional BN/BN PAGE and gels were activity stained for NADH oxidation (Fig. 4). As expected, the main form of complex I (1000 kDa) becomes visible as well as its peripheral arm (370 kDa). Both complexes are also visible as dissection products of the I + III<sub>2</sub> supercomplex.

The peripheral arm of complex I additionally is visible on the diagonal line on the two-dimensional gel system, indicating that a small proportion of complex I was dissected into its arms within our mitochondrial fraction. The GLDH containing 850-kDa complex I\* has NADH oxidation activity. Furthermore, the 850-kDa complex is also partially dissected into its arms on the second gel dimension. The peripheral arm of the 850-kDa complex has the same size as the peripheral arm of the 1000-kDa main form of complex I. We conclude that the peripheral arm of the 850-kDa complex I\* includes a complete set of subunits. Therefore, the unknown subunits of complex I, which are absent in complex I\*, must form part of the membrane arm.

In the second experiment, a mitochondrial fraction of *Arabidopsis* was separated by two-dimensional BN/BN PAGE and the resulting gels were used for immunoblotting experiments using antibodies directed against GLDH and the carbonic anhydrase subunit CA2 of complex I (Fig. 5). The latter subunit is known to form part of the membrane arm of complex I (23, 28). As expected, the CA antibody recognizes complex I (1000 kDa) and its membrane arm (570 kDa) (Fig. 5, center). Furthermore, complex I\* (850 kDa) is recognized as well as its membrane arm (470 kDa), which is of slightly reduced size compared with the membrane arm of the holoenzyme (550 kDa). Finally, the 470- and 420-kDa complexes are recognized on the diagonal line. This verifies the MS data indicating that the 470- and 420-kDa complexes represent parts of the membrane arm of complex I (including the CA2 subunit). The GLDH antibody does not recognize complex I (1000 kDa), which was expected because it was never reported to form part of the main form of the NADH dehydrogenase complex. In contrast, the 850-kDa complex I\* is recognized as well as its membrane arm at 470 kDa. As expected, the 470- and 420-kDa complexes are additionally recognized on the diagonal line of protein complexes visible on the two-dimensional BN/BN gels. We conclude that GLDH is attached to the membrane arm of complex I\* (470 kDa), which

## GLDH Forms Part of Three Complex I Subcomplexes in Arabidopsis

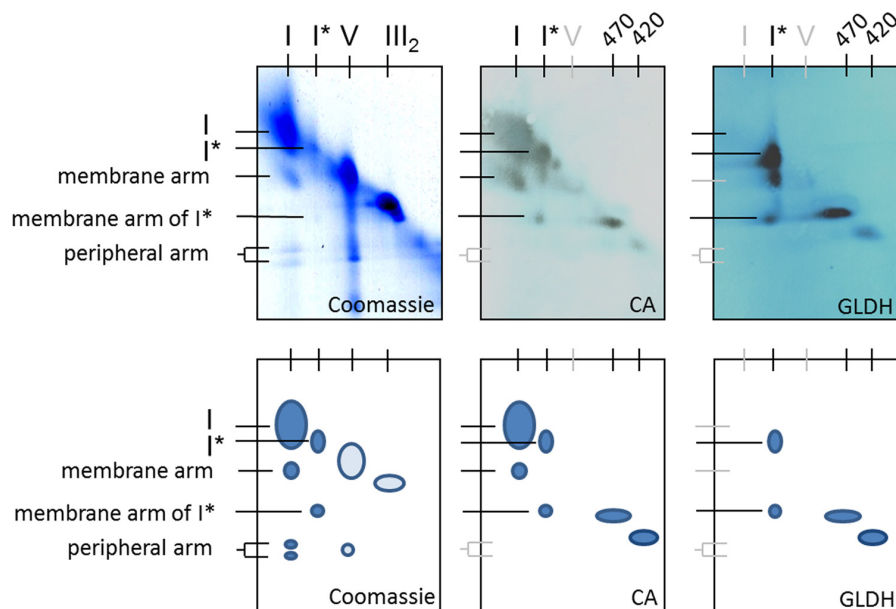


**FIGURE 5. Detection of CA- and GLDH-containing protein complexes on a two-dimensional BN/BN gel using antibodies.** Isolated mitochondria from *Arabidopsis* were treated with digitonin for protein solubilization and protein complexes were subsequently separated by two-dimensional BN-digtonin/BN-Triton X-100 PAGE. The resulting two-dimensional gels were either stained by Coomassie Blue (left) or blotted onto nitrocellulose membranes for immunological detection of CA (center) or GLDH (right). Identities of protein complexes are given on the top and left of the gels (for nomenclature see Fig. 1; black letters, visible spots; gray letters, positions of protein complexes not visible on one or two of the subfigures). The schemes below further illustrate the identity of the resolved protein complexes (dark blue circles, complex I and derived protein complexes; light blue circles, other protein complexes).

represents a large but incomplete fragment of the membrane arm of complex I.

## DISCUSSION

Using native gel electrophoresis procedures, which are combined with *in gel* activity stains and immunoblotting, novel insights into GLDH localization in plant mitochondria were achieved: (i) GLDH forms part of three mitochondrial protein complexes of 850, 470, and 420 kDa; (ii) all three complexes exhibit GLDH activity upon analysis by a newly developed *in gel* GLDH activity assay; (iii) the 850-kDa complex represents a known smaller version of complex I (13, 22, 26), here termed complex I\*, but also the 470- and 420-kDa complexes representing subcomplexes of complex I; (iv) 850-kDa complex I\* has a complete peripheral arm; and (v) The GLDH containing 470 kDa complex represents the membrane arm of complex I\*, which represents a large fragment of the membrane arm of the holoenzyme.

Very recently, the x-ray structure of bacterial complex I, which has a much simpler subunit composition, was resolved by x-ray crystallography (38, 40). Also, the overall structure of mitochondrial complex I is known by single particle electron microscopy and meanwhile also by partial x-ray crystallography (39, 41–43). All complex I particles analyzed so far have the characteristic L-like shape. Mitochondrial complex I from plants is very special, because the L-motif is markedly modified (28, 44–46). Most notably, it has a second matrix exposed domain, which is attached to the membrane arm at a central position. It was shown to include carbonic anhydrase subunits (25, 28), which belong to the set of subunits special to complex I in plants (23, 47). GLDH is another protein of this set of plant-

specific complex I subunits. However, it is absent in the 1000-kDa holo complex but present only in a slightly smaller 850-kDa complex I\*, which is of comparatively low abundance. Because the amount of complex I is very much reduced in an *Arabidopsis* knock-out line lacking the gene for GLDH, its involvement in complex I assembly was suggested (26).

Assembly of complex I was extensively studied in fungi and mammals (reviewed in Refs. 48 and 49–51) but not much is known about this process in plants. Due to its unique shape, the assembly pathway of plant complex I most likely differs substantially from the pathways taking place in other groups of organisms. Using low-SDS treatment of isolated complex I from *Arabidopsis*, subcomplexes were systematically generated and analyzed for subunit composition (23, 47). This experimental approach gave insights into subunit arrangement within plant complex I. However, disassembly of complex I does not necessarily reflect its assembly pathways. Other insights into complex I assembly in plants came from analyses of mutants defective in complex I accumulation (26, 52). Most recently, *Arabidopsis* knock-out lines defective in 7 different complex I subunits were systematically analyzed by native gel electrophoresis procedures (53). Assembly of the membrane arm of complex I was shown to involve intermediates of 200, 400, 450, and 650 kDa. Because abundances of these assembly intermediates are extremely low, they were only detectable by immunoblotting. Their subunit compositions therefore are largely unknown. However, based on information about which intermediates accumulate in which knock-out line, some first results became clear. Most notably, the plant-specific carbonic anhydrase subunit CA2 forms part of all assembly intermediates and

## GLDH Forms Part of Three Complex I Subcomplexes in Arabidopsis

therefore is involved in the initial events leading to the formation of the membrane arm.

We present evidence that the newly described GLDH containing protein complexes of 470 and 420 kDa represent assembly intermediates of complex I. Due to the fact that the GLDH only is attached to the subcomplexes and not to the holo-complex I, it is unlikely that they represent degradation fragments of intact complex I. Because the assembly intermediates are of very low abundance, they are only detectable by immunoblotting or by the GLDH *in gel* activity assay. Their subunit composition therefore is not known. However, analyses by mass spectrometry and immunoblotting allowed identifying subunits of the membrane arm of complex I, most notably CA2, CAL2, CA3, NAD2, and Grim-19 (Fig. 3, Table 1). All other identified proteins form part of protein complexes of very high abundance, which are localized on the BN/BN gels in close proximity to the 470- and 420-kDa complexes and that most likely were detected due to spot overlappings. We presume that GLDH containing 470- and 420-kDa complexes represent the 450- and 400-kDa assembly intermediates described by Meyer *et al.* (53), which were both shown to include CA2 (the size difference of the complexes as described by the two studies can be explained by a slight variation in molecular mass calibration of the native gels used for electrophoresis). The 850-kDa complex I\* is partially dissected into a 470-kDa membrane fragment, which includes GLDH and CA and which exactly co-migrates on our gels with the 470-kDa complex identified by GLDH *in gel* activity staining (Fig. 5). The 470-kDa dissection product of the 850-kDa complex also exhibits GLDH activity (supplemental Fig. S2).

In summary, our data point to a more extensive role of GLDH in complex I assembly. GLDH binds to the 420- and 470-kDa complex I assembly intermediates, which at a later stage form the 850-kDa intermediate. Formation of the 1000-kDa complex I holoenzyme is preceded by detachment of GLDH. Because we do not see smaller complex I subcomplexes on our GLDH activity stained two-dimensional BN/BN gels, we believe that the 420-kDa complex is the smallest complex I subcomplex that includes GLDH. We so far cannot answer if GLDH binding to the 420- and 470-kDa complexes is a prerequisite for formation of the 850-kDa complex.

GLDH integrated into the 850-, 470-, and 420-kDa complexes is active in ascorbate formation as revealed by our *in gel* activity assay. It currently cannot be decided whether GLDH activity (conversion of GL into ascorbate) is required for its assembly function. The biological reason of the bifunctionality of this protein so far remains a mystery and should be further investigated.

*Acknowledgment*—We thank Dagmar Lewejohann for expert technical assistance.

### REFERENCES

- Pignocchi, C., and Foyer, C. H. (2003) Apoplastic ascorbate metabolism and its role in the regulation of cell signaling. *Curr. Opin. Plant Biol.* **6**, 379–389
- de Pinto, M. C., Paradiso, A., Leonetti, P., and De Gara, L. (2006) Hydrogen peroxide, nitric oxide, and cytosolic ascorbate peroxidase at the crossroad between defense and cell death. *Plant J.* **48**, 784–795
- Barth, C., Moeder, W., Klessig, D. F., and Conklin, P. L. (2004) The timing of senescence and response to pathogens is altered in the ascorbate-deficient *Arabidopsis* mutant vitamin C-1. *Plant Physiol.* **134**, 1784–1792
- Barth, C., De Tullio, M., and Conklin, P. L. (2006) The role of ascorbic acid in the control of flowering time and the onset of senescence. *J. Exp. Bot.* **57**, 1657–1665
- Conklin, P. L., and Barth, C. (2004) Ascorbic acid, a familiar small molecule intertwined in the response of plants to ozone, pathogens, and the onset of senescence. *Plant Cell Environ.* **27**, 959–970
- Gao, Q., and Zhang, L. (2008) Ultraviolet-B-induced oxidative stress and antioxidant defense system responses in ascorbate-deficient vtc1 mutants of *Arabidopsis thaliana*. *J. Plant Physiol.* **165**, 138–148
- Larkindale, J., Hall, J. D., Knight, M. R., and Vierling, E. (2005) Heat stress phenotypes of *Arabidopsis* mutants implicate multiple signaling pathways in the acquisition of thermotolerance. *Plant Physiol.* **138**, 882–897
- Müller-Moulé, P., Golan, T., and Niyogi, K. K. (2004) Ascorbate-deficient mutants of *Arabidopsis* grow in high light despite chronic photooxidative stress. *Plant Physiol.* **134**, 1163–1172
- Wheeler, G. L., Jones, M. A., and Smirnoff, N. (1998) The biosynthetic pathway of vitamin C in higher plants. *Nature.* **393**, 365–369
- Mapson, L. W., Isherwood, F. A., and Chen, Y. T. (1954) Biological synthesis of L-ascorbic acid. The conversion of L-galactono- $\gamma$ -lactone into L-ascorbic acid by plant mitochondria. *Biochem. J.* **56**, 21–28
- Mapson, L. W., and Breslow, E. (1958) Biological synthesis of ascorbic acid. L-Galactono- $\gamma$ -lactone dehydrogenase. *Biochem. J.* **68**, 395–406
- Bartoli, C. G., Pastori, G. M., and Foyer, C. H. (2000) Ascorbate biosynthesis in mitochondria is linked to the electron transport chain between complexes III and IV. *Plant Physiol.* **123**, 335–344
- Millar, A. H., Mittova, V., Kiddle, G., Heazlewood, J. L., Bartoli, C. G., Theodoulou, F. L., and Foyer, C. H. (2003) Control of ascorbate synthesis by respiration and its implications for stress responses. *Plant Physiol.* **133**, 443–447
- Oba, K., Ishikawa, S., Nishikawa, M., Mizuno, H., and Yamamoto, T. (1995) Purification and properties of L-galactono- $\gamma$ -lactone dehydrogenase, a key enzyme for ascorbic acid biosynthesis, from sweet potato roots. *J. Biochem.* **117**, 120–124
- Ostergaard, J., Persiau, G., Davey, M. W., Bauw, G., and Van Montagu, M. (1997) Isolation of a cDNA coding for L-galactono- $\gamma$ -lactone dehydrogenase, an enzyme involved in the biosynthesis of ascorbic acid in plants. Purification, characterization, cDNA cloning, and expression in yeast. *J. Biol. Chem.* **272**, 30009–30016
- Leferink, N. G., van den Berg, W. A., and van Berkel, W. J. (2008) L-Galactono- $\gamma$ -lactone dehydrogenase from *Arabidopsis thaliana*, a flavoprotein involved in vitamin C biosynthesis. *FEBS J.* **275**, 713–726
- Leferink, N. G., Jose, M. D., van den Berg, W. A., and van Berkel, W. J. (2009) Functional assignment of Glu-386 and Arg-388 in the active site of L-galactono- $\gamma$ -lactone dehydrogenase. *FEBS Lett.* **583**, 3199–3203
- Leferink, N. G., van Duijn, E., Barendregt, A., Heck, A. J., and van Berkel, W. J. (2009) Galactonolactone dehydrogenase requires a redox-sensitive thiol for optimal production of vitamin C. *Plant Physiol.* **150**, 596–605
- Leferink, N. G., Fraaije, M. W., Joosten, H. J., Schaap, P. J., Mattevi, A., and van Berkel, W. J. (2009) Identification of a gatekeeper residue that prevents dehydrogenases from acting as oxidases. *J. Biol. Chem.* **284**, 4392–4397
- Imai, T., Karita, S., Shiratori, G., Hattori, M., Nunome, T., Oba, K., and Hirai, M. (1998) L-Galactono- $\gamma$ -lactone dehydrogenase from sweet potato. Purification and cDNA sequence analysis. *Plant Cell Physiol.* **39**, 1350–1358
- Siendones, E., Gonzalez-Reyes, J. A., Santos-Ocana, C., Navas, P., and Cordoba, F. (1999) Biosynthesis of ascorbic acid in kidney bean. L-Galactono- $\gamma$ -lactone dehydrogenase is an intrinsic protein located at the mitochondrial inner membrane. *Plant Physiol.* **120**, 907–912
- Heazlewood, J. L., Howell, K. A., and Millar, A. H. (2003) Mitochondrial complex I from *Arabidopsis* and rice. Orthologs of mammalian and fungal components coupled with plant-specific subunits. *Biochim. Biophys. Acta* **1604**, 159–169
- Klodmann, J., Sunderhaus, S., Nimtz, M., Jansch, L., and Braun, H. P. (2010) Internal architecture of mitochondrial complex I from *Arabidopsis*

## GLDH Forms Part of Three Complex I Subcomplexes in Arabidopsis

- thaliana*. *Plant Cell* **22**, 797–810
24. Klodmann, J., and Braun, H. P. (2011) Proteomic approach to characterize mitochondrial complex I from plants. *Phytochemistry* **72**, 1071–1080
  25. Braun, H. P., and Zabaleta, E. (2007) Carbonic anhydrase subunits of the mitochondrial NADH dehydrogenase complex (complex I) in plants. *Physiol. Plant* **129**, 114–122
  26. Pineau, B., Layoune, O., Danon, A., and De Paep, R. (2008) L-Galactono-1,4-lactone dehydrogenase is required for the accumulation of plant respiratory complex I. *J. Biol. Chem.* **283**, 32500–32505
  27. Alhagdow, M., Mounet, F., Gilbert, L., Nunes-Nesi, A., Garcia, V., Just, D., Petit, J., Beauvoit, B., Fernie, A. R., Rothan, C., and Baldet, P. (2007) Silencing of the mitochondrial ascorbate synthesizing enzyme L-galactono-1,4-lactone dehydrogenase affects plant and fruit development in tomato. *Plant Physiol.* **145**, 1408–1422
  28. Sunderhaus, S., Dudkina, N. V., Jansch, L., Klodmann, J., Heinemeyer, J., Perales, M., Zabaleta, E., Boekema, E. J., and Braun, H. P. (2006) Carbonic anhydrase subunits form a matrix-exposed domain attached to the membrane arm of mitochondrial complex I in plants. *J. Biol. Chem.* **281**, 6482–6488
  29. Werhahn, W., Niemeyer, A., Jansch, L., Kruff, V., Schmitz, U. K., and Braun, H. (2001) Purification and characterization of the preprotein translocase of the outer mitochondrial membrane from *Arabidopsis*. Identification of multiple forms of TOM20. *Plant Physiol.* **125**, 943–954
  30. Heinemeyer, J., Lewejohann, D., and Braun, H. P. (2007) Blue native gel electrophoresis for the characterization of protein complexes in plants. *Methods Mol. Biol.* **355**, 343–352
  31. Sunderhaus, S., Eubel, H., and Braun, H. P. (2007) Two-dimensional blue native/blue native polyacrylamide gel electrophoresis for the characterization of mitochondrial protein complexes and supercomplexes. *Methods Mol. Biol.* **372**, 315–324
  32. Neuhoff, V., Arold, N., Taube, D., and Ehrhardt, W. (1988) Improved staining of proteins in polyacrylamide gels including isoelectric focusing gels with clear background at nanogram sensitivity using Coomassie Brilliant Blue G-250 and R-250. *Electrophoresis* **9**, 255–262
  33. Neuhoff, V., Stamm, R., Pardowitz, I., Arold, N., Ehrhardt, W., and Taube, D. (1990) Essential problems in quantification of proteins following colloidal staining with Coomassie Brilliant Blue dyes in polyacrylamide gels, and their solution. *Electrophoresis* **11**, 101–117
  34. Kruff, V., Eubel, H., Jansch, L., Werhahn, W., and Braun, H. P. (2001) Proteomic approach to identify novel mitochondrial proteins in *Arabidopsis*. *Plant Physiol.* **127**, 1694–1710
  35. Zerbetto, E., Vergani, L., and Dabbeni-Sala, F. (1997) Quantification of muscle mitochondrial oxidative phosphorylation enzymes via histochemical staining of blue native polyacrylamide gels. *Electrophoresis* **18**, 2059–2064
  36. Klodmann, J., Senkler, M., Rode, C., and Braun, H. P. (2011) Defining the protein complex proteome of plant mitochondria. *Plant Physiol.* **157**, 587–598
  37. Eadie, M. J., Tyrer, J. H., Kukums, J. R., and Hooper, W. D. (1970) Aspects of tetrazolium salt reduction relevant to quantitative histochemistry. *Histochemistry* **21**, 170–180
  38. Efremov, R. G., Baradaran, R., and Sazanov, L. A. (2010) The architecture of respiratory complex I. *Nature* **465**, 441–445
  39. Hunte, C., Zickermann, V., and Brandt, U. (2010) Functional modules and structural basis of conformational coupling in mitochondrial complex I. *Science* **329**, 448–451
  40. Efremov, R. G., and Sazanov, L. A. (2011) Structure of the membrane domain of respiratory complex I. *Nature* **476**, 414–420
  41. Grigorieff, N. (1998) Three-dimensional structure of bovine NADH:ubiquinone oxidoreductase (complex I) at 22 Å in ice. *J. Mol. Biol.* **277**, 1033–1046
  42. Radermacher, M., Ruiz, T., Clason, T., Benjamin, S., Brandt, U., and Zickermann, V. (2006) The three-dimensional structure of complex I from *Yarrowia lipolytica*. A highly dynamic enzyme. *J. Struct. Biol.* **154**, 269–279
  43. Clason, T., Ruiz, T., Schagger, H., Peng, G., Zickermann, V., Brandt, U., Michel, H., and Radermacher, M. (2010) The structure of eukaryotic and prokaryotic complex I. *J. Struct. Biol.* **169**, 81–88
  44. Dudkina, N. V., Heinemeyer, J., Keegstra, W., Boekema, E. J., and Braun, H. P. (2005) Structure of dimeric ATP synthase from mitochondria. An angular association of monomers induces the strong curvature of the inner membrane. *FEBS Lett.* **579**, 5769–5772
  45. Peters, K., Dudkina, N. V., Jansch, L., Braun, H. P., and Boekema, E. J. (2008) A structural investigation of complex I and I+III2 supercomplex from *Zea mays* at 11–13-Å resolution. Assignment of the carbonic anhydrase domain and evidence for structural heterogeneity within complex I. *Biochim. Biophys. Acta* **1777**, 84–93
  46. Bultema, J. B., Braun, H. P., Boekema, E. J., and Kouril, R. (2009) Mega-complex organization of the oxidative phosphorylation system by structural analysis of respiratory supercomplexes from potato. *Biochim. Biophys. Acta* **1787**, 60–67
  47. Klodmann, J., Lewejohann, D., and Braun, H. P. (2011) Low-SDS blue native PAGE. *Proteomics* **11**, 1834–1839
  48. Brandt, U. (2006) Energy converting NADH:quinone oxidoreductase (complex I). *Annu. Rev. Biochem.* **75**, 69–92
  49. Vogel, R. O., Smeitink, J. A., and Nijtmans, L. G. (2007) Human mitochondrial complex I assembly. A dynamic and versatile process. *Biochim. Biophys. Acta* **1767**, 1215–1227
  50. Remacle, C., Barbieri, M. R., Cardol, P., and Hamel, P. P. (2008) Eukaryotic complex I. Functional diversity and experimental systems to unravel the assembly process. *Mol. Genet. Genomics* **280**, 93–110
  51. Lazarou, M., Thorburn, D. R., Ryan, M. T., and McKenzie, M. (2009) Assembly of mitochondrial complex I and defects in disease. *Biochim. Biophys. Acta* **1793**, 78–88
  52. Perales, M., Eubel, H., Heinemeyer, J., Colaneri, A., Zabaleta, E., and Braun, H. P. (2005) Disruption of a nuclear gene encoding a mitochondrial  $\gamma$ -carbonic anhydrase reduces complex I and supercomplex I + III2 levels and alters mitochondrial physiology in *Arabidopsis*. *J. Mol. Biol.* **350**, 263–277
  53. Meyer, E. H., Solheim, C., Tanz, S. K., Bonnard, G., and Millar, A. H. (2011) Insights into the composition and assembly of the membrane arm of plant complex I through analysis of subcomplexes in *Arabidopsis* mutant lines. *J. Biol. Chem.* **286**, 26081–26092

## Supplementary material

**Table S1:** MS analysis of the 75 kDa spot/smear from the 2D BN/SDS PAGE (Figure 1)

<sup>a</sup> [kDa]	<sup>b</sup> accession no	<sup>c</sup> protein	<sup>d</sup> mass [kDa]	<sup>e</sup> mascot score	<sup>f</sup> no peptides	<sup>g</sup> sequence-coverage [%]
75 kDa	At3g07770	HSP89	90.5	1816	38	42.1
75 kDa	At2g04030	HSP90	88.6	300	1	9.0
75 kDa	At4g26970	aconitate hydratase 2	108.4	202	6	8.9
75 kDa	At5g07440	glutamate dehydrogenase 2	44.7	181	4	14.1
75 kDa	At2g05710	aconitate hydratase 3	108.1	169	4	5.1
75 kDa	At4g39690	unknown protein	70.5	120	4	9.7
75 kDa	At4g37910	HSP70	73.0	109	2	2.9
75 kDa	At5g27540	miro-related GTP-ase 1	72.3	88	3	4.5

<sup>a</sup> analyzed protein spot (spot/smear at 75 kDa, Figure 1)

<sup>b</sup> accession numbers of identified proteins as given by TAIR (<http://www.arabidopsis.org/>)

<sup>c</sup> names of identified proteins

<sup>d</sup> calculated molecular mass of the identified proteins as deduced from the corresponding gene. Note that the mature molecular masses normally are smaller due to removal of mitochondrial targeting sequences.

<sup>e</sup> probability score for the protein identifications based on MS analysis and MASCOT search

<sup>f</sup> number of unique peptides

<sup>g</sup> sequence coverage of the proteins by identified peptides

We conclude that the immune signal visible at ~75 kDa on the blot of the 2D BN/SDS gel (Figure 1) does not represent GLDH but is due to a cross-reaction of the GLDH antibody with one of the identified proteins given above.

Figure S1:

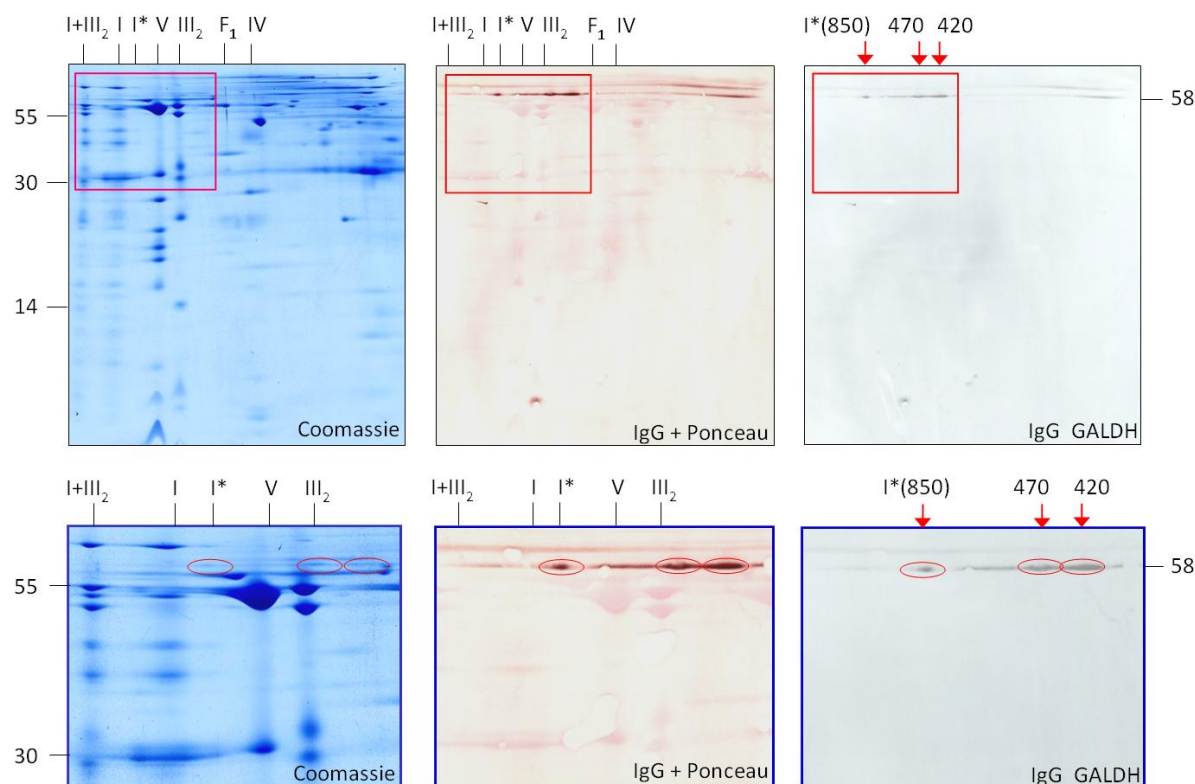


**Figure S1: Immunological detection of L-galactono-1,4-lactone dehydrogenase in a mitochondrial protein fraction of *Arabidopsis thaliana* (repetition of the experiment shown in Figure 1 of the paper).** Proteins were separated by BN/SDS PAGE and either stained by Coomassie-blue (left) or blotted onto nitrocellulose membranes for immunological GLDH detection (centre and right). The blot in the centre additionally was stained with Ponceau for background visualization. Enlargements of the boxed regions are given in the lower line of the figure. Red circles indicate GLDH. A molecular mass standard is given to the left of the figure. Nomenclature of protein complexes: I: complex I; I\*: 850 kDa subcomplex of complex I; V: complex V; III<sub>2</sub>: dimeric complex III; F<sub>1</sub>: F<sub>1</sub> part of complex V; IV: complex IV; I+III<sub>2</sub>: supercomplex composed of complex I + dimeric complex III; 850, 470 and 420 kDa: GLDH containing protein complexes (the 850 kDa complex corresponds to I\*). GLDH is detected on the second gel dimension at 58 kDa.

This experiment represents a repetition of the experiment shown in Figure 1 of our paper. Results are identical, except that the immune signal at 75 kDa, which is due to a cross reaction of the GLDH antibody, is hardly visible. We conclude that GLDH only is represented by the immune signal at 58 kDa, which is confirmed by analysis by mass spectrometry (table 1 of our paper, table S1).

Figure S2

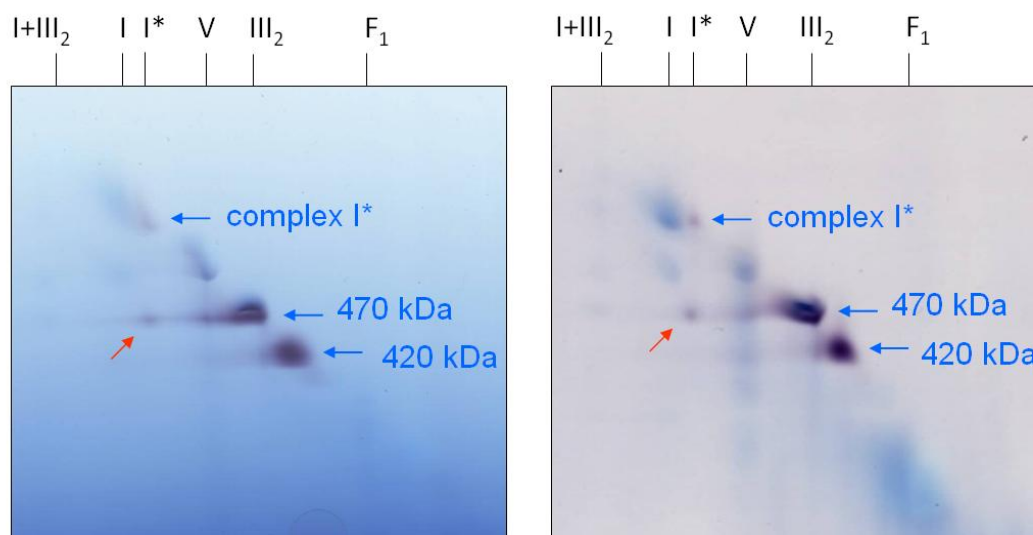


**Figure S2: Detection of GLDH-containing protein complexes on a 2D BN/BN gel by activity staining (two repetitions of Figure 3 of our paper):** Isolated mitochondria from *Arabidopsis thaliana* were treated with digitonin for protein solubilization and protein complexes were subsequently separated by two dimensional BN-digitonin/BN-Triton X-100 PAGE. The gel was stained for GLDH activity (purple spots). Background complexes are visible due to Coomassie blue present during the electrophoresis run (the gel was not stained with Coomassie after completion of the electrophoresis run). Identities of protein complexes are given on top of the gels (for nomenclature see Figure 1). The arrows indicate GLDH-containing complexes identified by the *in gel* activity assay.

Upon prolonged activity staining of the BN/BN gel, not only the 850 kDa complex I\*, the 470 kDa and the 420 kDa complexes become visible (purple spots), but also a dissection product of complex I\* (red arrow), which exactly co-migrates with the 470 kDa complex.



## Supplementary Figure 3

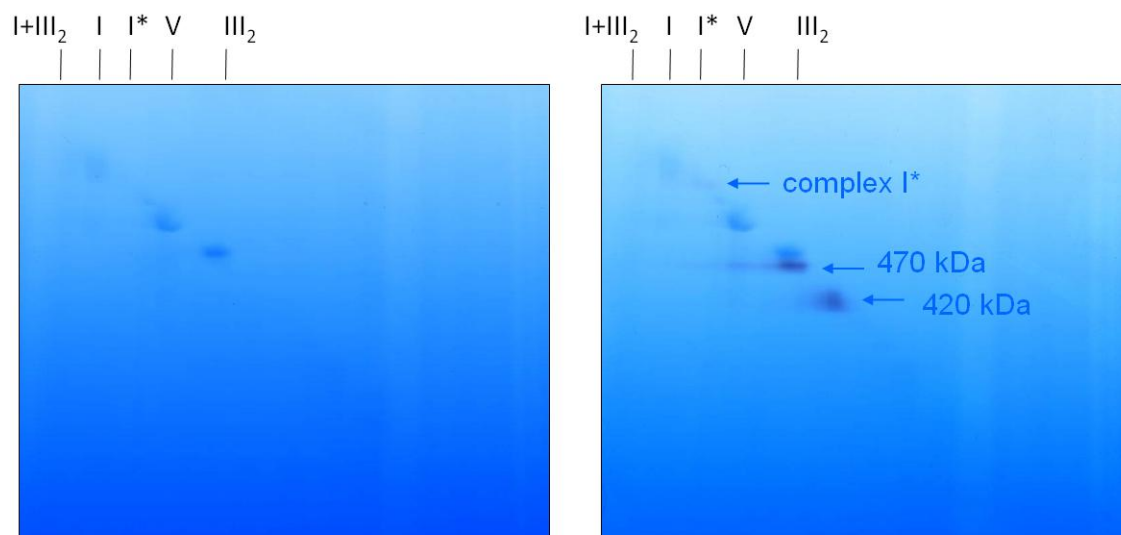


**Figure S3: Detection of GLDH-containing protein complexes on a 2D BN/BN gel by activity staining: GLDH visualization ± GLDH activity staining (gel to the left: without activity stain, gel to the right: with activity stain)**

Isolated mitochondria from *Arabidopsis thaliana* were treated with digitonin for protein solubilization and protein complexes were subsequently separated by two dimensional BN-digitonin/BN-Triton X-100 PAGE. The gel to the right was stained for GLDH activity (purple spots). Background complexes are visible due to Coomassie blue present during the electrophoresis run (the gel was not stained with Coomassie after completion of the electrophoresis run). Identities of protein complexes are given on top of the gels (for nomenclature see Figure 1). The arrows indicate GLDH-containing complexes identified by the *in gel* activity assay.

This figure illustrates the low abundance of the 420 and 470 kDa complex: without GLDH activity staining, these complexes are not visible on the 2D BN/BN gels.

**Table S2:** Proteins of the 2D BN / BN gel (Figure 3) identified by MS (complete list)

<sup>a</sup> sample	<sup>b</sup> accession no	<sup>c</sup> protein	<sup>d</sup> mass [kDa]	<sup>e</sup> mascot score	<sup>f</sup> no peptides	<sup>g</sup> s.c. [%]	complex
470 kDa	At3g02090	beta MPP	59.1	1744	31	67.6	complex III
470 kDa	At1g51980	alpha MPP	54.4	1372	28	57.5	complex III
470 kDa	At3g16480	alpha MPP	54.0	888	9	36.7	complex III
470 kDa	At3g27240	cytochrome c1	33.6	492	11	53.7	complex III
470 kDa	At5g40810	cytochrome c1	33.7	347	2	37.5	complex III
470 kDa	At4g32470	14kDa subunit	14.5	256	5	49.2	complex III
470 kDa	At3g47930	GLDH	68.5	201	4	11.8	complex I
470 kDa	At1g47260	CA2	30.0	178	4	25.5	complex I
470 kDa	At5g13430	FeS subunit	29.6	168	4	13.2	complex III
470 kDa	At3g52730	QCR9	8.4	158	3	41.7	complex III
470 kDa	At2g07727	Cytochrome b	44.1	155	3	8.1	complex III
470 kDa	At3g48680	CAL2	27.9	154	3	17.6	complex I
470 kDa	At3g10860	QCR8	8.5	104	2	26.4	complex III
470 kDa	At1g04630	GRIM-19	16.1	65	1	7.0	complex I
420 kDa	At3g23990	HSP60-1	61.2	873	17	36.6	HSP60
420 kDa	At4g00570	malic enzyme 2	66.6	836	15	33.6	ME complex
420 kDa	At2g33210	HSP60-2	61.9	597	2	27.4	HSP60
420 kDa	At5g08670	ATP synt. beta	59.6	591	12	29.9	ATP synt. (F1)
420 kDa	At2g07698	ATP synt. alpha	85.9	454	8	14.2	ATP Synth. (F1)
420 kDa	At2g13560	malic enzyme 1	69.6	432	7	16.7	ME complex
420 kDa	At3g13860	HSP60-3A	60.4	258	6	14.2	HSP60
420 kDa	At1g47260	CA2	30.0	204	4	24.5	complex I
420 kDa	At3g48680	CAL2	27.9	177	3	13.7	complex I
420 kDa	At3g47930	GLDH	68.5	170	4	8.5	complex I
420 kDa	At4g37910	HSP70-1	73.0	126	2	6.3	HSP70
420 kDa	At5g12290	DGS1	68.9	102	1	4.7	
420 kDa	At5g66510	CA3	27.8	101	1	15.5	complex I
420 kDa	AtMg00285	NAD2A	54.8	84	2	4.2	complex I
850 kDa	At3g23990	HSP60-1	61.2	1611	29	49.6	HSP60
850 kDa	At2g33210	HSP60-2	61.9	1213	8	39.0	HSP60
850 kDa	At5g40770	prohibitin 3	30.4	718	15	57.0	prohibitin
850 kDa	At4g28510	prohibitin 1	31.7	554	10	43.1	prohibitin
850 kDa	At1g03860	prohibitin 2	31.8	452	5	41.3	prohibitin
850 kDa	At3g27280	prohibitin 4	30.6	409	1	30.8	prohibitin
850 kDa	At3g13860	HSP60-3A	60.4	349	9	17.1	HSP60
850 kDa	At1g47260	CA2	30.0	305	8	28.1	complex I
850 kDa	At5g37510	75 kDa subunit	81.1	292	5	13.4	complex I
850 kDa	At2g20530	prohibitin 6	31.6	275	1	26.2	prohibitin
850 kDa	AtMg00070	NAD9	22.7	269	5	27.9	complex I
850 kDa	At2g20360	39 kDa subunit	43.9	207	7	12.7	complex I
850 kDa	AtMg00510	NAD7	44.5	184	3	9.9	complex I
850 kDa	At3g48680	CAL2	27.9	180	4	22.7	complex I
850 kDa	AtMg00285	NAD2A	54.8	154	3	6.2	complex I
850 kDa	At5g08670	ATP synth. beta	59.6	144	4	10.8	ATP synt. (F1)
850 kDa	At5g52840	B13	19.2	125	3	20.7	complex I
850 kDa	At2g07698	ATP synth. alpha	85.9	119	3	4.2	ATP synt. (F1)
850 kDa	At4g16450	compl. I su	11.3	108	2	18.9	complex I

850 kDa	At5g08530	51 kDa subunit	53.4	103	2	6.2	complex I
850 kDa	At3g08580	ADP/ATP carrier	41.4	96	2	4.5	
850 kDa	At3g50930	BCS1	66.1	95	3	6.3	
850 kDa	At1g67350	compl. I su	11.8	73	2	19.4	complex I
850 kDa	At2g07785	NAD1	10.6	61	1	14.1	complex I
850 kDa	At2g33220	GRIM-19	16.1	40	1	16.1	complex I
850 kDa	At1g16700	TYKY-2	11.9	38	1	4.1	complex I
850 kDa	At2g27730	compl. I su	25.4	38	1	26.5	complex I

<sup>a</sup> analyzed protein complex (Figure 3)

<sup>b</sup> accession numbers of identified proteins as given by TAIR (<http://www.arabidopsis.org/>)

<sup>c</sup> names of identified proteins

<sup>d</sup> calculated molecular mass of the identified proteins as deduced from the corresponding gene

<sup>e</sup> probability score for the protein identifications based on MS analysis and MASCOT search

<sup>f</sup> number of unique peptides

<sup>g</sup> sequence coverage of the proteins by identified peptides

Colour code for protein complexes:

- complex I
- HSP60 or HSP70
- prohibitin
- ATP synthase
- complex III
- malic enzyme

## Publication V

### ***2.5 Activity measurements of mitochondrial enzymes in native gels***

Peter Schertl and Hans-Peter Braun

From the Institute of Plant Genetics, Plant Proteomics, Leibniz University Hannover,  
Herrenhäuser Str. 2, 30419 Hannover, Germany

Type of authorship:	first author
Type of article:	book chapter
Share of the work:	85 %
Contribution to the publication:	performed experiments, prepared the figure and wrote the paper
Journal:	Methods in Molecular Biology (Humana Press)
Volume:	Plant mitochondria: Methods and Protocols
Date of publication:	in press

## **Activity measurements of mitochondrial enzymes in native gels**

**Peter Schertl and Hans-Peter Braun**

From the Institute of Plant Genetics, Plant Proteomics, Leibniz University Hannover,  
Herrenhäuser Str. 2, 30419 Hannover, Germany

To whom correspondence should be addressed:

Hans-Peter Braun, Institute of Plant Genetics, Plant Proteomics, Leibniz University Hannover,  
Herrenhäuser Str. 2, 30419 Hannover, Germany, Tel.: +49 511 7622674, Fax: +49 511 7623608, E-  
mail: [braun@genetik.uni-hannover.de](mailto:braun@genetik.uni-hannover.de))

## Summary

In-Gel activity assays are useful tools to identify and characterize enzymes within gels. Prerequisite are electrophoretic protein separations that are carried out under conditions compatible with enzyme activity. While blue native (BN) polyacrylamide gel electrophoresis (PAGE) is widely used for activity assays of the five enzyme complexes of the oxidative phosphorylation system, the blue background of this electrophoretic system is not compatible with activity assays for some other mitochondrial enzymes. As an alternative system, clear native (CN) PAGE can be used for visualizing activities of mitochondrial enzymes. Here, we describe enzyme activity assays for mitochondrial enzymes in BN- and CN gels.

## 1. Introduction

Blue native (BN) polyacrylamide gel electrophoresis (PAGE), in contrast to SDS PAGE, allows protein separations under native conditions (1). BN PAGE is based on the usage of the dye Coomassie blue. Originally, Coomassie blue was used after completion of electrophoretic runs to stain and thereby visualize proteins within gels (2). In contrast, during BN-PAGE, Coomassie blue is added to protein fractions before gel electrophoresis. Due to its anionic properties it introduces negative charge into proteins, thereby allowing their separation according to molecular mass. In contrast to the anionic detergent SDS, Coomassie does not denature proteins and therefore is perfectly compatible for characterizing enzyme activities. In-Gel enzyme assays offer the direct identification of enzymes in gels based on their activity. In contrast to immunoblotting procedures for protein identification, in-Gel enzyme assays do not require the availability of antibodies. Furthermore, in-Gel activity assays offer characterizing enzymes within gels, e.g. by usage of specific inhibitors. Protocols to visualize enzyme activities within BN gels first were established for the enzyme complexes of the oxidative phosphorylation (OXPHOS) system (3 and references within). Later, in-Gel activity assays were successfully used to characterize dysfunctions of OXPHOS complexes caused by mutations (4,5,6). Numerous further enzyme activity assays meanwhile were established for BN gels (e.g. 7). However, some enzyme assays are not compatible with BN PAGE because the blue background of the gels interferes with the activity signals. As an alternative system, clear native (CN) PAGE (8) can be used under these circumstances. During CN PAGE Coomassie blue is omitted. As a result, protein separation is exclusively based on the intrinsic charge of proteins. Separation capacity of CN gels is slightly reduced and molecular mass determinations cannot be carried out. However, CN PAGE is an especially mild procedure and not associated with blue background formation. It ideally can be used for visualization of the enzymatic activities that only result in faint color changes or for assays that are based on usage of blue redox dyes.

Here we present protocols for activity assays of the five OXPHOS complexes and for L-galactono-1,4-Lactone dehydrogenase (GALDH) within BN gels. GALDH catalyzes the terminal step of the

ascorbate biosynthesis pathway which in plants takes place in mitochondria. Furthermore, a proline dehydrogenase assay, which is carried out within a CN gel, is presented.

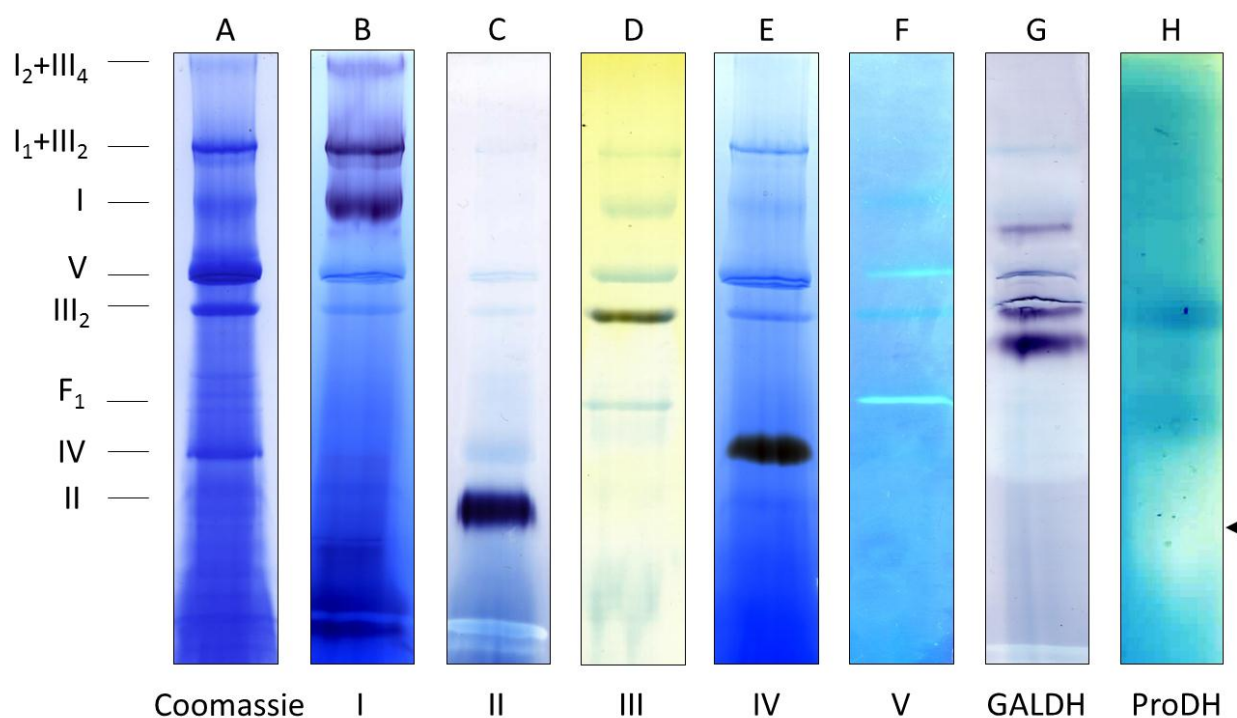


Figure 1: In-Gel activity assays of mitochondrial enzymes in native gels. *Arabidopsis thaliana* mitochondrial proteins (500  $\mu$ g) were solubilized by digitonin and subsequently separated by 1D BN-PAGE (A-G) or by 1D CN-PAGE (H). Designations to the bottom: Coomassie, Coomassie stained gel strip. I, II, III, IV, V: gel strips after in-Gel activity stainings for complexes I, II, III, IV and V. GALDH, gel strip after L-galactono-1,4-lactone dehydrogenase activity staining. ProDH, gel strip after proline dehydrogenase activity staining. For ProDH activity staining, mitochondria from proline treated *Arabidopsis* cells were isolated and separated on a 1D CN-PAGE. Identities of the separated protein complexes and supercomplexes are given to the left:  $I_2 + III_4$ , supercomplex consisting of two copies of complex I and two copies of dimeric complex III;  $I_1 + III_2$ , supercomplex consisting of one copy of complex I and one copy of dimeric complex III; I, complex I; V, ATP synthase;  $III_2$ , dimeric complex III; IV, complex IV; II, complex II,  $F_1$ ,  $F_1$  subcomplex of complex V.

## 2. Materials

All Buffers are prepared with analytical grade chemicals and with pure deionized water. It is not necessary to prepare stock solutions fresh. All other solutions are prepared freshly.

### 2.1. Components for Casting and Running a BN Gel

1. Acrylamide solution: 40 %, acryl/bisacryl = 32/1 (AppliChem, Darmstadt, Germany).
2. BN gel buffer (6×): 1.5 M aminocaproic acid, 150 mM BisTris, pH 7.0 (adjust at 4 °C).
3. Glycerol 100 % (AppliChem, Darmstadt, Germany).
4. N, N, N', N' -tetramethylethylenediamine (TEMED): 99 %, (Sigma, St. Louis, Missouri, USA).
5. Ammonium persulfate solution (APS): 10 % (w/v) ammonium persulfate.
6. BN cathode buffer (5×): 250 mM tricine, 75 mM BisTris, 0.1 % (w/v) Coomassie G250, pH 7.0 (adjust at 4 °C).
7. BN anode buffer (6×): 300 mM BisTris, pH 7.0 (adjust at 4 °C).
8. Gradient former (for example: Model 485 Gradient Former #165-4120; Bio-Rad, Richmond, Ca, US).
9. Protean II gel unit (Bio-Rad, Richmond, Ca, US).

### 2.2. Components for CN-Gel run

1. Precasted mini Gels: NativePAGE™ Novex® 4-16 % Bis-Tris Protein Gels, 1.0 mm, 10 wells (Life Technologies GmbH, Darmstadt, Germany).
2. Anode and cathode running buffer (10x): 250 mM Tris and 192 mM glycine.
3. XCell SureLock® Mini-Cell (Life Technologies GmbH, Darmstadt, Germany).

### 2.3. Components for Sample Preparation

1. Solubilization buffer with 5 % Digitonin, pH 7.4: 30 mM HEPES, 150 mM potassium acetate, 10 % (v/v) glycerol, 5 % digitonin (see Note 1). Buffer is stored at -20 °C.
2. Blue loading buffer (20x) for BN PAGE: 750 mM aminocaproic acid, 5 % (w/v) Coomassie G250, stored at 4 °C.
3. Solubilization buffer for proline dehydrogenase: 2.5 % digitonin in 50 mM Tris-HCl pH 7.2.
4. Native loading buffer (5x) for CN PAGE: 62.5 mM Tris-HCl pH 6.8, 10 % (w/v) glycerol, 0.00125 (w/v) bromphenol blue.

### 2.4. Components for in-Gel activity assays

Buffer stock solutions:

1. Tris-HCl buffer stock solution pH 7.4: 2 M Tris-HCl, pH 7.4.
2. Tris-HCl buffer stock solution pH 8.8: 2 M Tris-HCl, pH 8.8.
3. Phosphate buffer stock solution: 0.5 M KH<sub>2</sub>PO<sub>4</sub>, 0.5 M K<sub>2</sub>HPO<sub>4</sub>, pH 7.4.



Staining solutions:

4. NADH dehydrogenase staining solution (Complex I): 0.1 M Tris-HCl, pH 7.4, 0.14 mM NADH (Sigma, St. Louis, Missouri, USA), 0.1 % (w/v) nitroblue tetrazolium (AppliChem, Darmstadt, Germany) (9).
5. Succinate dehydrogenase staining solution (Complex II): 50 mM phosphate buffer, pH 7.4, 84 mM succinic acid, 0.2 mM phenazine methosulfate, 0.2 % (w/v) nitroblue tetrazolium, 4.5 mM ethylenediaminetetraacetic acid (EDTA), 10 mM KCN (10).
6. Cytochrome-c reductase staining solution (Complex III): Pierce 1-Step TMB-Blotting Substrate (Pierce, Rockford, IL, USA) (11).
7. Cytochrome-c oxidase staining solution (Complex IV): 10 mM phosphate buffer, pH 7.4, 0.1 % (w/v) 3,3'-diaminobenzidine (DAB), 7.5 % (w/v) sucrose, 19 U/mL catalase, and 16 mM cytochrome-c (Sigma-Aldrich, St. Louis, MO, USA) (12).
8. ATPase staining solution (Complex V): 35 mM Tris-HCl pH 7.4, 270 mM glycine, 14 mM, MgSO<sub>4</sub>, 0.2 % Pb(NO<sub>3</sub>)<sub>2</sub> and 8 mM ATP (13).
9. L-galactono-1,4-lactone dehydrogenase staining solution (GALDH): 40 mM Tris-HCl pH 8.8, 2 mM L-galactono-1,4-lactone, 0.1 % (w/v) nitroblue tetrazolium (AppliChem, Darmstadt, Germany), 0.2 mM phenazine methosulfate (7).
10. Pre-incubation solution for Proline dehydrogenase (ProDH) activity: 1.2 mM 2,6-dichlorophenolindophenol (DCPIP), 50 mM Tris-HCl pH 7.2 (14).
11. ProDH staining solution: 50 mM Tris-HCl pH 7.2, 5 mM MgCl<sub>2</sub>, 0.25 mM flavin adenine dinucleotide (FAD), 0.5 mM phenazine methosulfate (PMS), 100 mM L-proline (14).
8. Fixing solution: 40 % (v/v) methanol, 10 % (w/v) acetic acid.

### 3. Methods

#### 3.1. Preparation of a BN Gel

The following instructions refer to the Protean II electrophoresis unit (Bio-Rad, Richmond, CA, USA; gel dimensions 0.15 × 16 × 20 cm). However, units from other manufacturers are of comparable suitability for BN PAGE, e.g., the Hoefer SE-400 or SE-600 gel systems (GE Healthcare, Munich, Germany).

1. 4.5 % separation gel solution is prepared by mixing 2.4 ml of acrylamide solution with 3.5 mL of BN gel buffer and 15.1 mL of deionized water.
2. 16 % separation gel solution is prepared by mixing 7.4 mL of acrylamide solution with 3 mL of BN gel buffer, 4.6 mL deionized water and 3.5 mL glycerol.
3. Use a gradient former and connect it with a tube and a needle with the space in-between two glass plates which are pre-assembled in a gel casting stand. Transfer the two gel solutions into the two chambers of the gradient former. Gradient gels can either be casted from the top (16% gel solution has to enter the gel sandwich first) or from the bottom (4.5% gel solution has to enter the glass plates

first). For casting the gel from the bottom, an adjustable pump (e.g., Bio-Rad Econo Pump) is required.

4. 95  $\mu$ l APS and 9.5  $\mu$ l TEMED are added to the 4.5 % gel solution. To the 16 % gel solution 61  $\mu$ l APS and 6.1  $\mu$ l TEMED has to be added.

5. Cast the gradient gel and overlay it with deionized water to get a sharp line at the top after polymerization. The gel is polymerized within 60 min.

6. Discard the deionized water.

7. For the stacking gel mix 1.5 ml of acrylamide solution with 2.5 ml of BN gel buffer and 11 ml of deionized water.

8. For polymerization add 65  $\mu$ l APS and 6.5  $\mu$ l TEMED and cast the stacking gel on top of the separation gel. Use a comb according to the number of samples you want to analyze. The gel is polymerized within 30 min.

9. Prepare 1 $\times$  BN anode buffer and 1 $\times$  BN cathode buffer by diluting the corresponding stock solutions (see Note 2).

10. After removing the comb add the BN cathode and anode buffers to the upper and lower chambers of the gel unit, respectively. Cool the unit down to 4  $^{\circ}$ C.

### ***3.2. Sample Preparation for BN Gel and CN Gel***

The samples should be treated carefully in order to keep proteins in their native conformation (avoid high salt, ionic detergents, high temperatures, urea, etc.). All steps of the sample preparation should be carried out on ice. The BN and CN gel should be prepared and cooled down before the sample preparation is started. Here we describe sample preparation for isolated mitochondria from Arabidopsis cell culture but mitochondria from any other source can be used accordingly.

#### Sample Preparation for BN Gel

1. Mitochondria (corresponding to about 500  $\mu$ g mitochondrial protein) are centrifuged at 15000 g for 10 min at 4  $^{\circ}$ C using an Eppendorf centrifuge.

2. The mitochondrial pellet is resuspended in 100  $\mu$ l of 5 % digitonin solubilization buffer, pH 7.4, and incubated for 15 min on ice.

3. Afterwards samples are centrifuged for 10 min, 4  $^{\circ}$ C at 20000 g using an Eppendorf centrifuge to remove insoluble material.

4. The supernatant contains solubilized proteins and protein complexes. Mix the supernatant with 5  $\mu$ l blue loading buffer.

#### Sample Preparation for CN Gel:

5. Mitochondria including 45  $\mu$ g protein are centrifuged at 15000 g for 10 min at 4  $^{\circ}$ C using an Eppendorf centrifuge.

6. The mitochondrial pellet is resuspended in 30  $\mu$ l of 2.5 % digitonin solubilization buffer (solubilization buffer for proline dehydrogenase; subheading 2.3) and incubated for 15 min on ice.
7. Afterwards samples are centrifuged for 10 min, 4 °C at 20000 g using an Eppendorf centrifuge to remove insoluble material.
8. Mix the supernatant with 7.5  $\mu$ l native loading buffer.

### **3.3. BN PAGE run**

1. Load samples mixed with blue loading buffer (see Subheading 3.2.) into the gel pockets.
2. Connect the gel unit to a power supply. Start electrophoresis at constant voltage (100 V for 45 min) and continue at constant current (15 mA for about 11 h). Electrophoresis should be carried out at 4°C. Bands of the OXPHOS complexes are already visible during the gel run.

### **3.4. CN PAGE run**

1. Load the samples mixed with native loading buffer into the gel pockets.
2. Run the gel at 375 V, 4 °C for approximately 3.5 h using a XCell SureLock Mini-Electrophoresis System (Life Technologies GmbH, Darmstadt, Germany) or a mini gel chamber from another manufacturer.

### **3.5. In-Gel activity assays for BN PAGE**

1. Incubate the gel with 50 mL freshly prepared staining solution at room temperature (NADH dehydrogenase staining solution, succinate dehydrogenase staining solution, cytochrome-c reductase staining solution (see Note 3), cytochrome-c oxidase staining solution, ATPase staining solution (see Note 4), or GALDH staining solution (see Note 5), (preparation of staining solutions see subheading 2.4).

Staining takes 10 – 30 min for NADH dehydrogenase, up to several hours for succinate dehydrogenase, minimum of 6 hours for cytochrome-c reductase, 2 hours for cytochrome-c oxidase, 3 hours to overnight incubation for ATPase and approximately 30 min for GALDH.

2. The reactions are stopped by transferring the gel into fixing solution (see Note 6).

### **3.6. In-Gel activity assay for CN PAGE**

1. Incubate the gel for 10 min with 50 ml Pre-incubation solution for Proline dehydrogenase (ProDH) activity while gently shaking. Subsequently discard the solution and incubate the gel with ProDH activity staining solution without shaking (see Note 7) for 1.5 h in the dark.
2. Scan the gel immediately after activity staining. The staining solution can be washed out with water. Subsequently the gel can be Coomassie stained.

#### 4. Notes

1. Digitonin is necessary for the solubilization of membrane bound protein complexes of cellular or organellar fractions. Solubilization buffer with digitonin should be heated to dissolve digitonin.
2. It is recommended to use cold water for dilution of the anode and cathode buffer otherwise you have to wait to start the gel run until the buffers are cold.
3. After completion of the staining reaction visibility of precipitated TMB can be optimized using an image processing software (e.g. Adobe photoshop) by decreasing the blue channel of the RGB image file. The blue Coomassie background is not altered (for details see *11*).
4. After complex V staining do not transfer the gel to fixing solution. Acidic solutions can dissolve lead phosphate precipitates. Instead use 50 % methanol for stopping the activity assay (*15*).
5. Incubate in the dark because PMS is light sensitive.
6. For some activity assays it is advisable to scan gels after incubation with fixing solution again. Coomassie blue background should be decreased after this step.
7. Do not shake the gel in the staining solution. Otherwise DCPIP will be washed out and activity bands are not visible anymore.

#### Acknowledgments

We thank Dagmar Lewejohann for expert technical assistance.

#### References

- 1 Schagger H., von Jagow G. (1991) Blue native electrophoresis for isolation of membrane protein complexes in enzymatically active form. *Anal. Biochem.* **199**, 223-231.
- 2 Fazekas de St Groth S., Webster R.G., Datyner A. (1963) Two new staining procedures for quantitative estimation of proteins on electrophoretic strips. *Biochim Biophys Acta.* **71**, 377-391.
- 3 Zerbetto E., Vergani L., Dabbeni-Sala F. (1997) Quantification of muscle mitochondrial oxidative phosphorylation enzymes via histochemical staining of blue native polyacrylamide gels. *Electrophoresis* **18**, 2059-2064.
- 4 Jung C., Higgins C.M., Xu, Z. (2000) Measuring the quantity and activity of mitochondrial electron transport chain complexes in tissues of central nervous system using blue native polyacrylamide gel electrophoresis. *Anal. Biochem.* **286**, 214-223.

- 5 van Coster R., Smet J., George E., et al. (2001) Blue native polyacrylamide gel electrophoresis: a powerful tool in diagnosis of oxidative phosphorylation defects. *Pediatr. Res.* **50**, 658–665.
- 6 Sabar M., Gagliardi D., Balk J. Leaver C.J. (2003) ORFB is a subunit of F1F(O)-ATP synthase: insight into the basis of cytoplasmic male sterility in sunflower. *EMBO Rep.* **4**, 381–386.
- 7 Schertl P., Sunderhaus S., Klodmann J., et al. (2012) L-galactono-1,4-lactone dehydrogenase (GLDH) forms part of three subcomplexes of mitochondrial complex I in *Arabidopsis thaliana*. *J. Biol. Chem.* **287**, 14412–14419.
- 8 Schägger H., Cramer W.A., von Jagow G. (1994) Analysis of molecular masses and oligomeric states of protein complexes by blue native electrophoresis and isolation of membrane protein complexes by two-dimensional native electrophoresis. *Anal. Biochem.* **217**, 220-230.
- 9 Lojda Z., Gossrau R., Schiebler T. (1979) *Enzyme Histochemistry: A Laboratory Manual*. Heidelberg: Springer-Verlag, Berlin-Heidelberg-New-York, pp 1-270.
- 10 Dubowitz V. (1985) *Muscle Biopsy, a Practical Approach*, Bailliere Tindall, London.
- 11 Smet J., de Paepe B., Seneca S., et al. (2011) Complex III staining in blue native polyacrylamide gels. *J. Inherit. Metab. Dis.* **34**, 741–747.
- 12 Seligman A., M.; Karnovsky M.J., Wasserkrug H.L. et al. (1968) Nondroplet ultrastructural demonstration of cytochrome oxidase activity with a polymerizing osmiophilic reagent, diaminobenzidine (DAB). *J. Cell Biol.* **38**, 1–14.
- 13 Cox G.B., Downie J.A., Fayle D.R. et al. (1978) Inhibition, by a protease inhibitor, of the solubilization of the F1-portion of the  $Mg_2^+$ -stimulated adenosine triphosphatase of *Escherichia coli*. *J. Bacteriol.* **133**, 287–292.
- 14 Schertl P., Cabassa C., Saadallah K. et al. (2014) Biochemical characterization of ProDH activity in *Arabidopsis* mitochondria. *FEBS J. in revision*

- 15 Wittig I., Karas M., Schägger H. (2007) High resolution clear native electrophoresis for in-gel functional assays and fluorescence studies of membrane protein complexes. *Mol. Cell Proteomics* **6**, 1215–1225.

## Chapter 3 - Supplementary Discussion

The production of ATP and thereby the supply of cells with energy can be seen as the most important metabolic function of mitochondria. This is especially true during the night and for tissues not exposed to light (e.g. roots). Due to the diurnal cycle and other external influences it is clear that mitochondrial metabolism has to be highly dynamic and flexible. As a consequence multiple alternative electron entry pathways into the ETC exist in plants and have to be tightly regulated. In this supplementary discussion, additional aspects are presented which are not addressed in the frame of the discussion sections of the manuscripts: (I) On the role of mitochondrial metabolism in the light, (II) on the mechanism of regulating proline dehydrogenase in plants, and (III) on the functional relevance of the linkage between ascorbate biosynthesis and complex I assembly. Finally, a search for additional mitochondrial dehydrogenases is presented.

### 3.1 On the Role of Mitochondrial Metabolism in the Light

Energy metabolism in plants is affected by changes during the diurnal cycle. As a consequence, ATP formation constantly has to be adjusted in dependence to external factors and internal demands. Due to the fact that energy consumption of plants is not constant, it is clear that cells have to adjust the production mechanisms of ATP in a specific manner. First of all the plant cell has to monitor the current energy status or available ATP. Afterwards this status has to be brought in line with the required level of ATP. Several factors have to be integrated by the plant cell. The required level of energy is specific for each cell and depends on intrinsic factors, like tissue type and developmental stage. In addition there are several external factors which influence the amount of energy necessary to fuel specific metabolic pathways in plant cells. Plants have to cope with numerous external influences due to their sessile mode of life. They have to handle temperature changes, pathogens, toxic metals, different accessibility of water and nutrient deficiencies. One of the most important aspects in plant energy metabolism that has to be considered is the diurnal cycle. During the day, ATP is produced by photophosphorylation in chloroplasts. What does this mean for mitochondrial metabolism? Two important processes in mitochondria are considerably changed in the light. The pyruvate decarboxylase complex

(PDC) is reversibly inactivated (Budde and Randall 1990) and the export of TCA cycle intermediates is elevated (Hanning and Heldt 1993, Hodges 2002). These intermediates are mainly used for nitrogen fixation (Hodges 2002). Several studies report a substantial reduction in TCA cycle activity in the light (Tcherkez *et al.* 2005). At the same time, mitochondrial ETC is still active in the light (Atkin *et al.* 2000, reviewed in Padmasree *et al.* 2002, Yoshida *et al.* 2006). Since mitochondria possess a malic enzyme, mitochondria are able to run the TCA cycle also when PDC is inactivated. Nevertheless the function of plant mitochondria in illuminated leaves is poorly understood. Three mitochondrial functions are considered to be of special importance in the light (Nunes-Nesi and Fernie 2007). (I) Mitochondrial ATP can be used to support cytosolic sucrose biosynthesis. A decreased cytosolic ATP/ADP ratio was observed in barley leaf protoplasts when mitochondrial ATP-synthase was specifically inhibited (Krömer and Heldt 1991, Krömer *et al.* 1993), indicating a possible important role of mitochondrial ATP during sucrose synthesis. In addition experimental evidence has been presented that a decrease in mitochondrial and cytosolic ATP/ADP ratios leads to a reduced activity of the sucrose-phosphate synthase (Krömer *et al.* 1993). In contrast, other studies suggest that mitochondrial ATP is not necessary for cytosolic sucrose production (Carrari *et al.* 2003). Hence, the amount of ATP derived from mitochondria that is necessary to drive sucrose synthesis is still a matter of debate. (II) Another possible function of mitochondrial energy metabolism in illuminated leaves is the supply of  $\alpha$ -ketoglutarate for chloroplastic nitrogen assimilation (reviewed in Hodges 2002). Mitochondrial derived citrate is converted via isocitrate into  $\alpha$ -ketoglutarate in the cytosol. The  $\alpha$ -ketoglutarate is transported to the chloroplast to support nitrogen assimilation into amino acids by the glutamine synthetase - glutamate synthase (GS/GOGAT) pathway (Fernie *et al.* 2004). (III) Finally, the export of redox equivalents from mitochondria required for hydroxypyruvate reduction in peroxisomes is considered to represent another important function of mitochondrial energy metabolism in the light (Nunes-Nesi and Fernie 2007).

In addition several studies show supportive effects of mitochondrial metabolism on photosynthesis (Krömer *et al.* 1988, Padmasree and Raghavendra 1999a,b, Noguchi and Yoshida 2008, Sweetlove *et al.* 2006). This might be explained by the fact that mitochondrial respiration is able to decrease excess of reducing equivalents produced by the light reaction of photosynthesis (reviewed in Raghavendra *et al.* 1994, Hurry *et al.* 1995). Another hypothesis is that all ATP produced by the photophosphorylation is used for carbon



reduction, and that also in the light, mitochondrial derived ATP is necessary for all other cellular operations (reviewed in Jacoby *et al.* 2012). In summary, it is clear that also in the illuminated leaf mitochondrial metabolism and ATP production is of great importance. In leaves in the dark and in non-green tissues at all times cellular respiration forms the basis for nearly all processes taking place in cells.

### 3.2 Regulation of Proline Dehydrogenase (ProDH) activity

Mitochondrial metabolism is not only affected by the light–dark cycle. Drastic changes concerning energy metabolism also can be observed in the presence of certain stress conditions (reviewed in Jacoby *et al.* 2012). Plants have to adjust the ATP production to fuel all metabolic processes necessary to handle the specific stress situation. Similar to bacteria and fungi, proline levels in plants highly increase during stress, whereby proline concentrations can be up to 100 fold higher in comparison to control conditions (reviewed in Verslues and Sharma 2010). This increase in proline concentration is completely reversible after stress release. The two enzymes ProDH and P5CDH connect proline catabolism with the respiratory chain. Under stress release conditions proline therefore can be considered as an alternative respiratory substrate. The high  $K_m$  value of 31.69 mM indicates a very low substrate affinity of ProDH (Chapter 2: Biochemical characterization of proline dehydrogenase in Arabidopsis mitochondria). A high proline concentration is necessary to approach half of  $V_{max}$ . Sharma and Verslues 2010 measured the proline concentration in seven-days-old Arabidopsis seedlings which were transferred to low water potential polyethylene glycol (PEG) agar plates. The seedlings were held at 1.2 MPa for four days and then transferred back to high water potential media (Sharma and Verslues 2010). After four days at low water potential the proline concentration reached approximately 50  $\mu\text{mol/g}$  fresh weight (approximately 55 mM assuming that 90 % of the fresh weight represents soluble fraction). Therefore, the  $K_m$  value of ProDH is exactly within the range of physiological proline concentrations occurring under stress conditions. The  $K_m$  of 31.69 mM shows that ProDH activity can contribute to ATP production after stress release. Oxygen electrode measurements clearly show respiration with proline as substrate exclusively in seedlings which were treated with 50 mM proline for 24 h to induce ProDH (Chapter 2: Molecular and functional characterization of the mitochondrial proline dehydrogenase 1 in *Arabidopsis thaliana*).

For the first time it was shown that D-lactate as well as L-lactate competitively inhibit ProDH activity in plants (Chapter 2: Biochemical characterization of proline dehydrogenase in *Arabidopsis* mitochondria). Previously, this was only reported for mammalian ProDH and bacterial PutA (Kowaloff *et al.* 1977, Scarpulla and Soffer 1978). Much is known about PutA the bacterial homolog of ProDH. The crystal structure for PutA from *E.coli* revealed that the L-lactate hydroxyl forms hydrogen bonds to Asp370, Tyr540 and a water molecule (Lee *et al.* 2003). The authors defined the exact binding of L-lactate to PutA by accident. During the crystallization process they used PEG3000 (polyethylene glycol 3000) which was contaminated with L-lactate (Lee *et al.* 2003). The physiological reason why lactate inhibits ProDH still remains unclear. For mammalian ProDH it was suggested that the inhibition of ProDH by lactate coordinates hepatic fuel allocation with muscle requirements during exercise (Kowaloff *et al.* 1977). During and after exercise muscle proteolysis is prevented. The inhibition of enzymes involved in amino acid degradation would spare amino acids for protein synthesis after exercise (Kowaloff *et al.* 1977). In plants it is known that D-lactate is mainly formed from methylglyoxal (MG), a toxic by-product of glycolysis. The MG-side way of glycolysis is enhanced during stress (Yadav *et al.* 2005). The inhibitory effect of D-lactate on ProDH could prevent usage of this amino acid as a substrate for OXPHOS under high carbohydrate conditions in plants when glycolysis is enhanced. Another possible function of regulating ProDH activity by D-lactate is that after stress release ProDH is induced in order to remove excess of proline. In the case, the plant gets a new stress impulse, for example a new drought period occurs, ProDH activity has to be stopped immediately. Under stress conditions D-lactate concentration increases rapidly (Yadav *et al.* 2005) and thereby possibly prevents the degradation of the osmoprotective molecule proline.

Like D-lactate metabolism also L-lactate metabolism in plant mitochondria is not really understood so far. It is known that lactic fermentation represents a signal triggering ethanol production in hypoxic maize root tips (Roberts *et al.* 1984). In potato tubers a L-lactate dehydrogenase (LLDH) was identified (Paventi *et al.* 2007). Potato tubers are special with respect to mitochondrial metabolism. They represent ideal model systems to analyze hypoxia in plants because the oxygen concentration may drop below 5 % in the centre of potato tubers (Geigenberger *et al.* 2005). The physiological benefit of the inhibition of ProDH by L-lactate remains to be shown. In addition to the identification of D- and L-lactate as competitive inhibitors for *Arabidopsis* ProDH, pyruvate shows a similar effect on ProDH

activity (unpublished results, appendix Figure 7). The inhibitory effect of pyruvate on ProDH seems to be identical to the inhibition of D-lactate (Figure 7). It can be assumed that the physiological function of a pyruvate mediated inhibition of ProDH is the same as suggested for D-lactate. Under high carbohydrate conditions plant cells are not able to use proline as an alternative respiratory substrate, as far as the proline concentration is low. This may change if the proline concentration is high enough that proline can compete successfully with the competitive inhibitor. Finally, proline can be degraded when the plant cell does not need the protective function of this amino acid anymore. All ProDH inhibition measurements were repeated with membrane fractions that did not contain any matrix proteins. It therefore can be excluded that pyruvate or D- L-lactate were metabolized by other matrix localized enzymes and that another intermediate caused the observed inhibition of ProDH (data not shown).

### **3.3 L-Galactono-1,4-Lactone Dehydrogenase (GLDH) as an Assembly Factor of Complex I**

Besides ProDH, GLDH is the second mitochondrial dehydrogenase which stands in the focus of this thesis. Like ProDH also GLDH can be seen as an alternative electron donor for the mitochondrial respiratory chain. Two molecules cytochrome *c* are reduced during the oxidation of one L-galactono-1,4-lactone molecule. Cytochrome *c* can subsequently transfer its electron to complex IV of the respiratory chain (Bartoli *et al.* 2000). GLDH forms part of three distinct mitochondrial complexes (Chapter 2: L-Galactono-1,4-Lactone dehydrogenase (GLDH) Forms Part of Three Subcomplexes of Mitochondrial Complex I in *Arabidopsis thaliana*). Three lines of experimental evidence support these results. Using immunoblotting, in gel activity assays and mass spectrometry it was shown that enzymatically active GLDH is attached to a ~850 kDa, 470 kDa and a 420 kDa complex. Since GLDH is only attached to assembly intermediates and not to the holo-complex I (~1000 kDa) it can be ruled out that the discovered complexes represent artifacts of digitonin solubilization or that the complexes are degradation fragments of complex I. These fragments would not have GLDH attached. Until now it is not known at which point GLDH is detached from complex I during the assembly process. Besides GLDH acting as an assembly factor for complex I, Perales *et al.* 2005 showed that the carbonic anhydrase (CA2) At1g47260 is also important for complex I assembly. Both, GLDH and CA2, are plant specific complex I subunits essential for the

assembly process of complex I. Since these proteins only occur in plants the assembly of plant complex I has to occur in a unique way. Bartoli *et al.* 2000 and Millar *et al.* 2003 have demonstrated that GLDH activity strongly depends on the availability of oxidized cytochrome *c*. In this way the L-ascorbate production is not only physically linked to the respiratory chain but also physiologically. Much is known about the physiologic function of ascorbate in plants. It is involved in growth (Pignocchi and Foyer 2003), programmed cell death (de Pinto *et al.* 2006), pathogen response (Barth *et al.* 2004) and signal transduction (Barth *et al.* 2006). Ascorbate is also important for plants to handle environmental stress factors like ozone (Conklin and Barth 2004), UV-radiation (Gao and Zhang 2008), high temperatures (Larkindale *et al.* 2005) and high light conditions (Müller-Moulé *et al.* 2004). In addition, several enzymes require ascorbate as a co-factor. Thereby ascorbate often acts as a reductant keeping iron as Fe(II) (Prescott and John 1996). The prolyl hydroxylase, which catalyses posttranslational hydroxylation of proline residues, mainly in the cell wall, is one of these enzymes requiring ascorbate as a co-factor (Smirnoff and Wheeler 2000). One of the most important functions of ascorbate in chloroplasts is the ascorbate - glutathione cycle which consists of four enzymes; ascorbate peroxidase (APX), monodehydroascorbate reductase (MDHAR), glutathione-dependent dehydroascorbate reductase (DHAR), and glutathione reductase (GR). Plants use the cycle to detoxify reactive oxygen species (ROS). In all eukaryotes superoxide occurs in different organelles. The superoxide dismutase converts superoxide to hydrogenperoxid. Ascorbate acts as a co-factor of APX to reduce hydrogenperoxid to water. This reaction oxidizes ascorbate to monodehydroascorbate (MDHA). Subsequently MDHA undergoes a non-enzymatic disproportionation to ascorbate and dehydroascorbate (DHA) or MDHA is reduced to ascorbate by the action of MDHAR. Afterwards DHAR reduces DHA to ascorbate. DHAR uses glutathione as a co-factor. The oxidized glutathione is recycled by the glutathione reductase (GR) which receives the electrons for the reduction process from NADPH (Hancock and Viola 2005). Chew *et al.* 2003 demonstrated that the ascorbate - glutathione cycle is also present in Arabidopsis mitochondria. APX, MDHAR, and GR gene products are dual targeted to chloroplast and mitochondria in Arabidopsis. Only a DHAR isoform is specifically targeted to mitochondria (Chew *et al.* 2003). It is known that high amounts of ROS can be produced within mitochondria (Rhoads *et al.* 2006). For plant cells it is favorable to have the detoxification machinery at the place where it is needed.

Combining these insights with the findings that only assembly intermediates of complex I are connected with the respiratory chain via GLDH but not the holo-complex, it can be speculated that assembly intermediates of complex I are already catalytically active. Due to the absence of specific subunits, the correct function of these assembly intermediates is not possible. This could lead to an enhanced production of ROS by the assembly intermediates. In this way ascorbate would directly act as a scavenger of ROS at the site of its production.

It remains to be investigated how complex I accumulation and L-ascorbate synthesis can be regulated separately and what the benefit is of GLDH having to completely different functions. If the activity of GLDH is necessary to assemble complex I it would be interesting to know the direction of the catalytic activity of GLDH. Does the enzyme need ascorbate and reduced cytochrome *c* as substrates to assemble complex I or does it work *vice versa*, using L-galactono-1,4-lactone and oxidized cytochrome *c* as substrates. The first possibility would imply that ascorbate is essential for complex I assembly.

### 3.4 Supramolecular Structure of Plant Mitochondrial Enzymes

Although mitochondrial metabolism and ATP production are well studied, several aspects still remain unclear. The regulation of mitochondrial energy metabolism is currently not fully understood. For the respiratory chain complexes it is known that one possible level of regulation is the formation of higher order structures. Several mitochondrial enzymes form multienzyme complexes (discussed in more detail in chapter 2: Respiratory electron transfer pathways in plant mitochondria, section “Supramolecular structure of the ETC System”). Formation of protein complexes accelerates the activity of two or more successively acting enzymes. Also ProDH seems to form a small complex (Chapter 2: Molecular and functional characterization of the mitochondrial proline dehydrogenase 1 in *Arabidopsis thaliana*). ProDH might form a complex with P5CDH under certain environmental conditions. Possibly catabolism of proline in plants works similar to the catabolic pathway in bacteria, where ProDH and P5CDH are combined within the multifunctional flavoprotein PutA. With the difference that ProDH and P5CDH in plants are encoded by two separate genes. BN-PAGE combined with *in-gel* activity staining methods (Chapter 2: Activity measurements of mitochondrial enzymes in native gels) would represent a powerful tool to investigate this issue.

### 3.5 Identification of Putative Mitochondrial Dehydrogenases

Besides characterizing the already known enzymes involved in the multiple electron entry pathways into the plant respiratory chain it is of great importance to identify new electron entry points to better understand the complex regulation of the alternative electron transfer pathways and the resulting high flexibility of the plant respiratory system. As already mentioned 11 dehydrogenases are known to channel electrons to the ETF – ETFQO system in mammals. In plants there only is evidence for IVDH and D-2HGDH to interact with the ETF – ETFQO system. It seems likely that in plants by far not all dehydrogenases are discovered which are able to deliver electrons to ETF. Several of the dehydrogenases of the ETF – ETFQO system in mammals are involved in mitochondrial localized  $\beta$ -oxidation (reviewed in Watmough and Frerman 2010). In plants it was controversially discussed if  $\beta$ -oxidation takes place in mitochondria (Dieuaide *et al.* 1993, Masterson and Wood 2001) or in peroxisomes (reviewed in Graham 2008). Today it seems that  $\beta$ -oxidation of straight chain fatty acids in higher plants exclusively occurs in peroxisomes (Graham and Eastmond 2002). Bearing this in mind it is clear that not all dehydrogenases involved in the mammalian ETF – ETFQO system can be found in plant mitochondria. But it seems likely that the ETF – ETFQO system is not only used by two mitochondrial dehydrogenases in plants. A “shot gun proteomic approach” of mitochondria isolated from Arabidopsis suspension cells was carried out in order to identify possible new dehydrogenases or oxidoreductases which are able to fuel the mitochondrial electron transport chain. More than 1600 were detected (Table 1; Appendix). Data reduction was achieved by filtering proteins using known function and motif categories. The mitochondrial localization of unknown proteins was confirmed using “The subcellular localization database for Arabidopsis proteins”, SUBA, (<http://suba.plantenergy.uwa.edu.au/> Tanz *et al.* 2013). Table 1 (Appendix) includes known mitochondrial dehydrogenases and possible new dehydrogenases. The list contains 49 known mitochondrial dehydrogenases, including isoforms and subunits of protein complexes. 25 proteins were identified whose function has not been clarified so far. Most of them belong to the FAD/NAD(P)-binding oxidoreductase family or to the NAD(P)-binding rossmann-fold superfamily. In order to investigate the function of these proteins, knock out mutants have to be generated and analyzed. In addition, the characterization of recombinantly expressed putative mitochondrial dehydrogenases would allow to understand the processes of mitochondrial metabolism in more detail. This list of identified proteins only includes enzymes which are

expressed under standard growth conditions. Shot gun experiments should be repeated using mitochondria isolated from suspension cells or plants which were grown under different stress conditions. Investigation of mitochondria from plants cultivated under carbon starvation, osmotic stress, cold and heat stress or pathogen infections might help to reveal the roles of other dehydrogenases on the respiratory system in plants.

## Appendix

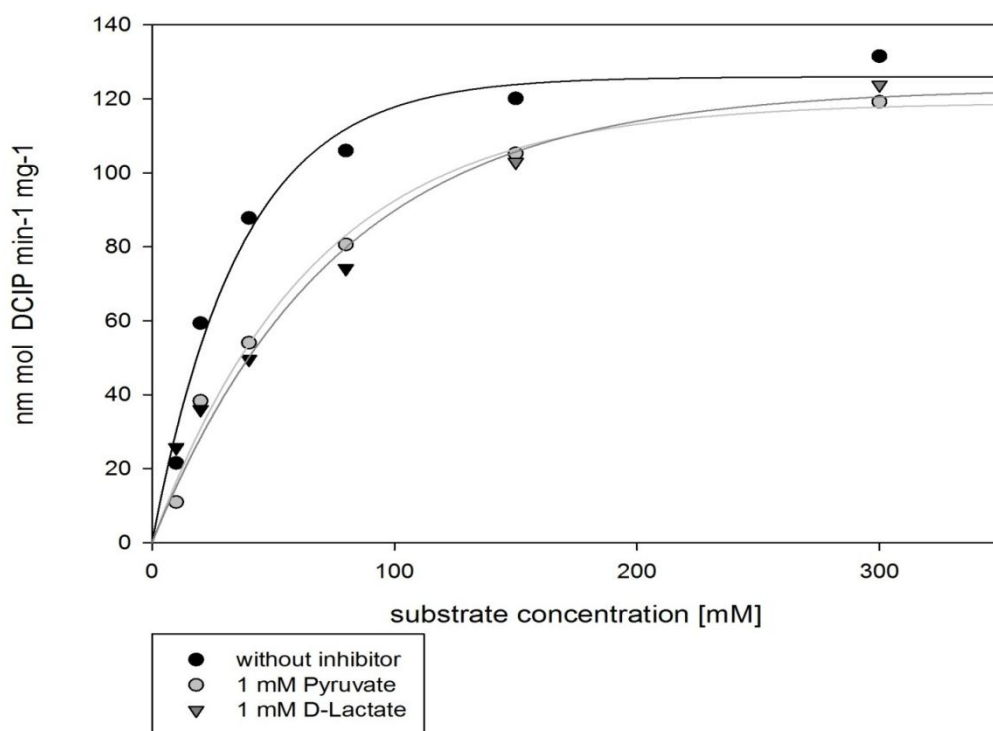


**Figure 7: Inhibitory effect of pyruvate and D-lactate on ProDH activity.** ProDH activity was measured in the absence of inhibitors (black dots) and in the presence of 1 mM pyruvate (grey dots) and 1 mM D-lactate (triangle) at different substrate concentrations (proline concentrations).



**Table 1: Known and putative mitochondrial dehydrogenases of *Arabidopsis thaliana* identified by a “shot gun proteomic approach” (P. Schertl, H.P. Braun and H. Eubel, unpublished work).**

<sup>a</sup> Accession	<sup>b</sup> Description	<sup>c</sup> s.c. [%]	<sup>d</sup> No. peptides	<sup>e</sup> MW [kDa]	<sup>f</sup> calc. pl
AT3G55410.1	2-oxoglutarate dehydrogenase, E1 component	52,90	27	115,1	6,93
AT5G65750.1	2-oxoglutarate dehydrogenase, E1 component	59,51	31	116,3	7,3
AT5G41670.1	6-phosphogluconate dehydrogenase family protein	45,59	7	53,3	5,8
AT4G20930.1	6-phosphogluconate dehydrogenase family protein	6,34	2	37,3	7,37
AT4G29120.1	6-phosphogluconate dehydrogenase family protein	40,12	8	35,3	8,4
AT3G48000.1	aldehyde dehydrogenase 2B4	63,75	24	58,6	7,46
AT1G23800.1	aldehyde dehydrogenase 2B7	10,30	5	58,1	7,33
AT2G29990.1	alternative NAD(P)H dehydrogenase 2	38,58	13	56,5	9,28
AT2G38660.4	amino acid dehydrogenase family protein	35,54	8	36,3	6,99
AT4G36400.1	D-2-hydroxyglutarate dehydrogenase	40,43	13	61,4	6,98
AT4G34200.1	D-3-phosphoglycerate dehydrogenase	45,11	19	63,3	6,58
AT5G23300.1	dihydroorotate dehydrogenase	47,17	14	48,5	9,2
AT5G06580.1	D-lactate dehydrogenase	21,69	9	62,1	6,9
AT1G50940.1	electron transfer flavoprotein alpha	38,29	9	38,4	6,92
AT5G43430.3	electron transfer flavoprotein beta	69,86	10	23,8	5,35
AT2G43400.1	electron-transfer flavoprotein:ubiquinone oxidoreductase	38,70	15	70,1	7,61
AT5G20080.1	FAD/NAD(P)-binding oxidoreductase	49,39	11	36	8,69
AT1G24340.1	FAD/NAD(P)-binding oxidoreductase family protein	26,94	13	78,3	7,25
AT2G29720.1	FAD/NAD(P)-binding oxidoreductase family protein	18,27	6	46,9	9,47
AT3G24200.1	FAD/NAD(P)-binding oxidoreductase family protein	44,75	14	55	7,96
AT5G49555.1	FAD/NAD(P)-binding oxidoreductase family protein	44,78	13	60,5	6,8
AT5G48440.2	FAD-dependent oxidoreductase family protein	13,41	5	46,6	7,31
AT5G14780.1	formate dehydrogenase	16,41	4	42,4	7,5
AT5G18170.1	glutamate dehydrogenase 1	58,88	14	44,5	6,86
AT5G07440.1	glutamate dehydrogenase 2	65,21	14	44,7	6,54
AT3G10370.1	Glycerol-3-phosphate dehydrogenase	23,37	11	68,4	8
AT3G10370.1	Glycerol-3-phosphate dehydrogenase	23,37	11	68,4	8
AT3G15090.1	GroES-like zinc-binding alcohol dehydrogenase family protein	54,37	13	39,4	9,03
AT5G63620.1	GroES-like zinc-binding alcohol dehydrogenase family protein	43,56	11	45,5	7,65
AT5G63890.1	histidinol dehydrogenase	17,92	6	48,9	5,44
AT4G35260.1	isocitrate dehydrogenase 1	52,86	10	39,6	8,13
AT2G17130.2	isocitrate dehydrogenase subunit 2	44,08	7	39,1	6,33
AT3G09810.1	isocitrate dehydrogenase VI	41,44	7	40,5	7,17
AT5G14590.1	Isocitrate/isopropylmalate dehydrogenase family protein	46,60	18	54,2	7,97

AT3G45300.1	isovaleryl-CoA-dehydrogenase	49,63	14	44,7	7,53
AT1G53240.1	lactate/malate dehydrogenase family protein	78,89	8	35,8	8,35
AT3G15020.1	lactate/malate dehydrogenase family protein	76,83	7	35,9	8,19
AT3G47930.1	L-galactono-1,4-lactone dehydrogenase	42,95	21	68,5	8,56
AT3G17240.1	lipoamide dehydrogenase 2	60,55	14	54	7,03
AT2G14170.2	Methylmalonate semialdehyde dehydrogenase	52,41	14	53,4	6
AT1G48030.1	mitochondrial lipoamide dehydrogenase 1	60,75	14	54	7,4
AT2G20360.1	NAD(P)-binding Rossmann-fold superfamily protein	54,48	16	43,9	9,23
AT2G33600.1	NAD(P)-binding Rossmann-fold superfamily protein	15,89	4	35,6	8,28
AT3G26760.1	NAD(P)-binding Rossmann-fold superfamily protein	69,00	13	31,7	7,44
AT3G26770.1	NAD(P)-binding Rossmann-fold superfamily protein	57,84	10	31,8	7,88
AT4G03140.1	NAD(P)-binding Rossmann-fold superfamily protein	7,29	1	36,8	8,87
AT4G20760.1	NAD(P)-binding Rossmann-fold superfamily protein	6,38	2	32,5	9,63
AT4G33360.3	NAD(P)-binding Rossmann-fold superfamily protein	23,24	5	36	7,46
AT5G10730.1	NAD(P)-binding Rossmann-fold superfamily protein	52,61	9	31	9,55
AT5G15910.1	NAD(P)-binding Rossmann-fold superfamily protein	33,46	6	28,8	9,67
AT4G28220.1	NAD(P)H dehydrogenase B1	26,80	9	63,3	6,73
AT4G05020.2	NAD(P)H dehydrogenase B2	34,09	16	69,2	8,48
AT2G20800.1	NAD(P)H dehydrogenase B4	35,22	17	65,3	8,92
AT5G08740.1	NAD(P)H dehydrogenase C1	6,55	2	57	6,96
ATMG00070.E	NAD9 NADH dehydrogenase subunit 9 RNA Edit	73,68	13	22,9	7,44
AT2G13560.1	NAD-dependent malic enzyme 1	55,54	22	69,6	5,45
AT4G00570.1	NAD-dependent malic enzyme 2	59,31	25	66,6	7,06
AT5G37510.1	NADH-ubiquinone dehydrogenase (complex I)	50,60	22	81,1	6,64
AT3G27890.1	NADPH:quinone oxidoreductase	51,02	6	21,5	7,5
AT3G30775.1	proline Dehydrogenase	4,61	2	54,9	6,89
AT5G62530.1	pyrroline-5-carboxylate dehydrogenase	53,60	20	61,7	6,73
AT1G59900.1	pyruvate dehydrogenase complex E1 alpha subunit	37,53	10	43	7,49
ATMG00516.E	RNA Edit NAD1C, NAD1 NADH dehydrogenase 1C	16,92	5	36,1	8,59
ATMG00285.E	RNA Edit NAD2A, NAD2.1, NAD2 NADH dehydrogenase 2A	17,64	8	55,4	8,46
ATMG00580.E	RNA Edit NAD4 NADH dehydrogenase subunit 4	6,87	3	55,8	8,54
ATMG00513.E	RNA Edit NAD5A, NAD5.1, NAD5 NADH dehydrogenase 5A	16,44	8	74,3	6,99
ATMG00510.E	RNA Edit NAD7 NADH dehydrogenase subunit 7	50,51	15	44,9	7,12
AT5G39410.1	saccharopine dehydrogenase	53,08	16	49,6	8,29

AT1G14810.1	semialdehyde dehydrogenase family protein	29,60	7	40,7	7,01
AT5G66760.1	succinate dehydrogenase 1-1	58,20	24	69,6	6,29
AT3G27380.1	succinate dehydrogenase 2-1	42,65	2	31,2	8,44
AT5G40650.1	succinate dehydrogenase 2-2	38,93	2	31,1	8,62
AT1G47420.1	succinate dehydrogenase 5	39,30	8	28,1	6,65
AT1G79440.1	succinic semialdehyde dehydrogenase	56,82	25	56,5	6,92

<sup>a</sup> accession numbers of identified proteins as given by TAIR (<http://www.arabidopsis.org/>)

<sup>b</sup> names / descriptions of identified proteins

<sup>c</sup> sequence coverage of the proteins by identified peptides

<sup>d</sup> number of unique peptides

<sup>e</sup> calculated molecular mass of the identified proteins as deduced from the corresponding gene

<sup>f</sup> calculated isoelectric points

light blue background: putative mitochondrial dehydrogenases

Remark: MASCOT scores are not given due to the fact that the list consists of four independent MS runs with four different scores for each protein

## References

- Abrahams, J. P.; Leslie, A. G.; Lutter, R.; Walker, J. E. (1994): Structure at 2.8 Å resolution of F<sub>1</sub>-ATPase from bovine heart mitochondria. In *Nature* 370 (6491), pp. 621–628.
- Araújo, W.; L.; Ishizaki, K.; Nunes-Nesi, A.; Larson, T. R.; Tohge, T.; Krahnert, I. et al. (2010): Identification of the 2-hydroxyglutarate and isovaleryl-CoA dehydrogenases as alternative electron donors linking lysine catabolism to the electron transport chain of Arabidopsis mitochondria. In *P. Cell* 22 (5), pp. 1549–1563.
- Atkin, O. K.; Evans, J. R.; Ball, M. C.; Lambers, H.; Pons, T. L. (2000): Leaf respiration of snow gum in the light and dark. Interactions between temperature and irradiance. In *Plant Physiol.* 122 (3), pp. 915–923.
- Bari, R.; Kebeish, R.; Kalamajka, R.; Rademacher, T.; Peterhänsel, C. (2004): A glycolate dehydrogenase in the mitochondria of Arabidopsis thaliana. In *J. Exp. Bot.* 55 (397), pp. 623–630.
- Barth, C.; Moeder, W.; Klessig, D. F.; Conklin, P. L. (2004): The timing of senescence and response to pathogens is altered in the ascorbate-deficient Arabidopsis mutant vitamin c-1. In *Plant Physiol.* 134 (4), pp. 1784–1792.
- Barth, C.; Tullio, M. de; Conklin, P. L. (2006): The role of ascorbic acid in the control of flowering time and the onset of senescence. In *J. Exp. Bot.* 57 (8), pp. 1657–1665.
- Bartoli, C. G.; Pastori, G. M.; Foyer, C. H. (2000): Ascorbate biosynthesis in mitochondria is linked to the electron transport chain between complexes III and IV. In *Plant Physiol.* 123 (1), pp. 335–344.
- Binder, S. (2010): Branched-Chain Amino Acid Metabolism in Arabidopsis thaliana. In *Arabidopsis Book* 8, pp. e0137.
- Budde, R. J.; Randall, D. D. (1990): Pea leaf mitochondrial pyruvate dehydrogenase complex is inactivated in vivo in a light-dependent manner. In *Proc. Natl. Acad. Sci. U.S.A.* 87 (2), pp. 673–676.
- Carrari, F.; Nunes-Nesi, A.; Gibon, Y.; Lytovchenko, A.; Loureiro, M. E.; Fernie, A. R. (2003): Reduced expression of aconitase results in an enhanced rate of photosynthesis and marked shifts in carbon partitioning in illuminated leaves of wild species tomato. In *Plant Physiol.* 133 (3), pp. 1322–1335.
- Chew, O.; Whelan, J.; Millar, A. H. (2003): Molecular definition of the ascorbate-glutathione cycle in Arabidopsis mitochondria reveals dual targeting of antioxidant defenses in plants. In *J. Biol. Chem.* 278 (47), pp. 46869–46877.
- Clifton, R.; Millar, A. H.; Whelan, J. (2006): Alternative oxidases in Arabidopsis: a comparative analysis of differential expression in the gene family provides new insights into function of non-phosphorylating bypasses. In *Biochim. Biophys. Acta* 1757 (7), pp. 730–741.

- Conklin, P. L. and Barth, C. (2004): Ascorbic acid, a familiar small molecule intertwined in the response of plants to ozone, pathogens, and the onset of senescence. In *Plant, Cell & Environ.*, 27: pp. 959–970
- Däschner, K.; Couée, I.; Binder, S. (2001): The mitochondrial isovaleryl-coenzyme a dehydrogenase of Arabidopsis oxidizes intermediates of leucine and valine catabolism. In *Plant Physiol.* 126 (2), pp. 601–612.
- Dieuaide, M.; Couée, I.; Pradet, A.; Raymond, P. (1993): Effects of glucose starvation on the oxidation of fatty acids by maize root tip mitochondria and peroxisomes: evidence for mitochondrial fatty acid beta-oxidation and acyl-CoA dehydrogenase activity in a higher plant. In *Biochem. J.* 296 (Pt 1), pp. 199–207.
- Engqvist, M.; Drincovich, M. F.; Flügge, U.-I.; Maurino, V. G. (2009): Two D-2-hydroxy-acid dehydrogenases in Arabidopsis thaliana with catalytic capacities to participate in the last reactions of the methylglyoxal and beta-oxidation pathways. In *J. Biol. Chem.* 284 (37), pp. 25026–25037.
- Fabro, G.; Kovács, I.; Pavet, V.; Szabados, L.; Alvarez, M. E. (2004): Proline accumulation and AtP5CS2 gene activation are induced by plant-pathogen incompatible interactions in Arabidopsis. In *Mol. Plant Microbe Interact.* 17 (4), pp. 343–350.
- Fernie, A. R.; Carrari, F.; Sweetlove, L. J. (2004): Respiratory metabolism: glycolysis, the TCA cycle and mitochondrial electron transport. In *Curr. Opin. Plant Biol.* 7 (3), pp. 254–261.
- Friedrich, T.; Böttcher, B. (2004): The gross structure of the respiratory complex I: a Lego System. In *Biochim. Biophys. Acta* 1608 (1), pp. 1–9.
- Gao, Q.; Zhang, L. (2008): Ultraviolet-B-induced oxidative stress and antioxidant defense system responses in ascorbate-deficient vtc1 mutants of Arabidopsis thaliana. In *J. Plant Physiol.* 165 (2), pp. 138–148.
- Geigenberger, P.; Fernie, A. R.; Gibon, Y.; Christ, M.; Stitt, M. (2000): Metabolic activity decreases as an adaptive response to low internal oxygen in growing potato tubers. In *Biol. Chem.* 381 (8), pp. 723–740.
- Graham, I. A. (2008): Seed storage oil mobilization. In *Annu Rev Plant Biol* 59, pp. 115–142.
- Graham, I. A.; Eastmond, P. J. (2002): Pathways of straight and branched chain fatty acid catabolism in higher plants. In *Prog. Lipid Res.* 41 (2), pp. 156–181.
- Hancock, R. D.; Viola, R. (2005): Improving the nutritional value of crops through enhancement of L-ascorbic acid (vitamin C) content: rationale and biotechnological opportunities. In *J. Agric. Food Chem.* 53 (13), pp. 5248–5257.
- Hanning, I.; Heldt, H. W. (1993): On the Function of Mitochondrial Metabolism during Photosynthesis in Spinach (*Spinacia oleracea* L.) Leaves (Partitioning between Respiration and Export of Redox Equivalents and Precursors for Nitrate Assimilation Products). In *Plant Physiol.* 103 (4), pp. 1147–1154.

- Heazlewood, J. L.; Howell, K. A.; Millar, A. H. (2003): Mitochondrial complex I from Arabidopsis and rice: orthologs of mammalian and fungal components coupled with plant-specific subunits. In *Biochim. Biophys. Acta* 1604 (3), pp. 159–169.
- Hodges, M. (2002): Enzyme redundancy and the importance of 2-oxoglutarate in plant ammonium assimilation. In *J. Exp. Bot.* 53 (370), pp. 905–916.
- Hurry, V.; Tobiaeson, M.; Krömer, S.; Gardeström, P. and Öquist, G. (1995): Mitochondria contribute to increased photosynthetic capacity of leaves of winter rye (*Secale cereale* L.) following cold-hardening. In *Plant, Cell & Environ.*, 18: pp. 69–76
- Ishizaki, K.; Larson, T. R.; Schauer, N.; Fernie, A. R.; Graham, I. A.; Leaver, C. J. (2005): The critical role of Arabidopsis electron-transfer flavoprotein:ubiquinone oxidoreductase during dark-induced starvation. In *P. Cell* 17 (9), pp. 2587–2600.
- Ishizaki, K.; Schauer, N.; Larson, T. R.; Graham, I. A.; Fernie, A. R.; Leaver, C. J. (2006): The mitochondrial electron transfer flavoprotein complex is essential for survival of Arabidopsis in extended darkness. In *Plant J.* 47 (5), pp. 751–760.
- Jacoby, R. P.; Li, L.; Huang, S.; Pong L., C.; Millar, A. H.; Taylor, N. L. (2012): Mitochondrial composition, function and stress response in plants. In *J Integr Plant Biol* 54 (11), pp. 887–906.
- Kenney, W. C. (1975): The reaction of N-ethylmaleimide at the active site of succinate dehydrogenase. In *J. Biol. Chem.* 250 (8), pp. 3089–3094.
- Klodmann, J.; Sunderhaus, S.; Nimtz, M.; Jänsch, L.; Braun, H.-P. (2010): Internal architecture of mitochondrial complex I from Arabidopsis thaliana. In *Plant Cell* 22 (3), pp. 797–810.
- Kowaloff, E. M.; Phang, J. M.; Granger, A. S.; Downing, S. J. (1977): Regulation of proline oxidase activity by lactate. In *Proc. Natl. Acad. Sci. U.S.A.* 74 (12), pp. 5368–5371.
- Krömer, S.; Stitt, M.; Heldt, H.-W. (1988): Mitochondrial Oxidative-Phosphorylation Participating in Photosynthetic Metabolism of a Leaf Cell. In *FEBS Let.*, 226(2), pp. 352-356.
- Krömer, S.; Malmberg, G.; Gardeström, P. (1993): Mitochondrial Contribution to Photosynthetic Metabolism (A Study with Barley (*Hordeum vulgare* L.) Leaf Protoplasts at Different Light Intensities and CO<sub>2</sub> Concentrations). In *Plant Physiol.* 102 (3), pp. 947–955.
- Krömer, S.; Heldt, H. W. (1991): On the Role of Mitochondrial Oxidative Phosphorylation in Photosynthesis Metabolism as Studied by the Effect of Oligomycin on Photosynthesis in Protoplasts and Leaves of Barley (*Hordeum vulgare*). In *Plant Physiol.* 95 (4), pp. 1270–1276.
- Larkindale, J.; Hall, J. D.; Knight, M. R.; Vierling, E. (2005): Heat stress phenotypes of Arabidopsis mutants implicate multiple signaling pathways in the acquisition of thermotolerance. In *Plant Physiol.* 138 (2), pp. 882–897.
- Lee, Y.-H.; Nadaraia, S.; Gu, D.; Becker, D. F.; Tanner, J. J. (2003): Structure of the proline dehydrogenase domain of the multifunctional PutA flavoprotein. In *Nat. Struct. Biol.* 10 (2), pp. 109–114.

- Masterson, C.; Wood, C. (2001): Mitochondrial and peroxisomal beta-oxidation capacities of organs from a non-oilseed plant. In *Proc. Biol. Sci.* 268 (1479), pp. 1949–1953.
- Millar, A. H.; Eubel, H.; Jänsch, L.; Kruff, V.; Heazlewood, J. L.; Braun, H. P. (2004): Mitochondrial cytochrome c oxidase and succinate dehydrogenase complexes contain plant specific subunits. In *Plant Mol. Biol.* 56 (1), pp. 77–90.
- Millar, A. H.; Mittova, V.; Kiddle, G.; Heazlewood, J. L.; Bartoli, C. G.; Theodoulou, F. L.; Foyer, C. H. (2003): Control of ascorbate synthesis by respiration and its implications for stress responses. In *Plant Physiol.* 133 (2), pp. 443–447.
- Millenaar F.F.; Lambers H. (2003): The alternative oxidase: in vivo regulation and function. In *Plant Bio.* 5, pp. 2–15.
- Müller-Moulé, P.; Golan, T.; Niyogi, K. K. (2004): Ascorbate-deficient mutants of Arabidopsis grow in high light despite chronic photooxidative stress. In *Plant Physiol.* 134 (3), pp. 1163–1172.
- Nicholls, D. G.; Rial, E. (1999): A history of the first uncoupling protein, UCP1. In *J. Bioenerg. Biomembr.* 31 (5), pp. 399–406.
- Noguchi, K.; Yoshida, K. (2008): Interaction between photosynthesis and respiration in illuminated leaves. In *Mitochondrion* 8 (1), pp. 87–99.
- Nunes-Nesi, A. and Fernie, A. R. (2007): Mitochondrial Metabolism, in Annual Plant Reviews Volume 31: Plant Mitochondria (ed D. C. Logan), John Wiley & Sons, Inc., Hoboken, NJ, USA. doi: 10.1002/9780470986592.ch8
- Padmasree, K.; Padmavathi, L.; Raghavendra, A. S. (2002): Essentiality of mitochondrial oxidative metabolism for photosynthesis: optimization of carbon assimilation and protection against photoinhibition. In *Crit. Rev. Biochem. Mol. Biol.* 37 (2), pp. 71–119.
- Padmasree, K. and Raghavendra, A. S. (1999a): Importance of oxidative electron transport over oxidative phosphorylation in optimizing photosynthesis in mesophyll protoplasts of pea (*Pisum sativum* L.). In *Physio. Plantarum*, 105: pp. 546–553
- Padmasree K. & Raghavendra A.S. (1999b): Response of photosynthetic carbon assimilation in mesophyll protoplasts to restriction on mitochondrial oxidative metabolism: metabolites related to the redox status and sucrose biosynthesis. In *Photosynthesis Research* 62, pp. 231–239.
- Paventi, G.; Pizzuto, R.; Chieppa, G.; Passarella, S. (2007): Mitochondria isolated from local market potato tubers contain L-lactate dehydrogenase in an inactive state. In *Ital. J. Biochem.* 56 (4), pp. 289–294.
- Perales, M.; Eubel, H.; Heinemeyer, J.; Colaneri, A.; Zabaleta, E.; Braun, H.-P. (2005): Disruption of a nuclear gene encoding a mitochondrial gamma carbonic anhydrase reduces complex I and supercomplex I + III2 levels and alters mitochondrial physiology in Arabidopsis. In *J. Mol. Biol.* 350 (2), pp. 263–277.

- Pignocchi, C.; Foyer, C. H. (2003): Apoplastic ascorbate metabolism and its role in the regulation of cell signalling. In *Curr. Opin. Plant Biol.* 6 (4), pp. 379–389.
- Pineau, B.; Layoune, O.; Danon, A.; Paepe, R. de (2008): L-galactono-1,4-lactone dehydrogenase is required for the accumulation of plant respiratory complex I. In *J. Biol. Chem.* 283 (47), pp. 32500–32505.
- Pinto, M. C. de; Paradiso, A.; Leonetti, P.; Gara, L. de (2006): Hydrogen peroxide, nitric oxide and cytosolic ascorbate peroxidase at the crossroad between defence and cell death. In *Plant J.* 48 (5), pp. 784–795.
- Prescott, A. G.; John, P. (1996): Dioxygenases: Molecular Structure and Role in Plant Metabolism. In *Annu. Rev. Plant Physiol. Plant Mol. Biol.* 47, pp. 245–271.
- Sazanov, L. A.; Baradaran, R.; Efremov, R. G.; Berrisford, J. M.; Minhas, G. (2013): A long road towards the structure of respiratory complex I, a giant molecular proton pump. In *Biochem. Soc. Trans.* 41 (5), pp. 1265–1271.
- Raghavendra, A. S.; Padmasree, K.; Saradadevi, K. (1994): Interdependence of photosynthesis and respiration in plant cells—interactions between chloroplasts and mitochondria. In *Plant Sci.* 97, pp.1–14
- Rasmusson, A. G.; Geisler, D. A.; Møller, I. M. (2008): The multiplicity of dehydrogenases in the electron transport chain of plant mitochondria. In *Mitochondrion* 8 (1), pp. 47–60.
- Rasmusson, A. G.; Soole, K.n L.; Elthon, T. E. (2004): Alternative NAD(P)H dehydrogenases of plant mitochondria. In *Annu Rev Plant Biol* 55, pp. 23–39.
- Rhoads, D. M.; Umbach, A. L.; Sweet, C. R.; Lennon, A. M.; Rauch, G. S.; Siedow, J. N. (1998): Regulation of the cyanide-resistant alternative oxidase of plant mitochondria. Identification of the cysteine residue involved in alpha-keto acid stimulation and intersubunit disulfide bond formation. In *J. Biol. Chem.* 273 (46), pp. 30750–30756.
- Rhoads, D. M.; Umbach, A. L.; Subbaiah, C. C.; Siedow, J. N. (2006): Mitochondrial reactive oxygen species. Contribution to oxidative stress and interorganellar signaling. In *Plant Physiol.* 141 (2), pp. 357–366.
- Roberts, J. K.; Callis, J.; Wemmer, D.; Walbot, V.; Jardetzky, O. (1984): Mechanisms of cytoplasmic pH regulation in hypoxic maize root tips and its role in survival under hypoxia. In *Proc. Natl. Acad. Sci. U.S.A.* 81 (11), pp. 3379–3383.
- Scarpulla, R. C.; Soffer, R. L. (1978): Membrane-bound proline dehydrogenase from *Escherichia coli*. Solubilization, purification, and characterization. In *J. Biol. Chem.* 253 (17), pp. 5997–6001.
- Sharma, S.; Verslues, P.E. (2010): Mechanisms independent of abscisic acid (ABA) or proline feedback have a predominant role in transcriptional regulation of proline metabolism during low water potential and stress recovery. In *Plant Cell Environ.* 33 (11), pp. 1838–1851.



- Sharma, S. S.; Dietz, K.-J. (2009): The relationship between metal toxicity and cellular redox imbalance. In *Trends Plant Sci.* 14 (1), pp. 43–50.
- Shen, W.; Wei, Y.; Dauk, M.; Tan, Y.; Taylor, D. C.; Selvaraj, G.; Zou, J. (2006): Involvement of a glycerol-3-phosphate dehydrogenase in modulating the NADH/NAD<sup>+</sup> ratio provides evidence of a mitochondrial glycerol-3-phosphate shuttle in Arabidopsis. In *Plant Cell* 18 (2), pp. 422–441.
- Shen, W.; Wei, Y.; Dauk, M.; Zheng, Z.; Zou, J. (2003): Identification of a mitochondrial glycerol-3-phosphate dehydrogenase from Arabidopsis thaliana: evidence for a mitochondrial glycerol-3-phosphate shuttle in plants. In *FEBS Lett.* 536 (1-3), pp. 92–96.
- Smirnoff, N.; Wheeler, G. L. (2000): Ascorbic acid in plants: biosynthesis and function. In *Crit. Rev. Biochem. Mol. Biol.* 35 (4), pp. 291–314.
- Sweetlove, L.J.; Lytovchenko, A.; Morgan, M.; Nunes-Nesi, A.; Taylor, N. L.; Baxter, C. J. et al. (2006): Mitochondrial uncoupling protein is required for efficient photosynthesis. In *Proc. Natl. Acad. Sci. U.S.A.* 103 (51), pp. 19587–19592.
- Szabados, L.; Savouré, A. (2010): Proline: a multifunctional amino acid. In *Trends Plant Sci.* 15 (2), pp. 89–97.
- Tanz, S. K.; Castleden, I.; Hooper, C. M.; Vacher, M.; Small, I.; Millar, H. A. (2013): SUBA3: a database for integrating experimentation and prediction to define the SUBcellular location of proteins in Arabidopsis. In *Nucleic Acids Res.* 41 (Database issue), pp. D1185-91.
- Tcherkez, G.; Cornic, G.; Bligny, R.; Gout, E.; Ghashghaie, J. (2005): In vivo respiratory metabolism of illuminated leaves. In *Plant Physiol.* 138 (3), pp. 1596–1606.
- Tobin, A.; Djerdjour, B.; Journet, E.; Neuburger, M.; Douce, R. (1980): Effect of NAD on Malate Oxidation in Intact Plant Mitochondria. In *Plant Physiol.* 66 (2), pp. 225–229.
- Ullrich, A.; Knecht, W.; Piskur, J.; Löffler, M. (2002): Plant dihydroorotate dehydrogenase differs significantly in substrate specificity and inhibition from the animal enzymes. In *FEBS Lett.* 529 (2-3), pp. 346–350.
- Van Der Straeten, D.; Chaerle, L.; Sharkov, G.; Lambers, H.; and Van Montagu M. (1995): Salicylic acid enhances the activity of the alternative pathway of respiration in tobacco leaves and induces thermogenicity. In *Planta* 196, pp. 41 2-41 9.
- Vanlerberghe; McIntosh; Yip (1998): Molecular localization of a redox-modulated process regulating plant mitochondrial electron transport. In *Plant Cell* 10 (9), pp. 1551–1560.
- Verslues, P. E.; Bray, E. A. (2006): Role of abscisic acid (ABA) and Arabidopsis thaliana ABA-insensitive loci in low water potential-induced ABA and proline accumulation. In *J. Exp. Bot.* 57 (1), pp. 201–212.
- Verslues, P. E.; Sharma, S. (2010): Proline metabolism and its implications for plant-environment interaction. In *Arabidopsis Book* 8, pp. e0140.

Wagner A. M ; Krab K. (1995): The alternative respiration pathway in plants: role and regulation. In *Physiol Plant* 95, pp. 318-325

Watmough, N. J.; Frerman, F. E. (2010): The electron transfer flavoprotein: ubiquinone oxidoreductases. In *Biochim. Biophys. Acta* 1797 (12), pp. 1910–1916.

Yadav, S. K.; Singla-Pareek, S. L.; Ray, M.; Reddy, M. K.; Sopory, S. K. (2005): Methylglyoxal levels in plants under salinity stress are dependent on glyoxalase I and glutathione. In *Biochem. Biophys. Res. Commun.* 337 (1), pp. 61–67.

Yoshida, K.; Terashima, I.; Noguchi, K. (2006): Distinct roles of the cytochrome pathway and alternative oxidase in leaf photosynthesis. In *Plant Cell Physiol.* 47 (1), pp. 22–31.

## Curriculum Vitae

---

Name:	Peter Schertl
Date of Birth:	13.07.1984
Place of Birth:	Hannover, Germany
Citizenship:	German

---

### Academic Education

since Jan. 2011	PhD-Student in the group of Prof. Dr. Hans-Peter Braun, Department "Plant Proteomics" at the "Leibniz Universität Hannover"
Oct. 2010	Master of Science in Biochemistry
2008-2010	Student at Hannover Medical School (MHH) major: Biochemistry
Sept. 2008	Bachelor of Science in Plant biotechnology
2005-2008	Student at the "Leibniz Universität Hannover" major: Plant biotechnology

---

### Civilian Service

Sept.2004-June 2005:	Daycare facility for children
----------------------	-------------------------------

---

### School Education

June 2004	Qualification "Abitur"
1997-2004:	"Gymnasium" in Hannover
1995-1997:	„Orientierungsstufe“ in Hannover
1991-1995:	Primary School in Hannover

---

## Publications

Petereit J., Katayama K., Lorenz C., **Schertl P.**, Kitsche A., Wada H., Frentzen M., Braun H. P., Eubel H. (2014) Cardiolipin deficiency has pleiotropic effects on the plant mitochondrial electron chain (submitted)

Cabassa-Hourton C., **Schertl P.**, Bordenave-Jacquemin M., Saadallah K., Guivarc'h A., Planchais S., Klodmann J., Eubel H., Lefebvre-De Vos D., Ghelis T., Richard L., Lebreton S., Abdelly C., Carol P., Braun H. P., Savaur  A. (2014) Molecular and functional characterization of the mitochondrial proline dehydrogenase 1 in *Arabidopsis thaliana* in revision. *Plant Physiology*, in revision

**Schertl P.** and Braun H. P. (2014a) Activity measurements of mitochondrial enzymes in native gels. *Mol. Meth. Biol.*, in press

**Schertl P.**, Cabassa C., Saadallah K., Bordenave M., Savaur  A., and Braun H. P. (2014) Biochemical characterization of ProDH activity in *Arabidopsis* mitochondria. *FEBS J.* doi: 10.1111/febs.12821

**Schertl P.** and Braun H. P. (2014b) Respiratory electron transfer pathways in plant mitochondria. *Front. Plant Sci.* 5:163. doi: 10.3389/fpls.2014.00163

**Schertl P.**, Sunderhaus, S., Klodmann, J., Grozeff, G. E. G., Bartoli, C. G., and Braun, H. P. (2012). L-galactono-1,4-lactone dehydrogenase (GLDH) forms part of three subcomplexes of mitochondrial complex I in *Arabidopsis thaliana*. *J. Biol. Chem.* 287, 14412–14419. doi: 10.1074/jbc.M111.305144

---

## Conference Presentations

### Oral Presentations

**20th Arbeitstagung – „Micromethods in Protein Chemistry”** June 24-26, 2013, Bochum (Germany)  
„Ein In-Gel Aktivit tstest f r die L-Galactono-1,4-Lacton Dehydrogenase (GLDH)“

**International Congress on Plant Mitochondrial Biology**, May 14-19, 2011, Hohenroda (Germany).  
“L-galactono-1,4-lactone dehydrogenase forms part of three distinct complexes in *Arabidopsis thaliana* mitochondria”

### Poster Presentations

**International Congress on Plant Mitochondrial Biology**, May 12-16, 2013, Rosario (Argentina).  
Schertl P. and Braun H. P. “Effects of proline on the activity of mitochondrial dehydrogenases”

---

## Award

**Winner of the Young Investigator Award 2013 (500  ), “ 20th Arbeitstagung - Micromethods in Protein Chemistry”** June 24-26, 2013, Bochum (Germany)

---

**Research Internships**

Federal University of Vicosa, Brazil, Department of Biology (Prof. Dr. Adriano Nunes Nesi, Prof. Dr. Wagner Luiz Araújo), 26<sup>th</sup> of october – 8<sup>th</sup> of november 2014 (supported by Deutscher Akademischer Austauschbund [DAAD])

Université Pierre et Marie Curie, Paris, Department “Adaptation de Plantes aux Contraintes Environnementales” 25<sup>th</sup> of october – 9<sup>th</sup> of november 2013 (Prof. Dr. Arnould Saviouré), (supported by Deutscher Akademischer Austauschbund [DAAD])

La Plata University, Argentina, Instituto de Fisiología Vegetal (INFIVE) (Prof. Dr. Carlos Bartoli), 27<sup>th</sup> of november – 11<sup>th</sup> of december 2011 (supported by Deutscher Akademischer Austauschbund [DAAD])

---

## **Danksagung**

**Lieber Hans-Peter**, an dieser Stelle möchte ich mich als erstes bei Dir dafür bedanken, dass du mir die Möglichkeit gegeben hast in deiner Abteilung zu promovieren. Vielen Dank für die Betreuung und Unterstützung. Vielen Dank auch dafür, dass du mir die Teilnahme an internationalen Konferenzen und Auslandsaufenthalte ermöglicht hast, die mich nicht nur wissenschaftlich voran gebracht haben, sondern die mir auch privat sehr viel Freude bereitet haben und an die ich mich noch lange und gerne zurück erinnern werde.

**Prof. Dr. Christoph Peterhänsel, Prof. Dr. Stefan Binder** und **Prof. Dr. Traud Winkelmann**, dass sie sich als Korreferenten bzw. als Prüfungsvorsitz für meine Dissertation zur Verfügung gestellt haben.

**Der gesamten AG Braun** möchte ich ganz herzlich für die schöne Zeit danken. Ohne das freundschaftliche Arbeitsklima hätte die Arbeit hier mit Sicherheit nicht so viel Spaß gemacht.